Investigation of the controls on the cadmium isotope composition of modern marine sediments

Allison Bryan

St Cross College
University of Oxford

A thesis submitted for the degree of Doctor of Philosophy

Trinity 2018

Abstract

Cadmium (Cd) isotopes have provided insights into the bigeochemical cycling of Cd in the modern oceans, and may be used to provide information about past ocean chemistry. Cadmium is removed from seawater into marine sediments, but the isotopic composition of this output flux, and the processes that control the isotope composition of marine sediments, are not well understood. This lack of understanding is partly due to the currently unknown influence of Cd-sulphide formation on the isotopic composition of sediments forming in low oxygen settings, which limits the application of Cd-isotopes to palaeoenvironmental reconstruction of past ocean Cd cycling, and potentially as a tracer of past ocean conditions.

It is important to know if the biogeochemically important processes that are recorded in the modern cycling of Cd are robustly recorded in ocean sediments after remineralization and diagenesis. This comparison can be achieved through a systematic investigation of the Cd-isotope variations found in modern marine sedimentary environments and overlying waters. To address this unknown, this research involved measuring and interpreting the Cd isotopic composition and concentration of waters, sinking particles, and surface sediments accumulating under a range of primary productivity and redox conditions in the South Atlantic at 40°S, Saanich Inlet, and Black Sea. The sample sites are settings characterised by differing levels of dissolved oxygen, in order to test the influence of Cd-sulphide formation on the bulk sediment isotopic composition. Also, I conducted laboratory experiments to quantify the mechanism and magnitude of Cd isotope fractionation during precipitation of cadmium sulphides (CdS).

The findings support a link between the redox state at the water-sediment interface and the degree of Cd isotope fractionation of the core-top sediments and porewaters relative to the overlying waters. The Cd concentration and isotope composition of near-surface sediments with anoxic deep-waters and sub-oxic conditions in the near-surface sediment porewaters indicate near-quantitative removal of Cd compared to sites with oxygenated deep-waters and pore-waters that report a preferential removal of the light Cd isotopes, likely by precipitation of cadmium sulphide (CdS) complexes. These findings greatly improve our understanding of an important light sink of Cd in our global oceans, and how the signal of important biological processes in the surface-waters are recorded within the near-surface sediments in modern marine environments.

Investigation of the controls on the cadmium isotope composition of modern marine sediments



Allison Bryan

St Cross College

University of Oxford

A thesis submitted for the degree of

Doctor of Philosophy

Trinity 2018

Acknowledgements

Personal

I have been supported as a postgraduate student by my supervisors, my fellow postgraduate students and friends within my department, college, and boat club, and my family back in the States. I have many individuals that deserve recognition, and I will highlight a few of them now.

Thank you to my supervisors Gideon Henderson, Don Porcelli, and Alex Dickson for providing me the opportunity and freedom to develop my own ideas and create collaborations with other researchers. It has allowed me to engage and develop academic relationships with scientists around the world, in order to gain access to and/or collect sample from the locations presented in this thesis. Also, a thank you for providing me the opportunity to join a GEOTRACES research cruise over the Christmas holidays this past year. It was an amazing and unique opportunity that I will always remember.

A particularly thank you to my supervisor Alex Dickson for his continuous help in and out of the lab, and sharing of his wealth of knowledge and ideas to improve my project every step of the way. I am indebted to all of your support these past 4 years.

An important component in the life of a postgraduate student, beyond the lab, is spending time with friends. I had the opportunity of meeting and developing friendships with a large number of fellow postgraduate students and rowers during my 4 years at Oxford. Some of these special individuals include Hannah, Saher, Sarah, Mimi, Gemma, Naomi, Eleanor, Rebecca, Lauren, Ash, Tim, Chris, Christian, Sabin, Phil, Stef, Nicky, and many more individuals within the department, my college, and boat club.

A special acknowledgement to Simon, who has been my primary support system and tried to help me maintain a healthy work-life balance this past year. You always remind me that there are more important things in life besides Cd isotopes and rowing.

I would never have made it to Oxford without the continuous support and love from my family. A very special thank you to my parents and siblings for all their never ending encouragement and support in my decision to travel across the Atlantic Ocean to study another isotope system. These past four years would not have been possible to complete without all of these individuals, so thank you!

Abstract

Cadmium (Cd) isotopes have provided insights into the bigeochemical cycling of Cd in the modern oceans, and may be used to provide information about past ocean chemistry. Cadmium is removed from seawater into marine sediments, but the isotopic composition of this output flux, and the processes that control the isotope composition of marine sediments, are not well understood. This lack of understanding is partly due to the currently unknown influence of Cd-sulphide formation on the isotopic composition of sediments forming in low oxygen settings, which limits the application of Cd-isotopes to palaeoenvironmental reconstruction of past ocean Cd cycling, and potentially as a tracer of past ocean conditions.

It is important to know if the biogeochemically important processes that are recorded in the modern cycling of Cd are robustly recorded in ocean sediments after remineralization and diagenesis. This comparison can be achieved through a systematic investigation of the Cd-isotope variations found in modern marine sedimentary environments and overlying waters. To address this unknown, this research involved measuring and interpreting the Cd isotopic composition and concentration of waters, sinking particles, and surface sediments accumulating under a range of primary productivity and redox conditions in the South Atlantic at 40°S, Saanich Inlet, and Black Sea. The sample sites are settings characterised by differing levels of dissolved oxygen, in order to test the influence of Cd-sulphide formation on the bulk sediment isotopic composition. Also, I conducted laboratory experiments to quantify the mechanism and magnitude of Cd isotope fractionation during precipitation of cadmium sulphides (CdS).

The findings support a link between the redox state at the water-sediment interface and the degree of Cd isotope fractionation of the core-top sediments and porewaters relative to the overlying waters. The Cd concentration and isotope composition of near-surface sediments with anoxic deep-waters and sub-oxic conditions in the near-surface sediment porewaters indicate near-quantitative removal of Cd compared to sites with oxygenated deep-waters and pore-waters that report a preferential removal of the light Cd isotopes, likely by precipitation of cadmium sulphide (CdS) complexes. These findings greatly improve our understanding of an important light sink of Cd in our global oceans, and how the signal of important biological processes in the surface-waters are recorded within the near-surface sediments in modern marine environments.

Extended Abstract

Cadmium (Cd) isotopes have provided insights into the bigeochemical cycling of Cd in the modern oceans, and may be used to provide information about past ocean chemistry. Cadmium is removed from seawater into marine sediments, but the isotopic composition of this output flux, and the processes that control the isotope composition of marine sediments, are not well understood. This lack of understanding is partly due to the currently unknown influence of Cd-sulphide formation on the isotopic composition of sediments forming in low oxygen settings, which limits the application of Cd-isotopes to palaeoenvironmental reconstruction of past ocean Cd cycling, and potentially as a tracer of past ocean conditions.

It is important to know if the biogeochemically important processes that are recorded in the modern cycling of Cd are robustly recorded in ocean sediments after remineralization and diagenesis. This comparison can be achieved through a systematic investigation of the Cd-isotope variations found in modern marine sedimentary environments and overlying waters. To address this unknown, this research involved measuring and interpreting the Cd isotopic composition and concentration of waters, sinking particles, and surface sediments accumulating under a range of primary productivity and redox conditions in the South Atlantic at 40°S, Saanich Inlet, and Black Sea. The sample sites are settings characterised by differing levels of dissolved oxygen, in order to test the influence of Cd-sulphide formation on the bulk sediment isotopic composition. The South Atlantic at 40°S represents an open ocean settings with high primary productivity within an ocean basin known for low concentrations of critical micronutrients (Chapter 4). The Black Sea depicts a restricted, permanently anoxic basin with a sharp chemocline and significantly lower trace metal concentrations that the open ocean (Chapter5). Saanich inlet is a seasonally anoxic basin characterized by vertical variability in the chemocline depth and high trace metal concentrations in the basin seawater (Chapter 6) These field studies are supported by experiments to precipitate CdS under controlled laboratory conditions. The laboratory experiments were conducted to quantify the mechanism and magnitude of Cd isotope fractionation during precipitation of cadmium sulphides (CdS) using synthetic seawater in an anoxic environment (Chapter 3).

The findings support a link between the redox state at the water-sediment interface and the degree of Cd isotope fractionation of the core-top sediments and pore-waters relative to the overlying waters. The Cd concentration and isotope composition of

near-surface sediments with anoxic deep-waters and sub-oxic conditions in the near-surface sediment porewaters indicate near-quantitative removal of Cd compared to sites with oxygenated deep-waters and pore-waters that report a preferential removal of the light Cd isotopes, as seen in the South Atlantic ($\Delta^{114/110}\mathrm{Cd}_{\mathrm{core\text{–}top\text{–}deep\,waters}}$ ranges from -0.36 $\pm$ 0.08 ‰ to 0.10 $\pm$ 0.07 ‰), seasonally anoxic basin, Saanich Inlet (average $\Delta^{114/110}\mathrm{Cd}_{\mathrm{core\text{–}top\,sed\text{–}surface\,waters}}$ of -0.38 $\pm$ 0.07 ‰), and the oxygenated sites deposited above the chemocline (i.e. shelf and coast) in the Black Sea (average $\Delta^{114/110}\mathrm{Cd}_{\mathrm{core\text{–}top\,sed\text{–}surface\,waters}}$ = -0.30 $\pm$ 0.10 ‰). This light sink of Cd likely represent precipitation and non-quantitative removal of cadmium with trace $\mathrm{H_2S}$ to form cadmium sulphide (CdS) complexes, an interpretation supported by the low Cd concentrations in these sediments.

New experimental results confirm the preferential removal of isotopically light Cd during the precipitation of insoluble CdS complexes. The experiments displayed an enrichment of light Cd isotopes during precipitation of insoluble CdS species, reflecting Rayleigh behaviour with a fractionation factor of 1.00011. These observations indicate the important role of redox cycling in controlling Cd isotopes in marine sediments. Likewise, the experiments suggest that the most significant variability in Cd concentration and isotope compositions in the geological record likely coincide with redox transitions. These findings greatly improve our understanding of an important light sink of Cd in our global oceans, and how the signal of important biological processes in the surface-waters are recorded within the near-surface sediments in modern marine environments.

Contents

1 Introduction **1**

1.1 Expansion of low-oxygen zones in the ocean 1
1.2 Motivation to study trace metals in the ocean 2
1.3 Relationship between Cd and PO_4^{3-} 3
1.4 Isotopic composition of Cd in the modern ocean 5
1.4.1 Primary mechanism for Cd isotopic variations in the surface-waters 5
1.4.2 Potential biological function for Cd in the oceans 6
1.4.3 Cadmium isotopic trends in the intermediate and deep-waters . 7
1.5 Role of particulates on the Cd cycle 7
1.6 Cadmium-sulphide precipitation in the water column 8
1.7 Isotopic mass balance of Cd in the modern ocean 9
1.8 Authigentic enrichment of Cd in the sediments 11
1.9 Motivations for the thesis 12

2 Methodology **15**

2.1 Introduction 15
2.2 Digestion of sediment samples 16
2.3 Digestion of particulate samples 17
2.4 Measurement of trace metal concentrations 19
2.4.1 Analysis of metal concentrations in water, pore-water, and core-top water samples 19
2.4.2 Analysis of metal concentrations in sediment and particulate samples 20
2.5 Ion exchange chromatography procedure 21
2.6 Instrumental mass bias correction 25
2.7 Mass spectrometry procedure 27
2.8 Data reduction 28

3 Cadmium Isotope fractionation during precipitation of cadmium sulphides **31**

3.1 Introduction 32
3.2 Materials and method 35
3.2.1 Stock solution preparations 35

3.2.2 Experimental design for the precipitation experiments 35
3.2.3 Ion exchange chromatography procedure 38
3.2.4 Mass spectrometric methods and data validation 38
3.3 Results 38
3.3.1 Synthetic seawater precipitation experiments under anoxic conditions 38
3.4 Discussion 40
3.4.1 Explanation for the observed fractionation effect 40
3.4.2 Isotope effect influenced by complex speciation at high ionic strength 42
3.4.3 Implications for interpreting Cd isotope fractionation in natural waters and sediments 44
3.5 Conclusion 46

4 Cadmium isotope signatures in seawater, suspended particulates, and near-surface sediments from the South Atlantic at 40°S 47
4.1 Introduction 49
4.2 Sediment sampling procedures 51
4.3 Methods 53
4.4 Results 53
4.4.1 Cd concentrations and isotope variations in the water column . . 53
4.4.2 Cd concentrations and isotope variations in particulates 56
4.4.3 Cd concentrations and isotope compositions of sediment depth profiles 58
4.4.4 Cd concentrations and isotope compositions of water and near-surface sediment samples from the North Atlantic 68
4.5 Discussion 71
4.5.1 Cause of the observed isotope fractionation effect in the water column 71
4.5.2 Cadmium isotopic composition in the global ocean basins . . . 74
4.5.3 Cadmium isotopic composition in the global deep ocean basins 74
4.5.4 Relationship between the sediments and the overlying water column 77
4.5.5 Controls on $\delta^{114/110}\mathrm{Cd}$ in the near-surface sedimentary profile . 86
4.5.6 Cause of the observed isotope variations in the depth profile from the Deep Argentine Basin 91
4.5.7 Cadmium sulphide complexes: Primary geologic sink of Cd in the oceans 94
4.5.8 Correlation between the sedimentary enrichment of Cd with other chalcophile metals 94
4.5.9 Mass balance for Cd isotopes in the ocean 95
4.6 Conclusions 96

5 Cd isotope signatures in waters, pore-waters, and near-surface sediments from the Black Sea 99
5.1 Introduction . . . 100
5.1.1 Study site . . . 101
5.2 Sampling procedures . . . 103
5.2.1 Sediment and water sampling procedures from the Fe-Vici cruise 103
5.2.2 Measurement of nutrients and chemical parameters . . . 105
5.2.3 Sediment sampling procedures from the GEOTRACES, Med-Black Cruise . . . 105
5.3 Methods . . . 106
5.4 Results . . . 106
5.4.1 Cd concentrations and isotope compositions in the water column 106
5.4.2 Cd concentrations and isotope variations across the sediment-water interface . . . 110
5.4.3 Trace metal concentrations in sediment pore-waters . . . 116
5.4.4 Cd concentrations and isotopic compositions in near-surface sediments . . . 119
5.4.5 Interlab Comparison for Station 2 . . . 123
5.5 Discussion . . . 123
5.5.1 Cause of the observed Cd isotope fractionation effect in the water column . . . 123
5.5.2 Redox reaction zones defined by other trace metals in the water column . . . 125
5.5.3 Explanation for the Cd isotopic compositions in the deep-waters 126
5.5.4 Authigenic enrichment of Cd in sediments . . . 126
5.5.5 Source of Cd to the sediment-water interface . . . 127
5.5.6 Quantitative Cd removal from the waters and into the sediments 129
5.5.7 Cadmium-sulphide interactions in the sedimentary depth profile 130
5.6 Conclusions . . . 132

6 Redox cycling control on the cadmium isotope composition of waters, pore-waters, and near-surface sediments in a seasonally anoxic basin (Saanich Inlet, Vancouver) 133
6.1 Introduction . . . 135
6.1.1 Study site . . . 135
6.2 Sediment sampling procedures . . . 138
6.3 Methods . . . 140
6.3.1 Measurement of total organic carbon concentrations . . . 140
6.4 Results . . . 140

6.4.1 Cd concentrations and isotope compositions of water depth profiles 140
6.4.2 Cd concentrations and isotope compositions of sediment depth profiles . . . 142
6.4.3 Comparison of Cd concentrations with other trace metals in the near-surface sediment cores . . . 147
6.4.4 Cd concentrations and isotope compositions of pore-water depth profiles . . . 149
6.5 Discussion . . . 151
6.5.1 Origin of Cd isotopic variation in the Saanich Inlet water column 151
6.5.2 Explanation for the Cd isotopic composition of near-surface sediments . . . 153
6.5.3 Evidence for primary depositional signal record by Cd isotopes 155
6.5.4 A mechanism for the authigenic enrichment of Cd in sediments 155
6.5.5 Co-variance between Cd and select trace metals in sediments . . 157
6.6 Conclusion . . . 159

7 Conclusions and Outlook 161
7.1 Conclusions . . . 161
7.1.1 The precipitation of Cd with H_2S will preferentially remove the light Cd isotopes into the CdS complexes, with an alpha fractionation factor of 1.00005–1.00011 . . . 162
7.1.2 Redox conditions in benthic-waters controls the degree of Cd isotope offset between the near-surface sediments (core-tops) and overlying benthic-waters . . . 165
7.1.3 The majority of the Cd isotopic compositions in the near-surface sediment cores ranged from $\delta^{114/110}Cd$ range of ~-0.4 to 0.4‰ 166
7.1.4 CdS complexes may be unstable under frequently changing redox regimes . . . 167
7.2 Outlook . . . 167
7.3 Closing remarks . . . 168

References 169

1 Introduction

Contents

1.1 Expansion of low-oxygen zones in the ocean 1
1.2 Motivation to study trace metals in the ocean 2
1.3 Relationship between Cd and PO_4^{3-} 3
1.4 Isotopic composition of Cd in the modern ocean 5
1.4.1 Primary mechanism for Cd isotopic variations in the surface-waters 5
1.4.2 Potential biological function for Cd in the oceans 6
1.4.3 Cadmium isotopic trends in the intermediate and deep-waters 7
1.5 Role of particulates on the Cd cycle 7
1.6 Cadmium-sulphide precipitation in the water column 8
1.7 Isotopic mass balance of Cd in the modern ocean 9
1.8 Authigentic enrichment of Cd in the sediments 11
1.9 Motivations for the thesis 12

1.1 Expansion of low-oxygen zones in the ocean

Oxygen deficient zones (ODZs) are regions of the ocean, typically found along continental margins, where nutrient-rich waters upwell to the surface, causing an increase in primary productivity. When the oxygen requirement by marine organisms during bacterial oxidation of organic matter outpaces the replacement of oxygen from the air-surface exchange, it causes low oxygen settings to form in the ocean [1]. These ODZs are

easily identified as low oxygen regions between two oxygen-rich water masses, at the surface and in the deep-waters, resulting from bottom water currents delivering younger, oxygen-rich waters throughout the global oceans [2, 3]. The environmental impact of ODZs is the production of carbon dioxide, nitrous oxides, methane, and other trace gases by marine microbes using alternative oxidizers to respire organic matter, impacting the climate system. This process is intensified by increasing global temperatures, resulting in decreased dissolved oxygen solubility and increased thermal stratification [4, 5]. These changes will cause a shift in the diversity and community structure of marine organisms [2]. It is critical to improve our understanding of these expanding ODZs as our global oceans become warmer and more acidic [6–8].

Trace metals have the potential to help decipher the underlying physical processes that play an essential role in the control of biogeochemical processes in our oceans, including the carbon cycle and marine life [9]. A better understanding of the processes governing trace metal cycling in the modern ocean can improve our projections of the oceans' responses to increasing global ocean warming and acidification. One of the promising trace metals to better understand our oceans and the expansions of ODZs is cadmium. Cadmium has been used as a tracer for nutrient utilization and water mass distribution in ancient oceans [10, 11].

1.2 Motivation to study trace metals in the ocean

Trace metals play a key role in many of the biogeochemical processes that occur in the oceans. For instance, these metals influence the growth and composition of marine phytoplankton communities as active centers in metalloproteins [12–17]. Despite the importance of trace metals to biology, however, the processes controlling their local and global distribution in the oceans are not fully understood. Likewise, the export of trace metals from seawater to sediments and their subsequent burial is scarcely quantified for most trace metal systems. The trace metal of interest in this thesis is cadmium.

Cadmium (Cd) is a transition metal with a single, divalent oxidation state. The first dissolved Cd concentrations in the oceans were reported by Boyle et al. (1976) [18], Bruland et al. (1978) [19], and Martin et al., (1976) [20]. After these pioneering

studies and with the advancements in trace metal-free sample collection protocols and instrumental capabilities, Cd has received significant attention in the oceans. The primary reason is that Cd exhibits a nutrient-like depth profile similar to those of biologically-active major elements like phosphorus [14, 18, 21–24]. The cycling of Cd in the ocean is predominately governed by biological uptake in surface-waters, organic matter decomposition and remineralization in intermediate waters, and global circulation patterns in deep-waters [25–27]. As a result of these processes, dissolved Cd concentrations range from <1 to 500 pmol kg^{-1} [28] in surface-waters and 0.3 to 1 nmol kg^{-1} in the deep Atlantic and Pacific Oceans [29–31]. Cadmium may be a promising tool to better understand past nutrient utilization and ocean mixing, if the processes controlling the biogeochemical cycling of Cd are constrained.

1.3 Relationship between Cd and PO_4^{3-}

The apparent coupling of Cd concentrations in seawater with the macronutrient phosphorus (P) has led to innovative research [10, 11, 18, 32–34]. Cadmium and P undergo biological uptake in surface-waters and regeneration in the intermediate waters at a similar depth. This coupling provides a powerful tool for reconstructing seawater phosphate (PO_4^{3-}) concentrations. The Cd/Ca ratio recorded in planktonic and benthic foraminifera has been used to reconstruct nutrient utilization and water mass distributions in ancient oceans [10, 11, 18, 32–34]. As we learn more about the Cd/ PO_4^{3-} ratio in the oceans, it is important to account for how differences between water mass origins, mixing relationships between water masses, remineralisation rates of organic matter in different basins, and the Cd/PO_4^{3-} ratio of the remineralised biomass have changed over geological history [35].

The relationship between Cd and PO_4^{3-} has been studied for many years in the modern ocean. However, the driving mechanism(s) for the relationship and the reason for deviation from linearity in the waters above 1000 m are not understood. The Cd/ PO_4^{3-} ratio in surface-waters of the ocean is mainly dictated by biological uptake-regeneration processes, while the ratio in deep-waters is attributed to conservative mixing [30]. Globally, the ratio of dissolved Cd to PO_4^{3-} displays minor variability in waters >1,000 m, with the ratio of Cd (nM) to PO_4^{3-} (µM) approximately 0.17–0.27 and 0.29–0.37 for the North

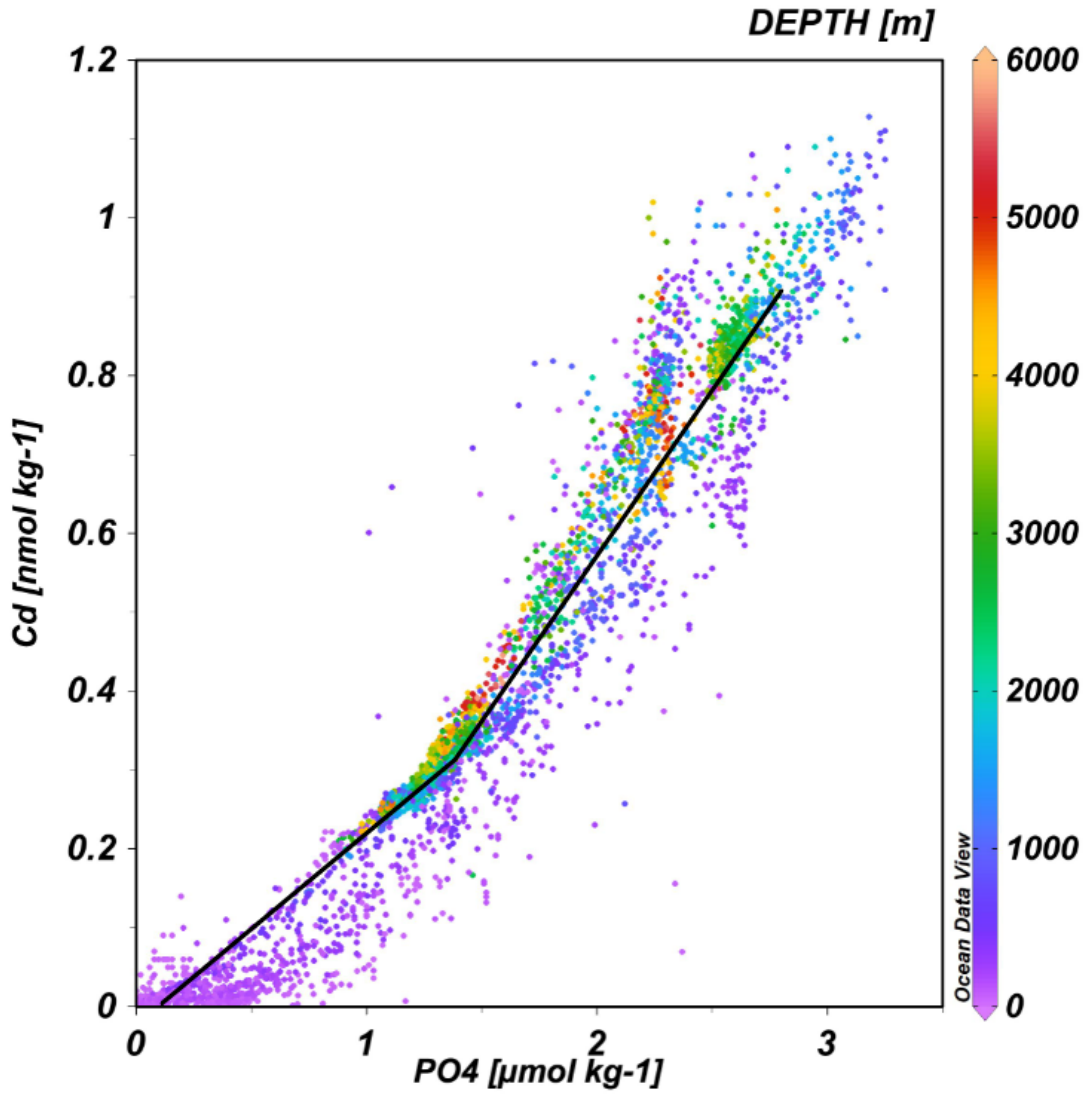


Figure 1.1: Dissolved concentrations of Cd compared to PO_4^{3-} from the GEOTRACES 2017 Intermediate Data product [41]. The 'kink' in the Cd/PO_4^{3-} trend is located at a PO_4^{3-} concentrations of approximately 1.3 µmol kg^{-1}, and it is denoted with a best visual fit, black line.

Atlantic and Indian-Southern-Pacific Oceans [36, 37], respectively. This Cd/ PO_4^{3-} trend may reflect the age of the deep-waters [11, 30]. However, significant variability exists in surface-water ratios, along with a characteristic 'kink' at PO_4^{3-} concentrations of approximately 1.3 µmol kg^{-1} (see Figure 1.1) [37–41].

Several explanations for the 'kink' in the global Cd/PO_4^{3-} dataset have been proposed [10, 37, 38, 42–45]. Previous authors have reported influences from biological uptake [15, 16, 37, 46, 47], preferential remineralization of PO_4^{3-} compared to Cd [32], variations in pCO_2 [48], water masses with different Cd concentrations [49–51], and

variations in the remineralization depth [35, 49, 51–53]. The most recent studies support that the kink is primarily caused by the mixing of water masses with different Cd/PO_4^{3-} ratios [28, 51, 54–56], while the remineralization of Cd and its release is a minor driver [35]. The different water masses have different ratios because the availability of Cd and the degree of Cd uptake by primary producers changes in different ocean basins, particularly between the northern and southern latitude oceans [35]. Solving the Cd/PO_4^{3-} conundrum is a significant step to better deciphering the Cd cycle in the global oceans.

1.4 Isotopic composition of Cd in the modern ocean

The biotic and abiotic processes dictating Cd speciation in waters, sinking particles and sediments may have characteristic isotopic signatures, which may therefore provide a fruitful approach for investigating the present and past biogeochemical cycling of Cd in the oceans [57, 58]. However, the literature on dissolved and particulate Cd concentrations was until recently extremely limited, and even sparser for Cd isotopes. The recent efforts of the GEOTRACES programme to increase the global database on trace metal concentrations and the isotopic compositions of the oceans has therefore been a highly significant advance [9, 28, 41, 59]. The studies emerging from this program have reported surface seawater to be enriched in heavy Cd isotopes (up to +5 ‰), while the global deep oceans (below >1000 m) are homogenous at a dissolved $\delta^{114/110}$Cd value of +0.3 ‰, relative to NIST 3108 [25, 27, 28, 31, 54, 56, 57, 59–63].

1.4.1 Primary mechanism for Cd isotopic variations in the surface-waters

The study of the Cd isotope system provides an additional dimension to understand the biogeochemical cycling of Cd in the oceans, and subsequently to aid in deciphering its potential as a tool to understand ocean conditions in the modern and ancient oceans. The surface-waters are dominated by biological uptake into marine phytoplankton preferentially removing the light Cd isotopes, and subsequently driving the depleted dissolved Cd composition to isotopically heavy values [25, 28, 54, 59]. This mechanism

is best depicted with a Rayleigh isotope fractionation effect, where continual biologically-mediated uptake of the light Cd isotopes causes the remaining dissolved fraction to become increasingly isotopically heavy (up to ~+5 ‰ [28]).

However, the fractionation factor in the surface-waters is variable amongst the different ocean basins, suggesting that the mechanism for isotope fractionation may differ in different ocean basins. This variability may be driven by small differences in the phytoplankton communities' structure and overall local physical, chemical, and biological processes [25]. Previous authors have attributed the deviation from approximately closed-system Rayleigh fractionation to external inputs of aeolian dust [27], dissolved and suspended riverine Cd, seasonal phytoplankton blooms [25, 26], or phytoplankton community compositions, causing Cd behaviour to reflect more of an open-system steady state model [25, 26, 54]. To address this conundrum, Xue et al. (2013) [61] proposed that the worldwide oceans can be divided by two different fractionation factors for high nutrient-low chlorophyll (HNLC) zones (e.g. Pacific, Sub-Arctic Pacific, and Antarctic Oceans) and non-HNLC waters where phytoplankton growth is limited by nutrients (e.g. Atlantic, Pacific, and Indian Oceans). The Cd isotopic signatures of surface-waters in HNLC regions are dictated by biological uptake.

1.4.2 Potential biological function for Cd in the oceans

A current debate exists whether Cd uptake by marine phytoplankton is driven by a biochemical requirement or by non-specific (or inadvertent) uptake into the organisms. It is known that Cd will substitute for zinc (Zn) in the carbonic anhydrase (CA) enzyme. This enzyme catalyzes the conversion of bicarbonate ions and CO_2 and is required for the uptake and fixation of inorganic carbon in diatoms [13, 64, 65]. Cadmium is able to substitute for Zn in specific phytoplankton taxa under low free Zn^{2+} conditions, like the Southern Ocean [13, 66]. This biological flexibility is expected considering the low concentrations of trace metals in the ocean. However, a biological requirement of Cd has been contested by Horner et al. (2013) [67], who reported that the addition of the gene for CA enzyme did not affect the magnitude or direction of Cd isotopic composition in cultured, genetically modified bacteria. This result supports the notion

that the biological uptake of Cd is an unintentional consequence of accumulating other nutrients. In response, the cell has implemented a detoxing mechanism to internally complex Cd [67]. Regardless of whether marine phytoplankton intentionally utilize Cd in CA or accidently accumulate Cd in pursuit of other trace metals, this process imparts an isotopic signature of isotopically 'lighter' Cd in algae and bacteria compared to the growth media [67].

1.4.3 Cadmium isotopic trends in the intermediate and deep-waters

Intermediate oceans waters (between ~200–500 m) show significant Cd isotope variations compared to surface and deep-waters, which likely reflects the remineralization of organic matter [54, 61]. The isotopic signature and levels of dissolved Cd for deep-waters will be governed by global water mixing and the input of Cd released from organic matter during remineralization from the overlying surface-waters [49, 52, 54]. For example, waters in the Subantarctic Ocean is mainly based on mixing seawater end-members of Antarctic Bottom Water (e.g. cold, low salinity, and Cd-rich) and North Atlantic Deep Water (e.g. warm, high salinity, and Cd-poor) components [54]. Despite scatter in the database from local and seasonal processes in surface-waters and/or inputs from external sources [54], the worldwide trend for Cd isotopic composition in deep-waters is relatively homogenous (~0.3 ‰) below ~1000 m due to the remineralization of organic matter and water mixing leading to a long resistance time of approximately 50,000 years [68].

1.5 Role of particulates on the Cd cycle

Bio-available, free-hydrated, cationic species of Cd only compose a very small fraction of the total Cd in surface-waters, with a majority complexed to labile organic or inorganic ligands and sorbed (via adsorption, absorption, and co-precipitation) onto colloidal organic or inorganic particles due to high stability constants [55, 69–74]. Surface chemical models that determine the equilibrium constants of metal-particulate matter relationships have improved our understanding of the interaction between trace metals and surfaces of marine particles, like metal oxides and organic ligands [75]. These models support that scavenging of trace metals by adsorption to organic surfaces is a likely candidate

to explain the range in residence times of some reactive elements [75]. Hunter (1983) expanded the model by accounting for ionization of surface ligand groups [76]. The bio-availability of Cd is regulated by the production of organic ligands, such as phytochelatins, which are metal-binding polypeptides that complex Cd in the cell. This complexation is a possible strategy for cell detoxification in case of increasing Cd concentrations in surface-waters or to extend the residence time of Cd in surface-waters [14, 54, 73, 77, 78]. For example, in the Northeast Pacific, dissolved Cd has been shown to form both strong complexes with organic ligands and weak complexes with inorganic ligands, mainly chloro complexes that are reactive and bio-available in surface-waters [69, 72, 73].

The particulate Cd fraction below ~200 m still accounts for ~35–65% of the total Cd in the water-column [55, 69, 79, 80]. These particulates are dominated by sinking organic material and aqueous Cd species [81–84], with a minor association with Fe-Mn oxides [85] and carbonates with a slight preferences for the light isotopes of Cd [86].

1.6 Cadmium-sulphide precipitation in the water column

Recent studies have reported evidence of cadmium-sulphide (CdS) complexes forming in oxygen deficient zones (ODZs) [28, 56, 80, 87]. As ODZs expand, this fraction of Cd may become an increasing mechanism for Cd removal from the dissolved phase. The conditions required for sulfate-reducing microbes are typically expected to occur after the complete utilization of other electron acceptors in anoxic settings. This view was recently challenged with the discovery of strong evidence to suggest the existence of sulfate-reducing microbes in prominent oxygen deficient zones [1, 88, 89]. Bianchi et al. (2018) proposed that sinking organic aggregates form microenvironments with increased respiration and inhibited O_2 diffusion in low oxygen settings, resulting in anaerobic respiration and the precipitation of chalcophile metals with trace hydrogen sulphide (H_2S), such as Cd to form insoluble cadmium sulphides (CdS) [90]. Prior to these studies, Cd was predicted to only form sulphide species within the water column of restricted, anoxic basins, such as the Cariaco Basin and the Black Sea [91].

A recent study by Janssen et al. (2014) observed particulate Cd in the North Atlantic ODZ with $\delta^{114}Cd$ values as low as -0.02 ‰ at 235 m, correlating with a maximum

concentration of particulate Cd [56]. The evidence for CdS formation in this study is the increased particulate load and a preferential enrichment of light Cd isotopes in the sinking particulates relative to dissolved Cd in the water column. This statement depends on the assumption that the mechanism for CdS precipitation is a removal of the light Cd isotopes. Previous studies support this assumption. Theoretical studies have shown a preferential incorporation of light Cd isotopes into sulphide species [92]. Likewise, direct Cd isotope measurements of a suite of oceanic and continental hydrothermal sulphides by Schmitt et al. (2009) found that the average Cd isotopic composition was 0.24 ± 0.12 ‰ lighter than the average deep-water Cd isotope value (~0.3 ‰) [31, 93]. However, no previous studies have determined the magnitude and degree of isotopic fractionation during precipitation of CdS complexes. This is the driving motivation for the experiments presented in Chapter 3.

While the process of CdS precipitation may be important in some ODZs, it was not observed in the Peru margin ODZ by John et al. (2017), suggesting that oxygen concentrations have to be below a minimum threshold amount to initiate the formation of CdS complexes [94]. Likewise, the stability of these newly-formed CdS precipitates is unknown. Further research is required to decipher the stability of CdS complexes from below the ODZ to the seafloor.

1.7 Isotopic mass balance of Cd in the modern ocean

Previous studies on oceanic waters have produced a wealth of Cd isotope data [25–28, 31, 54, 60, 61, 94–97], yielding many insights into the processes that regulate the vertical and horizontal distribution of Cd and its isotopes in the global ocean. However, critical questions remain about the magnitude and isotopic composition of Cd burial into marine sediments. Firstly, the mechanism(s) by which organically-bound Cd is transported from surface-waters to the seafloor are not well understood. Secondly, the composition of Cd burial in near-surface sediments is not well constrained.

Sedimentary archives may be a promising tool to understand past nutrient and ocean mixing in modern and ancient oceans, as Cd isotopes. A critical first step is to constrain the isotopic mass balance of Cd in the oceans. At a global scale, the Cd cycle is controlled

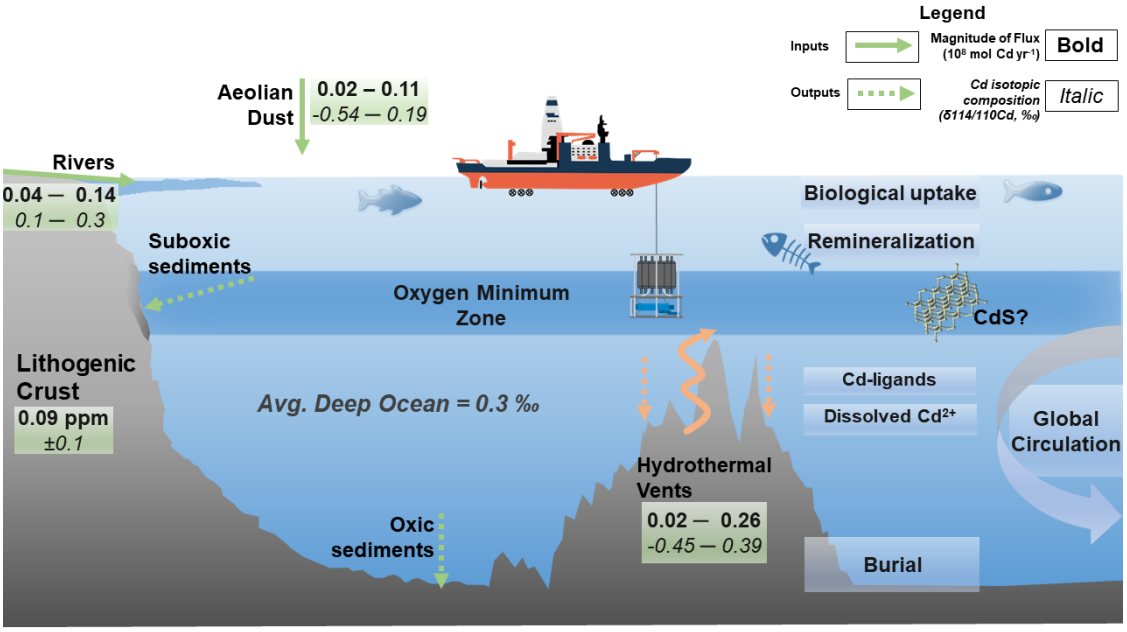


Figure 1.2: A schematic representing the main inputs and outputs of Cd in the ocean (left), along with the internal Cd cycle that influence the distribution of Cd and its isotopes in the ocean (right). The biogeochemical cycling of Cd in the surface-waters is dominated by biological uptake into marine phytoplankton and remineralization at depth. Cadmium in the deep-waters is predominately dissolved Cd^{2+} and Cd that is complexed to sinking refractory ligands (Cd-ligands), along with a minor association with Fe-Mn oxides, carbonates, and possible precipitation of CdS complexes in some ODZs [28, 80, 86, 87, 93, 98–104]. The figure above for the primary inputs and outputs of Cd in the ocean compiles data from previous studies [93, 105–112]

by inputs of Cd to the oceans from three main sources: rivers, dust [93, 110, 112, 113] and hydrothermal vents [93] (see Figure 1.2). The input flux of Cd from hydrothermal vents to seawater varies by ocean basin, and likely only influences the chemistry of ocean waters immediately surrounding each vent system [106, 107, 114]. Consequently, these vents are not considered an important source in this study.

The output fluxes of Cd from seawater into sediments are from abiotic and biotic processes. The biotic process is sinking organic material associated with trace metals from the surface-waters exported to the sediment-water interface. The abiotic processes are likely diffusion of dissolved Cd across the sediment-water interface as free and chloro complexes [27, 31, 60], adsorption of Cd to mineral surfaces including Fe-Mn oxides [85, 104] and carbonates [86], and possibly a component of CdS complexes, if an overlying ODZ exists.

While the principal fluxes of Cd to and from the ocean are mostly understood, the Cd

isotope compositions of these fluxes remain poorly constrained. Currently, the dissolved Cd in the global oceans has a $\delta^{114}\mathrm{Cd}$ value of approximately 0.3 ‰ and the crustal $\delta^{114}\mathrm{Cd}$ value is approximately 0.1 ‰ (relative to NIST SRM 3108) [28, 54, 57]. This means that the weighted sum of isotopic compositions of known sinks is heavier than the weighted sum for known sources, indicating a missing light sink of Cd [56, 93, 112]. The missing sink may be the preferential removal of light Cd isotopes during the precipitation of CdS complexes in the sediments and possibly CdS formation in the water column [28, 56]. This sink would balance the Cd isotopic budget in the global oceans.

1.8 Authigentic enrichment of Cd in the sediments

The enrichment of Cd into sediments is likely driven by its interactions with sulphide species to form insoluble CdS complexes. This hypothesis would mean that the primary burial flux of Cd to sediments is controlled by redox conditions in the overlying bottom-waters and pore-waters [56, 115]. Previous studies suggest that Cd is a redox-sensitive element, similar to Mo, V, and Zn [68, 116–118] and will respond to changing redox conditions, as a result of its strong affinity to form CdS species. In this study, sediments will be distinguished as oxic, suboxic or hypoxic, and anoxic. They are defined as the following: Oxic sediments imply that oxygen is present in the overlying bottom-waters and within the pore-waters and that aerobic bacterial oxidation degrades sinking organic matter within near-surface sediments. Suboxic sediments form where the overlying bottom-waters have oxygen concentrations less than 5 µmol l^{-1} and oxygen penetrates less than 1 cm into the sediments. Trace $\mathrm{H_2S}$ may be present, but limited, to the pore-waters below the sediment-water interface and below the depth of oxic respiration, such that the dominant oxidant is nitrate being used by denitrifying microbes for organic matter decomposition [119, 120]. This provides a scenario where dissolved Cd in the pore-waters could be immobilized with trace amounts of $\mathrm{H_2S}$ to form CdS species during the earliest stages of diagenesis [80, 110, 121]. Anoxic sediments form where oxygen is below detection (less than ~0.1 µmol l^{-1}) with complete consumption of other electron acceptors (e.g. N, Mn, Fe) and does not strictly imply the presence of sulphate-reducing microbes, although this may be a feature [120]. Examples of these

locations are the Black Sea and Cariaco Basin, where sulfate-reducing microbes are the primary bacteria in the deep-waters and pore-waters, and CdS formation is the dominant removal mechanism from the water column and into the sediments [68, 118, 122]. The significant coverage of the oceans compared to restricted anoxic basins, such as the Black Sea, Cariaco Basin, and the Saanich Inlet suggests that the primary removal of Cd occurs into open-marine suboxic sediments [68, 110, 113, 122]. The CdS complexes have a high stability constant and as such are unlikely to dissociate once formed in low oxygen sediments [123, 124], so the exchange of Cd with anoxic pore fluids during the earliest stages of diagenesis is probably not occurring in the sediments [121]. While studies have worked to understand the distribution of Cd in sedimentary phases, the question of how Cd isotopes are altered during the deposition and early diagenesis of CdS-containing phases is currently unstudied.

1.9 Motivations for the thesis

Marine sediments represent an important physical interface with the oceans. However, some fundamental questions remain unanswered:

- What is the relationship between Cd in seafloor sediments and the overlying water column?
- What is the concentration and isotopic composition of the output flux of Cd to seafloor sediments?
- What are the processes that control the Cd concentration and isotope composition of marine sediments?
- What is the relationship between Cd and sulphide, and the importance of this relationship on the global Cd cycle?
- What is the effect of remineralization and diagenesis on the fidelity of biogeochemical signals recorded by Cd in ocean sediments?

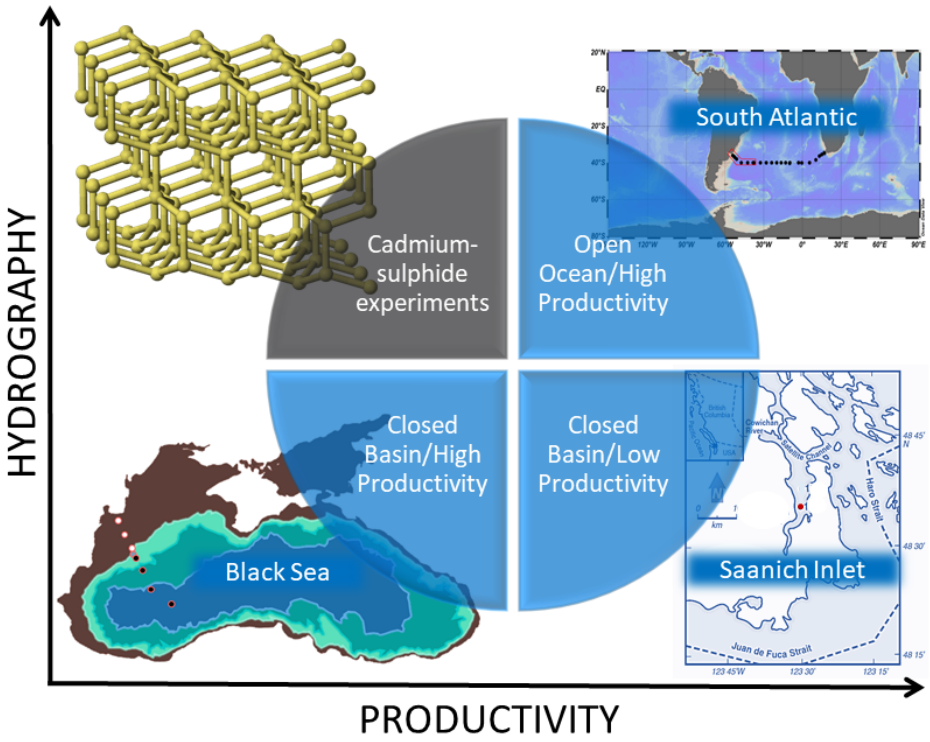


Figure 1.3: A schematic depiction of the studied sites and laboratory experiments (Chapter 3) that are presented this thesis, with a focus on end-member locations for hydrography and productivity. The studies sites include the South Atlantic at 40°S (Chapter 4), the Black Sea (Chapter 5), and Saanich Inlet (Chapter 6).

Answering these key questions is critical before Cd isotopes can be used as a tracer for past ocean cycling of this metal, and potentially as a tracer of past ocean chemistry and nutrients. These questions can be addressed through a systematic investigation of the Cd isotope variations found in modern sedimentary environments and overlying marine deep-waters. Given the potential impact of CdS complexes on the paleo-record, undertaking such a study in low oxygen, modern marine basins is especially important. To address the proposed questions, this thesis presents the Cd isotopic compositions and concentrations of waters, sinking particles, pore-waters, and surface sediments accumulating under a range of primary productivity and redox conditions in the South Atlantic at 40°S, Saanich Inlet, and the Black Sea (Figure 1.3). The sample sites represent settings that are characterised by differing levels of dissolved oxygen, in order to test the influence of CdS formation on the bulk sediment isotopic composition. The South

Atlantic at 40°S represents an open ocean settings with high primary productivity within an ocean basin known for low concentrations of critical micronutrients (Chapter 4). The Black Sea depicts a restricted, permanently anoxic basin with a sharp chemocline and significantly lower trace metal concentrations that the open ocean (Chapter 5). Saanich inlet is a seasonally anoxic basin characterized by vertical variability in the chemocline depth and high trace metal concentrations in the basin seawater (Chapter 6). These field studies are supported by experiments to precipitate CdS under controlled laboratory conditions, in order to constrain the fractionation factor between dissolved Cd and CdS (Chapter 3). An improved mechanistic understanding of the supply and enrichment of Cd to sediments in different redox settings and ocean basins will have an important bearing on our understanding of the biogeochemical cycle of Cd, and on our ability to apply Cd geochemistry to the understanding of ancient environments and ocean chemistry.

2
Methodology

Contents

2.1 Introduction 15
2.2 Digestion of sediment samples 16
2.3 Digestion of particulate samples 17
2.4 Measurement of trace metal concentrations 19
2.4.1 Analysis of metal concentrations in water, pore-water, and core-top water samples 19
2.4.2 Analysis of metal concentrations in sediment and particulate samples 20
2.5 Ion exchange chromatography procedure 21
2.6 Instrumental mass bias correction 25
2.7 Mass spectrometry procedure 27
2.8 Data reduction 28

2.1 Introduction

The natural concentration of cadmium (Cd) in the oceans is extremely low, down to <1 pmol kg^{-1} in surface-waters [28] and down to 0.3 nmol kg^{-1} in the deep-waters [29–31]. These low Cd concentrations requires that sample collection protocols, laboratory procedures, and instrument analyses are extremely careful to ensure minimal to negligible contamination of water, particulate, porewater, and sediment samples. All of the natural samples presented in this thesis were either collected on a GEOTRACES

cruise, on a cruise designated as a GEOTRACES process study, or sampled following GEOTRACES protocols for sample collection, handling, and storage. GEOTRACES is an international study to better constrain the biogeochemical cycles and mass balance of trace metals and their isotopes in the modern oceans [9]. GEOTRACES protocols aim to optimise all steps of the sampling process to retrieve contamination-free seawater samples. Once the samples are delivered to the lab, they require the same level of care during preparation and measurement, in order to avoid outside contamination. This aids in reporting accurate results that are representative of the sampling locations despite low trace metal concentrations.

This chapter details the laboratory and instrumental procedures employed for Cd concentration and isotopic composition analyses from a suite of sediment, particulate, pore-water, and water samples. The site descriptions and sample collection procedures for each of the studied basins are detailed in the following chapters. All of the collected samples were prepared for measurement of Cd concentrations and isotopic compositions in a Class 10 laminar flow workstation within a Class 1000 clean lab suite at the University of Oxford. The acids used in this study were purified by sub-boiling distillation in quartz glass stills or purchased as trace metal grade, as was the case for perchloric acid and sulphuric acid (sourced from Fisher Scientific).

2.2 Digestion of sediment samples

The digestion of near-surface sediments was completed following one of two procedures. A portion of the sediment samples from the GEOTRACES, South Atlantic cruise at 40°S were digested according to the method by Homoky et al. (2013) for trace metal analyses[125]. In this method, 6 mL of Aqua Regia (3:1, HCl:HNO_3) was added to between 100 to 300 mg of dried and homogenized sediments in acid-cleaned, Teflon vials in order to initiate the oxidation of organics for each sample. The samples were capped and heated at 60°C for a minimum of 18 hours. The partially digested samples were dried down to incipient dryness and a mixture of 3 mL of hydrofluoric acid (HF) followed by 2.25 mL of perchloric acid ($HClO_4$) was added, capped, and heated to 150°C for a minimum of 12 hours to promote the dissolution of silicates and intensify the

breakdown of organic content. An additional 2 mL of $HClO_4$ was added to break down any remaining organics and subsequently evaporated down at 180°C. A cycle of adding 2 mL of concentrated nitric acid (HNO_3), refluxing, and drying down was completed three times to ensure the elimination of $HClO_4$ in the samples before transferring to 3 M HNO_3 to analyse for Cd concentrations on a Thermo ELEMENT 2 ICPMS.

A separate portion of the sediment samples were digested following a slightly different methodology, using slight modifications in order to accommodate the digestion of large samples (up to ~2 g of sediment). At times, significant amounts of sample were required to have adequate Cd concentration for multiple replicates on the instrument. This procedure involved weighing out ~0.3 to 2 g of dried and homogenized sediments into acid-cleaned Teflon vials or jars. Then, adding 4 to 12 mL of inverse Aqua Regia (3:1, HNO_3:HCl), depending on the sample mass, and heated in a sealed Teflon container at 150°C for between 48 hours to one week. After this time, the large samples in jars (up to ~2 g) were placed inside an oven at 120°C to 130°C for one to two weeks. They were removed from the oven once digestion was complete, as evidenced by the presence of pale yellow leached silicates. Samples were dried to incipient dryness, before 3 mL of HNO_3 and 1 mL of HF were added to dissolve any silicates in the samples. The samples were left closed overnight, then dried and redissolved in 3 M HNO_3 in preparation for measurement of major and minor elemental concentrations on a Perkin Elmer NexION 350D ICP-MS at the University of Oxford.

2.3 Digestion of particulate samples

The particulate samples were collected by filtering very large quantities of seawater (~1000 L) on polyethersulfone (PES) filters. The PES filters required complete digestion to ensure no loss of Cd and no potential isotope fractionation from using a leaching procedure. The method development stage for these filters was extremely difficult given the chemical resistance and large mass of the PES filters (a quarter of a filter with a total 293 mm diameter) that was required to be digested for trace metal analysis. The few published methods, along with modified methods of the limited literature were tested

with mixed success. The following procedures exhibited a measurable degree of success but failed to completely dissolve the required amount of filter material:

- A mixture of concentrated HF and perchloric acid ($HClO_4$) [126].
- A microwave digestion method using a 1:1 ratio of HNO_3 to hydrochloric acid (HCl) and boric acid [127].
- A 3:1 ratio of sulfuric acid to hydrogen peroxide [128]. The method of Ohnemus et al. (2014) successfully digested the filter material; however, the amount of sulfuric acid required for the digestion required an extremely long time to dry down the sample (approximately 3 weeks). This is a dangerously long time for a vial to be left open to possible contamination, even in a clean fume hood.

Subsequently, I developed additional methods that all partially digested the PES filters. These methods included several microwave digestion procedures such as a 3:1 ratio of HNO_3 and HF, and inverse aqua regia (3:1 ratio of HNO_3 and HCl); and a method using solely dichloromethane (DCM).

I developed two methods that successful digested the large size of PES filters with low blanks:

- The first method involved ashing the samples with an electric Bunsen burner with quartz ceramic crucibles. The ash was transferred to an acid-cleaned Teflon vial and subsequently digested according to the method used for the sediment samples using inverse Aqua Regia.
- The second method employed the use of a HPA-S High Pressure Asher. This high pressure digestion method involved cutting each filter into 4 pieces, adding each slice to one pre-cleaned quartz vial, adding 10 mL of concentrated HNO_3, attaching a quartz lid with Teflon tape, and securing a carousel with all the samples into the HPA-S. The high pressure asher was heated for two cycles at 250°C for one hour and 320°C for 2 hours. The digested particulate samples were recombined, dried down, and subsequently digested according to the method used for the sediments

using inverse Aqua Regia. The digested particulate samples were visually clear of any solids after the digestion. However, to be sure of complete dissolution, the samples were also treated with the digestion procedure for sediments using inverse Aqua Regia. The Cd blanks for both methods on pre-cleaned, blank PES filters were near the detection limit of the ICP-MS. The main concern with the ashing method, using an electric Bunsen burner, is the inability to monitor the exact temperature inside the ceramic crucible during the heating stage, and Cd has a lower volatility point compared to other trace metals [129]. For this reason, the latter method was preferred and used for the digestion of the PES filters.

2.4 Measurement of trace metal concentrations

2.4.1 Analysis of metal concentrations in water, pore-water, and core-top water samples

The water, pore-water, and core-top water samples did not require a digestion procedure. The samples were filtered and acidified in preparation for the measurement of a range of major and minor elemental concentrations on a Perkin Elmer NexION 350D ICP-MS. Several challenges were overcome to measure the waters, pore-waters, and core-top waters on the ICP-MS. These included their high total dissolved solids (TDS) concentrations (up to a similar value as open ocean seawater at 35,000 ppm) and their low Cd concentration. The conventional procedure to prepare samples with a high TDS is to dilute the sample until the concentration is below 200 ppm to avoid the precipitation of large amounts of matrix material onto the interface of the ICP-MS [130]. This procedure is critical as a high amount of precipitate will cause contamination and instrumental instability, leading to high uncertainties and poor reproducibility. However, the already low concentration of Cd in the pore-waters means dilution is not an easily used method, since dilution may result in values below detection limits. Instead, a flow injection technique called FIAS (Flow Injection Automation System) was used. This approach involves the uptake of a small volume (less than 1 µL) of the undiluted porewater solution into the ICP-MS. The measurements are then completed using the rapid scanning capabilities of the Perkin Elmer NexION 350D ICP-MS, using a time series interpolation to capture the trace

elements from each injection. The reported value is an average of nine injections. This procedure allows for low uptake volumes and accurate measurements, while limiting the amount of matrix material introduced to the ICP interface [130].

2.4.2 Analysis of metal concentrations in sediment and particulate samples

A suite of major and minor elements for the solid phase component of the sediments was determined using an ELEMENT 2 ICP-MS or a Perkin Elmer NexION 350D ICP-MS at the University of Oxford. The concentrations were determined by calibration to a series of external standards. The majority of the sediment samples from the South Atlantic dataset and all of the samples from the other locations were measured on the Perkin Elmer NexION 350D ICP-MS. Three different modes for collision reaction cells were used during the analysis to minimize spectral interferences on the IPC-MS. The elements measured in standard mode included uranium (U), tin (Sn), and thorium (Th). The elements measured in kinetic energy discrimination mode (KED) encompassed Cd, molybdenum (Mo), vanadium (V), manganese (Mn), iron (Fe), aluminium (Al), chromium (Cr), cobalt (Co), nickel (Ni), copper (Cu), zinc (Zn), strontium (Sr), barium (Ba), and magnesium (Mg), and in dynamic reactive cell mode included calcium (Ca). Ammonia was used as a reactive cell gas for the measurement of Cd to increase sensitivity. The detection limit on the ICP-MS for the Cd samples varied from 5 to 10ppt, depending on the instrument session. The instrument detection limit for the other measured elements is 1ppt for U, 5ppt for Sn and Co, 10ppt for Sr and V, 15ppt for Mo and Cu, 20ppt for Th and Cr, 25ppt for Ca, Zn, and Ni, 50ppt for Mg, 70ppt for Ba, 150ppt for Mn and Al, and 100 to 750ppt for Fe (high variability). The digestion method was validated by measuring the USGS Devonian Shale (SDO-1) standard. All the reported elements were between 92% (Zn) and 110% (Fe) of the published elemental concentrations. An analytical blank and yield check was completed for all procedures related to sediment, particulate, pore-water, and water samples to confirm the quality of the methods and confidence in the reported results. The blanks were always near the detection limit on the ICP-MS for the above methods.

The Cd concentration data from the ICP-MS was used to spike each sample with an aliquot of a ^{111}Cd and ^{113}Cd double spike solution. The double spike used in this study was mixed and calibrated by Horner (2012) [131]. The optimal spike:sample ratio for the samples was ~1. Each sample was allowed to equilibrate at a low temperature (~90°C) overnight (at least 12 hours).

2.5 Ion exchange chromatography procedure

The measurement of Cd isotopic compositions of natural samples requires the completion of a column chromatography procedure to purify Cd from the surrounding matrix, particularly for the elements that represent spectral interferences. The downside of a wealth of Cd isotopes is a significant number of spectral interferences from elements like Sn, indium (In), and palladium (Pd) (see Figure 2.1). These complications require a Cd purification routine with good separation and yields. While the use of double spike technique does make it possible to accurately correct for poor yields, a large portion of the natural samples presented in this thesis suffer from low concentrations. Thus, it is ideal to use a separation procedure with near-complete yields.

The digested sediment, particulate, and pore-water samples were purified by a two-stage column procedure to isolate Cd from the matrix and prevent spectral interferences during isotopic analysis. For the first stage, all spiked samples were loaded onto 2 mL of AG 1-X8 resin using a procedure modified from Pearce et al. (2009), Wombacher et al. (2003) and Dickson et al. (2016) [133–135]. This two-stage column chemistry is detailed in Table 2.1 and the results shown graphically in Figure 2.2. The elution was dried down and converted to 8 M HCl in preparation for the second stage using a method modified from Wombacher et al. (2003) [134]. The sample was loaded onto 200 µL of Eichrom TRU extraction chromatographic resin in 8 M HCl. The Cd was eluted with 1.5 mL of 8 M HCl, while the matrix remained complexed to the resin (see Table 2.1 and Figure 2.3). In preparation for isotopic analysis, the samples were dried down and redissolved in 1 mL of 2 % HNO_3.

A three-column procedure was used to remove surrounding matrix from Cd in seawater. The seawater was spiked with an aliquot of ^{111}Cd and ^{113}Cd double spike

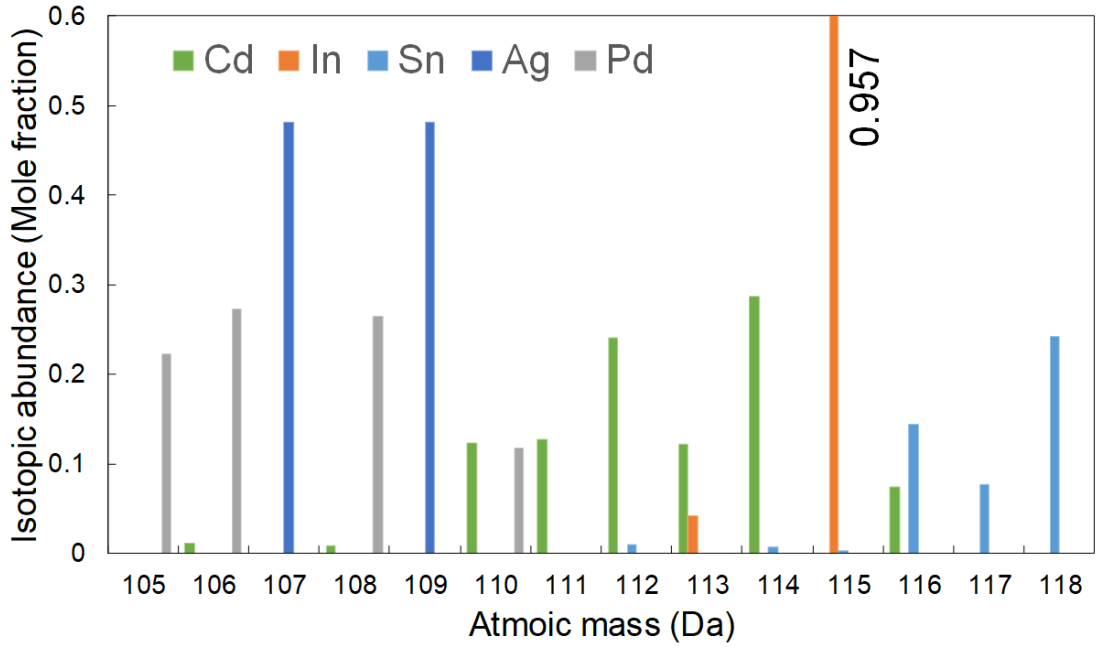


Figure 2.1: Cadmium mass spectrum in nature with the relative fraction of other elements within the range of Cd [132], including spectral interferences from Pd (masses 106, 108, and 110), In (mass 113), and Sn (masses 112, 114, 116).

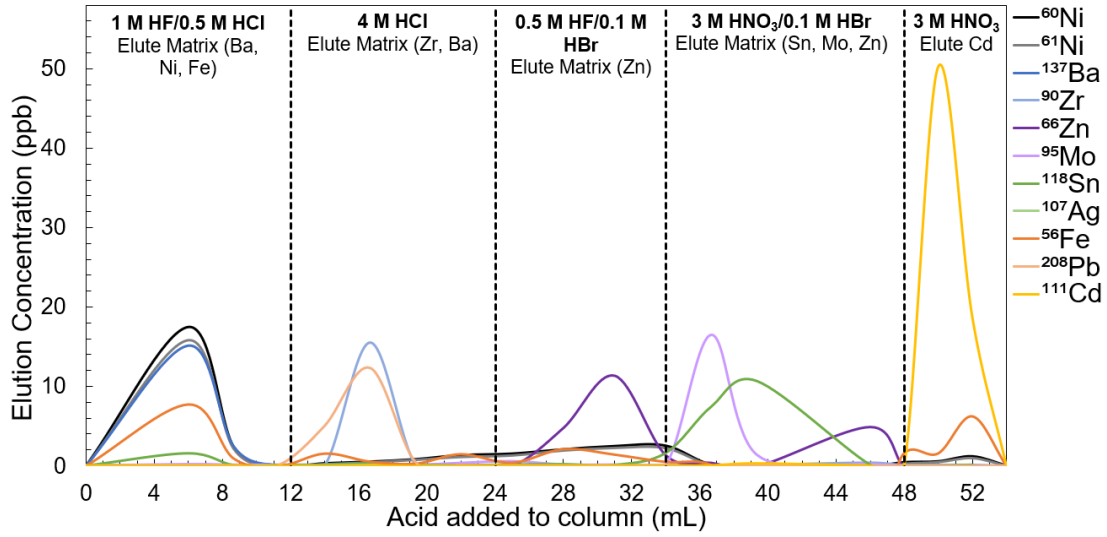


Figure 2.2: Cadmium column calibration for Biorad AG-1X8 resin with elution samples taken every 2 mL.

Table 2.1: Cd chromatography column chemistry for sediment, particulate, and pore-water samples

First stage columns		
Biorad AG 1 - X8 anion exchange resin (dry mesh: 200-400)		
2 mL resin in polypropylene columns		
Purpose	Quantity (mL)	Eluent
Resin Cleaning	10	7.5 M HNO_3
	5	H_2O
	10	6 M HCl
	10	1 M HCl
Resin Conditioning	6	1 M HF/0.5 M HCl
Sample Loading	6	1 M HF/0.5 M HCl
Matrix elution	6	1 M HF/0.5 M HCl
Elution of Zr, Ba	8	4 M HCl
Elution of Zn	8	0.5 M HF/0.1 M HBr
Elution of Sn, Mo, Zn	8	3 M HNO_3/0.1 M HBr
Elution of Cd	7	3 M HNO_3

Second stage columns		
TrisKem TRU Spec resin (dry mesh: 50-100 µm particles)		
0.2 mL resin in Teflon columns		
Purpose	Quantity (mL)	Eluent
Cleaning	2	0.32 M HNO_3
	0.2	H_2O
	2	8 M HCl
Conditioning	1	8 M HCl
Loading/elution of Cd	0.2	8 M HCl
Elution of Cd	1.5	8 M HCl

solution to achieve an optimal sample:spike ratio of ~1 prior to being loaded onto the column. The first Cd purification column followed a method developed by Wombacher et al. (2003) [134], and subsequently used successfully by Ripperger and Rehkämper (2007) [58] to isolate Cd from seawater. The first stage of the Cd purification scheme involved loading each spiked sample onto 1.5 mL of AG 1-X8 resin. The amount of seawater that was loaded on the cleaned resin varied between 1000 mL to 2000 mL, depending on their Cd concentration. This step required 3 to 6 days of loading the water sample into the large quartz column with a 200 mL reservoir. The other two column steps are the same as the procedure for the sediment samples detailed in Table 2.2.

Table 2.2: Cd chromatography column chemistry for seawater samples (adapted from Ripperger and Rehkämper (2007) for the first column stage [58])

First stage columns		
Biorad AG 1 - X8 anion exchange resin (dry mesh: 100-200)		
1.5 mL resin in large quartz columns		
Purpose	Quantity (mL)	Eluent
Resin Cleaning	11	2 M HNO_3
	0.5	H_2O
	25	6 M HCl
Resin Conditioning	11	0.7 M HCl
Sample Loading	Variable	Up to 2 L acidified seawater
Matrix elution	23	0.7 M HCl
	10	1 M HCl
	10	2 M HCl
	10	8 M HCl
	10	0.5 M HNO_3/0.1 M HBr
	2	2 M HNO_3
Elution of Cd	10	2 M HNO_3

Second stage columns		
Biorad AG 1 - X8 anion exchange resin (dry mesh: 200-400)		
2 mL resin in polypropylene columns		
Purpose	Quantity (mL)	Eluent
Resin Cleaning	10	7.5 M HNO_3
	5	H_2O
	10	6 M HCl
	10	1 M HCl
Resin Conditioning	6	1 M HF/0.5 M HCl
Sample Loading	6	1 M HF/0.5 M HCl
Matrix elution	6	1 M HF/0.5 M HCl
Elution of Zr, Ba	8	4 M HCl
Elution of Zn	8	0.5 M HF/0.1 M HBr
Elution of Sn, Mo, Zn	8	3 M HNO_3/0.1 M HBr
Elution of Cd	7	3 M HNO_3

Third stage columns		
TrisKem TRU Spec resin (dry mesh: 50-100 µm particles)		
0.2 mL resin in Teflon columns		
Purpose	Quantity (mL)	Eluent
Cleaning	2	0.32 M HNO_3
	0.2	H_2O
	2	8 M HCl
Conditioning	1	8 M HCl
Loading/elution of Cd	0.2	8 M HCl
Elution of Cd	1.5	8 M HCl

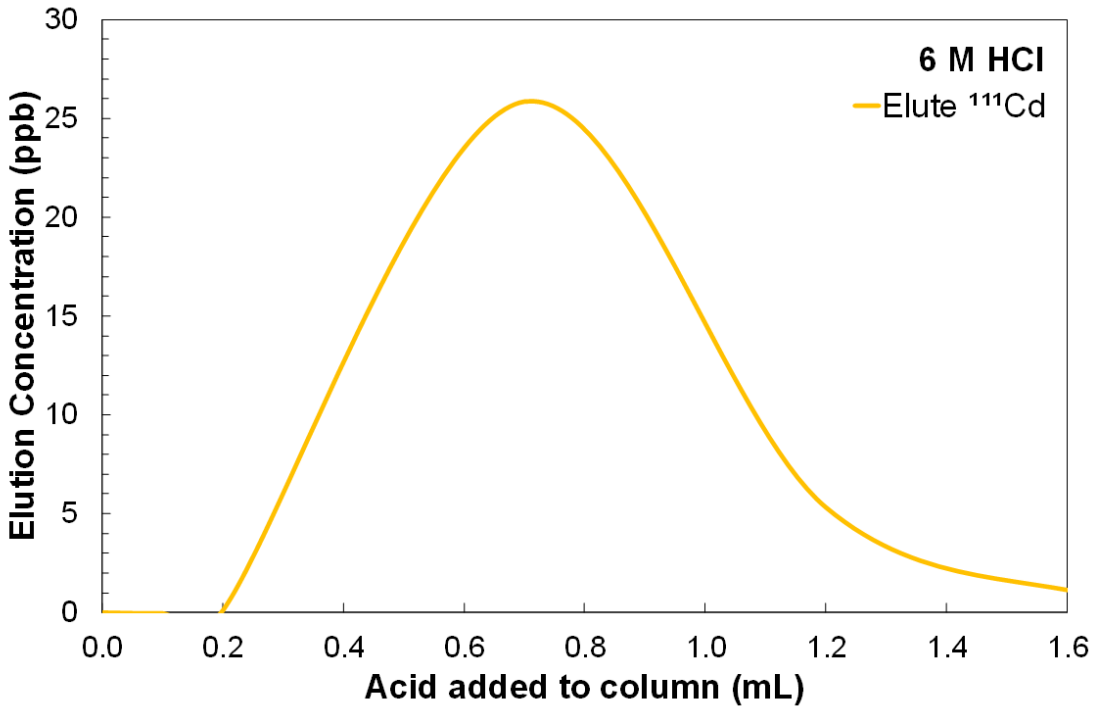


Figure 2.3: Cadmium column calibration for TrisKem TRU Spec resin with elution samples taken every 0.2 mL.

2.6 Instrumental mass bias correction

The use of a multi-collector inductively coupled mass spectrometer (MC-ICP-MS) was used for determination of Cd isotopic compositions. The MC-ICP-MS, similar to TIMS, is affected by instrumental mass bias. However, unlike TIMS, mass fractionation is independent of time, and subsequently a correction can be applied to determine the natural fractionation in the sample [136, 137]. The other benefits compared to TIMS include rapid data acquisition and the ability to measure the samples as a solution. These are significant benefits for the large number of samples processed in this thesis.

The use of a MC-ICP-MS necessitates a protocol to correct for instrument mass bias. Three primary approaches have been used to resolve the natural fractionation of stable isotopes from the artificial fractionation caused by the instrument during isotope measurements. These techniques include standard-sample bracketing [138], elemental doping [137, 139], and double spiking [140]. The principles, advantages, and disadvantages of each will be discussed below.

The approach of standard-sample bracketing involves bracketing each sample on either side with a standard during the session on the instrument [138]. The assumption is that the instrument will fractionate the sample to the same degree as the bracketing standards. However, this assumption may break down in the case of any differences between the standard and sample in terms of trace impurities, acid concentration, or solute concentration. This method when combined with double spike, discussed below, is a useful tool to produce a robust dataset. Another technique for mass bias correction is elemental doping [136, 137, 140–143]. The theory behind this approach is that elements with a similar mass will be fractionated to a similar degree by the instrument and thus may be used to calculate a mass bias correction for individual samples. This approach has been applied to several pairing of elements including Zn and Cu [139], Tl and Pb [137], along with others. For Cd, this approach would entail taking a known amount of Ag or Sb, and adding it to the sample and standard prior to the analysis. The resulting instrumental fractionation on Ag or Sb would be used to apply a correction to Cd. This approach has been successfully used by Wombacher et al. (2003) [134], but has some drawbacks. This technique does not provide concentration data, requires good chromatography yields, and requires an increased mass range on the instrument, causing a number of isobaric interferences and decreasing the number of Cd isotopes that can be simultaneously monitored.

The approach that provides the most robust analysis of Cd isotopes in natural samples is correcting instrumental mass bias with a double spike technique. The double spike equation involves a three-dimensional geometric scheme where each of the axes refers to an isotope pair [144]. Consequently, this technique requires the measured element to have at least four stable isotopes. Traditionally, two purified isotopes of the element are sourced, mixed, and calibrated on an instrument to establish a known isotopic ratio for the double spike solution. This approach is ideally combined with samples bracketed by standards with the same sample:spike ratio. The measurement of frequent standards is particularly important if the mass-dependent, instrumental fractionation varies significantly over time. This technique is a robust method to directly measure the isotopic composition of the sample, without relying on the assumption that the

instrument will be fractionating the element of interest to the same extent as an external element (such as Ag or Sb for Cd) or a bracketing standard. Also, this approach allows for the use of an optimal purification scheme over a procedure with high yields but less satisfactory separation from spectral interferences. The double spike solution is added prior to element purification procedures, and subsequently the double spike will correct for the fractionation caused by the instrument during isotope measurements and chemical purification procedures. The other significant benefits of the double spike technique are the output of highly accurate Cd concentration data and a high signal to noise ratio. Cadmium is found at very low concentrations within natural samples. Double spiking technique provides a scheme to increase the signal to noise ratio, as the sample mixtures has both natural and enriched isotopes of the element of interest. The Cd isotopic compositions reported in this thesis were measured with the instrumental mass bias corrected by using a $^{111}\mathrm{Cd}$ and $^{113}\mathrm{Cd}$ double spike solution that was previously mixed and calibrated by Horner (2012) at the University of Oxford [131]. Cadmium has eight stable isotopes that range in abundance from less than 1.5% ($^{106}\mathrm{Cd}$ and $^{108}\mathrm{Cd}$) to ~25% ($^{112}\mathrm{Cd}$ and $^{114}\mathrm{Cd}$) [132]. This provides an ideal element to apply the double spike approach for correcting instrumental fractionation in the sample. A measured amount of the double spike solution is added to each sample, following an ideal sample:spike ratio (~1). Given the mass spectrum range on the MC-ICP-MS, it is possible to measure $^{110}\mathrm{Cd}$, $^{111}\mathrm{Cd}$, $^{112}\mathrm{Cd}$, $^{113}\mathrm{Cd}$, and $^{114}\mathrm{Cd}$, while still monitoring interferences from $^{115}\mathrm{In}$, $^{115}\mathrm{Sn}$, and $^{117}\mathrm{Sn}$ in the same analysis run. While $^{113}\mathrm{Cd}$ has an interference with Sn, $^{111}\mathrm{Cd}$ isotope has no isobaric interferences.

2.7 Mass spectrometry procedure

The Cd isotopic analyses for the samples were completed on a Nu Instruments Nu Plasma multi-collector HR-ICP-MS at the University of Oxford in low resolution mode. An Elemental Scientific PFA MicroFlow Nebulizer was used for sample introduction with a Nu Instruments DSN-100 desolvation system. The sample and standard concentrations were chosen to ensure as high signal-to-noise ratio as was possible with a minimum of 0.1 V on $^{110}\mathrm{Cd}$ to generate SE below 0.1 within the 40 integration routine on the reported

$\delta^{114/110}\mathrm{Cd}$ isotope ratio. Signals were collected simultaneously for $^{110}\mathrm{Cd}$, $^{111}\mathrm{Cd}$, $^{112}\mathrm{Cd}$, $^{113}\mathrm{Cd}$, $^{114}\mathrm{Cd}$, along with $^{115}\mathrm{In}$ and $^{117}\mathrm{Sn}$ to correct for isobaric interferences. Signal voltages were recorded over 40 cycles of 10 s integration time. All voltages were corrected for background by subtracting the voltages measured on an acid blank before each measurement. Each sample was measured two to four times, and the mean value was taken for the samples with acceptable error. This value is presented in the thesis.

2.8 Data reduction

The spike-sample mixtures were deconvolved off-line using an excel-based routine, and isotopic compositions were corrected to Cd NIST SRM 3108 by normalizing to in-run bracketing standards to correct for mass discrimination. Cadmium NIST SRM 3108 (Lot# 060531, $\delta^{114/110}\mathrm{Cd}_{\mathrm{NIST}} \equiv 0$), double-spiked to match the concentrations and sample-spike ratios of the water, particulate, and sediment samples, bracketed every one or two sample analyses. The long-term precision on the standard over the course of all the studies in this thesis was ±0.08‰ (2 SE). The final Cd isotopic compositions are reported in delta notation relative to NIST SRM 3108 [111] using the following equation:

$$\delta^{114/110}\mathrm{Cd} = \left(\frac{^{114}\mathrm{Cd}/^{110}\mathrm{Cd}_{\mathrm{sample}}}{^{114}\mathrm{Cd}/^{110}\mathrm{Cd}_{\mathrm{standard}}} - 1 \right) \mathrm{x}\,1000$$

expressed in ‰. The final 2 SE of the reported isotope values are calculated by propagating the 2 SE counting statistics with the 2 SE of the two bracketing NIST standards. An in-house standard 'OXCAD' (Alfa Aesar Specpure Cd concentration standard, Lot# 81-081192A) was measured repeatedly in each analysis session to assess instrument stability and long-term reproducibility. The OXCAD relative to the Cd SRM NIST 3108 measured as -0.95 ± 0.09‰ ($\delta^{114/110}\mathrm{Cd}$; n = 139, 2 SE) over the course of all the studies. The deconvolution steps are described in Siebert et al. (2001) and are iterated in excel until a final, mass bias corrected $\delta^{114/110}\mathrm{Cd}$ is obtained [140]. Ideally, the column chromatography procedure reduces the amount of Sn to a trace amount, if remaining at all. To correct for any Sn that may be remaining in the sample, the deconvolution routine was run twice. In the first iteration, a mass fractionation factor was calculated from the $^{113}\mathrm{Cd}/^{111}\mathrm{Cd}$ ratio. This factor was used to correct the measured

$^{112}\mathrm{Cd}$, $^{114}\mathrm{Cd}$, and $^{115}\mathrm{In}$ signal voltages for Sn interference by using the monitored $^{117}\mathrm{Sn}$ signal. The deconvolution routine was subsequently iterated a second time to obtain final corrected isotope ratios. The $^{115}\mathrm{In}$ isotope was used to correct for $^{113}\mathrm{In}$ on $^{113}\mathrm{Cd}$. However, the ln correction was not applied in the deconvolution routine, as the measured signal intensities for In were never greater than the measured acid backgrounds. Many of the measured samples had sample:spike ratios that deviated from the ideal sample:spike of ~1. The cause of these deviations were mostly due to the Cd concentrations from the ICP-MS that were at times nearly double the concentration calculated by isotope dilution. The likely cause of the discrepancy is molybdenum oxides interfering with the measured $^{111}\mathrm{Cd}$. Samples that were over-spiked relative to the ideal sample-spike ratio leads to changes in the isotopic composition of the correcting standard. This deviation is most likely caused by the shift from the ideal calibration due to an increase in the minor impurities in the double spike solution [60, 131]. To counteract this problem, samples that exhibited deviation from optimal spike:sample ratios by more than 0.15 $‰$ were bracketed with standards with similar spike:sample ratios and Cd concentrations [58]. Previous work has confirmed that this technique produces accurate results [58].

3

Cadmium Isotope fractionation during precipitation of cadmium sulphides

Contents

3.1 Introduction 32
3.2 Materials and method 35
3.2.1 Stock solution preparations 35
3.2.2 Experimental design for the precipitation experiments 35
3.2.3 Ion exchange chromatography procedure 38
3.2.4 Mass spectrometric methods and data validation 38
3.3 Results 38
3.3.1 Synthetic seawater precipitation experiments under anoxic conditions 38
3.4 Discussion 40
3.4.1 Explanation for the observed fractionation effect 40
3.4.2 Isotope effect influenced by complex speciation at high ionic strength 42
3.4.3 Implications for interpreting Cd isotope fractionation in natural waters and sediments 44
3.5 Conclusion 46

Abstract

The dissolved cadmium (Cd) in the global deep ocean has a $\delta^{114}\mathrm{Cd}$ of approximately 0.3 ‰ and the lithogenic crust $\delta^{114}\mathrm{Cd}$ value is approximately 0.1 ‰ (relative to NIST

SRM 3108. The weighted sum of isotopic compositions of known sinks is therefore heavier than the weighted sum for known sources, indicating a missing light sink of Cd. Cadmium sulphide (CdS) complexes have been postulated to be the missing isotopically light sink required to balance the global Cd isotope cycle. The new experimental results demonstrate that precipitation of Cd with hydrogen sulphide gas in synthetic seawater results in preferential association of lighter isotopes with the precipitated CdS phase. The reported data is best fit by the Rayleigh isotope fractionation equation, with a fractionation factor of 1.00011. The magnitude of fractionation in the system is governed by the aqueous speciation of Cd in the synthetic seawater; wherein a large portion is associated with chloro complexes, which preferentially incorporate the heavier isotopes of Cd at equilibrium relative to the hydrated Cd^{2+} [92]. This effect drives the precipitated CdS forming from the hydrated Cd^{2+} to be isotopically lighter relative to the bulk solution. This study supports the hypothesis that the precipitation of CdS complexes in marine sediments is the missing sink for isotopically light Cd in the ocean.

3.1 Introduction

Recent studies report that dissolved cadmium (Cd) in waters and pore-waters likely precipitate with trace hydrogen sulphide to form insoluble cadmium sulphide complexes in low oxygen settings [28, 48, 56, 80, 87, 110, 145]. The conditions required for sulfate-reducing microbes to reduce sulfate to sulphide are typically taken to occur after the complete utilisation of other electron acceptors, such as nitrate and Fe(III) in anoxic settings. This view was recently challenged with the discovery of strong evidence to suggest the existence of sulfate-reducing microbes in prominent oxygen deficient zones (ODZs) [1, 88, 89]. Bianchi et al. (2018) proposed that sinking organic aggregates form microenvironments with increased respiration and inhibited O_2 diffusion in low oxygen settings, resulting in anaerobic respiration and the precipitation of chalcophile metals with trace hydrogen sulphide ($\mathrm{H}_2\mathrm{S}$), such as Cd to form insoluble cadmium sulphides (CdS) complexes [90].

The observed vertical profiles of Cd concentrations, and the decoupling of Cd and PO_4^{3-} through the water column may be driven by the degree of CdS precipitation

within microenvironments, resulting in water masses with different Cd:P ratios [28, 56, 90]. For example, in the ODZs within the Northeast Pacific and North Atlantic Oceans, particulate Cd:P ratio reaches a maximum in the hypoxic layer where dissolved PO_4^{3-} increases during remineralisation and particulate Cd increases, potentially due to the formation of CdS species [56]. The particulate Cd decreases in the deep-waters and the strong linear relationship between Cd and PO_4^{3-} returns, suggesting that CdS particulates disaggregate following a first-order rate once the water is oxygenated [56, 90]. This observation indicates that CdS particulates may not represent the sole source of Cd to the benthic-waters; however, it does confirm the strong potential for Cd to form insoluble CdS complexes in the presence of trace hydrogen sulphide. Likewise, it further supports the formation of CdS species within the sediment depth profile as oxygen concentrations rapidly decrease during degradation of organic material. These newly formed sedimentary CdS complexes likely remain immobilized unless redox conditions change in the sediments [110]. This process indicates that CdS precipitation may represent the missing sink of isotopically light Cd from the ocean. The dissolved Cd in the global deep ocean has a $\delta^{114}Cd$ of approximately 0.3 ‰ and the lithogenic crust $\delta^{114}Cd$ value is approximately 0.1 ‰ (relative to NIST SRM 3108) [28, 54, 57]. This means that the weighted sum of isotopic compositions of known sinks is heavier than the weighted sum for known sources, indicating a missing light sink of Cd [56, 93, 112]. Cadmium sulphide is likely the missing light sink required to build a robust mass balance model for Cd isotopes in the oceans and potentially use Cd isotopes to trace paleoredox conditions in ancient oceans [122].

Water column Cd sulphide precipitation has not been observed in the Peru margin ODZ [94]. These authors attributed the increased particulate Cd concentrations relative to PO_4^{3-} to the uptake of Cd by marine phytoplankton at the top of the ODZ [94, 146]. Other studies have similarly credited the disassociation of Cd and PO_4^{3-} between different water masses to preferential biological assimilation of Cd in the surface-waters [16, 37, 38, 43, 48, 146], mixing of water masses with different Cd:PO_4^{3-} ratios [25, 35, 54, 147], and variations in the depths of uptake and remineralisation [35, 51, 53].

The Cd stable isotope system may aid in deciphering the processes responsible for the variable Cd:PO_4^{3-} ratios in water masses and in identifying the primary sinks of Cd from the water column and their subsequent immobilization in the sediments. The recent study by Janssen et al. (2014) observed particulate Cd in the North Atlantic ODZ with $\delta^{114}Cd$ values as low as -0.02 ‰ at 235 m, correlating with a maximum concentration of particulate Cd [56]. Consequently, the formation of particulate Cd would be expected to drive the remaining dissolved Cd in seawater to isotopically heavy values. Theoretical studies have shown a preferential incorporation of light Cd isotopes into sulphide species [92]. Likewise, direct Cd isotopes measurements of a suite of oceanic and continental hydrothermal sulphides by Schmitt et al. (2009) found that the average Cd isotopic composition was 0.24 ± 1.2 ‰ lighter than the average deep-water Cd isotope value (~0.3 ‰) [31, 93].

These studies show that the precipitation of CdS species in low oxygen microenvironments in waters and sediments will likely lead to a preferential removal of lighter Cd isotopes from the dissolved Cd pool. Experimental studies are required to resolve the fractionation mechanisms and associated magnitudes of fractionation to determine if this process is the primary mechanism responsible for the different Cd:PO_4^{3-} ratios in water masses in prominent ODZs.

This study focuses on a precipitation reaction that is likely an important pathway for the removal of dissolved Cd from low oxygen settings in particulate Cd in the water column and ultimately as a sink into sediments [110].

The objective of this study is to determine experimentally the mechanism and magnitude of Cd isotope fractionation during the precipitation of cadmium sulphides under controlled anoxic conditions using synthetic seawater. The results improve our understanding of Cd cycling in ODZs and anoxic settings and provides insight into the role of Cd precipitation with trace H_2S as a mechanism for incorporating Cd into seafloor sediments.

3.2 Materials and method

3.2.1 Stock solution preparations

Cadmium stock solutions were prepared from aliquots of Cd NIST SRM 3108, and the stock solution was equally divided into four experiments. Synthetic seawater was used as a high ionic strength solution in these experiments to better mimic the seawater properties found in nature (see Table 3.1). The Cd stock solutions were mixed several times a day over the course of 5 days to achieve equilibration between the salts and $\delta^{114/110}\mathrm{Cd}_{\mathrm{NIST3108}}$ standard solution. The solution was then purged with $\mathrm{O_2\ free-N_2}$ gas for 1 hour to achieve anoxic conditions. The anoxic solution was placed inside an anoxic glovebox and mixed on a stir plate for one hour to remove any remaining oxygen in the system. This solution was equally divided into four experiments. The anoxic glovebox was maintained at 96% $\mathrm{N_2}$ and 4% $\mathrm{H_2}$ atmosphere. Additionally, palladium catalysts and anhydrous $\mathrm{CaSO_4}$ desiccant maintained oxygen concentrations below 1 ppm. The humidity levels were kept below 20%, with catalysts replaced if the humidity increased above 35%. Cadmium concentrations in the stock solutions were analysed by ICP-MS and isotopic compositions by MC-ICP-MS (Nu Plasma).

3.2.2 Experimental design for the precipitation experiments

The experiments were designed to result in the precipitation of cadmium sulphides in high ionic strength solutions under anoxic conditions (see Figure 3.1). Details on the concentration of Cd in the starting aliquots of each experiment and the amount of pure hydrogen sulphide gas added to these aliquots in each experiment is detailed in Table 3.2. A compressed gas cylinder of pure sulphide gas (sourced from Fisher Scientific) with a stainless steel regulator and pressure gauge and a needle valve was fitted to a lab stand using clamps to hold it safely in place. The needle valve was fitted with a segment of Teflon tubing with one end attached to the valve and the other side fitted with a septa. A Hamilton™ 1800 series gastight needle syringe was designed to pierce through the septa to take up a measureable amount of gas. The needle was closed to trap the gas, and then removed from the tubing, allowing the septa to maintain a seal to prevent escape of

Table 3.1: Salt species in synthetic ocean water

Component	Concentration (M)
Anhydrous Salts	
NaCl	4.20×10^{-1}
Na_2SO_4	2.88×10^{-2}
KCl	9.39×10^{-3}
$NaHCO_3$	2.38×10^{-3}
KBr	8.40×10^{-4}
H_3BO_3	4.85×10^{-5}
NaF	7.15×10^{-5}
Hydrous Salts	
$MgCl_2 \cdot 6H_2O$	5.46×10^{-2}
$CaCl_2 \cdot 2H_2O$	1.05×10^{-2}
$SrCl_2 \cdot 6H_2O$	6.38×10^{-5}
Composition of synthetic seawater (ionic strength of 0.8 M) based on a recipe by Morel et al. (1979) and Price et al. (1989)	

gas. The needle was transported with the gas to the reaction vessel. The reaction vessel is a sealed Teflon jar with two ports on the lid. The two ports are fitted with a septa to prevent escape of gases. One of the septa is pierced with the needle to inject the H_2S gas directly into the solution inside the closed vessel. The needle is then removed and the vessel is shaken vigorously by hand for 5 minutes. The reaction vessel remains sealed and kept on a platform shaker in the glovebox overnight to ensure the experiment reached equilibrium. While time series were not completed in this study, a recent publication reported that cadmium sulphide precipitation reaches equilibrium within one minute at both low and high ionic strength conditions [80].

The CdS precipitate and the remaining dissolved Cd were separated using a pre-cleaned polypropylene syringe fitted with an acid-cleaned 0.2 µm PTFE filter. The precipitate on the filter was then dissolved with 5 M nitric acid and dispensed into a separate PFA vial. The two sub-samples of Cd (precipitate and residual solution) were then dried down and prepared for ion exchange chromatography. The concentrations



Figure 3.1: Experimental setup to use pure H_2S gas to precipitate cadmium sulphides complexes. A compressed gas cylinder of pure sulphide gas (sourced from Fisher Scientific) with a stainless steel regulator and pressure gauge and a needle valve was fitted to a lab stand using clamps for safety, shown in the middle graphic with a blue box. In the top left corner, the procedure begins with piercing the septa to recover a measurable amount of pure H_2S gas for each experiment (1), followed by adding the measured amount of gas to the Teflon reaction vessel by piercing the septa (2). The needle is removed and the vessel is physically agitated for 5 minutes (3), then placed on a platform shaker overnight. The final step is to separate the dissolved Cd and precipitated CdS using a syringe fitted with an 0.2 µm PTFE filter, where the precipitated CdS was removed from the filter with 4 M nitric acid into a separate PFA vial (4). The procedure from step 1 onward is completed inside an anoxic glovebox. Further details are provided in Section 3.2.2.

of Cd in the solid and dissolved samples was initially analysed by quadrupole ICP-MS for all experiments. Each set of experiments included a procedural blank containing 50 mL of Cd-free stock solution. The experiments were filtered and analysed using the same procedure applied to the other experiments. The amount of Cd contamination in all blank samples was checked by ICP-MS. The procedural blanks were three orders of magnitude lower in Cd than the precipitation experiments.

3.2.3 Ion exchange chromatography procedure

Please refer to Chapter 2 for details on the chemical separation protocols for the precipitation experiments.

3.2.4 Mass spectrometric methods and data validation

Please refer to Chapter 2 for details on the procedure and instrumentation used to determine the Cd concentrations and isotopic compositions of the samples from the precipitation experiments.

3.3 Results

3.3.1 Synthetic seawater precipitation experiments under anoxic conditions

The experiments were designed to have similar concentrations of Cd with varying amounts of added hydrogen sulphide, in order to alter the fraction of dissolved Cd precipitated as CdS species. The fractional removal of Cd from the stock solutions after 12 hours ranged from 2–99 % (Table 3.2). Two different stock solutions of synthetic seawater were used during this study, resulting in small differences in the Cd concentrations and isotopic compositions from one stock to another. The isotopic compositions of Cd stock solutions ranged from $\delta^{114/110}\mathrm{Cd}_{\mathrm{stock\,solution}} = -0.69 \pm 0.06\,‰\,\mathrm{to}\,-0.92 \pm 0.05\,‰$. The small variation between the stocks may have been caused by contamination as the experiments were completed in a clean glove box, but not located in the clean laboratory facility. The validity of the experimental results is supported by clear trends and a satisfactory mass balance assessment for each experiment. To make the results from all the experiments easier to compare, they are isotopically normalized in the figures relative to a stock solution of -0.69 ‰. The tables contain the original, measured isotopic compositions of all samples. Cadmium sulphides were preferentially enriched in light Cd isotopes in all experiments. Results are detailed in Table 3.2 and shown graphically in Figure 3.2. Values of $\Delta^{114/110}\mathrm{Cd}_{\mathrm{precipitated-aqueous}}$ ranged from -3.78 ‰ to -1.47 ‰, with a greater offset as the percentage of Cd sequestered in the sulphide phase increased.

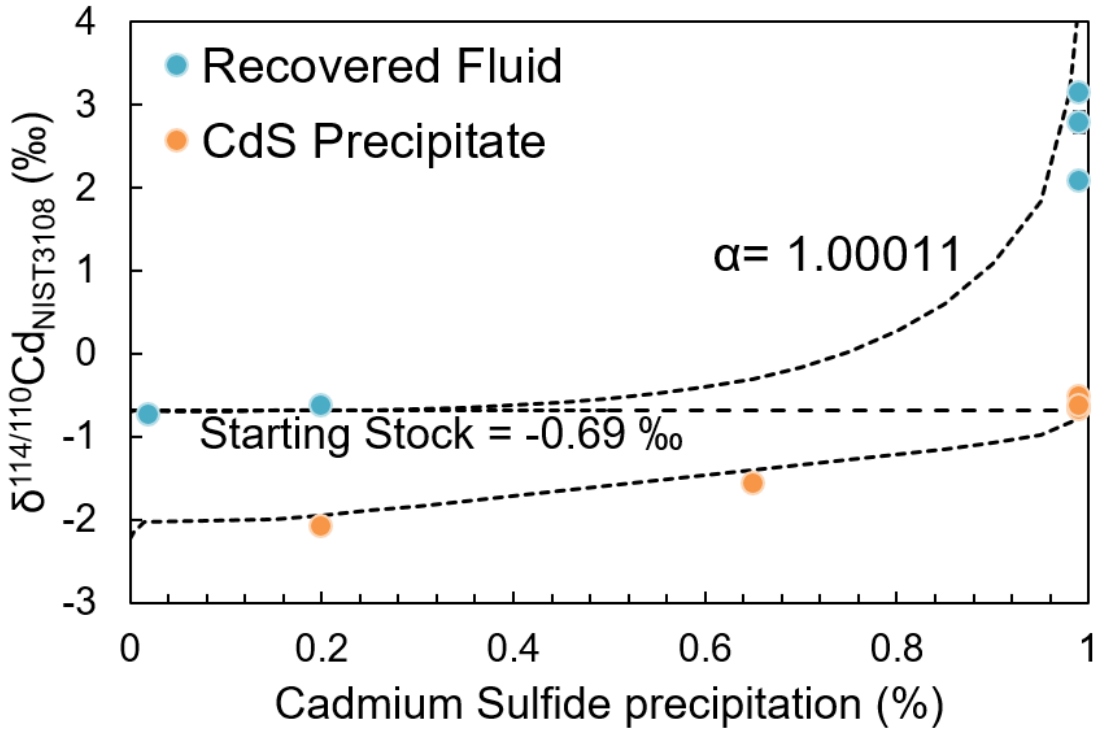


Figure 3.2: Isotopic compositions of dissolved Cd (filled, blue circles) and Cd sulphide precipitate (filled, orange squares) from experiments completed with synthetic seawater in an anoxic setting. The horizontal line at $\delta^{114/110}\mathrm{Cd} = -0.69‰$ represents the bulk starting composition. Error bars represent 2 SE of each sample. The dashed lines are Rayleigh fractionation curves calculated with an alpha value of 1.00011.

Cadmium recovery and isotope mass balance was calculated to verify the success of the experiments and confirm that no interferences of major contamination in any experiments following the use of the stock solutions. The Cd recovery for the reported experiments ranged from 98.7 to 102.7 %, with the higher amounts most likely to slight contamination from the glove box. The offset between the calculated isotope mass balance of the experiments and the measured isotope value of the corresponding starting stock solution was computed as $\delta^{114/110}\mathrm{Cd}_{\mathrm{stock}} - (\delta^{114/110}\mathrm{Cd}_{\mathrm{aqueous}} * (100 - \%\,\mathrm{precipitated}) + \delta^{114/110}\mathrm{Cd}_{\mathrm{precipitated}} * \%\,\mathrm{precipitated})$, and these values are listed in the last column of Table 3.2. All mass balances were within the reproducibility of Cd isotope measurements (approximately ±0.6 ‰), apart from one measurement from each experiment which average ±0.18 ‰. Three of the experiments do not have corresponding measurements of the solid or dissolved pool in the experiments. This was a result of complications during the filtration procedure completed in the glove box.

Table 3.2: Experimental system parameters and results

Each experiment is maintained at anoxic conditions and a pH ~8.2 and duration of 15 h.

H2S gas (µL)	Cd in expt. (µg g^{-1})	Precipitated Cd (%)	$\delta^{114/110}Cd_{aqueous}$ *	2 SE	$\delta^{114/110}Cd_{CdS}$ *	2 SE	$\delta^{114/110}Cd_{stock}$ **	2 SE	Mass balance offset ***
75	17.31	2	-0.97	0.06			-0.92	0.05	
500	400.02	20	-0.62	0.06	-2.09	0.06	-0.69	0.06	0.20
500	17.31	>99			-0.90	0.06	-0.92	0.05	
750	400.02	65			-1.57	0.06	-0.69	0.06	
1250	17.31	>99	2.56	0.13	-0.76	0.05	-0.92	0.05	-0.16
excess	400.02	>99	2.08	0.06	-0.68	0.07	-0.69	0.06	-0.01
excess	400.02	>99	3.15	0.08	-0.63	0.08	-0.69	0.06	-0.06

* Each sample is an average of two or three measurements on a Nu Plasma HR MC-ICPMS with a Nu Instruments DSN-100 desolvation system with the 2 SE values reported to reflect internal precision on replicates or our long-term 2 SE on the Cd NIST 3108 standard, whichever is larger.

** The table is showing the measured isotope values. In Figure 2, all values have been normalized to a stock value of -0.69 ‰ for clarity.

*** Mass balance offset = $\delta^{114/110}Cd_{stock} - (\delta^{114/110}Cd_{aqueous} \cdot (100 - \%\ \text{precipitated}) + \delta^{114/110}Cd_{precipitated} \cdot \%\ \text{precipitated})$

3.4 Discussion

3.4.1 Explanation for the observed fractionation effect

The data plotted in Figure 3.2 are consistent with a Rayleigh trend that signifies either an irreversible kinetic fractionation or equilibrium isotope fractionation effect. An irreversible kinetic isotope fractionation effect for this system would imply that the isotopically lighter Cd isotopes will react more rapidly with free H_2S to precipitate CdS complexes. In an equilibrium fractionation system, the Cd species in solution will remain in equilibrium as thermodynamically driven precipitation leads to the removal of isotopically light Cd species, likely Cd^{2+} and $CdCl^{+}$, from the solution into the solid fraction. As the experiments represent a closed-system, with finite amount of Cd, as increased amounts of dissolved Cd are removed from the system, the dissolved fraction will become isotopically heavier, resulting in a Rayleigh isotope fraction trend. In both cases, the precipitated CdS was insoluble under anoxic conditions. The data is best fit by the Rayleigh equation. The deviations from linearity are most apparent in the samples with very high proportions of total Cd precipitated. The preferential precipitation of lighter Cd isotopes followed a Rayleigh fractionation trend, with a magnitude of the isotope effect for the system best expressed as a fractionation factor of $\alpha = 1.00011$ in $\delta^{114/110}Cd$ notation, where,

$$\alpha = \left(\frac{1-f}{f \ln f}\right)\left(\frac{\delta^{114/110}Cd_{precipitated} + 1000}{\delta^{114/110}Cd_{aqueous} + 1000}\right)$$

f is the fraction of Cd remaining in the aqueous species in the solution.

The experiments show that $\Delta^{114/110}Cd_{precipitated–aqueous}$ increases exponentially, with each experiment left closed in an anoxic environment for 12 hrs after the injection of H_2S to ensure the reaction reached completion. As previously mentioned above, time series experiments were not completed to determine when the system reached equilibrium. However, a recent study showed that cadmium sulphide precipitation reaches equilibrium within one minute at both low and high ionic strength conditions [80]. The rapid rate of equilibrium for the system suggests that the system is in equilibrium instead of representing a kinetic isotope fractionation effect. As far as implications for natural samples are concerned, any short kinetic effect is likely unimportant when considering diffusion and sedimentation rates. The results are in agreement with the *ab initio* calculations of CdS species by Yang et al. (2015) and recent CdS precipitation experiments completed by Guinoiseau et al. (2018) [80, 92]. Guinoiseau et al. (2018) performed an in-depth experimental study on the synthesis of CdS under anoxic conditions in low and high ionic strength solutions to determine the isotope fractionation of Cd associated with formation of sulphide species [80]. These authors determined fractionation factors (α) that ranged from 1.00014–1.00024, depending on the ionic strength of the solution [80]. These findings indicate that the Cd isotope fractionation during precipitation of CdS complexes is sensitive to variations in ionic strength.

The Rayleigh isotope fractionation curves that best fit the data in the CdS precipitation experiments by Guinoiseau et al. (2018) under a range of ionic strengths and the measured dissolved and solid Cd fractions in this study are within analytical uncertainty at low percentages of CdS precipitation. This supports agreement between the two studies (see Figure 3.3) [80]. However, the Rayleigh isotope fractionation curves that best fit the dataset for the two studies show varying degrees of agreement across the range of percentage of CdS precipitation. Small differences in the ionic strength of our synthetic seawater relative to the synthetic seawater in Guinoiseau et al. (2018) experiments may explain the points of poor agreement, particularly at high percentage of CdS

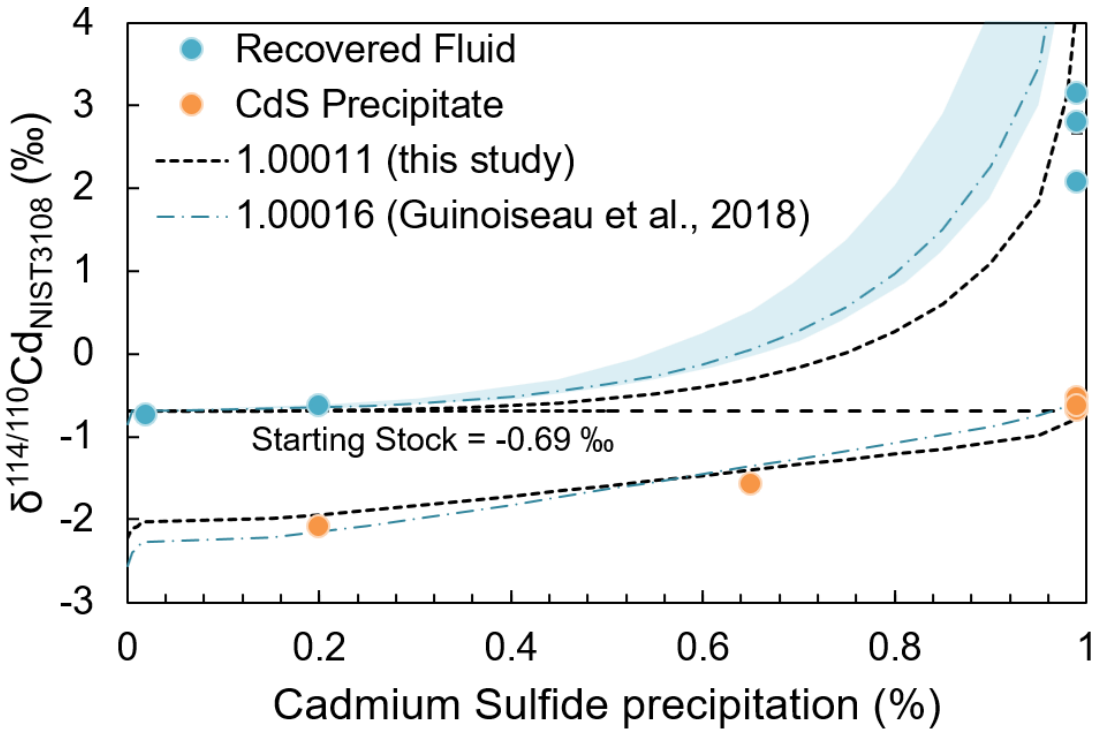


Figure 3.3: Isotopic compositions of dissolved Cd (filled, blue circles) and Cd sulphide precipitate (filled, orange squares) from experiments completed with synthetic seawater in an anoxic setting. The horizontal line at $\delta^{114/110}\mathrm{Cd} = -0.69‰$ represents the bulk starting composition. Error bars represent 2 SE of each sample, however in most cases are smaller than the size of the marker. The black, dashed lines are Rayleigh fractionation curves calculated with an alpha value of 1.00011. The blue, dashed lines are Rayleigh fractionation curves reported by Guinoiseau et al. (2018) for Cd sulphide precipitation experiments with synthetic seawater in an anoxic setting. The blue, shaded shape represents the reported range of fractionation factors ($\alpha = 1.00014 - 1.00024$) from experiments completed by Guinoiseau et al. (2018) from low to high ionic strengths [80].

precipitation. Also, the source of sulphide in the experimental system of this study is high purity, hydrogen sulphide gas (H_2S) compared to sodium sulphide (Na_2S). Some of the difference in the fractionation factor for this study compared to Guinoiseau et al. (2018) may be attributed to the source of H_2S [80]. Despite the different fractionation factors, the direction of fractionation is the same in all experiments, with a preferential precipitation of light Cd isotopes to form CdS species.

3.4.2 Isotope effect influenced by complex speciation at high ionic strength

Equilibrium speciation of Cd in the synthetic seawater, which includes the anhydrous and hydrous salts in the ocean (Table 3.3), was modelled at relevant conditions (pH =

Table 3.3: Equilibrium Cd speciation in synthetic ocean water used in the experiments

Primary aqueous Cd species	Distribution in the stock solution (%)	RPFR for $^{114/110}$Cd
Cd^{+2}	43.2	2.299
$CdCl^{+}$	21.6	2.210
$CdSO_4$	15.3	
$CdCl_2$	10.1	2.011
$CdCl_3^{-}$	5.4	1.796
$CdCl_4^{-}$	4.4	

Calculated using The Geochemist's Workbench with pH ~8.2, T = 25°C, and P = 1 bar

Reduced partition function ratios (RPER, ln (β)·1000) for $^{114/110}$ Cd at 298 K from Yang et al. (2015)

8.2, T = 25°C, P = 1 bar) using The Geochemist's Workbench and results are detailed in Table 3.3. The Cd^{2+} species represent approximately 43 % of all the dominant Cd species in the solution, and the residual species are dominated by various chloro complexes (~42 % of all Cd). We therefore expect that the observed fractionation in the experiments is impacted by fractionation amongst the salts and Cd^{2+} species. Previous *ab initio* calculations by Yang et al. (2015) indicate that Cd chloride species should preferentially incorporate heavier isotopes of Cd at equilibrium relative to hydrated Cd^{2+} with a low degree of isotope fractionation [92]. Chloride ligands complex with Cd to form mono-, di- and tri-chloro Cd complexes [92]. The authors also calculated reduced partition function ratios for various aqueous species of Cd, reporting that chloro complexes of Cd should be enriched in heavier isotopes relative to hydrated Cd^{2+} [92]. The resulting magnitude of fractionation from $Cd(H_2O)_6^{2+}$ for chloro complexes is from -0.04 ‰ for $Cd(H_2O)_5^{2+}$ to -0.50 ‰ for $CdCl_3(H_2O)^{-}$.

If the system is at equilibrium between all aqueous species at high ionic strength, then the observed fractionation is a representation of the distribution of Cd isotopes between the weighted average of all aqueous species in the solution. Guinoiseau et al. (2018) reported that the free Cd^{2+} will predominately precipitate with available trace hydrogen sulphide in low ionic strength solutions and with $CdCl_2$ at high ionic strengths [80]. Using the proportions of hydrated Cd^{2+} and Cd chloride species in Table 3.3, along with the *ab initio* calculations by Yang et al. (2015) for the Cd chloride species, a mass balance

calculation can be performed to determine the Cd isotopic composition of hydrated Cd^{2+}, or $\mathrm{Cd(H_2O)}^{6+}$, in the aqueous starting stock with a $\delta^{114/110}\mathrm{Cd}_{\mathrm{stock}} = -0.69‰$ [92]:

$$\delta^{114/110}\mathrm{Cd}_{\mathrm{Cd}^{2+}} = \frac{\delta^{\frac{114}{110}}\mathrm{Cd}_{\mathrm{Cd}_{\mathrm{stock}}} - \left(\mathrm{f}_{\mathrm{Cd}_{\mathrm{Cd(Cl)}^+}} * \delta^{\frac{114}{110}}\mathrm{Cd}_{\mathrm{Cd(Cl)}^+}\right) - \left(\mathrm{f}_{\mathrm{Cd}_{\mathrm{Cd(Cl)}_2}} * \delta^{\frac{114}{110}}\mathrm{Cd}_{\mathrm{Cd(Cl)}_2}\right) - \left(\mathrm{f}_{\mathrm{Cd}_{\mathrm{CdCl}_3^-}} * \delta^{\frac{114}{110}}\mathrm{Cd}_{\mathrm{CdCl}_3^-}\right)}{\mathrm{f}_{\mathrm{Cd}^{2+}}}$$

where f is the fraction of the individual Cd chloro species in the solution from Table 3.3, and Cd isotopes value of the Cd chloride species is determined using the differences in reduced partition functions ($10^3 \ln \beta^{114/110}$) from Yang et al. (2015) [92].

The resulting hydrated Cd^{2+} isotopic composition equals $\delta^{114/110}\mathrm{Cd} = -1.82 \pm 0.3‰$, supporting that CdS complexes preferentially remove the hydrated Cd^{2+}. The mass balance calculation, while simple, is consistent with the experimental results and suggests that the complex speciation at high ionic strength influences the isotopic behaviour of the system. The effect of aqueous salts on the kinetics of isotope fractionation between solution and substrate is difficult to constrain in this study; however, Guinoiseau et al. (2018) further explored the impact of ionic strength on the fractionation of Cd isotopes during this precipitation reaction [80]. These authors suggested that the fractionation factor decreases with increasing ionic strength. Similarly, with other substrates, Horner et al. (2011) observed that the presence of salts slowed the isotopic exchange and incorporation of Cd into calcite, resulting from competition with other major cations, like Na^+ and Mg^{2+} [86]. Likewise, Wasylenki et al. (2014) reported that a similar mechanism was occurring in synthetic seawater for Cd adsorption onto birnessite [85]. Consequently, complex aqueous speciation is likely to have a significant impact on the fractionation processes occurring as Cd precipitates with hydrogen sulphide to form insoluble CdS species [80].

3.4.3 Implications for interpreting Cd isotope fractionation in natural waters and sediments

The experimental results reported here indicate that fractionation during precipitation of Cd to sulphides can explain the light Cd isotopic compositions of sinking particulates in ODZ settings with oxygen concentrations $\leq 75\,\mathrm{mol\,kg^{-1}}$ [28, 56] and enrichment

of light Cd isotopes in low temperature, hydrothermal sulphides [93]. However, the degree of fractionation between average seawater and published literature values for Cd particulates containing low temperature hydrothermal sulphides is significantly smaller than the fractionation measured in laboratory experiments with the smallest fractionation removal of CdS from solution. This discrepancy between the experimental systems in this study and natural conditions could be a result of higher concentrations of Cd in the initial starting solution than found in seawater.

Another explanation for the differences in isotopic composition is the lack of other mineral surfaces in our experimental system. Cadmium is known to form inorganic complexes with an enrichment in light Cd isotopes during its incorporation into calcite [86] and adsorption to Mn oxides [85]. However, the global mass balance of Cd by Little et al. (2015) considers oxic sinks of Cd to be negligible [122]. The primary sink for Cd in the seafloor is into suboxic sediments.

Another possibility is that the experimental system lacks organic ligands, which are known to remove a majority of Cd in the surface-waters of the open ocean [55, 69, 79]. Below 200 m, a majority of the more labile Cd-bound organic ligands have undergone remineralisation and released the dissolved Cd species. However, refractory Cd-bound ligands still constitute a significant portion of the total Cd concentration in the deep ocean [55, 69, 79, 80]. At this point, Cd isotopic compositions of organic ligands are unconstrained, but likely enriched in light isotopes [67]. The combination of CdS precipitation in microenvironments and remaining Cd bound in organic ligands may in tandem explain the increased particulate Cd concentration and lighter Cd isotopic composition compared to seawater, resulting in the observed Cd:$\mathrm{PO_4^{3-}}$ ratio in the North Atlantic ODZ [97].

The re-oxygenated conditions below the ODZ may cause the CdS particulates to dissolve [90], causing the ultimate Cd source to the benthic-waters to possibly be dominated by free $\mathrm{Cd^{2+}}$ and a small percentage of refractory, organically bound Cd, as suggested by Georgiev et al. (2015) and Rosenthal et al. (1995) [110, 121]. Cadmium removal from the water column is likely governed by diffusion across the sediment-water interface, where microbial degradation of organic matter and reductive dissolution of Mn

oxides leads to mobilization of Cd into pore-waters. The ultimate sink of Cd is likely to be via the precipitation of dissolved Cd from pore-waters with trace hydrogen sulphide at the redox front in suboxic and anoxic sediments [68, 110, 113, 122].

3.5 Conclusion

This study quantified the Cd isotope fractionation during precipitation of cadmium with pure hydrogen sulphide gas in synthetic seawater under anoxic conditions. Calculations of the primary Cd species in solution were used to help constrain the fractionation mechanism for the observed isotope effect. The experiments displayed an enrichment of light Cd isotopes during precipitation of insoluble cadmium sulphides, reflecting Rayleigh behaviour with complexities in Cd speciation due to salts. The results provide a mechanistic explanation for the lighter Cd isotopes signature in Cd particulates within prominent ODZs, along with the different Cd:$\mathrm{PO_4^{3-}}$ ratios in various ODZs. An important aim for future work will be to determine the rate of dissolution of CdS particulates, building on the modelling results by Bianchi et al. (2018) [90], to investigate if CdS particulates formed in the ODZs reach the seafloor under oxic and suboxic conditions. Furthermore, it will be important to determine whether the same CdS species form under different ambient $\mathrm{H_2S}$ concentrations, and whether these species fractionate Cd similarly. This work advocates that CdS precipitation is likely the missing sink of isotopically light Cd from the ocean, and is able to explain the offset between the deep global ocean (~0.3 ‰) and lithogenic crust $\delta^{114}\mathrm{Cd}$ value of approximately 0.1 ‰ (relative to NIST SRM 3108) [28, 54, 57]. The following chapters will aim to further investigate how the magnitude of fractionation observed in natural waters and sediments from a range of redox conditions is driven by the precipitation of cadmium sulphides.

4

Cadmium isotope signatures in seawater, suspended particulates, and near-surface sediments from the South Atlantic at 40°S

Contents

4.1 Introduction 49
4.2 Sediment sampling procedures 51
4.3 Methods 53
4.4 Results 53
4.4.1 Cd concentrations and isotope variations in the water column . 53
4.4.2 Cd concentrations and isotope variations in particulates 56
4.4.3 Cd concentrations and isotope compositions of sediment depth profiles 58
4.4.4 Cd concentrations and isotope compositions of water and near-surface sediment samples from the North Atlantic 68
4.5 Discussion 71
4.5.1 Cause of the observed isotope fractionation effect in the water column 71
4.5.2 Cadmium isotopic composition in the global ocean basins . . 74
4.5.3 Cadmium isotopic composition in the global deep ocean basins 74
4.5.4 Relationship between the sediments and the overlying water column 77
4.5.5 Controls on $\delta^{114/110}$Cd in the near-surface sedimentary profile 86
4.5.6 Cause of the observed isotope variations in the depth profile from the Deep Argentine Basin 91
4.5.7 Cadmium sulphide complexes: Primary geologic sink of Cd in the oceans 94
4.5.8 Correlation between the sedimentary enrichment of Cd with other chalcophile metals 94

4.5.9 Mass balance for Cd isotopes in the ocean 95
4.6 Conclusions 96

Abstract

The cycling of Cd in the oceans is controlled by a range of biogeochemical processes throughout the water column. Within the surface-waters, the dominating process is biological uptake. This mechanism results in the removal of the light Cd isotopes, driving the residual dissolved Cd to isotopically heavy values. How, and if, this productivity signal is exported to the deep-waters, and subsequently recorded in the sediments is unknown. This relationship was investigated by measuring the Cd isotopic compositions and concentrations of near-surface seafloor sediments, waters, and suspended particulates across a transect at 40°S in the South Atlantic from the Argentine shelf to the East Mid-Ocean Ridge. The samples were collected by the UK GEOTRACES, JC068 research cruise aboard the RRS James Cook from December 2011 to January 2012. Cadmium isotopic compositions of the near-surface sediments are isotopically offset from the overlying oxygenated water column by between $\Delta^{114/110}\mathrm{Cd}_{\mathrm{core\,top-deep\,waters}}$ = -0.36 $\pm$ 0.08‰ and 0.10 $\pm$ 0.07‰, with an overall preferential removal of light Cd isotopes. Isotopically light Cd signatures likely indicate the non-quantitative capture and immobilisation of CdS in the sediments by trace hydrogen sulphide in oxic and sub-oxic conditions. Conversely, Cd isotope signatures close to that of overlying seawater likely reflect the quantitative capture and immobilisation of particulate and dissolved Cd as CdS in the sediments under sub-oxic to anoxic conditions. Consequently, the redox state within the overlying deep-waters and pore-waters at the sediment-water interface is likely the dominating control on the Cd isotopic composition of the near-surface sediments. The precipitation of insoluble CdS complexes represents a key sink of Cd to suboxic sediments. The results from Cd concentrations and isotopic compositions of the near-surface sediment cores and overlying water column, along with chemical and physical parameters are used to provide an updated global mass balance model for Cd in this chapter.

4.1 Introduction

The South Atlantic at 40°S is a region of high productivity in an ocean basin known for low concentrations of critical micronutrients. The sub-tropical convergence zone is characterized by the meeting of nutrient-rich, cold water from the Southern Ocean and nutrient-depleted, warm water from the North Atlantic. The physical and chemical parameters from this region of the ocean depict the layering of known water masses. Antarctic Intermediate Water (AAIW) is identified at approximately 750 m to 2000 m, known for low salinity water that originates from the Antarctic Convergence Zone. This water mass overlies North Atlantic Deep Water (NADW), which extends from approximately 2000–3500 m and is characterised by higher temperatures, salinity, and lower dissolved oxygen concentrations relative to the AAIW. NADW has low-nutrient levels, as it is formed in low-nutrient surface-waters in the North Atlantic Ocean. Conversely, the deep-waters below 3500 m are characterized by high nutrient levels and low temperatures from the Antarctic Bottom Water (AABW), formed from the downwelling of cold, nutrient-rich, near-surface-waters in the Southern Ocean. The deep-water masses in the South Atlantic Ocean upwell to the south and north to supply micronutrients to the Fe-starved Southern Ocean, and to the highly productive Equatorial Atlantic. The overall vertical trend across the zone is nutrient-depleted surface-waters and increased nutrients at depth. The processes that control the sources, sinks, and internal cycling of trace metals such as Cd in the South Atlantic are not fully understood. Application of the Cd stable isotope system will aid in investigations of the dominant sources, sinks, and cycling of Cd in the modern and ancient oceans.

Previous studies on these water masses have produced a wealth of Cd isotope data [25–28, 31, 54, 61, 94–97, 148]. However, critical questions remain about the ultimate incorporation of Cd into the sediments. The measurement of Cd isotopic compositions in the water column have allowed us to delineate key water mass zones and confirmed the importance of biological uptake in the surface-waters. The primary unknowns are how organically-bound Cd and its isotopic signature are exported from the surface-waters to the seafloor. Likewise, the primary sinks for Cd within near-surface sediments.

Marine sediments represent an important physical interface with the oceans. However, a first order understanding of the relationship between Cd in sediments and the overlying water column remains poorly constrained. Cadmium is removed from seawater into marine sediments, but the isotopic composition of this output flux, and the processes that control this isotope composition, are not understood. Such understanding is required before Cd isotopes can be used as a tracer for past ocean cycling of this metal, and potentially as a tracer of past ocean chemistry.

To improve our understanding of the processes controlling Cd cycling and deposition in the South Atlantic Ocean, the Cd concentrations and isotope compositions of water, particulate, and sediment samples were measured across a transect at 40°S in the South Atlantic from the Argentine shelf to the East Mid-Ocean Ridge. These data, in addition to complementary chemical and physical parameters and trace metal concentrations, will provide the information required to better constrain the distribution, sources, and sinks of Cd in the ocean.

The findings from the South Atlantic will be compared with Cd concentrations and isotopic compositions of water and sediment samples from the Bermuda Atlantic Time-Series (BATS) site, near Bermuda in the Sargasso Sea (see Figure 4.1). The BATS study is a long-term, time-series that examines the seasonal and long-term changes in the biogeochemical cycles in the Sargasso Sea. This is achieved through routine sampling trips once a month to analyse critical biochemical and hydrographic parameters at the BATS station and surrounding sites. The BATS program has enabled scientists worldwide to collected samples for a range of analyses. Specifically, it was the location for a GEOTRACES intercomparison exercise for dissolved Cd concentration and isotope variations in the water column [28, 59]. This study allows an assessment of any temporal variability in dissolved Cd concentration and isotope composition of water samples through the water column. Also, it provides an ideal opportunity to compare the isotopic offset between the core-top sediments and overlying bottom-waters in the Sargasso Sea to the measured isotopic offset in the South Atlantic. I collected the water samples following GEOTRACES protocols for sample collection, handling, and storage. The sediment samples were previously collected by another researcher using a grab sampler.

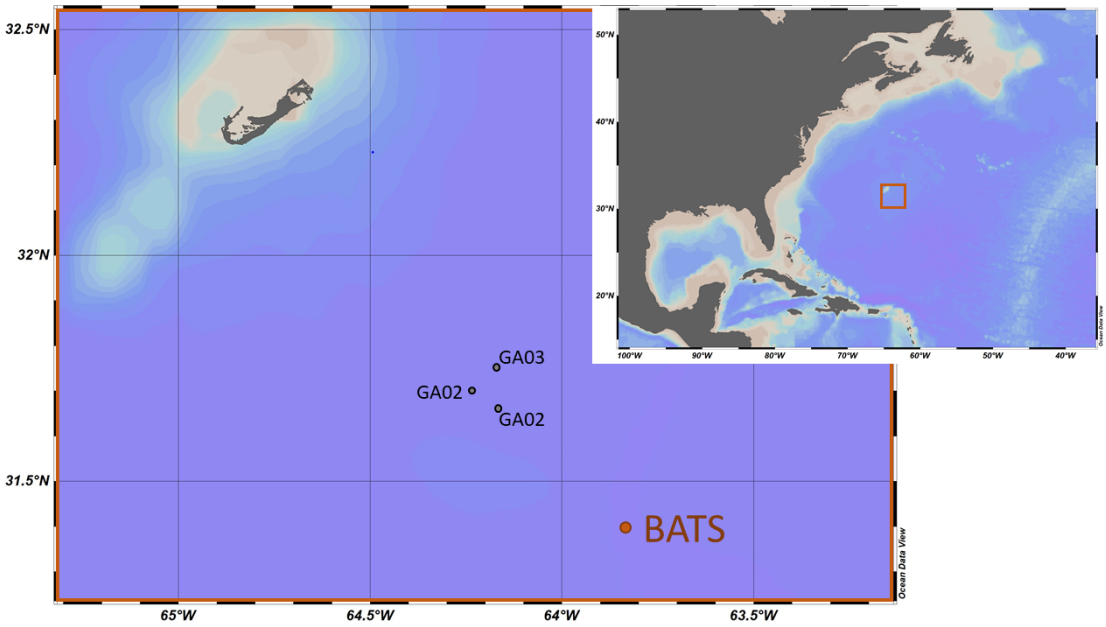


Figure 4.1: Geographic location of the Bermuda Atlantic Time-Series (BATS) site, near Bermuda in the Sargasso Sea. The orange circle marks the BATS site, where water and sediment samples were collected for this study. The small black dots denote the sampling sites for previous GEOTRACES cruises (GA02 and GA03).

4.2 Sediment sampling procedures

The water, particulate, core-top water, and sediment samples for Cd isotopes were collected by the UK GEOTRACES, JC068 research cruise aboard the RRS James Cook from December 2011 to January 2012 in the South Atlantic at 40ºS. Twenty three water samples were collected for Cd isotopes from three locations (see Figure 4.2). These sites were considered superstations and represented different environments along the transit. They were located at the Mid-Ocean Ridge (station 12), deep Argentine basin (station 18), and the Argentine slope (station 21). Water samples were retrieved through the vertical depth profile from the surface to the deep basin. All water sampling was completed with a titanium CTD frame equipped with a full sensor array and fitted with 24x 10 litre OTE (Ocean Test Eqipment) bottles with external springs. The unit was deployed on a Plasma Rope for optimal trace metal-free sampling. The retrieved bottles were transferred to a class 100 clean air container. The samples for Cd isotopes were immediately filtered through 0.2 μm AcroPak Supor polyethersulfone membrane filter capsules (Pall) into acid-cleaned, low density polyethylene bottles. Each sample was acidified to approximately

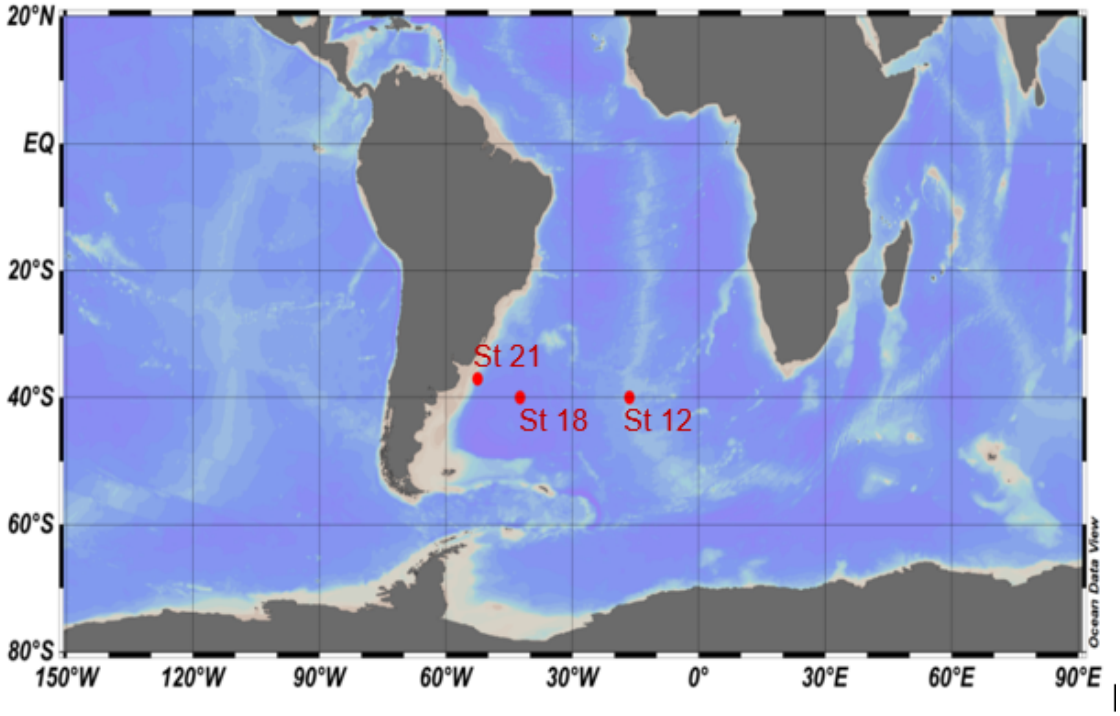


Figure 4.2: Schematic of the super stations on the UK GEOTRACES cruises, JC068 over the Mid-Ocean Ridge (station 12), deep Argentine basin (station 18), and the Argentine slope (station 21).

0.024 M with UpA HCl (Romil, Cambridge, UK) under a class 100 laminar flow hood and stored in polyethylene zip-lock bags. The collection of water and particulate samples was not completed as part of this thesis, but by the UK GEOTRACES participants. The processing and analysis of Cd isotopes for the water column samples presented in this thesis are unpublished and were completed by Fern Dowdall (University of Oxford).

Particulate samples were collected using Stand Alone Pumps (SAPs) to filter large volumes of seawater at the superstations (station 12, 18, and 21). The SAPs contained a filter housing unit that was fitted with acid-cleaned nyon mesh (10 μm) and paired 293 polyethersulfone filters (0.8 μm, Pall Gelman). The SAPs were deployed at six selected depths in the water column, with a focus on the bottom and near the surface. Once the SAPs were retrieved, the filter housing units were transferred to a clean container and opened under a laminar flow hood. The 293 mm PES filters were subdivided, folded, and placed into clean zip-lock plastic bags. The bags were frozen at -20°C for the duration of the cruise.

Core-top water, pore-water, and near-surface sediment samples were collected at additional stations along the transect (see Figure 4.3). A Bowers and Connelly Mega corer was deployed on a Plasma Rope to collect near-surface sediment cores and pore-waters from sites on the Argentine slope and deep Argentine Basin. The retrieved cores were immediately transferred to a temperature controlled laboratory, with a temperature similar to the bottom-waters. The cores were inserted into the air locks of a table mounted, Cole Palmer glove bag with an N_2 atmosphere. Once anoxic conditions were established in the glove bag, the overlying supernatant water in each core tube, referred to as core-top water, was collected, filtered, and acidified in the laboratory. The cores were sub-sampled at 1–2 cm resolution using a polycarbonate sectioning ring and a Teflon plate and spatula. The pore-water and sediment fractions were separated using a centrifugation and filtration procedure within the glove bag or a rhizon filtration procedure. The pore-water fractions were measured for a range of macronutrient and dissolved/colloidal metals. The solid fraction was double bagged and refrigerated for the duration of the research cruise. The solid fraction was freeze-dried and homogenized using an agate pestle and mortar prior to a range of analyse including organic and inorganic carbon concentrations and selected trace metal concentrations and isotopes. Sediment collection and pore-water analyses were completed by Dr Will Homoky (University of Oxford).

4.3 Methods

Please refer to Chapter 2 for details on the digestion and chemical separation protocols for the natural samples, along with analytical procedures.

4.4 Results

4.4.1 Cd concentrations and isotope variations in the water column

The vertical depth profiles for Cd exhibit a nutrient-like distribution in the water column, similar to phosphate, with low Cd concentrations and heavy Cd isotope values near the surface and increased Cd concentrations and lighter Cd isotope values in deep-waters. The results are detailed in Table 4.1 and shown graphically in Figure 4.4. The behaviour

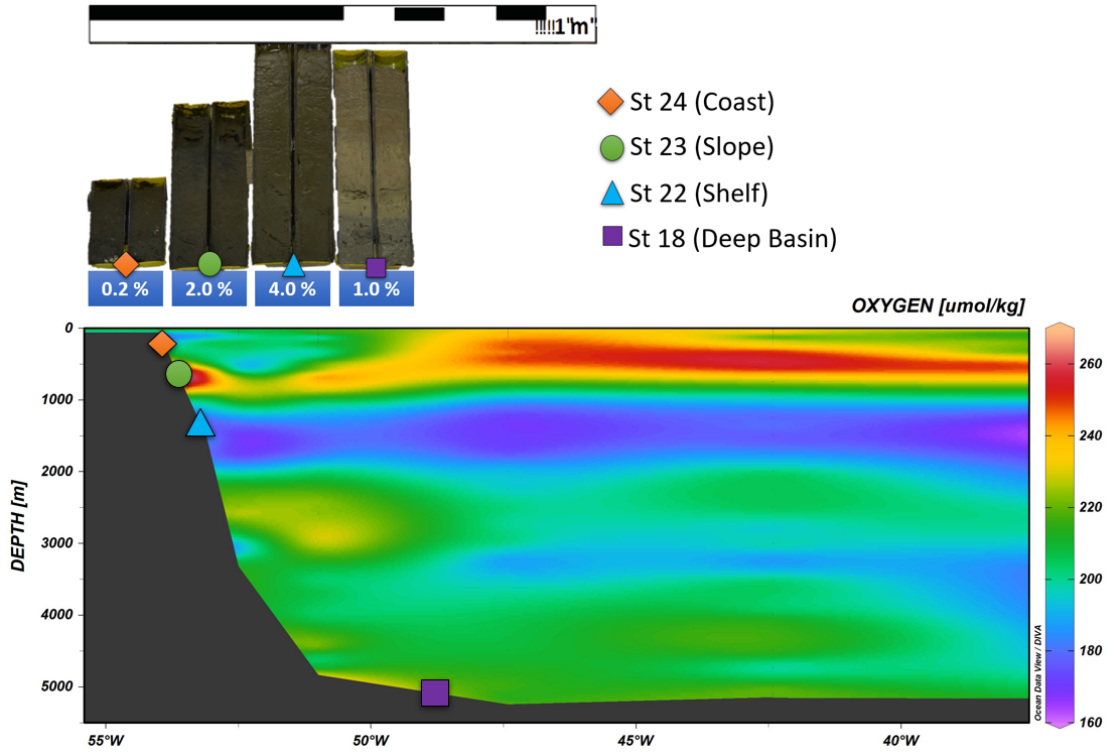


Figure 4.3: Station locations for UK GEOTRACES cruises JC068 along the Argentine continental margin, along with an image of near-surface sediment cores and corresponding TOC (%) labels that exhibit a gradient in organic matter enrichment.

of Cd in the surface-waters is governed by biological uptake and dissolution of sinking particles at depth in the remineralization zone [55, 69, 79, 147]. Dissolved Cd removal by marine phytoplankton in the surface-waters drives the isotopic composition of dissolved Cd to heavier values in the water column. The bacterial oxidation and dissolution in the remineralization zone found in intermediate waters releases Cd. This action significantly increases the dissolved Cd and shifts the Cd isotopes to lighter values in this zone. The Cd concentrations and isotopic compositions are relatively uniform through the deep-waters, and in all ocean basins (~0.3‰).

The three depth profiles display an inverse relationship between Cd concentrations and isotopic compositions. The nutrient-like vertical profile for Cd is most apparent at station 18. The full depth profile at station 18 shows surface-water depleted in Cd, with levels as low as $0.01\,\mathrm{nmol\,kg^{-1}}$ at 47 m, resulting in highly fractionated surface-waters with dissolved $\delta^{114/110}\mathrm{Cd}$ values up to $3.01 \pm 0.22\,‰$. In the deep ocean, Cd concentrations increase up to $0.65\,\mathrm{nmol\,kg^{-1}}$ at 5103 m while Cd isotope compositions

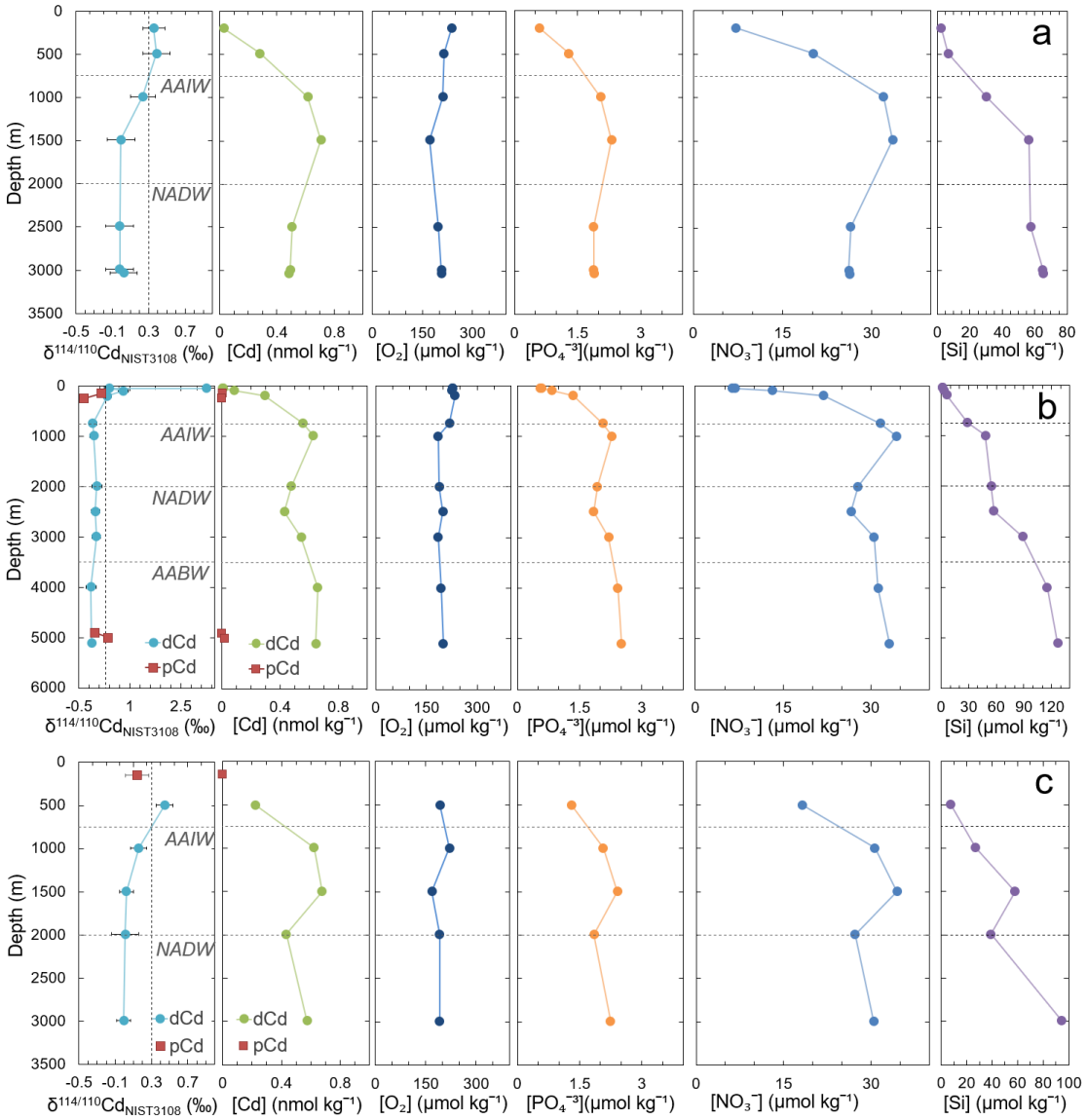


Figure 4.4: Vertical water column profiles of dissolved Cd concentrations and isotopic compositions (dCd), along with dissolved oxygen, phosphate, nitrate, and silica (Si) from the a) Mid-Ocean Ridge (St 12), b) deep Argentine basin (St 18), and c) Argentine slope (St 21). The measured particulate Cd concentrations and isotopic compositions (pCd) from the deep Argentine Basin (St 18) and Argentine slope (St 21) are depicted with filled, red squares. The vertical dashed line $\delta^{114/110}\mathrm{Cd} = 0.3‰$ represents the average deep ocean water value. Error bars for the Cd isotopes measurements represent the 2 SE on the sample.

are near constant at ~0.3 below ~800 m, as observed elsewhere in the global ocean [25, 28, 31, 54]. The data at stations 12 and 21 do not fully extend to the surface-waters, and thus reveal only smaller shifts in Cd isotopes to heavier values higher up the water column. Measurements were not undertaken at the most shallow water depths due to very low Cd concentrations near the surface (0.4 and $1.6\,\mathrm{pmol\,kg^{-1}}$). The measurement of Cd isotopes is extremely difficult to complete on samples at such low concentration levels. The Cd concentrations and isotopic compositions from Station 12 at 198 m was $0.03\,\mathrm{nmol\,kg^{-1}}$ and $\delta^{114/110}\mathrm{Cd} = 0.57 \pm 0.08\,‰$. The Cd concentrations and isotopic compositions for the deep-waters at Station 12 and 21 had the same values within analytical uncertainties as station 18.

The Cd concentrations in the depth profiles show a strong correlation with those of phosphate and nitrate. The phosphate and nitrate concentrations exhibit maximum and minimum peaks at the same depths. At station 18, the phosphate concentration in the surface-waters is as low as $0.6\,\mu\mathrm{mol\,kg^{-1}}$ at 47 m, with a maximum in the remineralization zone of $2.3\,\mu\mathrm{mol\,kg^{-1}}$ at 992 m. The deep-waters have a maximum phosphate concentration of $2.5\,\mu\mathrm{mol\,kg^{-1}}$ at 5103 m. Similarly, the minimum nitrate concentration in the surface-waters is $6.3\,\mu\mathrm{mol\,kg^{-1}}$ and increases to $34.4\,\mu\mathrm{mol\,kg^{-1}}$ at 992 m. The deep-waters exhibit a maximum nitrate concentration of $33.2\,\mu\mathrm{mol\,kg^{-1}}$ at 5103 m.

4.4.2 Cd concentrations and isotope variations in particulates

The trace metals in the oxygenated water column are either dissolved or in the particulate phases and associated with organic ligands or inorganic precipitates [55, 69–74]. The surface-waters are dominated by trace metals incorporated into marine phytoplankton. Below the sub-surface organic matter remineralization zone, dissolved trace metals exist as either aqueous Cd species or as particulate complexes. The particulate trace metals may occur in several forms, including in association with stable, refractory organic ligands, and/or adsorbed or incorporated into oxides and carbonates [85, 86, 104]. The particulate fraction obtained by filtration was measured for 5 samples from stations 18 and 21 (see Table 4.1). Cadmium concentrations at station 18 and 21 at 150 m have Cd concentrations of $0.006\,\mathrm{nmol\,kg^{-1}}$ and $0.01\,\mathrm{nmol\,kg^{-1}}$, respectively. The Cd isotopic

Water Depth (m)	Salinity (pss)	θ (°C)	$[O_2]$ (µmol/kg)	$[PO_4^{3-}]$ (µmol/kg)	[Si] (µmol/kg)	$[NO_3^-]$ (µmol/kg)	[Cd] (nmol/kg)	$\delta^{114/110}Cd_{NIST}$ (‰)	±2SD
Station 12, Mid-Ocean Ridge, 40.00'S, 16.46'W									
198	35.2	12.4	237.8	0.6	2.4	7.2	0.03	0.57	0.08
490	34.6	8.4	214.5	1.3	6.7	20.2	0.28	0.59	0.10
990	34.3	3.6	210.9	2.1	30.2	32.0	0.62	0.49	0.09
1488	34.5	2.9	171.7	2.3	56.5	33.6	0.71	0.33	0.10
2487	34.8	2.6	197.4	1.9	57.6	26.5	0.51	0.32	0.10
2988	34.8	2.1	206.6	1.9	64.9	26.2	0.49	0.32	0.10
3031	34.8	2.1	206.5	1.9	65.5	26.3	0.49	0.35	0.10
Station 18, deep Argentine basin, 40.00'S, 42.42'W									
47	35.1	13.0	227.4	0.6	1.8	6.3	0.01	3.01	0.22
49	35.1	13.1	226.9	0.6	1.9	6.8	0.01	0.72	0.22
95	35.0	11.3	225.9	0.8	3.3	13.1	0.09	1.05	0.12
*150							0.006	0.15	0.05
195	34.4	7.5	234.4	1.4	6.2	21.9	0.30	0.67	0.10
*250							0.002	-0.36	0.05
742	34.2	3.5	218.8	2.1	28.8	31.6	0.56	0.33	0.10
992	34.4	3.0	184.5	2.3	48.1	34.4	0.63	0.35	0.10
1990	34.8	2.9	188.5	1.9	54.7	27.8	0.48	0.42	0.12
2488	34.8	2.6	198.8	1.8	57.2	26.6	0.43	0.39	0.10
2995	34.8	1.7	184.5	2.2	88.7	30.6	0.55	0.41	0.10
3995	34.7	0.6	193.0	2.4	115.5	31.3	0.66	0.28	0.12
*4900							0.02	0.36	0.05
*5000							0.001	-0.04	0.08
5103	34.7	0.3	199.9	2.5	127.0	33.2	0.65	0.3	0.07
Station 21, Argentine slope, 37.03'S, 52.49'W									
*150							0.01	0.14	0.13
498	34.8	9.9	192.5	1.3	7.4	18.2	0.22	0.63	0.06
995	34.2	3.6	220.5	2.1	27.1	30.7	0.62	0.44	0.06
1499	34.5	2.9	168.2	2.4	57.9	34.5	0.68	0.35	0.05
1993	34.8	3.5	190.9	1.9	39.1	27.3	0.43	0.34	0.10
2993	34.7	1.4	191.7	2.2	94.4	30.5	0.57	0.33	0.05
**Denotes particulate samples*									

Table 4.1: Cadmium concentrations and isotope compositions of waters and particulates, along with other nutrient and physical parameters from water column profiles in the South Atlantic

compositions are $\delta^{114/110}\mathrm{Cd} = 0.15 \pm 0.05\,‰$ and $\delta^{114/110}\mathrm{Cd} = 0.14 \pm 0.13\,‰$, which are indistinguishable within analytical uncertainty. The other three samples were all from station 18 at the surface and in the bottom-waters. The Cd concentrations and isotope compositions were highly variable. The Cd concentration and isotopic composition for the sample from 250 m was at a lower level ($0.002\,\mathrm{nmol\,kg^{-1}}$) and isotopically lighter (-0.36‰), than the particulate sample at 150 m (~0.15‰). In the benthic-waters, the Cd concentration and isotopic composition at 5000 m was $0.001\,\mathrm{nmol\,kg^{-1}}$ and $\delta^{114/110}\mathrm{Cd} = -0.04 \pm 0.08\,‰$.

4.4.3 Cd concentrations and isotope compositions of sediment depth profiles

The Cd concentrations and isotopic compositions of near-surface sediments collected from a transect across the Argentine coast to the deep Argentine basin are detailed in Table 4.2 and shown graphically in Figure 4.5. Most of the samples have a higher Cd concentration compared to the average upper crustal rocks at ~0.1 $\mu g\ g^{-1}$ [149]. All the cores are distinguished by a significant or minor excursion to isotopically light values of Cd at one or more depths in the core. The Cd isotopes and concentrations of the solid fractions show a mostly positive relationship down core, except for the core from the deep Argentine basin (station 18). The coastal site (station 24) is characterized by the most isotopically heavy core-top values (~0.40‰) relative to the other core-top samples. Station 24 shows the least variability down core for Cd concentrations and Cd isotopes. The Cd concentrations in the down core sediments from station 24 ranged from $0.11\,\mu g g^{-1}$ to $0.24\,\mu g\,g^{-1}$. Cadmium isotopic compositions for all samples from station 24 varied from $\delta^{114/110}\mathrm{Cd} = -0.33 \pm 0.04\,‰$ to $0.71 \pm 0.06\,‰$, with the largest shift to isotopically light isotopes of Cd at 21 cm.

Table 4.2: Cadmium concentrations and isotope compositions of sediments from a transect of shallow multi-cores obtained from the Argentine Continental Margin and Deep Basin, along with TOC (wt%), $CaCO_3$ (wt%), and major and trace metal concentrations data

Depth interval (cm)	[Cd] (µg g^{-1})	$\delta^{114/110}Cd_{NIST}$ (‰)	2σ	TOC (%)	1σ	$CaCO_3$ (wt. %)	1σ	[V] (µg g^{-1})	[U] (µg g^{-1})	[Mo] (µg g^{-1})
Station 18, deep Argentine Basin, -40.001'N, -42.416'E, 5156 m (water depth)										
0.5	0.10	0.16	0.08	0.97	0.25	0.26	0.23	102.55	1.75	1.42
1.5	0.08	-0.02	0.07	0.85	0.23	0.08	0.03	93.08	1.97	1.94
2.5	0.07	0.03	0.08	0.81	0.24	0.09	0.13	117.95	1.83	3.71
3.5	0.06	-0.01	0.13	0.80	0.24	0.05	0.13	118.45	1.93	3.05
7	0.06	-0.08	0.16	0.82	0.24	0.01	0.13	113.97	1.96	0.77
9	0.05	-0.02	0.09	0.64	0.24	0.01	0.13	112.16	1.95	0.69
13	0.05	-0.03	0.09					112.69	1.98	0.68
15	0.05	-0.03	0.10	0.38	0.24	-0.01	0.13	105.71	1.92	0.66
19	0.04	-0.08	0.29	0.31	0.24	-0.01	0.13	113.87	2.15	1.17
27	1.62	-0.01	0.05	0.67	0.24	0.00	0.13	186.21	3.94	0.87
29	3.31	0.30	0.06					199.28	11.60	1.60
30	0.52	0.31	0.08					150.46	11.54	1.67
33	0.23	0.23	0.05					111.14	9.56	1.11
35	0.18	0.20	0.07					136.11	9.05	1.45
Station 22, Shelf, -36.538'N, -53.102'E, 1483 m (water depth)										
0.5	0.17	-0.06	0.08	4.21	0.25	7.27	1.42			
1.5	0.21	0.06	0.07	3.97	0.25	8.48	1.42	81.37	1.87	1.12
2.5	0.26	0.25	0.06	3.66	0.25	8.52	1.42	85.20	2.44	1.22
3.5	0.23	0.08	0.07	3.92	0.25	8.61	1.42	83.39	2.83	1.29
5.5	0.23	0.23	0.07	3.75	0.25	8.61	1.42	85.77	2.61	1.35
7	0.18	-0.02	0.07	3.50	0.25	7.90	1.42	81.25	2.47	1.28
9	0.21	0.02	0.06					81.97	3.23	1.73
13	0.24	0.11	0.07					81.60	2.87	1.44
15	0.28	0.12	0.08	3.34	0.25	9.33	1.42	81.25	3.65	1.41
17	0.36	0.28	0.06	3.41	0.25	8.50	1.42	82.61	3.98	1.43
19	0.43	0.40	0.08					82.10	4.17	1.78
21	0.40	0.19	0.06					82.06	4.47	2.19
23	0.35	0.13	0.07	3.46	0.25	9.50	1.42	81.70	4.25	2.17
25	0.36	0.12	0.05					83.00	4.00	2.14

Table 4.2: continued

Depth interval (cm)	[Cd] (µg g^{-1})	$\delta^{114/110}Cd_{NIST}$ (‰)	2σ	TOC (%)	1σ	$CaCO_3$ (wt. %)	1σ	[V] (µg g^{-1})	[U] (µg g^{-1})	[Mo] (µg g^{-1})
Station 23, Continental slope, -36.338'N, -53.337'E, 705 m (water depth)										
0.5	0.25	0.09	0.07	1.68	0.10	2.09	0.18	49.06	1.48	0.77
1.5	0.28	0.21	0.07	2.08	0.08	1.91	0.04	51.03	1.61	0.76
2.5	0.27	0.17	0.07	1.47	0.10	1.80	0.17	50.03	1.67	0.75
3.5	0.27	0.23	0.06	1.51	0.11	1.87	0.24	55.20	1.73	0.97
4.5	0.31	0.25	0.05	1.50	0.11	1.88	0.26	57.04	1.86	1.17
5.5	0.31	0.07	0.08	1.57	0.10	2.36	0.18	55.90	2.11	1.11
7	0.28	-0.02	0.05	1.56	0.10	2.67	0.18	56.47	2.16	1.24
9	0.29	0.03	0.06	1.26	0.10	3.01	0.18	55.55	2.17	1.49
11	0.42	0.27	0.07					49.26	2.49	1.36
17	0.28	0.24	0.05	1.56	0.10	3.92	0.18	51.89	2.84	2.16
19	0.31	0.31	0.05					59.00	3.10	3.19
21	0.30	0.27	0.05	1.75	0.10	4.33	0.18	57.70	3.13	3.96
25	0.34	0.29	0.05	1.98	0.10	4.85	0.18	62.47	2.91	4.50
Station 24, Argentine coast, -36.000'N, -54.000'E, 60 m (water depth)										
0.5	0.15	0.40	0.07	0.39	0.02	-0.02	0.03	46.62	1.29	0.38
2.5	0.16	0.44	0.06	0.13	0.02	-0.08	0.03	73.16	1.36	0.46
3.5	0.15	0.57	0.06	0.11	0.02	0.12	0.03	63.40	1.25	0.39
4.5	0.14	0.51	0.06	0.13	0.02	0.09	0.03	48.64	1.21	0.38
5.5	0.15	0.71	0.06	0.23	0.02	0.01	0.03	50.51	1.24	0.38
7	0.17	0.21	0.06	0.17	0.02	0.12	0.03	51.51	1.52	0.41
9	0.12	0.22	0.04	0.48	0.02	0.12	0.03	49.55	1.40	0.39
11	0.11	0.24	0.08	0.18	0.02	0.68	0.03	44.27	1.57	0.43
17	0.24	0.34	0.05	0.18	0.02	2.89	0.03	46.60	2.09	0.82
21	0.11	-0.33	0.04							
25	0.11	0.12	0.06							
27	0.11	-0.25	0.04							

Table 4.2: continued

Depth interval (cm)	[Mn] (mg g^{-1})	[Cr] (µg g^{-1})	[Co] (µg g^{-1})	[Ni] (µg g^{-1})	[Cu] (ng g^{-1})	[Th] (µg g^{-1})	[Re] (ng g^{-1})
Station 18, deep Argentine Basin, -40.001'N, -42.416'E, 5156 m (water depth)							
0.5	1.78	32.22	15.80	34.11	88.13	7.74	0.12
1.5	2.25	38.60	18.88	42.48	104.48	8.69	0.12
2.5	2.45	39.28	20.53	42.34	99.31	7.79	0.12
3.5	1.96	35.32	19.95	37.43	97.23	8.37	0.11
7	0.78	45.77	12.61	25.10	94.67	8.16	0.12
9	0.67	36.28	11.86	20.99	84.32	8.42	0.12
13	0.81	45.90	14.86	20.57	79.68	8.81	0.12
15	0.95	38.74	19.44	24.13	68.57	9.21	0.13
19	1.61	41.45	20.72	28.27	54.49	10.00	0.13
27	0.93	54.24	13.26	29.96	144.94	11.18	
29	0.52	55.74	15.92	42.97	80.60	11.75	
30	0.52	49.47	16.83	44.69	53.41	11.92	
33	0.46	41.38	17.49	46.43	44.33	11.05	
35	0.49	45.92	18.68	50.69	49.31	10.79	
Station 22, Shelf, -36.538'N, -53.102'E, 1483 m (water depth)							
0.5							
1.5	0.40	43.84	7.09	29.17	32.78	6.11	0.07
2.5	0.40	43.79	7.31	29.67	33.87	6.27	0.09
3.5	0.39	47.00	7.33	29.68	34.05	6.29	0.10
5.5	0.41	49.53	7.55	29.85	34.75	6.36	0.11
7	0.38	46.85	7.00	28.24	33.13	6.22	0.10
9	0.39	46.32	7.04	29.11	33.82	6.45	0.10
13	0.38	45.20	7.04	27.92	32.40	6.45	0.09
15	0.39	43.56	6.98	27.28	31.45	6.36	0.11
17	0.39	45.77	7.01	27.36	31.93	6.31	0.12
19	0.38	42.67	6.93	27.45	31.77	6.30	0.13
21	0.38	44.19	6.90	28.33	32.34	6.22	0.15
23	0.38	44.52	6.92	28.24	32.65	6.37	0.15
25	0.39	46.01	7.07	28.75	33.43	6.44	0.14

Table 4.2: continued

Depth interval (cm)	[Mn] (mg g^{-1})	[Cr] (µg g^{-1})	[Co] (µg g^{-1})	[Ni] (µg g^{-1})	[Cu] (ng g^{-1})	[Th] (µg g^{-1})	[Re] (ng g^{-1})
Station 23, Continental slope, -36.338'N, -53.337'E, 705 m (water depth)							
0.5	0.43	33.82	6.01	18.11	13.03	5.66	
1.5	0.09	33.30	6.03	18.78	12.85	5.97	
2.5	0.19	36.55	6.19	18.29	12.55	5.72	
3.5	0.23	36.73	6.55	18.96	12.64	5.70	
4.5	0.17	34.09	6.60	19.03	12.62	5.80	
5.5	0.23	36.60	6.64	18.95	12.37	7.13	
7	0.38	39.07	6.42	19.91	13.07	6.22	
9	0.30	32.71	5.86	18.68	11.89	6.07	
11	0.38	31.55	5.93	18.96	12.01	5.91	
17	0.44	35.31	5.98	19.47	12.83	5.87	
19	0.43	33.88	6.25	20.19	13.10	6.59	
21	0.40	33.41	5.98	20.04	12.95	5.54	
25	0.25	34.69	6.27	21.27	14.22	5.44	
Station 24, Argentine coast, -36.000'N, -54.000'E, 60 m (water depth)							
0.5	0.36	23.88	4.85	5.93	4.84	4.57	0.10
2.5	0.54	41.97	7.03	7.74	5.83	4.87	0.07
3.5	0.49	37.81	6.10	7.08	5.72	4.22	0.04
4.5	0.39	30.83	4.85	6.07	5.16	4.69	0.08
5.5	0.41	30.25	4.98	6.12	5.16	4.12	0.03
7	0.41	33.77	5.05	6.38	5.09	5.34	0.02
9	0.38	30.28	4.68	5.74	4.58	4.35	0.06
11	0.35	30.36	4.35	5.62	4.66	4.61	0.03
17	0.35	32.35	4.37	6.22	4.85	5.08	0.23

Table 4.2: continued

Depth interval (cm)	[Al] (mg g^{-1})	[Fe] (mg g^{-1})	[Mg] (mg g^{-1})	[Ca] (mg g^{-1})	[Ba] (mg g^{-1})	[Sr] (µg g^{-1})	[Zn] (µg g^{-1})
Station 18, deep Argentine Basin, -40.001'N, -42.416'E, 5156 m (water depth)							
0.5	74.39	38.60	11.05	25.07	1.00	181.3	59.1
1.5	75.88	40.37	11.72	14.44	1.08	187.3	9.4
2.5	75.56	40.45	11.47	12.46	1.00	177.7	14.5
3.5	73.98	41.20	11.43	10.96	0.98	163.7	17.1
7	76.60	39.89	11.68	11.64	1.10	207.4	15.0
9	77.85	41.37	11.38	15.39	1.04	206.0	19.9
13	77.40	40.50	11.19	11.79	1.03	199.2	9.4
15	80.41	44.90	11.91	11.04	1.02	203.5	8.9
19	87.99	46.69	13.00	10.13	0.89	162.9	9.5
27	93.90	60.13	14.18	9.16	0.57	154.5	21.0
29	91.37	44.29	13.56	22.58	0.53	144.9	69.1
30	96.56	45.87	13.54	9.39	0.57	149.1	61.6
33	85.96	39.01	11.02	9.87	0.57	143.6	23.9
35	87.92	41.73	11.93	11.61	0.56	149.7	28.3
Station 23, Continental slope, -36.338'N, -53.337'E, 705 m (water depth)							
0.5	74.47	21.72	6.19	32.37	0.45	274.0	85.6
1.5	72.82	20.42	5.59	30.09	0.44	287.8	9.0
2.5	73.34	21.02	5.28	31.63	0.45	356.0	18.7
3.5	74.17	21.29	5.72	29.93	0.47	369.6	23.0
4.5	75.29	21.82	5.93	31.70	0.46	372.7	16.7
5.5	75.79	22.32	6.09	32.77	0.48	381.9	22.9
7	74.15	21.89	5.92	33.69	0.46	370.8	37.9
9	75.00	21.63	5.07	35.32	0.48	375.5	29.5
11	73.38	21.38	4.96	38.73	0.37	377.0	38.4
17	73.59	21.85	6.05	40.25	0.46	393.7	88.1
19	74.72	22.41	5.44	46.00	0.46	402.2	21.8
21	69.95	21.17	5.50	41.12	0.42	387.9	33.4
25	71.67	22.00	5.38	42.36	0.43	382.9	25.0

The progression to the shelf site (station 23) is marked by a slight increase in the Cd concentration of the core-top ($0.25\,\mu g\,g^{-1}$). The Cd isotopic compositions of the core-top shelf sediments is $\delta^{114/110}Cd = 0.09 \pm 0.07\,‰$. The Cd concentrations of the down core sediments station 23 ranged from $0.25\,\mu g\,g^{-1}$ to $0.42\,\mu g\,g^{-1}$. Cadmium isotopic compositions for all samples from station 23 varied from $\delta^{114/110}Cd = -0.02 \pm 0.05\,‰$ to $0.31 \pm 0.05\,‰$.

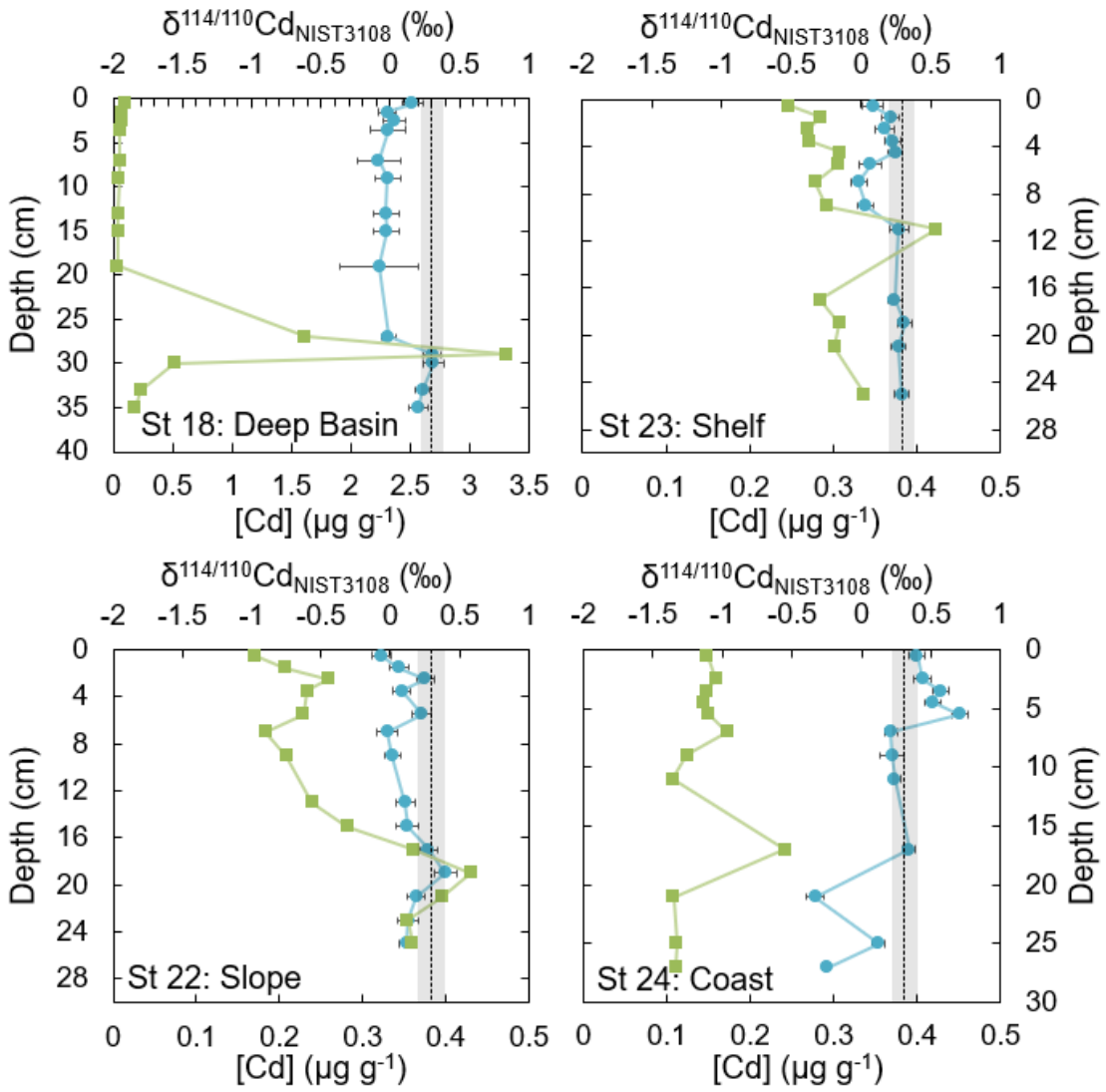


Figure 4.5: Cadmium isotopic compositions (blue, filled circles) and Cd concentrations (green, filled squares) for four sites from a transect of shallow multi-cores obtained from the deep Argentine Basin (St 18), shelf (St 22), continental slope (St 23), and Argentine coast (St 24). The vertical, dashed line $\delta^{114/110}\mathrm{Cd} = 0.3‰$ represents the deep ocean water composition, and the grey shading represents the error on this value. Error bars represent the 2 SE on the sample.

The transition from station 23 to the continental slope (station 22) is characterized by a shift to isotopically lighter values of Cd in the core-tops ($\delta^{114/110}\mathrm{Cd} = -0.06 \pm 0.08‰$) and a slight decrease in Cd concentration ($0.17 \mu g\, g^{-1}$). The sediments at Station 22 are positioned under the oxygen deficient zone (ODZ), supported with the highest TOC value in all the cores (up to 4.2 %). The Cd concentrations of the down core sediments from station 22 ranged from $0.17 \mu g\, g^{-1}$ to $0.43 \mu g\, g^{-1}$. Cadmium isotopic compositions for all samples from station 22 spanned from $\delta^{114/110}\mathrm{Cd} = -0.06 \pm 0.08‰$ to $0.40 \pm 0.08‰$.

The deepest site in this study has a water depth of 5156 m and is in the deep Argentine basin (station 18). The core-top has the lowest Cd concentration of all the measured core-top samples ($0.10\,\mu g\,g^{-1}$). The Cd isotopic composition of the core-top in the deep basin is lighter than the overlying deep-waters, but heavier than the core-top under the ODZ at a value of $\delta^{114/110}\mathrm{Cd} = 0.16 \pm 0.08\,‰$. The Cd concentrations at station 18 ranged from 0.04 to $3.31\mu g\,g^{-}1$, with the largest concentration peak ($3.31\,\mu g\,g^{-1}$) of all the sediment samples at 29 cm. Cadmium isotopic compositions for all samples varied from $\delta^{114/110}\mathrm{Cd} = –0.08 \pm 0.16\,‰$ to $0.31 \pm 0.08\,‰$.

A comparison of the various geochemical parameters obtained from core pore-waters and sediments suggests that Cd concentrations and isotopes in near-surface sediment profiles are sensitive to changes in redox state, detailed in Table 4.3 and shown graphically in Figure 4.6. This argument is supported by the similar trends between Cd, U, and V concentrations (see Table 4.2), where Cd concentrations reach maxima at similar depths as vanadium (V) and uranium (U) in the deep basin (station 18), on the slope (station 22), and on the shelf (station 23). The most significant increase in Cd, V, and U concentrations are associated with peak nitrate reduction at station 18 at 29 cm. The relationship between peak nitrate reduction and Cd isotopes is an important observation in all the cores. The point where nitrate levels diminish to low levels coincides with an excursion to heavier isotopes of Cd, and in the case of station 18, driving the sedimentary Cd isotopic composition to within analytical error of the overlying deep-waters.

Table 4.3: Cadmium concentrations and isotope compositions of core-top waters and pore-waters from a transect of shallow multi-cores obtained from the Argentine Continental Margin and Deep Basin, along with nutrients concentration data

Core-top waters				Porewaters				
Depth interval (cm)	[Cd] (ng g^{-1})	$\delta^{114/110}Cd_{NIST}$ (‰)	2σ	O_2 (µM)	Nitrate (µM)	NH_4^+ (µM)	Silicate (µM)	PO_4 (µM)
Station 18, deep Argentine Basin, -40.001'N, -42.416'E, 5156 m (water depth)								
0.5	0.07	0.26	0.06	199.9	38.2	20.6	167.7	2.3
1.5				139.7				
2.5				121.0	37.3	11.8	170.9	2.3
3.5				98.0				
7				41.6	35.6	12.1	276.8	4.7
9				32.7	32.7	9.7	296.9	4.8
13					29.1	57.9	311.8	5.0
15					21.3	43.8	323.8	7.8
19					15.4	33.8	331.1	8.6
27					1.9	30.9	349.4	12.5
30					1.5	34.4	356.8	12.9
Station 22, Shelf, -36.538'N, -53.102'E, 1483 m (water depth)								
0.5	0.06	0.25	0.05	186.7	13.6	2.6	119.5	2.3
2.5				nd	2.2	21.8	211.1	11.0
3.5				nd	1.5	30.0	122.7	10.7
7				nd	2.2	52.1	240.0	10.6
9				nd	1.5	52.6	223.5	10.0
15				nd	1.3	73.8	291.9	12.5
17				nd	1.0	85.3	183.9	14.4
21				nd	0.7	89.7	120.1	15.7
25				nd	0.7	104.2	106.1	15.9

Table 4.3: continued

Core-top waters				Porewaters				
Depth interval (cm)	[Cd] (ng g^{-1})	$\delta^{114/110}Cd_{NIST}$ (‰)	2σ	O_2 (µM)	Nitrate (µM)	NH_4^+ (µM)	Silicate (µM)	PO_4 (µM)
0.5				250.0	3.4	8.9	79.0	12.6
1.5				nd	1.2	16.7	126.3	13.4
2.5				nd	1.7	35.3	135.8	17.1
3.5				nd	0.7	38.1	159.8	17.6
4.5				nd	0.3	47.0	210.6	15.0
7				nd	0.1	61.1	273.1	19.9
9				nd	-0.1	68.5	203.8	22.3
11				nd	0.0	62.9	196.8	15.4
17				nd	-0.1	63.8	109.9	11.8
21				nd	0.1	76.4	106.8	12.4
25				nd	0.1	82.2	131.4	11.8
Station 24, Argentine coast, -36.000'N, -54.000'E, 60 m (water depth)								
0.5				196.6	19.9	4.2	75.3	5.3
3.5				nd	4.7	36.3	63.8	5.6
4.5				nd	3.6	36.0	52.4	3.4
5.5				nd	1.7	35.0	55.1	2.7
7				nd	1.6	33.0	44.7	2.2
9				nd	1.1	29.9	35.0	2.4
11				nd	0.8	25.8	32.4	2.0

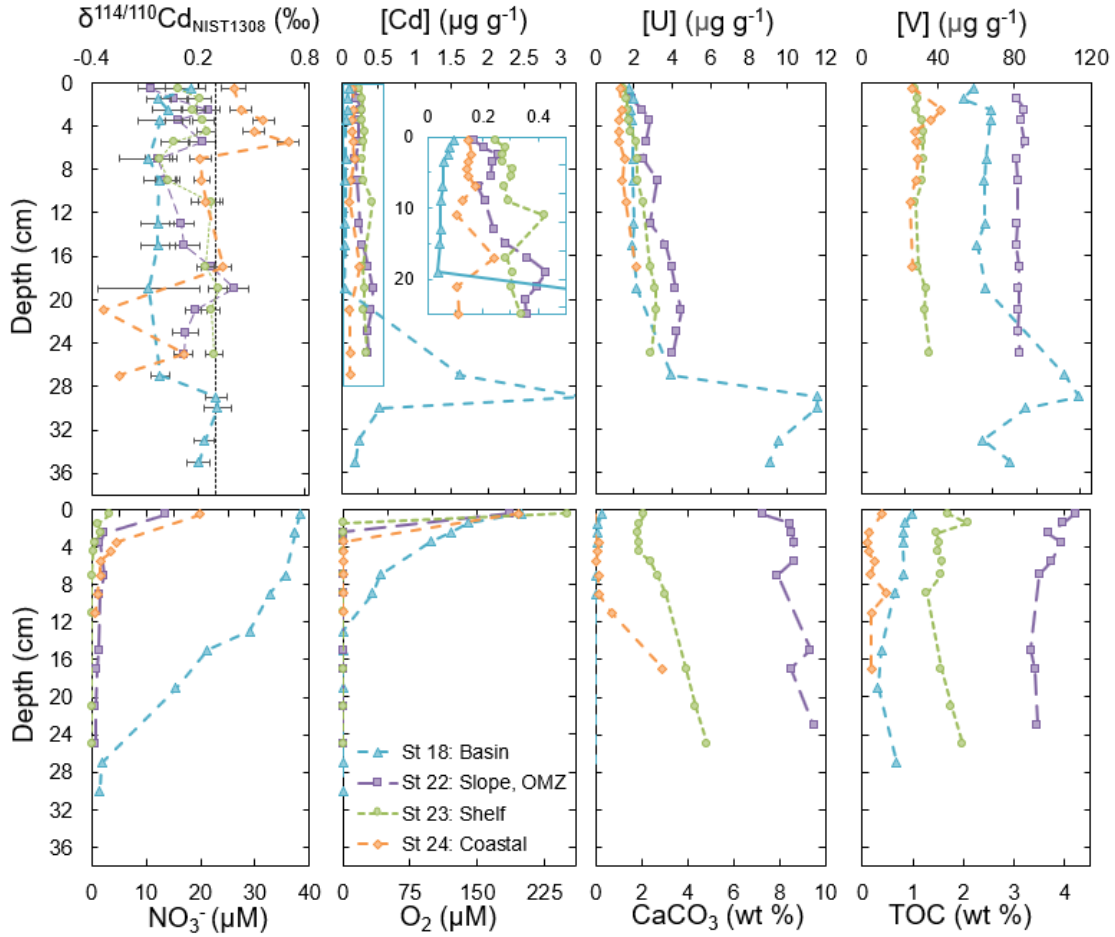


Figure 4.6: Down core sediment profiles of cadmium isotopic compositions and cadmium, uranium, vanadium, calcium carbonate, and total organic carbon concentrations, along with dissolved oxygen and nitrate concentrations in the pore-waters, from a transect of shallow multi-cores obtained from the coast (orange diamond), continental shelf (green circles), slope (purple squares), and deep basin (blue triangle) of the Argentine Basin. The vertical dashed line $\delta^{114/110}\mathrm{Cd} = 0.3‰$ represents the deep ocean water value. Error bars for the Cd isotope measurements represent the 2 SE on the measurement.

4.4.4 Cd concentrations and isotope compositions of water and near-surface sediment samples from the North Atlantic

The water and sediment results from the South Atlantic dataset were compared with samples collected and measured from the deep basin in the North Atlantic Ocean during a routine sampling trip with the Bermuda Atlantic Time Series (BATS) study. Water samples from between 200 m and 4500 m were measured, with results detailed in Table 4.4 and shown graphically in Figure 4.7. The behaviour of Cd through the water column in the North Atlantic was similar to that observed in all the ocean basins, with biological uptake

Table 4.4: Cadmium concentrations and isotope compositions of waters and sediments from the BATS site near Bermuda in the North Atlantic

Water Depth (m)	[Cd] (nmol kg^{-1})	$\delta^{114/110}Cd_{NIST}$ (‰)	±2SD
200	0.01	1.21	0.14
400	0.02	0.34	0.11
800	0.27	0.42	0.09
1000	0.22	0.47	0.06
1200	0.19	0.49	0.05
2000	0.19	0.43	0.15
3000	0.20	0.43	0.08
4500	0.36	0.46	0.04
Sediment grab samples underlying this station			
	0.14*	0.13	0.06
	0.14*	0.11	0.07
	0.15*	0.19	0.05

**Cd concentration is in ug g^{-1}*

preferentially removing light isotopes of dissolved Cd in the surface-waters, bacterial degradation in the remineralization zone shifting the isotope composition of dissolved Cd to isotopically lighter values, and the deep-waters having a relatively homogenous Cd concentration and isotopic composition (~0.4‰) [59]. The Cd concentrations exhibit an increase with depth from $0.01\,\mathrm{nmol\,kg^{-1}}$ in the surface-waters at 200 m to $0.36\,\mathrm{nmol\,kg^{-1}}$ at 4500 m. The average Cd concentration in the deep-waters (below 800 m) was $0.23\,\mathrm{nmol\,kg^{-1}}$. The Cd isotopic compositions of the water samples below 800 m varied from $\delta^{114/110}\mathrm{Cd}$ values of 0.42 ± 0.09 ‰ to 0.49 ± 0.06 ‰, with the average value of 0.45 ± 0.15 ‰. The Cd concentrations and isotopic compositions of the water samples agrees well with previous studies by Boyle et al. (2012) at the same location (see Figure 4.7) [59].

The sedimentary Cd concentrations and isotopic compositions of sediment grab samples from the same location exhibited a minimal range, as expected. The Cd concentrations varied from $0.04\,\mathrm{\mu g\,g^{-1}}$ to $0.05\,\mathrm{\mu g\,g^{-1}}$. The Cd isotopic compositions of

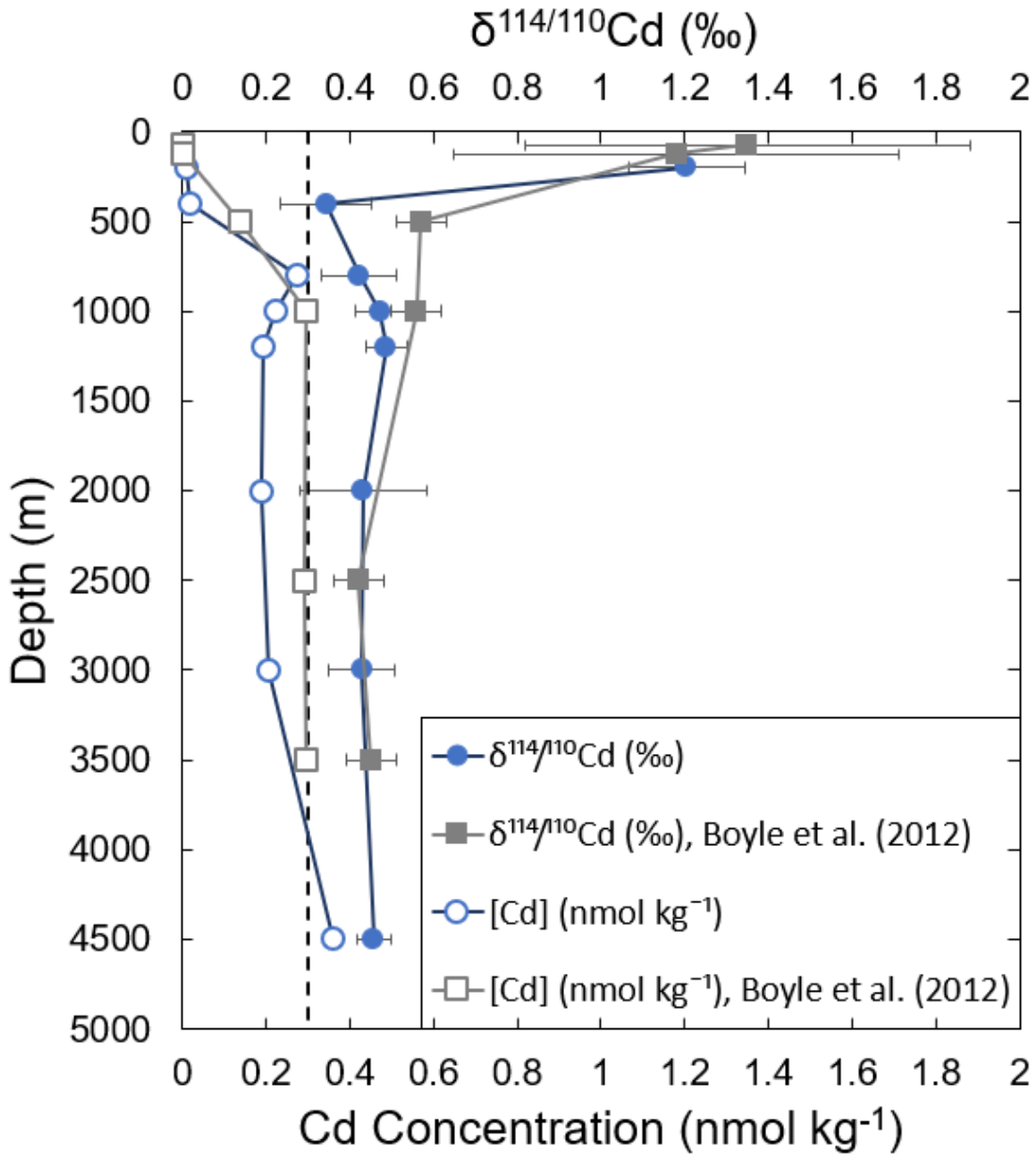


Figure 4.7: Vertical water column profiles of cadmium isotopic compositions and cadmium concentrations from the BATS site in the North Atlantic from this study and from Boyle et al (2012) [59]. The vertical dashed line $\delta^{114/110}\mathrm{Cd} = 0.3‰$ represents the average deep ocean water value. Error bars for the Cd isotope measurements represent the 2 SE on the sample.

the sediment grab samples were all within analytical error of each other with an average $\delta^{114/110}\mathrm{Cd}$ of $0.14 \pm 0.07‰$. The isotopic offset between the near-surface sediments and the overlying bottom-waters is $\Delta^{114/110}\mathrm{Cd}_{\mathrm{core\,top\,sed-deep\,water}} = -0.32 \pm 0.07‰$. This value is similar to the results from the South Atlantic.

4.5 Discussion

4.5.1 Cause of the observed isotope fractionation effect in the water column

The Cd concentrations and isotopic compositions of the surface-waters in the global oceans are driven by biological uptake. The surface-waters in the South Atlantic at 40°S in the water column profiles exhibit large variability for Cd concentrations and isotopic compositions, resulting from the near-quantitative removal by marine phytoplankton (see Figure 4.8). Previous authors have attributed the observed trend in the surface-waters to a Rayleigh isotope fractionation effect. The use of this equation assumes that incremental removal by a fractionation process, with a constant fractionation factor, is occurring from a well-mixed reservoir. In this case, the removal is by biological uptake, with a preferential incorporation of the light isotopes of Cd, leaving the remaining, dissolved Cd fraction isotopically heavy [57, 63, 147]. This process is best observed in the deep basin at station 18. The surface-waters (at 47 m) have the lowest Cd concentration ($0.01\,\mathrm{nmol\,kg^{-1}}$) and the heaviest Cd isotopic composition (~3.01‰) in this dataset. As remineralization begins to break down the organic material and release the Cd, the dissolved Cd concentration increases ($0.09\,\mathrm{nmol\,kg^{-1}}$) and the Cd isotopic composition returns to lighter values (~1.05‰) at 95 m. The particulate Cd at a similar depth (150 m) has a lower Cd concentration ($0.01\,\mathrm{nmol\,kg^{-1}}$) and lighter Cd isotope value compared to the dissolved fraction at a similar depth, with the particulate phase measuring $\delta^{114/110}\mathrm{Cd}$ = 0.15 ± 0.05‰. These results suggest that a large fraction of the total Cd is still retained in organic material at 150 m [55, 69, 79], as organic matter is likely to be associated with lighter Cd isotope values [57, 63, 147]. Studies have reported that below 200 m water depth, 25 to 65% of Cd remains associated with organic ligands [55, 69, 80].

The application of a Rayleigh isotope fractionation equation was applied to the results in this study (see Figure 4.9). The starting Cd concentration ($0.56\,\mathrm{nmol\,kg^{-1}}$ at 742 m) and isotopic composition (~0.33‰) is set at a depth where the Cd isotopes are representative of the deep-waters. Cadmium removal is assumed to be by marine phytoplankton taking up isotopically light Cd. This equation assumes that the incorporated Cd is no longer

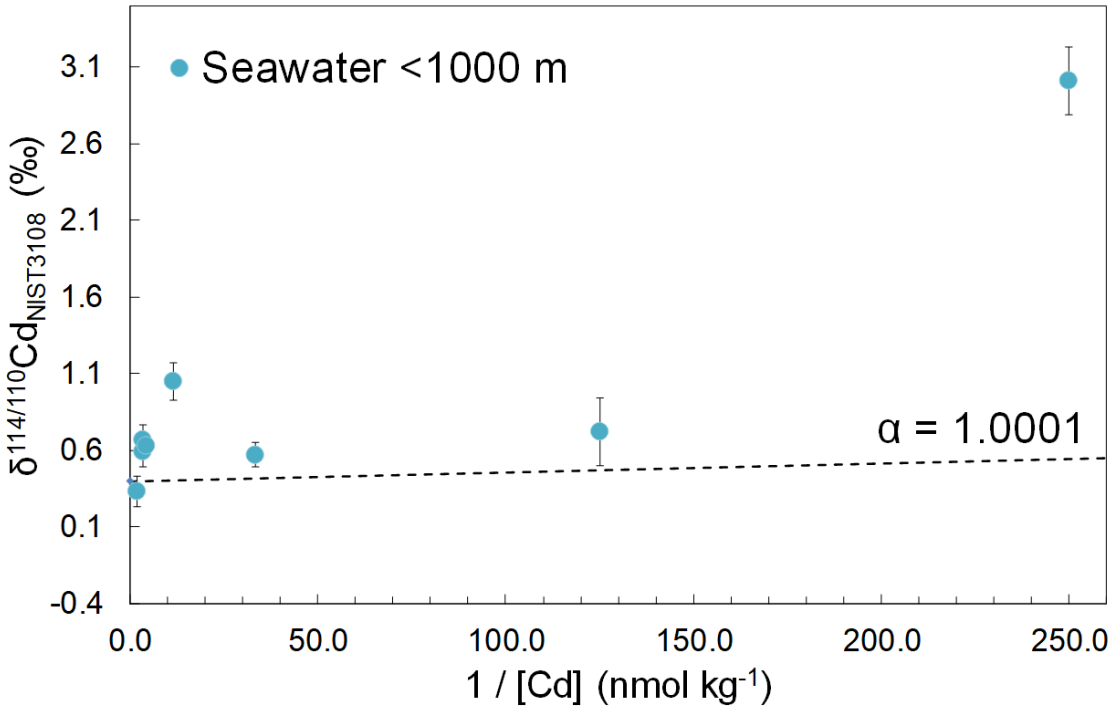


Figure 4.8: Cadmium isotopic compositions relative to 1/Cd concentrations of the waters (above 1000 m water depth) at all three stations in this chapter, with a fractionation factor of 1.0001.

isotopically exchanging with the dissolved Cd in the system. As removal continues, the cumulative Cd within marine microorganisms will tend towards the starting seawater composition (~0.3‰), resulting in a significantly fractionated dissolved pool of Cd. The Rayleigh trend lines that best fit the data support a fractionation factor of $\alpha = 1.0001$, indicating that the study site is best described with a closed-system Rayleigh fractionation model with a fractionation factor of 1.0001. This alpha value agrees with the proposed range by Ripperger et al. (2007) and Abouchami et al. (2014) for the global ocean Cd isotope dataset [31, 54]. Likewise, this is within the range of values that Abouchami et al. (2014) reported for different regions of the sub-Antarctic [54]. These values are included on Figure 4.9. It is worth noting that one data point does not agree with the trend, and is providing evidence for open system behaviour.

However, the fractionation factor is variable amongst the different ocean basins. This variability may be driven by small differences in the phytoplankton communities' structure and overall local physical, chemical, and biological processes [25]. Likewise, the mechanism for isotope fractionation may be different in other ocean basins. Previous

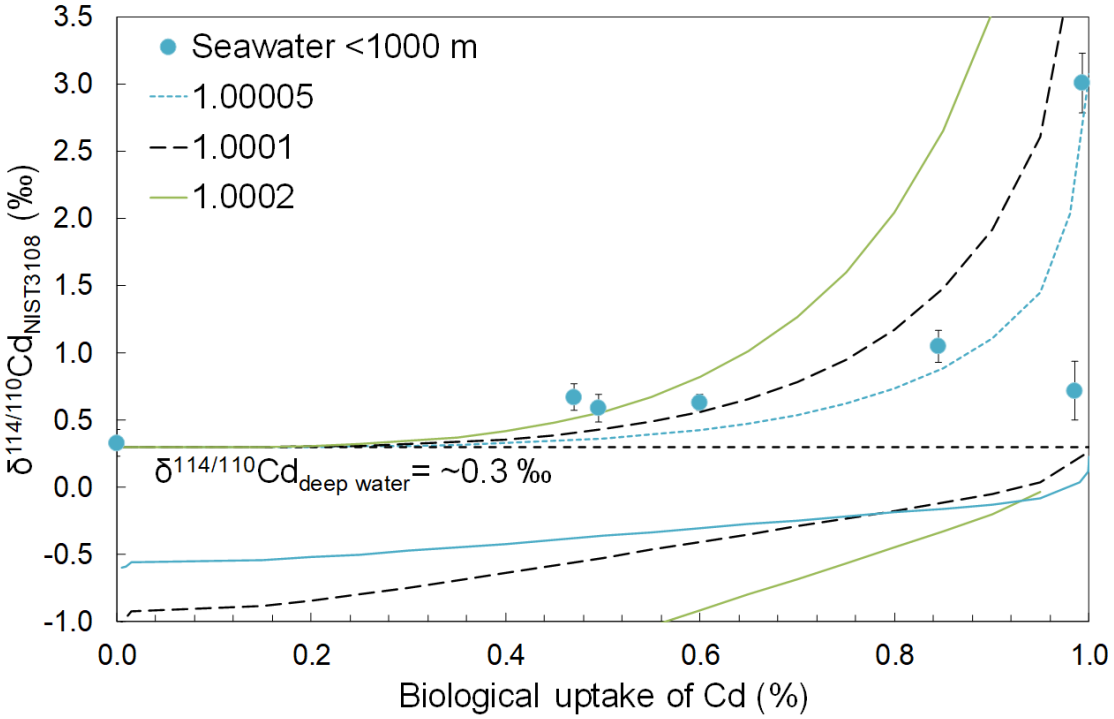


Figure 4.9: Application of a closed-system Rayleigh fractionation equation for Cd removal during biological uptake in the surface-waters of the South Atlantic Ocean at 40°S for all water samples above a water depth of 1000 m, with a fractionation factor of 1.0001. Additionally, superimposed are fractionation factors observed in the global ocean Cd isotope dataset, as reported by Abouchami et al. (2014) [54].

authors have attributed the deviation from a system that is best described as a closed-system Rayleigh fractionation model to external inputs of Aeolian [27], rivers, or seasonal phytoplankton blooms [25, 54], causing Cd behaviour to reflect more of an open-system steady state model [26, 54, 147].

The Cd concentrations and isotopic compositions in the deep-waters remains relatively uniform in the vertical water column and within the basin. The deep-water structure is formed from waters originating from the Southern Ocean and the North Atlantic, reflecting their own signatures in nutrient concentrations. At station 18, a decrease in Cd concentrations between approximately 2000-3500 m reflects the difference in Cd concentrations in the NADW compared to the overlying AAIW and the underlying AABW. Cadmium exhibits a strong correlation with phosphate concentrations, resulting from its association with marine phytoplankton in the surface-waters. The relationship between dissolved Cd and PO_4^{3-} and Cd and NO_3^- for deep-waters below 500 m have

an R-squared value of 0.97, confirming strong correlation between Cd and PO_4^{3-} and Cd and NO_3^- in the South Atlantic (see Figure 4.10). This agreement persists, despite variations in the Cd concentrations in the different water masses.

Hydrothermal vents are known to be a localized sink for CdS complexes [93]; however, a hydrothermal signal was not recorded in the Cd concentrations and Cd isotopes above the Mid-Ocean Ridge (station 12). The results are in good agreement between station 12 and station 18, supporting a well-mixed ocean basin. The Cd concentration and isotopic composition at a depth of 198 m ($0.03\,\mathrm{nmol\,kg^{-1}}$ and 0.57‰) are similar to those for samples from the same depth at station 18 ($0.30\,\mathrm{nmol\,kg^{-1}}$ and 0.67‰). Despite sampling occurring above the ridge, no resolvable fractionation from the surrounding deep-water is observed at this site. A hydrothermal signal would generate decreased dissolved Cd concentrations with a preferential removal of light Cd isotopes with sulphides [93], driving the remaining dissolved Cd isotopes to heavier values relative to the deep-water signal (~0.3‰). The lack of any such signal near the ocean floor at station 12 suggests that any hydrothermal signal is a short-lived signal, at least in this location at the time of sampling.

4.5.2 Cadmium isotopic composition in the global ocean basins

A compilation of all published Cd isotopic compositions of all seawater from the Atlantic, Pacific, and Southern Oceans is shown in Figure 4.11. The high variability for Cd isotopes at low concentrations reflects biological uptake and fractionation in the surface-waters from uptake of dissolved Cd by marine phytoplankton. Alternatively, the significant Cd isotopic variations in the surface-waters at low Cd concentrations may reflect analytical limitations and should be examined further. The deep-water remains at a relatively uniform Cd isotopic composition (~0.3‰).

4.5.3 Cadmium isotopic composition in the global deep ocean basins

A relatively uniform $\delta^{114/110}\mathrm{Cd}$ value of 0.33 ± 0.05 ‰ has been recorded for global ocean basins; however, subtle differences do exist between different oceanic regions [31, 54, 61]. Xue et al. (2013) observed a trend towards heavier Cd isotope signatures

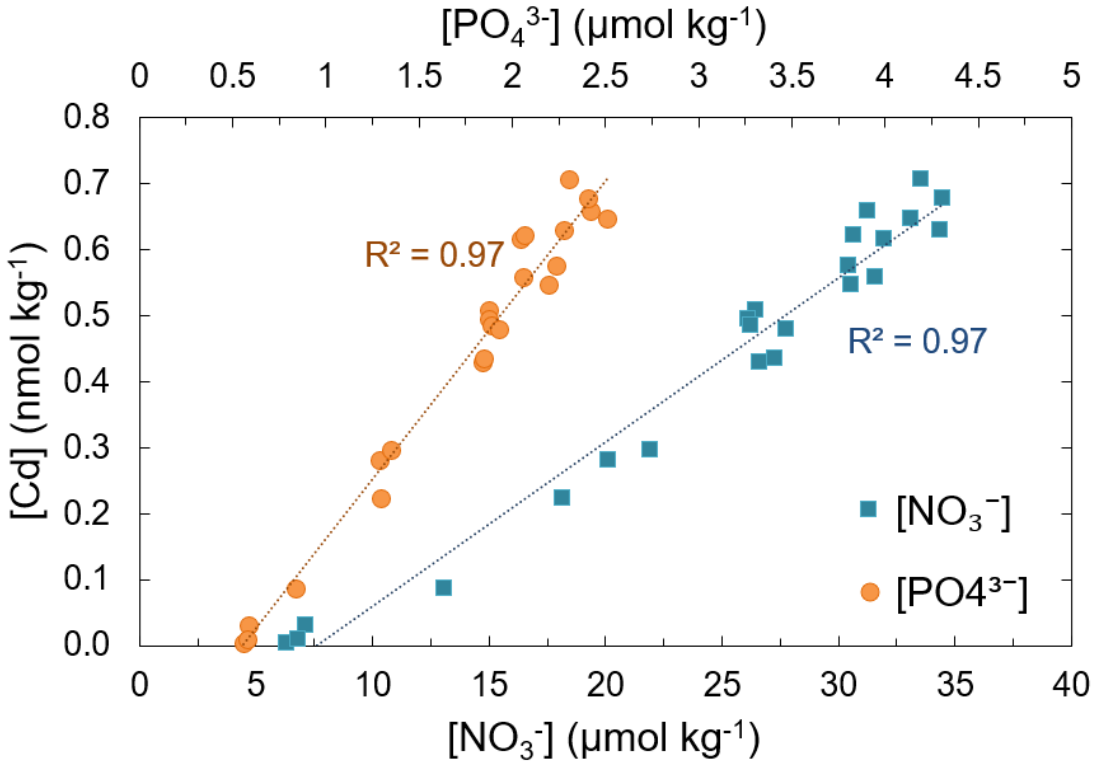


Figure 4.10: Dissolved Cd concentrations compared to dissolved PO_4^{3-} and NO_3^- concentrations for all the water samples below a depth of 500 m, along with the resulting R-square value of 0.97 for dissolved PO_4^{3-} and NO_3^-.

in the younger, North Atlantic deep-waters compared to the Southern and Pacific deep-waters [61]. The authors attributed this difference to the advection of a surface water signal, as the surface-waters in these regions tend to be slightly isotopically heavier from biological removal compared to the other basins. The samples from this thesis provide an ideal location to look at subtle differences in the water masses and to trace the possible signature of NADW during its transit southwards. At Station 18, the deep-water can be grouped into two distinct pools: Southern Ocean and North Atlantic. The water masses from the North Atlantic Ocean, between ~1500 m to ~3000 m depths are characterized by slightly decreased Cd concentrations and phosphate concentrations compared to the deep-water at 3000 m from the Southern Ocean. While the Cd isotopic composition is expected to be uniform in the deep-waters, a slightly discernible shift is observed between the two water masses. The Cd isotopic composition of the NADW water mass is heavier (~0.4‰) relative to the deeper, Lower Circumpolar Deep Water (LCDW)

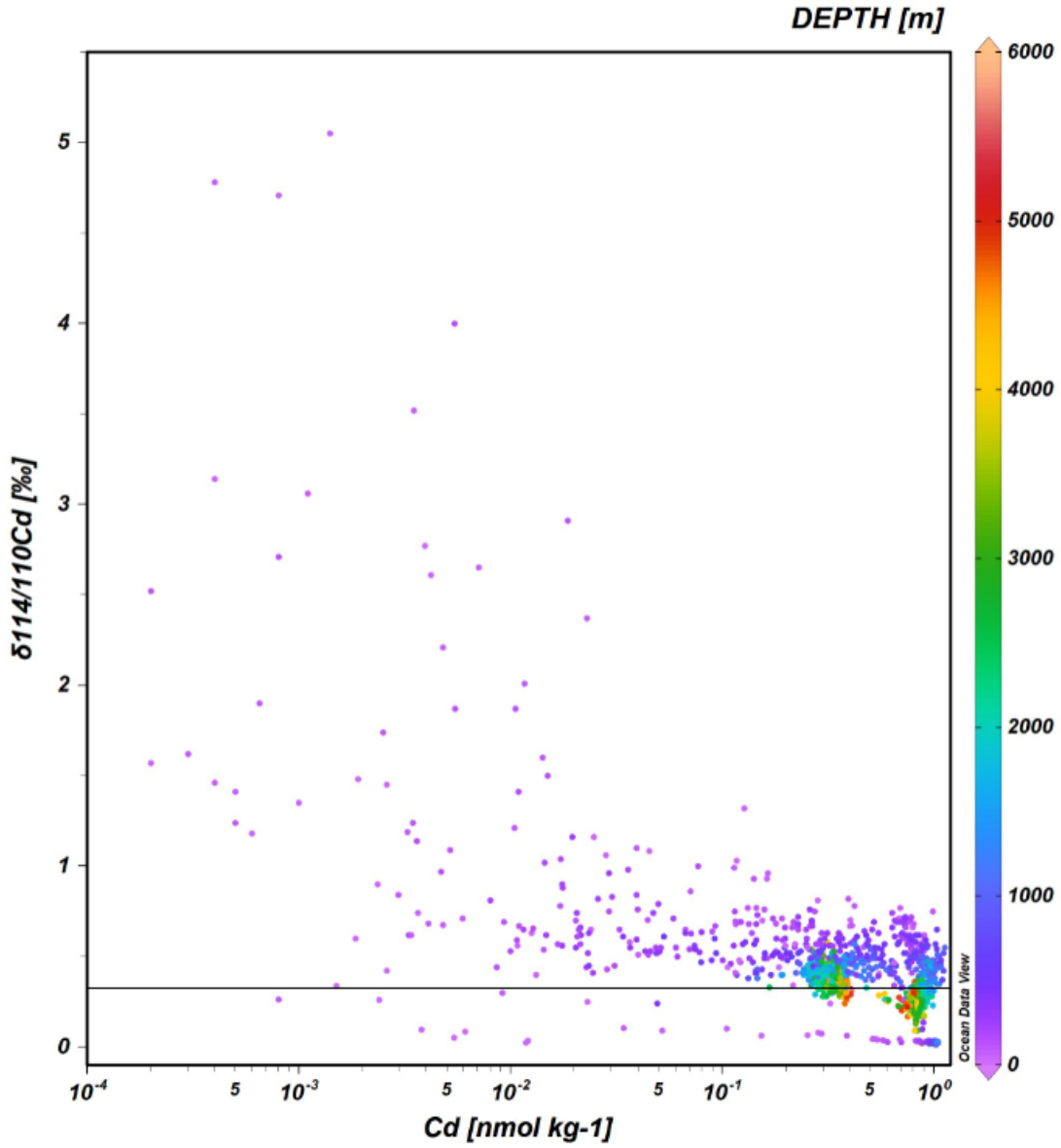


Figure 4.11: Comparison of dissolved Cd concentrations and isotopic compositions in seawater from data that was included in the GEOTRACES 2017 Intermediate Data product [40, 41], along with the data from this study. The colours distinguish water depth [25–28, 31, 60–62, 95–97].

at ~0.3‰. However, the error bars for these water masses overlap, so the magnitude of the fractionation cannot be truly distinguished given analytical uncertainties. This water mass isotopic signature was not observed for the other two stations, because station 21 is on the basin shelf and station 12 is over the Mid-Atlantic Ridge. Consequently, neither profile extended to depths below ~3500 m.

While the Cd concentrations and isotopic compositions are relatively uniform in the global dataset for Cd isotopes for deep-waters, some minor variability is likely from scavenging by oxides and other sinking particulates [28, 85, 86]. It is likely that a very small fraction of Cd will be removed from the seawater and undergo abiotically mediated partitioning into calcite [86] and adsorption to Mn- and Fe-oxides [85]. However, the primary fractions of Cd that reach the benthic-waters are likely associated with organically-bound Cd to refractory ligands and aqueous Cd species, such as $CdCl^{+}$ [55, 79, 80].

4.5.4 Relationship between the sediments and the overlying water column

The sediments collected from the Argentine coast to the deep Argentine basin provide an opportunity to quantify the flux of Cd from the oceans to ocean margin and deep ocean sediments. However, the processes at this critical physical interface are poorly constrained. These study sites are particularly important as the primary burial flux of Cd in the modern ocean occurs at continental marginal environments into suboxic and anoxic sediments [68, 113, 122]. Cadmium removal into oxic and euxinic sediments is reported to be minimal [68, 122]. As mentioned in Chapter 1, suboxic sediments are defined as those sediments that are at depths below where oxygen is the oxidant for bacterial respiration and where nitrate is the primary electron acceptor [119].

The sediments collected from the Argentine coast to the deep Argentine basin exhibit significant gradients in Cd concentrations and isotopic compositions through the cores. The behaviour of Cd in the cores is primarily dictated by the source of Cd exported to the sediments, the extent of Cd removal, the level of oxygen in the benthic-waters, and the depth of nitrate reduction in the sediments.

Our current knowledge on the Cd cycle suggests that the primary sources of Cd exported to the seafloor are aqueous Cd species, such as $CdCl^+$ and Cd associated with sinking organic matter [55, 69, 79, 80]. Other minor sources of Cd include incorporation into calcium carbonates ($CaCO_3$), adsorption to Fe-Mn oxides, and possibly *in situ* precipitation of CdS in the overlying ODZ. The sections below will discuss why dissolved $CdCl^+$ and organically-bound Cd are likely the primary sources of Cd to the sediments.

Relative enrichment of Cd in the sediments

First, the influence of a detrital signal was explored by calculating the relative enrichment of Cd in the sediments using the elemental enrichment factor (EF). In this process, the Cd concentrations were normalized to Th in order to determine the detrital contribution to the sediments, then subsequently compared to the average of the upper continental crust [149], using the following equation:

$$\mathrm{EF_{Cd}} = (\mathrm{Cd/Th})_{\mathrm{sediment\,sample}}/(\mathrm{Cd/Th})_{\mathrm{upper\,continental\,crusts}}$$

where an EF greater than 1 indicates authigenic enrichment of the trace metal and less than 1 implies depletion in the sediments.

In all the near-surface sediment cores, except the deep Argentine basin, the average enrichment factor was 5.1 and ranged between 2.7 and 8.2 (see Table 4.5), supporting an overall authigenic signal with values similar to or above the predicted upper continental crusts values at 0.1 $\mu g\,g^{-1}$ [149]. Cadmium enrichment factors in near-surface sediments from the deep basin exhibit a large range from 0.4 to 32.3. The lowest enrichment factors are observed in the oxic zone of the deep basin core, while the highest enrichment factors are attributed to the Cd enrichment peak at the peak nitrate reduction zone. These differences in enrichment factors are reflected in the Cd isotopic compositions of the sediment samples from the deep Argentine Basin. When enrichment factors are very low, then the Cd isotopic compositions are similar to values of crustal Cd (~0.1‰). Conversely, when enrichment factors are high, then the Cd isotopic compositions are similar to values of the overlying deep-waters (~0.3‰).

For all the sediment cores, the relationship between Cd and other redox-sensitive elements provide support against a solely lithogenic source for these elements in the

Table 4.5: Calculated enrichment factors for select trace metals

Depth interval (cm)	EF [Cd]	EF [U]	EF [Mo]	EF [V]	EF [Fe]
Station 18, deep Argentine Basin, -40.001'N, -42.416'E, 5156 m (water depth)					
0.5	1.4	0.9	1.3	2.6	1.7
1.5	1.0	0.9	1.6	2.1	1.5
2.5	1.1	1.0	3.5	2.9	1.7
3.5	0.8	1.0	2.7	2.7	1.6
7	0.8	1.0	0.7	2.7	1.6
9	0.7	1.0	0.6	2.6	1.6
13	0.6	0.9	0.6	2.5	1.5
15	0.6	0.9	0.5	2.2	1.6
19	0.4	0.9	0.9	2.2	1.6
27	16.5	1.5	0.6	3.2	1.8
29	32.3	4.1	1.0	3.3	1.3
30	5.0	4.0	1.0	2.5	1.3
33	2.4	3.6	0.7	2.0	1.2
35	1.9	3.5	1.0	2.5	1.3
Station 22, Shelf, -36.538'N, -53.102'E, 1483 m (water depth)					
0.5					
1.5	3.9	1.3	1.4	2.6	
2.5	4.7	1.6	1.4	2.6	
3.5	4.3	1.9	1.5	2.6	
5.5	4.1	1.7	1.6	2.6	
7	3.4	1.6	1.5	2.5	
9	3.7	2.1	2.0	2.5	
13	4.2	1.8	1.6	2.5	
15	5.1	2.4	1.6	2.5	
17	6.5	2.6	1.7	2.5	
19	7.8	2.7	2.1	2.5	
21	7.3	3.0	2.6	2.6	
23	6.4	2.7	2.5	2.5	
25	6.4	2.6	2.4	2.5	

**Reference Th concentration data to calculate enrichment factors is 10.3 $\mu g\ g^{-1}$, as detailed in Wedepohl (1995)*

suboxic, marine sediments. The results have lower Mo and U and higher Cd compared to the ratio for Mo:Cd and U:Cd of the upper continental crust [149]. This suggests that another source is the primary export of Cd to the sediments.

Table 4.5: continued

Depth interval (cm)	EF [Cd]	EF [U]	EF [Mo]	EF [V]	EF [Fe]
Station 23, Continental slope, -36.338'N, -53.337'E, 705 m (water depth)					
0.5	5.0	1.1	1.0	1.7	1.3
1.5	5.5	1.1	0.9	1.7	1.1
2.5	5.4	1.2	1.0	1.7	1.2
3.5	5.4	1.3	1.2	1.9	1.2
4.5	6.1	1.3	1.5	1.9	1.3
5.5	4.9	1.2	1.1	1.5	1.0
7	5.1	1.4	1.5	1.8	1.2
9	5.5	1.5	1.8	1.8	1.2
11	8.2	1.7	1.7	1.6	1.2
17	5.5	2.0	2.7	1.7	1.2
19	5.3	1.9	3.6	1.7	1.1
21	6.2	2.3	5.3	2.0	1.3
25	7.1	2.2	6.1	2.2	1.3
Station 24, Argentine coast, -36.000'N, -54.000'E, 60 m (water depth)					
0.5	3.7	1.2	0.6	2.0	
2.5	3.7	1.1	0.7	2.9	
3.5	4.0	1.2	0.7	2.9	
4.5	3.5	1.1	0.6	2.0	
5.5	4.2	1.2	0.7	2.4	
7	3.7	1.2	0.6	1.9	
9	3.3	1.3	0.7	2.2	
11	2.7	1.4	0.7	1.9	
17	5.4	1.7	1.2	1.8	

**Reference Th concentration data to calculate enrichment factors is 10.3 μ g g^{-1}, as detailed in Wedepohl (1995)*

Cd partitioning into carbonates and adsorption onto Fe-Mn oxyhydroxides

The adsorption of Cd onto Fe-Mn oxyhydroxides in pelagic clays and partitioning into marine carbonates is likely to represent a small fraction of the Cd exported to the sediments [68, 86, 110, 113]. The relationship between Cd and $CaCO_3$ was investigated in this study. The percentage of $CaCO_3$ in the cores was highly variable from below detection to 9.5 %. However, marine $CaCO_3$ is unlikely to be an important sink for Cd in the sediments, as Cd concentrations are very low in pelagic calcifying organisms

[11, 32, 86, 100].

Adsorption to Fe-Mn oxyhydroxides as a carrier phase in the deep-waters is unlikely to represent an important source of sedimentary Cd. Dissolved Cd profiles show little variation in global deep-waters ([25, 27, 31, 60–62]), as it is not shown to scavenge onto sinking particulates, as seen for zinc [63]. Similarly, diffusion of seawater is unlikely to be a source of Cd to the pore-waters, as previous studies have confirmed a subsurface peak in pore-water Cd that would act as a barrier to inward diffusion of seawater Cd beyond the core-top layer [110, 150]. Additionally, the Cd isotopic composition of core-top sediments for suboxic sites is lighter than deep ocean seawater by $\delta^{114/110}\mathrm{Cd} = –0.21‰$ on the shelf and -0.36 ‰ on the slope, suggesting that sedimentary Cd must be mostly sourced from another pore-water phase.

In-situ precipitation of CdS species in the overlying ODZ

Oxygen deficient zones produce an additional complexity within the water column, particularly at St 22 on the continental slope. Water samples were not collected in the overlying bottom-waters; however, the sediments have a Cd isotopic composition ($\delta^{114/110}\mathrm{Cd} = –0.064 \pm 0.08‰$) that is lighter than the other core-top samples. Recent studies focused on ODZs have suggested that the production of hydrogen sulphide by sulphate-reducing microbes in short-lived microenvironments where oxygen diffusion is limited results in the formation of CdS complexes [28, 56, 90]. The export of Cd to the seafloor from the formation of CdS particles in the water column is not well constrained. However, this process appears to be limited to ODZs below a threshold concentration of oxygen. The existence of CdS particulates in the water column was not observed in the Peru Margin ODZ [94, 97]. Similarly, in the deep basin (St 18), the sample within the ODZ (at 1990 m) does show a slight decrease in dissolved Cd concentration and a slight shift to isotopically heavier values, but not outside of analytical error of the surrounding water samples. Consequently, the ODZ in the South Atlantic does not appear to be at low enough oxygen concentration to initiate the formation of oxygen-depleted microenvironments for the formation of *in-situ* CdS complexes.

If CdS complexes did form; however, the stability of particulates once below the ODZ is unknown. Oxic particles in the deep-water have a high stability constant and are likely to be preserved and exported to the benthic-waters [151], while the survival of any precipitated CdS likely depends on its size. A recent study by Bianchi et al. (2018) presented a size-resolved particle model using dissolution constants to predict formation of CdS complexes in these microenvironments [90]. The survival of the CdS particulates to the ocean seafloor depends on oxygen levels and size of the particles. Further studies on the Cd concentrations and isotopic compositions of particles in water column are required to investigate the global importance of CdS precipitation on the Cd cycle.

Organically-bound Cd complexes

This leaves organically-bound Cd and lithogenic Cd as the likely source of Cd to the sediments. Dissolved Cd is removed from the surface-waters by marine phytoplankton and is the likely source for any material that is not detrital. This means most of the solid fraction of Cd was once associated with sinking organic material from the surface-waters to the sediments on the coast, continental margin, and in the deep basin. If this is the case, then a relationship should exist between concentrations of Cd and organic carbon.

The expected Cd concentration from marine phytoplankton and detrital contribution can be predicted using the Cd concentration in the upper continental crusts (UCC) from Wedepohl et al. (1995) and the Cd:C ratio of cultured marine phytoplankton from Ho et al. (2003) (see Figure 4.12) [149, 152]:

Detrital [Cd] = [Th] • $[\mathrm{Cd/Th}]_{\mathrm{UCC}}$

Bulk [Cd] = TOC (wt%) • $[\mathrm{Cd/C}]_{\text{Ho et al. (2003)}}$

Total [Cd] = Detrital [Cd] + Bulk [Cd]

The measured Cd concentration for the core-top sediments is lower than would be predicted based on the stoichiometry of marine plankton ($0.016\ \mathrm{ngg^{-1}}$ for Cd:C ratio) and detrital contributions for all the core-tops, except for the core-top from the coast. Also, a weak correlation exists between TOC (%) and Cd concentrations throughout the core. However, these observations do not rule out Cd export to the sediments via association with organic material. Cadmium in the core-top sample from the coastal site is above

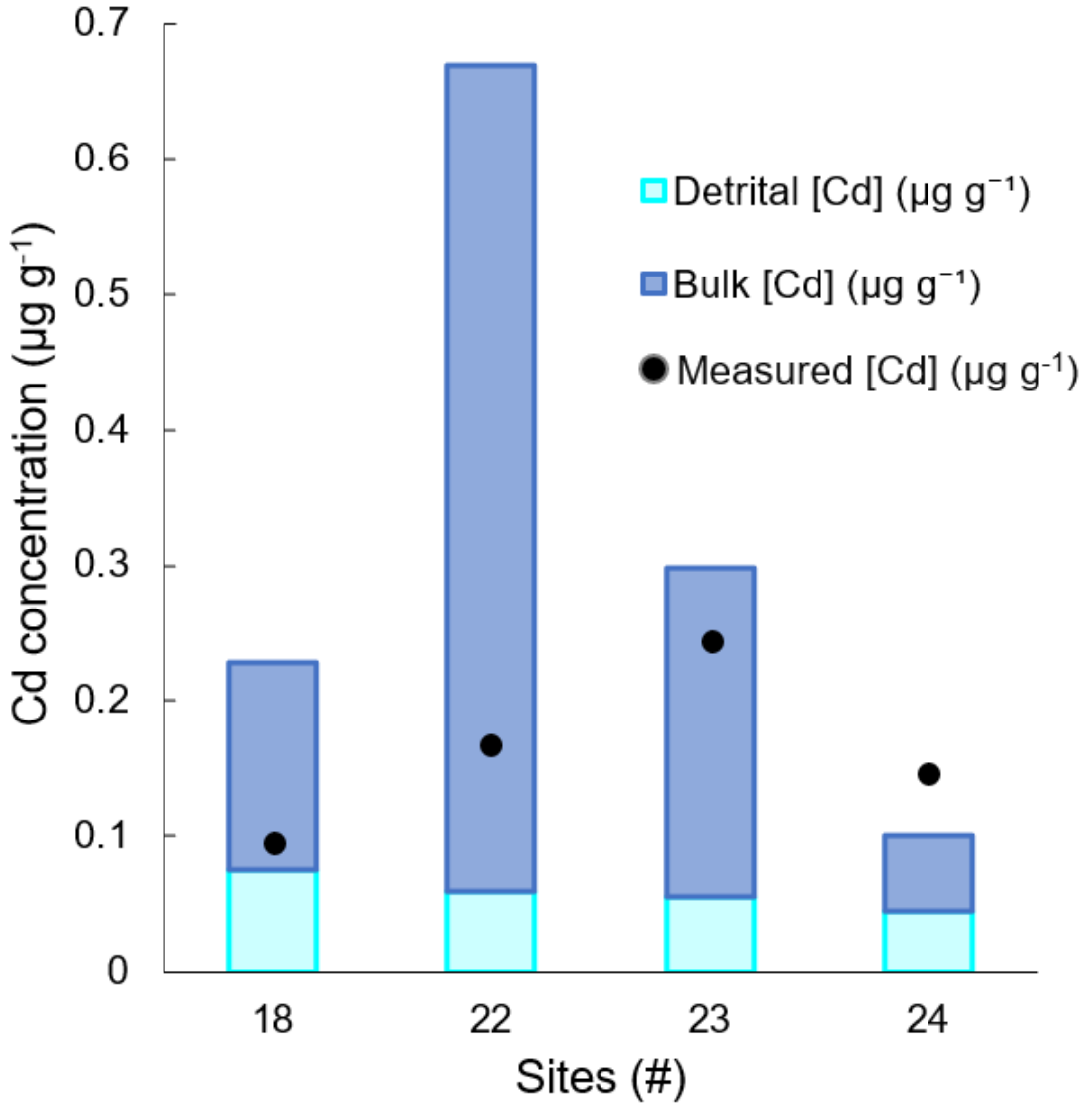


Figure 4.12: Predicted Cd concentration contribution in the samples from sinking organic material and detrital sources compared to the measured Cd concentration in the samples.

the peak remineralization zone in the water column. Consequently, any removal step of dissolved Cd by marine phytoplankton from the surface-waters likely remains mostly intact to the sediment-water interface. Conversely, the core-tops from the continental margin and deep basin sites represent variable degrees of remineralization through the water column, suggesting that organically-bound Cd that reaches the seafloor will likely be below the measured Cd concentration of cultured marine phytoplankton species [152]. It is likely that the relationship between organic material and Cd breaks down within the remineralization zone and during sedimentary aerobic respiration. The released Cd

to the pore-waters after sedimentary aerobic respiration is either preferentially retained in the sediments by formation of a secondary authigenic phase, lost by diffusion to the overlying deep-water column, or exported deeper into the core.

A previous study by McCorkle and Klinkhammer (1991) noted a subsurface excursion to increased pore-water Cd concentrations within suboxic marine sediments off the coast of California, supporting the source to be the release of Cd during the degradation of organic material [150, 153, 154]. The subsurface pore-water peak would cause a diffusion gradient, preventing the inward diffusion of Cd from the seawater, if the pore-water Cd concentrations is greater than the deep-waters. While pore-water Cd concentrations were not measured in this study, the solid fraction at the deep basin site shows a distinct decrease at the top of the core and a shift to isotopically lighter values. This trend supports the degradation of organic material that reach the seafloor, thus leaving the sediments with a Cd isotopic signature of detrital Cd below. The pore-water Cd is either exported deeper into the core or released to the overlying deep-water.

Most likely, pore-water Cd diffuses deeper into the core until it adsorbs to and/or is incorporated within Fe-Mn oxyhydroxides, representing a temporary removal mechanism until reaching depths with suboxic to sulphidic pore-waters. At this depth, Cd will be precipitated as CdS complexes. Cadmium sulphide complexes are known to be stable, unless redox zones are altered [110]. At this zone, pore-water Cd is immobilized into the sediments while dissolved organic carbon remains in the pore-waters, resulting in authigenic enrichment of Cd relative to organic carbon, as can be seen in the deep basin and on the continental slope at depth [150, 153, 154]. This process will induce an isotopic shift in the sediments according to the fractionation exerted by the secondary authigenic phase, unless removal of the liberated Cd from solution into a solid phase is quantitative. This study supports that quantitative removal will correspond to a $\delta^{114/110}\mathrm{Cd}$ value within error of global deep-water values at approximately $0.3‰$.

Consequently, Cd is likely dominated by export to the sediments via association with organic material and as aqueous Cd species that diffuse into the surface sediment pore-waters. Also, the core-top sediment data support an organic pathway as an important source of Cd, as they are isotopically lighter than the overlying deep-waters or the same

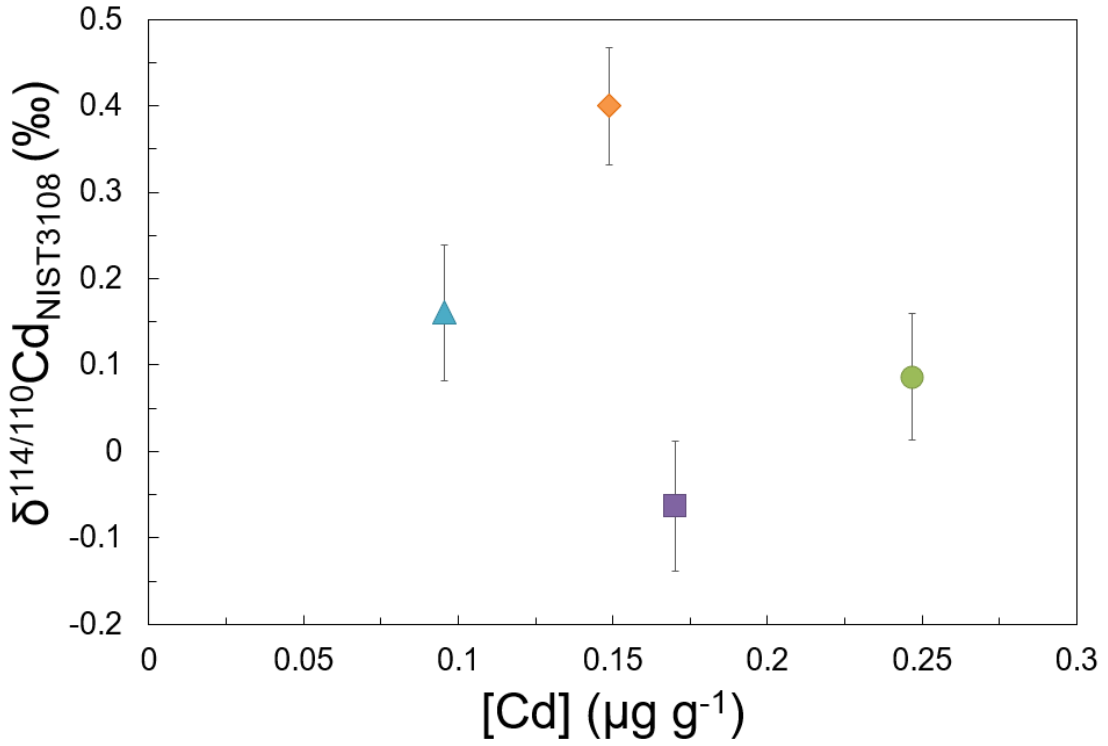


Figure 4.13: Cadmium isotopic compositions compared to Cd concentrations for core-top samples including station 18 (blue triangle), station 22 (purple square), station 23 (green circle), and station 24 (orange diamond).

as the overlying deep-water within analytical uncertainties. [57, 63, 67, 147]. The isotopic offset between the sedimentary Cd in the core-tops and the dissolved Cd in the overlying deep-waters at ~0.3‰ ranged from $\Delta^{114/110}\mathrm{Cd}_{\mathrm{core\,top-deep\,waters}} = -0.36 \pm 0.08\,‰$ to $0.10 \pm 0.07\,‰$ for all the core-top sediments (see Figure 4.13). As the organic matter undergoes bacterial oxidation, Cd is released into the pore-waters. A mechanism is required to capture and remove Cd from the pore-waters and into the sediments. This mechanism is likely the precipitation of Cd from the pore-waters with trace hydrogen sulphide (H_2S) to form cadmium sulphide (CdS) complexes [110].

Cd isotopic offset between sediments and overlying bottom waters in the North Atlantic at the BATS site

The measured site in the North Atlantic Ocean at the Bermuda Atlantic Time Series recorded a similar isotopic offset between the core-top sediments and overlying bottom-waters as the measure sites on the Argentine continental margin. The recorded average

offset for $\Delta^{114/110}\mathrm{Cd}_{\mathrm{core-top\,sediments-deep\,water}}$ was $-0.32 \pm 0.07\,‰$. The similar Cd isotopic offset between the core-top sediments and overlying deep-waters for the South Atlantic and North Atlantic is expected because both sites have oxygenated deep-waters, and the Cd isotopes value of the deep-waters is relatively homogeneous in all ocean basins.

4.5.5 Controls on $\delta^{114/110}\mathrm{Cd}$ in the near-surface sedimentary profile

Redox conditions in the pore-waters control the reported Cd concentrations and isotopic compositions of sedimentary samples during the early stages of diagenesis. If the Cd isotopic composition of each sediment sample is distinguished by the redox condition in the pore-waters, then a trend emerges in the data (see Figure 4.14). As mentioned in Chapter 1, suboxic sediments are defined as those where oxygen penetrates less than 1 cm into the sediments. Trace $\mathrm{H_2S}$ may be present, but limited, to the pore-waters below the sediment-water interface and below the depth of oxic respiration, such that the dominant oxidant is nitrate being used by denitrifying microbes for organic matter decomposition [119, 120]. This provides a scenario where dissolved Cd in the pore-waters could be immobilized with trace amounts of $\mathrm{H_2S}$ to form CdS species during the earliest stages of diagenesis [80, 110, 121]. Sulfidic sediments in this study are defined as depths where oxygen is below detection (less than ~0.1 μmol $\mathrm{l^{-1}}$) with complete consumption of other electron acceptors (e.g. N, Mn, Fe), and supports the presence of sulfate-reducing microbes [120].

In general, pore-waters with suboxic conditions fit a Rayleigh frationation model with a fractionation factor ($\alpha_{\mathrm{sediments-seawater}}$) of 1.0003, while those with sulfidic pore-waters fit a fraction factor of 1.0002. Any deviation in nearly all the samples is likely either attributed to low Cd concentrations and Cd isotopic compositions similar to lithogenic material ($\tilde{}0.1‰$) or isotopic equilibration between sediments and overlying deep-waters.

Transition from oxic to suboxic conditions in pore-waters from the coast

The Cd concentration and isotopic composition of the near-surfaces sediments in the oxidizing portion of the coastal core is likely controlled by adsorption reactions to Mn and Fe oxyhydroxides and possibly precipitation with trace $\mathrm{H_2S}$ to form cadmium

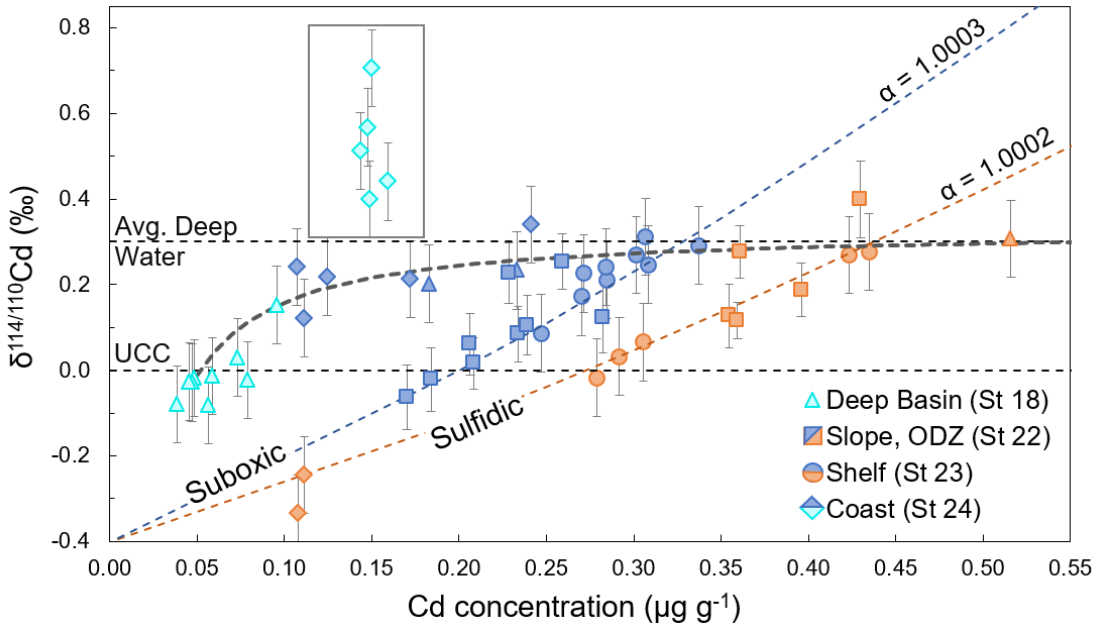


Figure 4.14: Sedimentary Cd data evidence for redox conditions controlling the observed Cd trends within near-surface sediments. Cadmium concentration relative to Cd isotopic composition of near-surface sediments from the coast (turquoise or blue diamonds), continental shelf (orange or blue circles), continental slope (orange or blue squares), and deep Argentine Basin (turquoise triangles) are plotted with colors indicating their redox conditions of the pore-waters: turquoise marks oxic, blue indicates suboxic, and orange denotes sulfidic conditions. The dashed lines represent the best visual fit for Rayleigh fractionation with $\delta^{114/110}$Cd isotopic fractionation factors ($\alpha_{\text{sediment–seawater}}$) of 1.0002 for the sulfidic zone (dashed, orange line) and 1.0003 for the suboxic zone (dashed, blue line), using an initial sedimentary Cd = 0.005 µg g^{-1} and $\delta^{114/110}$Cd = -0.4‰. The dashed line denotes an asymptotic mixing relationship of detrital Cd (0.085 µg g^{-1}; M1 and 0.1 ‰; δ_1) with the deep-water (0.3 ‰; δ_2) at a starting Cd concentration of 0.05 µg g^{-1}($M_{OBSERVED}$):
$\delta_{OBSERVED} = \delta_2 + (\delta_1 - \delta_2)(M_1/M_{OBSERVED})$
The dashed, horizontal lines denote the average Cd isotopic composition of the deep ocean water and the upper continental crust (UCC). The grey box highlights samples from the coast (St 24) that are deposited above the remineralization zone on the coast at 60 m and with nitrate conditions above 1 µM, and thus possibly controlled by a different process than the other reported samples. Please note this figure omits two points from the deep Argentine Basin, as they likely represent evidence for a glacial-interglacial transition, and they will be discussed in section 4.5.6.

sulphide complexes. Some short-live precipitation of CdS complexes may temporarily exist within the oxic portion of the core, as a result of degrading organic aggregates, forming microenvironments with increased respiration and inhibited diffusion, resulting in precipitation of chalcophile metals with trace hydrogen sulphide. This is a similar mechanism that is predicted to be occurring in low oxygen waters in ODZs. However, the stability of CdS complexes within oxic pore-waters or those with high nitrate concentrations is unknown.

What is observed in the shallow, oxic zone on the coast is a small increase in sedimentary Cd concentrations that corresponds to solid phase increases in Mn, supporting the formation of Mn oxyhydroxides with subsequent adsorption and/or incorporation of Cd to Mn oxyhydroxides. Previous experimental studies have shown that the isotope fractionation during adsorption of Cd to Mn oxyhydroxides decreases over time to a $\delta^{114/110}\mathrm{Cd}$ value within 0.1‰ of the isotopic composition of deep-water [85]. Likewise, a similar range was observed for the Cd isotopic composition of ferromanganese crusts with no isotopic fractionation during adsorption and/or incorporation of Cd to Fe-Mn oxyhydroxides outside of analytical uncertainties [104]. This lack of significant isotope variation in measured and experimental samples implies that the action of Cd adsorption to and/or incorporation of Cd into Mn and Fe oxyhydroxides is not a significant driver of isotope variation in the oxic portions of the cores.

The starting Cd concentration and isotopic composition of the core-top from the coast is at a different stage of remineralization compared to the other sites, as it is only at a water depth of 60 m and above the peak remineralization zone. At the top of the core, the solid phase $\delta^{114/110}\mathrm{Cd}$ value is 0.4‰, heavier than the deep-water value, and becoming progressively heavier relative to the deep-water with increased depth. This observed trend supports preferential release of light Cd isotopes as organic material is degrading, leaving heavy organically-bound Cd. While these values are very heavy at 0.71 ± 0.06‰, it is still within the values of recorded sinking particulates [155]. The transition from oxic to suboxic conditions occurs at approximately 3 cm. It is distinguished by oxygen levels below detection, low nitrate concentrations (<5 μM), and an increase in pore-water Fe, suggesting dissolution of Fe and Mn oxyhydroxides.

Suboxic zone

Nearly all the $\delta^{114/110}\mathrm{Cd}$ values of the near-surface sediments that are located below 700 m water depth recorded values that fall between two isotopic endmembers: lithogenic crusts ($0 \pm 0.1‰$) and deep-water (approx. $0.3‰$). The cause of the observed Cd isotope variations between these two endmembers is redox-controlled processes in the cores.

The primary removal mechanism of pore-water Cd in the suboxic and sulfidic zones is by preferential precipitation of isotopically light isotopes with trace hydrogen sulphide to form cadmium sulphide (CdS) complexes [80, 110, 156]. The traditional sequence of oxidants after oxygen is nitrate reduction followed by Fe and Mn reduction, and then sulfate reduction. The results support that CdS complexes are precipitating before the onset of sulfate reduction. This is plausible as Cd is known to precipitate with trace hydrogen sulphide that is below detection limits [110]. Recent studies have supported the coexisting of sulfur-reducing microbes with denitrifying microbes in the nitrate reduction zone as well [90]. An additional source of $\mathrm{H_2S}$ to the suboxic zone may be upward diffusion of pore-water from the zone of sulfate reduction [110].

The source of Cd to the suboxic and sulfidic zone is predominately from the release of adsorbed and/or incorporated Cd to the pore-waters during dissolution of Mn-Fe oxyhydroxides and degradation of any remaining organic material [124]. This process is observed on the continental shelf where a subsurface peak in pore-water Fe and a decrease in sedimentary Mn concentrations support dissolution of Fe-Mn oxyhydroxides and a release of Cd to the pore-waters. Similarly, on the slope, an increase in pore-water Fe concentrations corresponds to a small decrease in sedimentary Cd, suggesting dissolution of Fe oxyhydroxides and release of Cd to the pore-waters. Further down-core, pore-water Fe decreases while solid phase Cd increases, indicating that Cd is either adsorbing to FeS species or precipitating with $\mathrm{H_2S}$ to form CdS complexes. This trend continues till you reach the transition to sulfidic conditions.

Sulfidic zone

The sulfidic zone is characterized by the rapid and likely complete removal of pore-water Cd to precipitate CdS complexes. This process maintains the downward directed, Cd

concentration gradient in the core. The released, pore-water Cd, from the dissolution of metal oxides, will likely diffuse deeper into the core till sufficient sulphide concentrations exist to precipitate CdS complexes. The sulfidic zone in this study is marked as a depth with nitrate concentrations in the pore-waters at 1 μM or below. The location of this redox boundary in the sediments will likely fluctuate in response to variable organic carbon input. It is important to remember that any CdS complexes in the sediments when the redox boundary moves downward will likely be oxidized, released to pore-waters, diffuse deeper, react with sulphides and reprecipitate to form CdS species [110]. The stability of CdS complexes is unknown outside of anoxic conditions, however the conversion of dissolved Cd to CdS complexes is known to be a rapid process with preferential removal of the light Cd isotopes from recent laboratory experiments [80]. The movement of the redox boundaries and rapid precipitation of CdS species would explain how Cd is ultimately concentrated into a thin layer of enrichment at the lower limit of the redox excursion [110, 124].

A significant observation in all the measured cores is a distinct, authigenic Cd enrichment peak that correlates with peak nitrate penetration depth, typically occurring at the suboxic/sulfidic redox boundary. This diagenetic feature is formed when the redox boundary deepens, causing subsequent remobilization and downward diffusion of Cd to depths below the new suboxic/sulfidic redox boundary where sufficient H_2S drives the rapid precipitation of CdS complexes [110, 157]. This sharp, authigenic Cd enrichment peak results in an excursion in the isotopic composition of Cd to within error of the overlying deep-water value.

Cadmium adsorption to newly-precipitated FeS complexes may represent a pool of solid phase Cd, as pore-water Fe is decreasing at the suboxic/sulfidic redox boundary on the continental slope, attesting to the precipitation of FeS complexes. This mechanism may preferentially adsorb heavy isotopes of Cd to FeS complexes, as the sedimentary Cd isotopic composition is heavier than overlying deep-waters. However, the error bars for the deep-waters and sedimentary Cd samples overlap, so the magnitude of the fractionation cannot be truly distinguished given analytical uncertainties. At this time, the isotopic fractionation caused by Cd adsorption to FeS is unknown.

Minimal changes are observed in the Cd profile below the enrichment peaks in the cores, expect for some fluctuations observed in the near-surface cores from the coast and continental shelf. The sharp, zigzag pattern in the Cd isotopes at the bottom of the Cd profile from the coast may either represent a sampling artifact or indicate a physical movement of sediment on the seafloor. While on the continental shelf, at depths below the suboxic/sulfidic redox boundary, the pore-waters return to suboxic conditions. This shift in redox zones may represent a recent perturbation in the sediments, suggesting the system is in the process of returning to equilibrium conditions.

4.5.6 Cause of the observed isotope variations in the depth profile from the Deep Argentine Basin

Two processes were only observed at the deep Argentine basin site. The first is preferential release of Cd relative to POC during aerobic respiration of recently deposited organic matter. Cadmium concentrations decrease to below lithogenic levels in the subsurface, oxic portion of the core, as solid phase Mn concentrations decrease and $\delta^{114/110}\mathrm{Cd}$ values remain within error of the isotopic composition of the upper continental crusts, suggesting preferential remineralization of Cd compared to POC [149]. This process was previously reported to be active within the euphotic zone of the water column [155, 158]. A similar mechanism is likely active during sedimentary aerobic respiration of recently deposited organic matter, where preferentially released Cd is diffused to deeper in the core until reaching the oxic/suboxic redox front. The transition to the suboxic zone is marked by an authigenic Cd enrichment peak.

The deep basin site shows the highest Cd enrichment peak of all the measured cores, and it is located at the oxic/suboxic redox boundary. The Cd concentrations increase from below expected UCC levels to 3.31 $\mu\mathrm{gg}^{-1}$. This 80-fold increase in sedimentary Cd drives the $\delta^{114/110}\mathrm{Cd}$ values within analytical error of the overlying deep-waters. Other known redox elements show elevated concentrations at this transition with a corresponding decrease in solid-phase Mn concentrations. A Cd enrichment peak occurs at the transition from the suboxic to the sulfidic zone in the other measured cores. However, it is possible that the magnitude of the enrichment peak in the deep

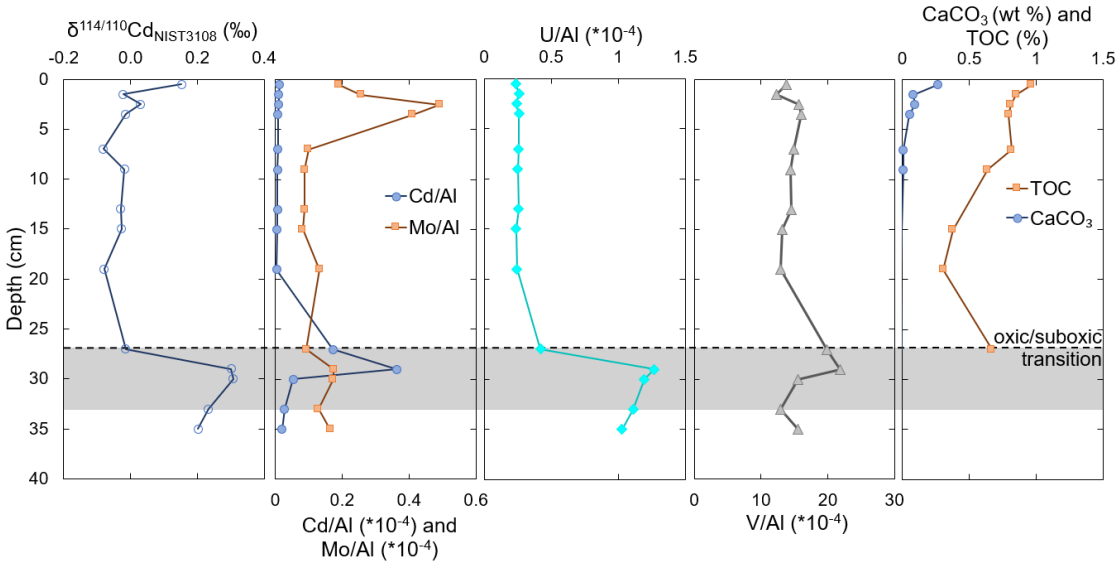


Figure 4.15: Down-core Cd concentration and isotopic composition in the near-surface sediment core from the deep Argentine Basin, along with trends for Cd/Al, Mo/Al, U/Al, and V/Al and weight percentage of $CaCO_3$ and TOC. The grey box represents the active enrichment peaks forming at the oxic/suboxic boundary, as a result of a shift in biological flux during the last glacial-interglacial transition.

basin is not a consequence of steady-state, early diagenetic processes in the core. This peak may reflect the active postdepositional redistribution of Cd as a consequence of decreased biological flux to seafloor during the transition from the last glacial maximum to the current interglacial epoch.

Last glacial-interglacial transition

The transition from a glacial to an interglacial period is likely captured in the core from the deep Argentine Basin (see Figure 4.15). The observed enrichment of redox-sensitive elements is in response to reducing bottom water conditions driven by an increase in biological productivity [159, 160]. This increased flux of organic carbon to the sediments is confirmed by an increase in TOC. Likewise, an increase in biogenic silica concentrations at this depth further support that elevated surface productivity led to a decrease in bottom water oxygen content and a corresponding increase in organic material flux to the sediments during the last glacial maximum (LGM). This explanation for the reported Cd profile is similarly proposed for sediments from the Subantarctic Ocean and Cape Basin (South Atlantic) [159].

It has been previously proposed that the last glacial-interglacial transition lead to a decrease in the biological flux of organic carbon to the sediments [161]. This transition causes a subsequent migration of the oxic/suboxic redox boundary to deeper depths, resulting in a deeper penetration of oxic pore-waters. A similar Cd profile is observed for "burn down" events in turbidites, where authigenic phases of Cd and other elements experience postdepositional redistribution as redox fronts deepen in the sediments [124, 159, 161]. Conversely, in modern continental margin sediments, increased organic carbon flux to the sediments relate to a shallower redox boundary, as observed in this study in the other cores. At the redox front in both cases, the redox-sensitive elements will form sedimentary authigenic enrichment peaks.

As discussed above, CdS precipitation at redox boundaries is the primary removal mechanism for Cd from pore-waters [110]. However, the magnitude of the Cd peak at this redox boundary is significantly higher at this site than the others on the coast and continental margin, with excess amounts of Cd relative to the average Cd/Th ratio observed in measure upper continental crusts of 96.9 % and a Cd/Th of 0.282 compared to the UCC of 0.009. Likewise, the location of the sedimentary Cd enrichment and similar, sharp peaks observed for other redox-sensitive elements further support that this formation is not from sedimentation, but a diagenetic signature of a deepening redox front perhaps caused by a shift in the flux of organic material during the last glacial-interglacial transition.

The observed peak shapes, magnitudes, and locations show some variation at the redox front, as a result of different mechanisms for immobilization in the sediments, however the peaks may continue to form and shift until a steady-state profile is achieved at the oxic/suboxic redox boundary. This was previously observed by Thomson et al. (1996) for cores from the Armorican Seamount in the deep northeast Atlantic [157]. This means that the Cd profile may experience further enrichment until an equilibrium at the oxic/suboxic boundary with the current biological flux to the seafloor is achieved in the sediments. Likewise, the Cd peak will likely become offset compared to other redox-sensitive elements during early stages of diagenesis, controlled by their removal mechanisms [157].

4.5.7 Cadmium sulphide complexes: Primary geologic sink of Cd in the oceans

The above results suggest that the down-core Cd concentrations and isotopic compositions are recording a story of the earliest stages of diagenesis, where organically-bound Cd is oxidized, released into the pore-waters at a subsurface depth and subsequently precipitated as CdS with trace H_2S. Unless the process is quantitative, leading to an isotopic composition similar to the overlying deep-waters, then it will fractionate the isotopes with a preference for the light isotopes in forming CdS species. This process likely overprints any signal of surface processes from biological uptake, although the isotopic composition of the initial Cd flux to the seafloor will be set by the degree of upper-ocean Cd utilization.

As CdS formation is likely the dominant process governing Cd burial in ancient sediments as now, it is not a surprise that similar isotope ratios are observed in Late Permian shales and Cenomanian-Turonian (Late Cretaceous) shales with a range of ~-0.5‰ to ~0.5‰ [121, 162]. Thus, the resulting Cd isotope values of the sediments will be controlled by redox conditions in the overlying water column and pore-waters. Likewise, the narrow isotopic range supports that deep seawater Cd isotopic composition has undergone minimal variability over time.

4.5.8 Correlation between the sedimentary enrichment of Cd with other chalcophile metals

The covariance of Cd with other redox-sensitive elements like Mo, U, and V through the cores further confirms that the Cd enrichment spikes are driven by redox reactions in the sediments. The concentrations of Cd, Mo, U, and V display enrichment spikes associated with peak nitrate penetration depth. The ratio of Cd/U concentrations and of Cd/Mo concentrations exhibit particularly strong correlations at the slope site overlying the ODZ (St 22) and on the coast (St 24) with an R-square of 0.870 for the Cd/U ratio and 0.816 for the Cd/Mo ratio (see Figure 4.16). The relationship between these redox-sensitive elements and Cd is less satisfactory in the deep basin (St 18) and on the shelf (St 23), possibly as a result of the deeper nitrate reduction zone for the deep basin. For the shelf station, it is marked by the sharpest decline in nitrate reduction. This observation may

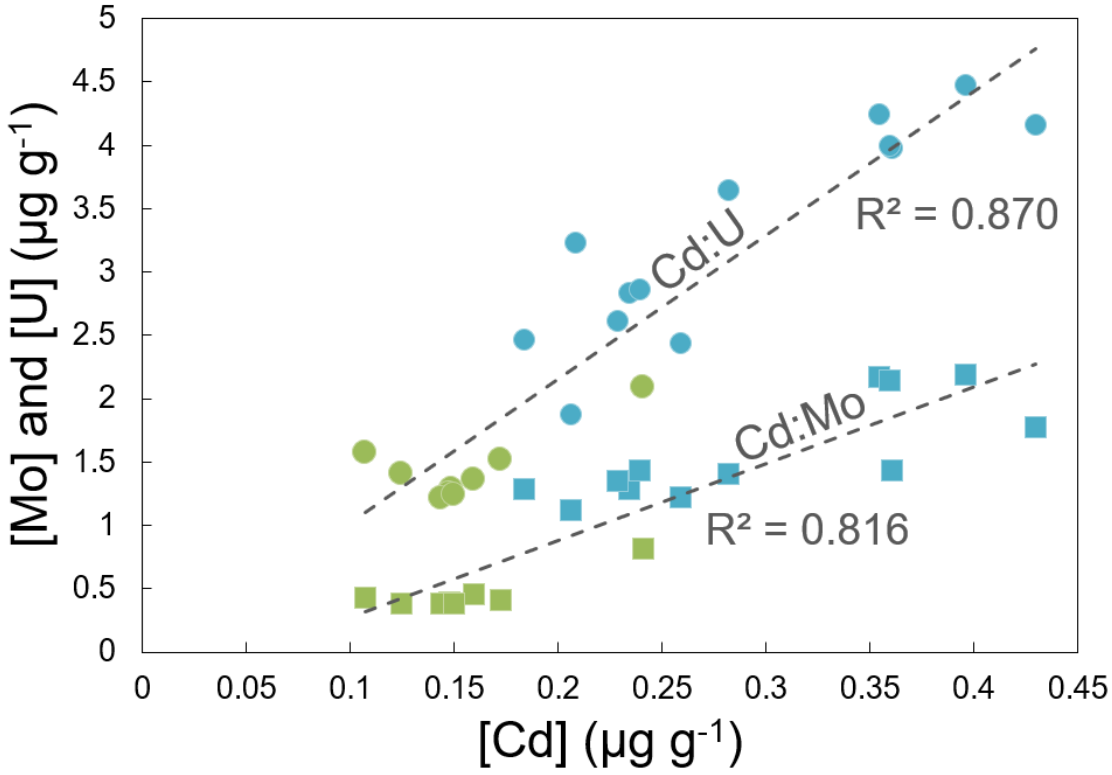


Figure 4.16: Cadmium concentrations compared to molybdenum (squares) and uranium (circles) concentrations for all the samples from station 22 (blue circles and squares) and station 24 (green circles and square), along with the resulting R-square value.

indicate that trace hydrogen sulphide is leading to precipitation of Cd near the top of the core before concentrations are above a necessary threshold for removal of U and Mo from the pore-waters at stations 18 and 23.

4.5.9 Mass balance for Cd isotopes in the ocean

The Cd concentrations and isotopic compositions of the near-surface sediment cores and overlying water column, along with chemical and physical parameters provide the information needed to better constrain the primary sources and sinks of Cd in the ocean (see Figure 4.17). A previous mass balance model for Cd was recently completed by Little et al. (2015) [122]. The below model builds on the previous model and better constrains the sink of Cd into oxic, suboxic, and anoxic sediments. Likewise, this work shows that immobilization of Cd with CdS precipitates within suboxic sediments is able to complete the global mass balance for Cd in the ocean.

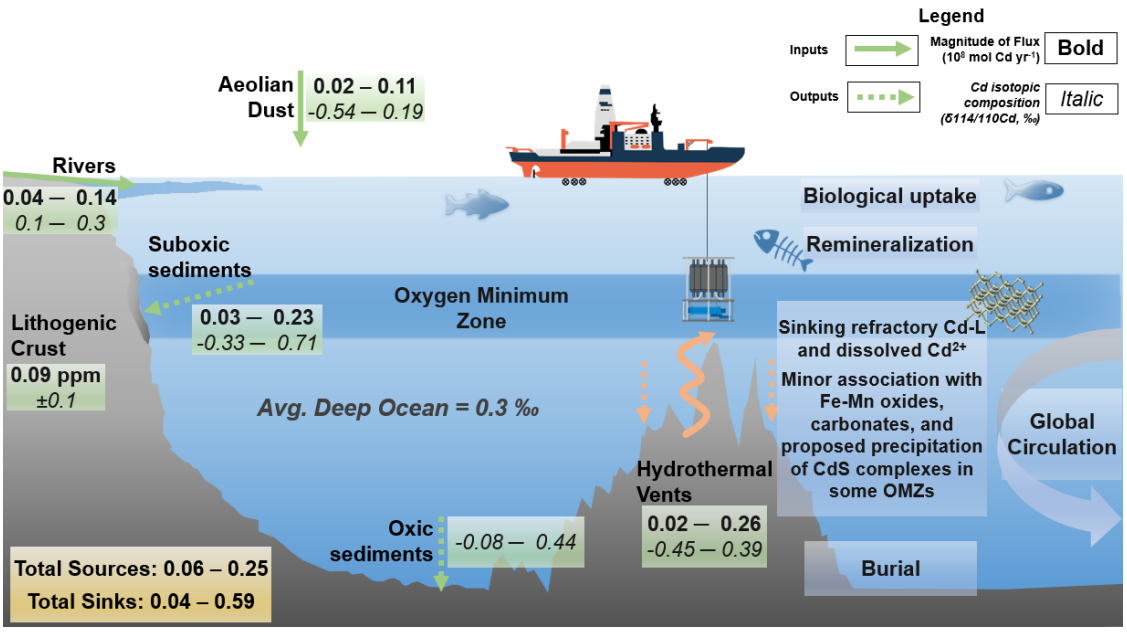


Figure 4.17: Schematic representing the mass balance of the primary sources and sinks for Cd in the ocean (left), along with the primary processes occurring for Cd in the water column (right). The model compiles data from previous studies related to the main sources and sinks of Cd to the oceans, including atmospheric dust [93, 108–111], rivers [93, 109, 110, 112] and hydrothermal activity [93, 105–107, 111], suboxic and anoxic sediments [68, 113, 163], pelagic clays [99–101], Fe-Mn oxides [93, 98, 102–104], and carbonates [86].

The main sources of Cd to the oceans are atmospheric dust fluxes [93, 108–111], rivers [93, 109, 110, 112] and hydrothermal activity [93, 105–107, 111]. Within the water column, Cd is associated with clays, carbonates, and Fe-Mn oxides that form in the water column. The primary sinks of Cd from seawater are mainly suboxic sediments, along with anoxic sediments [68, 113, 163], pelagic clays [99–101], Fe-Mn oxyhydroxides [93, 98, 102–104], and carbonates [86].

4.6 Conclusions

The potential of Cd isotopes to be used as a paleoredox proxy requires a further constraint of the primary sources and sinks of dissolved and particulate Cd pools to the seafloor. This study is the first to constrain the isotopic compositions of Cd in modern marine suboxic sediments relative to the directly overlying oxygenated water column across a transect from the Argentine coast to the deep basin. The Cd concentrations and isotopic

compositions of the core-tops capture a picture of the interactions at the sediment-water interface.

The core-tops are likely primarily impacted by the amount of oxygen and sedimentation rates in the bottom-waters, depicting either non-quantitative or quantitative removal. This is distinguished by the redox conditions in the pore-waters. If the sediments are dominated by aerobic bacterial oxidation within the pore-waters, then they will record open system behaviour and non-quantitative removal. This process leads to a reported Cd isotopic composition that is lighter than the overlying deep-waters. Conversely, if the sediments are dominated by denitrifying microbes using nitrate for organic decomposition, then trace H_2S may be present. In this situation, the rapid conversion of dissolved pore-water Cd with trace H_2S to form CdS complexes would lead to quantitative removal, reporting a Cd isotopic signature that is the same as the overlying deep-waters. The strong relationship between Cd and sulphide, along with the covariance between U and Mo concentrations further confirm Cd as a redox-sensitive element. The following chapters on the Black Sea and Saanich Inlet will explore how varying productivity and redox conditions impact the Cd cycle in the water column and near-surface sediments.

5

Cd isotope signatures in waters, pore-waters, and near-surface sediments from the Black Sea

Contents

5.1 Introduction 100
5.1.1 Study site 101
5.2 Sampling procedures 103
5.2.1 Sediment and water sampling procedures from the Fe-Vici cruise 103
5.2.2 Measurement of nutrients and chemical parameters 105
5.2.3 Sediment sampling procedures from the GEOTRACES, Med-Black Cruise 105
5.3 Methods 106
5.4 Results 106
5.4.1 Cd concentrations and isotope compositions in the water column 106
5.4.2 Cd concentrations and isotope variations across the sediment-water interface 110
5.4.3 Trace metal concentrations in sediment pore-waters 116
5.4.4 Cd concentrations and isotopic compositions in near-surface sediments 119
5.4.5 Interlab Comparison for Station 2 123
5.5 Discussion 123
5.5.1 Cause of the observed Cd isotope fractionation effect in the water column 123
5.5.2 Redox reaction zones defined by other trace metals in the water column 125
5.5.3 Explanation for the Cd isotopic compositions in the deep-waters 126
5.5.4 Authigenic enrichment of Cd in sediments 126
5.5.5 Source of Cd to the sediment-water interface 127

5.5.6 Quantitative Cd removal from the waters and into the sediments 129
5.5.7 Cadmium-sulphide interactions in the sedimentary depth profile 130
5.6 Conclusions 132

Abstract

Cadmium (Cd) is a redox-sensitive element with a high affinity to form cadmium sulphide (CdS) species within sulphidic waters and sediments of the Black Sea [91, 122, 164, 165]. Consequently, this permanently anoxic basin provides the ideal study site to systematically examine the behaviour of Cd in seawater and accumulating sediments as they are formed from oxygenated to sulfidic conditions. This chapter reports the Cd concentrations and isotopic compositions of waters, pore-waters, and sediments from a transect of shallow multi-cores obtained from the Black Sea coast to the deep basin, along with complementary chemical and physical parameters and trace metal concentrations. The results depict a strong link between redox state in the bottom-waters and the degree of Cd isotope fractionation of the core-top sediments relative to the overlying surface-waters. Oxygenated waters drive the isotopic compositions of the near-surface sediments to lighter values relative to the overlying surface-waters, with very similar average $\Delta^{114/110}\mathrm{Cd}_{\mathrm{core\,top-surface\,waters}}$ values to the South Atlantic seafloor, of ~-0.30 $\pm$ 0.10 ‰ for most sites. Conversely, anoxic deep-waters in the Black Sea exhibit negligible isotopic offset of near-surface sediments relative to the overlying water column. This finding supports the hypothesis that the CdS species that formed across the chemocline remain stable through the deep-waters, before being quantitatively removed into the accumulating sediments. These findings provide critical information to better constrain the relationship between Cd and hydrogen sulphide within the marine environment.

5.1 Introduction

Cadmium (Cd) is a redox-sensitive element with a high affinity to form cadmium sulphides within sulfidic water columns, such as the Black Sea. In Chapter 3, experiments were

conducted to quantify Cd isotope fractionation during precipitation with hydrogen sulphide (H_2S) in synthetic seawater under anoxic conditions. These experiments constrained the fractionation mechanism for the observed isotope effects. The experiments exhibited a behaviour best fit by a Rayleigh trend, indicating closed-system equilibrium fractionation. This chapter allows the comparison of the experimental results presented in chapter 3 with natural samples from the Black Sea. The Black Sea provides an ideal setting to understand how the transition from oxygenated surface-waters across a permanent chemocline to euxinic deep-waters impacts the partitioning of Cd isotopes between the dissolved and particulate phases.

This chapter will focus on analysing the Cd isotope compositions and concentrations of waters, pore-waters, and sediments to investigate the relationship between the isotopic composition of Cd in the water column and in near-surface sediments and pore-waters. The first aim of this study is to gain insight into the mechanisms of Cd removal into the sediments on the northwestern shelf of the Black Sea and to decipher shallow-burial diagenetic processes across a depth transect from the coast to the adjacent anoxic basin. The second aim is to investigate the relationship between Cd isotope fractionation during export into the sediments and bottom water oxygen concentrations. The samples were collected by the Fe-Vici cruise as part of the Vici Project, "Response of the Iron Biogeochemical Cycle on Continental Shelves to Seawater Deoxygenation" funded by the Netherlands Organization for Scientific Research. Also, the Fe-Vici cruise measured nutrients in the pore-waters. The new and unpublished Black Sea water data presented in this chapter was measured by Claudine Stirling, Ejin George and John Rolison at the University of Otago, New Zealand, using samples collected on the GEOTRACES MedBlack cruise. All other analyses (sediments and pore-waters) were undertaken as part of this thesis at the University of Oxford.

5.1.1 Study site

The Black Sea is the largest, permanently anoxic, silled basin in the world at 423,000 km^3 and a maximum depth of 2240 m resulting from a 33 m sill that restricts the two-layer inflow and outflow with the Mediterranean Sea through the shallow Bosphorus

and Dardanelles Straits and the Sea of Mamara [166–169]. The inflow of saline Mediterranean waters is likely responsible for the observed residence time of the seawater at different depths, with the deep-water below 500 m having an estimated residence time of 625 yrs [168, 169]. Other inflows come from rivers including the Danube, Dneper, and Dnestr on the northwest shelf, which have highly variable seasonal and yearly discharges [166], The overall basin has an estuarine-type circulation and maintains a positive water balance [169].

The vertical water column has distinct gradients in temperature and salinity. The surface-waters are colder and less saline than deep-waters, resulting from freshwater runoff at the surface and from subsurface Mediterranean Sea inflows [166]. The deep-water is relatively stable below 500 m except near the bottom, where a 400–500 m thick convection layer driven by geothermal heating exists at approximately 1700 m [166]. Similar bottom convection layers have been observed in other systems, but not as large [170, 171]. The homogenisation time scale of the convective layer is approximately 40 years, and the overall age is similar to that of the deep-waters [166, 172].

The vertical transition from oxic to anoxic waters in the Black Sea is distinguished by a relatively stable chemocline and halocline between 50 m to 150 m water depth [169, 173, 174]. Below the chemocline, euxinic conditions persist with low Cd concentrations [175]. This trend has been observed for other trace metals, like Mo [176] and Zn [177]. Cadmium speciation is expected to change from mainly $\mathrm{CdCl_2}$, $\mathrm{CdCl^+}$, and $\mathrm{Cd^{2+}}$ species in the oxic layer to predominately CdS species in euxinic waters [91].

The deep-waters and pore-waters in the sediments maintain similar levels of $\mathrm{H_2S}$, with a maximum concentration reaching 380 $\mu\mathrm{M}$ at the bottom [173, 178]. Overall, the basin experiences low rates of organic carbon accumulation (~0.31-10 g $\mathrm{m^{-2}\ yr^{-1}}$), with bulk mass accumulation rates of between 10 g $\mathrm{m^{-2}\ yr^{-1}}$ in the deep basin and up to 200 g $\mathrm{m^{-2}\ yr^{-1}}$ at the basin margin [169, 179, 180].

5.2 Sampling procedures

5.2.1 Sediment and water sampling procedures from the Fe-Vici cruise

Please note that all the near-surface sediments and water samples, along with dissolved nutrient and chemical data were not collected by myself but by the participants of the Fe-Vici cruise and GEOTRACES, MedBlack cruise following the listed below procedures.

The sampling of sediments and pore-waters was focused on capturing a redox transect from the anoxic deep basin to the oxic Romanian shelf in the northwestern section of the Black Sea. The Fe-Vici cruise was a GEOTRACES process study, following International GEOTRACES protocols related to methodology and data management. Similarly, the water samples presented in this study from the GEOTRACES, MedBlack cruise were collected following GEOTRACES procedures for collection and processing of the samples. The reported results includes Cd concentrations and isotopes, along with the concentrations of other trace metals and physical and chemical parameters to aid in the interpretation of the Cd dataset.

The water samples presented in this study were collected from a single, vertical depth profile in the water column in the deep basin, from the oxygenated surface-waters to the euxinic deep-waters (see Figure 5.1). The water sampling site is located at 42°52.2'N, 31°40.2'E (see Table 5.1). The depth at the sampling site was approximately 2120 m. Each sample was collected with a titanium CTD frame fitted with 24, 20 litre bottles with external springs. The cast collected a full water depth profile from the surface to the benthic-waters. The data collected from the water samples included select trace metal concentrations, along with hydrographic and nutrient concentrations. The samples for Cd concentration and isotopic analyses were collected in acid-cleaned containers at depths throughout the water column. The samples were immediately filtered and acidified to a pH of 1.7 (0.024 M).

The near-surface sediments and pore-waters were retrieved from seven multicores, across a transition from the oxygenated coast to the euxinic, deep basin (see Figure 5.1). The sample site locations, depths and overlying water column chemistry are reported in Table 5.1. In summary, Station 1 and 2 are situated in the deepest portion of the basin

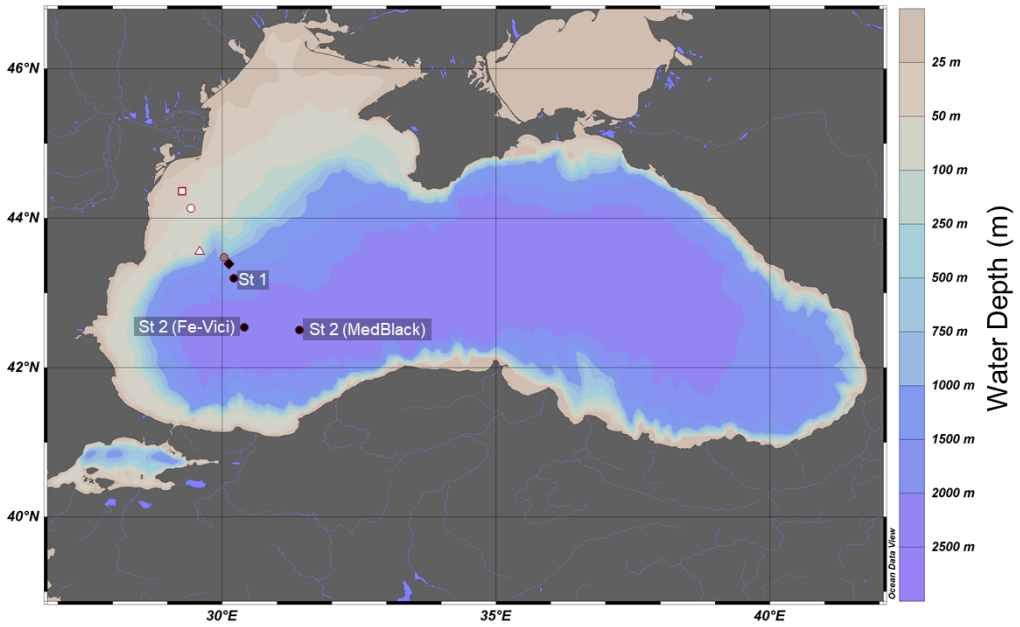


Figure 5.1: Geographic locations of the sediment sampling sites of the Fe-Vici cruise transiting from the NW coast to deep-waters, along with St 2 of the GEOTRACES MedBlack cruise in the deep-waters of the Black Sea using Ocean Data View (ODV). The marked sites are St 13 (white square), St 8 (white circle), St 7 (white triangle), St 14 (grey circle), St 4 (black diamond), and St 1 and St 2 (black circles). The location of the stations in the deep basin for the Fe-Vici and GEOTRACES MedBlack cruises are labelled in the figure. The site markers are filled with white for oxygenated overlying bottom-waters, grey for suboxic conditions, and black for anoxic conditions.

with euxinic overlying bottom-waters and laminated, fine-grained sediments. Station 4 is on the slope with anoxic overlying bottom-waters, while station 14 is located on the shelf with hypoxic overlying bottom-waters and sediments containing macrofauna shells. The other three stations are St 7 (shelf), St 8 (mid-shelf), and St 13 (coast), and they have oxygenated overlying bottom-waters with highly bioturbated sediments containing benthic fauna and no discernible sub-surface production of H_2S.

All near-surface cores were recovered with a 10 cm diameter multicorer using an Oktopus multicoring apparatus. Twelve cores were recovered per cast. One core was transferred to a nitrogen-filled glovebox inside a temperature-controlled container. Each core was sliced following a general scheme. Each slice was placed into a 15 mL glass vial for water and solid fraction analyses and 50 mL centrifuge tubes for the porewater fraction. The glass vials were heat-sealed in a gas-tight aluminium-laminated bag and frozen at -20°C. The porewater fraction was centrifuged at 4500 rpm for 20–30 min.

Table 5.1: Details on the collected near-surface multi-cores from the Fe-Vici cruise

Table 1: Details on the collected near-surface multi-cores from the Fe-Vici cruise

Station number	Latitude	Longitude	Water Depth (m)	Bottom water redox, location
1	43°21.05'N	30°22.3'E	1596	anoxic, deep basin
2	42°53.8'N	30°40.7'E	2107	anoxic, deep basin
2*	42°52.2'N	31°40.2'E	2120	anoxic, deep basin
4	43°40.6'N	30°07.5'E	380	anoxic, slope
14	43°45.9'N	30°04.0'E	114	hypoxic, shelf edge
7	43°53.8'N	29°58.6'E	78	oxic, shelf
8	44°14.7'N	29°43.4'E	64	oxic, mid-shelf
13	44°36.45'N	29°27.4'E	39	oxic, coastal

* This station is from the GEOTRACES, MedBlack Cruise

This procedure yielded >10 mL of porewater for most samples. After centrifugation, the tubes were transferred to the glovebox and filtered through a 0.45 μm filter into a 15 mL centrifuge tube. A subsample was taken from the tubes for a range of on-board and laboratory analyses of dissolved organic and inorganic constituents.

5.2.2 Measurement of nutrients and chemical parameters

All nutrients and chemical parameters were measured in on-board laboratories equipped with QuAAtro Gas Segmented Continuous Flow Analysers. This included ammonium (NH_4^+), nitrite (NO_2^-), nitrate with nitrite (NO_3^-+ NO_2^-), phosphate (PO_4^{3-}), silicate (Si), dissolved inorganic carbon (DIC), and sulphide (H_2S). Additionally, TOC (%) was measured on the core-top samples from the mid-shelf (station 8), the shelf (station 7), and a down-core depth profile from station 13, representing a location with oxygenated coastal waters.

5.2.3 Sediment sampling procedures from the GEOTRACES, MedBlack Cruise

The GEOTRACES, MedBlack Cruise also collected a near-surface sediment core from the deepest part of the basin. The sediment core was collected with a multicorer from

a site at 42°52.2'N, 31°40.2'E and at a water depth of 2120 m (see Figure 5.1 and Table 5.1). Similar to the Fe-Vici cruise, the core was subsampled following a general scheme. The Cd concentrations and isotopic compositions from this core was compared to the results from the Fe-Vici cruise at station 2.

5.3 Methods

Details on the digestion and Cd separation protocols for the natural samples, along with analytical procedures, are fully described in Chapter 2.

5.4 Results

5.4.1 Cd concentrations and isotope compositions in the water column

The dominant influence on the Cd concentration and isotopic composition of the surface-waters is the inflow of oxygen-rich, saline water from the Mediterranean Sea with a high concentration of trace metals at ~60 m (see Table 5.2 and Figure 5.2). This inflow is distinguished by an increase from $69.9\,\mathrm{pmol\,kg^{-1}}$ to $180.6\,\mathrm{pmol\,kg^{-1}}$ in the dissolved Cd concentration of the subsurface-waters relative to the surface-waters, with a similar increase observed for Zn and V, but not for Fe or Mo. The input from the Mediterranean Sea drives the dissolved Cd isotopic composition from $\delta^{114/110}\mathrm{Cd}$= 0.68 ‰ at 39 m to $\delta^{114/110}\mathrm{Cd}$= 0.37 ‰ at 60 m. This value represents the composition of the water right above the chemocline, and it is similar to that for the deep ocean worldwide [58]. The chemocline in the Black Sea is distinguished by an abrupt transition from anoxic to euxinic conditions, resulting in a significant shift in the Cd concentrations and isotopic compositions of the waters (see Table 5.2 and Figures 5.2 and 5.3). The oxygen concentrations are below detection limit at ~100 m and $\mathrm{H_2S}$ is detectable below ~105 m. This change in redox chemistry coincides with a decrease in the dissolved Cd concentration to $3.5\,\mathrm{pmol\,kg^{-1}}$ at ~105 m. Dissolved Zn and V concentrations display similar decreases across the chemocline.

Table 5.2: Cadmium concentrations and isotope compositions from a water column in the anoxic, deep basin of the Black Sea, along with physical and trace metal concentrations data

Water Depth (m)	Salinity	O_2 (µmol kg^{-1})	H_2S (µmol kg^{-1})	[Cd] (pM)*	$\delta^{114/110}Cd_{NIST}$ (‰)**	2σ	NO_3^- (µM)	[V] (pM)	[Mn] (µM)	[Fe] (nM)	[Co] (pM)	[Ni] (nM)	[Cu] (nM)	[Zn] (nM)	[Mo] (nM)
Station 2, 42°52.1'N, 31°40.1'E, anoxic deep basin															
9	18.23	235	0	71.7	0.83	0.10	0.1	5.2	0.1	0.6	272	11.2	4.1	2.7	44.1
19				83	0.97	0.10	0.0	5.9		0.5	275	12.7	4.8	2.1	
24				58	0.83	0.10	0.0	4.5	0.1	0.4	214	11.3	4.1	0.8	41.2
39	18.45	299	0	69.6	0.68	0.10	0.0	3.8	0.0	0.3	170	11.3	3.9	1.0	43.3
45				74.2			0.0	5.3		0.3	139	11.3	3.7	1.2	
45				98.9	0.71	0.10	0.0	13.5	0.1	0.3	105	13.9	3.9	2.1	39.6
50				122.9	0.58	0.10	1.9	16.0		0.4	52	13.4	3.6	2.8	
55				156.3	0.28	0.10	3.5	16.2		0.4	39	12.7	3.2	3.9	
60				166.4	0.37	0.10	4.0	14.8		0.3	28	12.4	2.8	4.8	
65				180.6	0.37	0.10	4.1			0.3	28	12.7	2.8	4.6	
70				160.9	0.25	0.10	4.1	15.3	0.1	0.3	28	12.0	2.3	4.3	41.6
75				141.5	0.37	0.10	3.3	14.3		0.5	29	12.6	1.9	3.9	
80				114.8	0.14	0.10	2.6	12.5		0.5	48	12.2	1.5	3.1	
84					0.42	0.10	1.6	12.2		5.1	261	11.6	0.9	3.0	
85				81.9	0.33	0.10	1.7	11.2	0.3	0.5	60	12.7	1.0		
90				63.6	0.30	0.10	1.2	12.0		0.7	168	13.0	0.8	2.7	
95		*Chemocline*		46			1.2	11.9		0.6	365	13.3	0.6	2.6	
99	20.86	0	0	15.9	0.44	0.10	0.0	11.3		14.0	4199	12.7	0.2	2.5	
100				21.4			0.0	11.9	4.2	2.9	3802	14.3	0.3	2.5	40.8
105		*Euxinic*		3.5	0.43	0.10	0.0	12.4		92.5	7193	15.1	0.2	2.4	
110				2.2	0.70	0.10	0.0	11.5		112.5	6628	13.4	0.2	1.7	
114				2.8			0.0	12.0		139.6	5991	13.6	0.2	1.2	
115				2.2	1.79	0.10	0.0	11.6	8.2	158.3	6498	14.1	0.2	1.1	42.3
120				2	2.23	0.10	0.0	14.5		182.3	7115	15.1	0.2	1.0	

Table 5.2: continued

Water Depth (m)	Salinity	O_2 (μmol kg^{-1})	H_2S (μmol kg^{-1})	[Cd] (pM)*	$\delta^{114/110}Cd_{NIST}$ (‰)**	2σ	NO_3^- (μM)	[V] (pM)	[Mn] (μM)	[Fe] (nM)	[Co] (pM)	[Ni] (nM)	[Cu] (nM)	[Zn] (nM)	[Mo] (nM)
125				2.4			0	14.3		244.9	6914	15	0.2	1.0	
129	21.22	0	16	3.1			0	16.5		249.9	5831	12.1	0.2	0.6	
130				2.8	3.89	0.10	0	17	9.1	277.5	6249	13.8	0.2	0.7	40.1
135				2.7			0	15.3		322.7	6105	13.9	0.2	0.5	
140				3.2			0	16.3		377.1	6022	13.6	0.2	0.5	
145				3.1	5.51	0.10	0	17.3	9.2	379.2	5342	13.2	0.1	0.4	40.8
150				3.2	5.07	0.10	0	16.2		392.7	4938	12.9	0.1	0.4	
157				2.3			0	17.8		409	5029	13.5	0.2	0.4	
160				2.8			0	15.6	9.1	373.1	5373	10.8	0.1	0.4	37.7
174				5.7			0	12.3	8.6	311.2	3538	10.2	0.1	0.9	36.2
204	21.61	0	46	0.4	3.51	0.10	0	11.3	7.6	173.8	2158	10.3	0.1	0.2	28.7
250				0.9	1.49	0.10	0	10.1	6.8	64	878	10.3	0.1	0.2	20.8
300	21.85	0	94	0.9			0	9	6.2	48.1	575	10.5	0.1	0.2	21.7
399				1.6	0.96	0.10	0	9	5.5	31.7	352	11.3	0.1	0.2	10.6
498	22.09	0	192	0.6	-0.04	0.10	0	7.9	5.3	27.8	321	10.9	0.1	0.2	10.7
749				1.3			0	5.1	5.1	24.6	403	10.9	0.1	0.3	7.2
999	22.31	0	348	0.7			0	4.5	4.9	13.9	330	11.1	0.0	0.2	6.0
1249				0.7			0	2.2	4.9	10.1	303	11.4	0.0	0.2	7.4
1499	22.34	0	398	0.4			0	2.7	4.9	9.7	240	12	0.0	0.3	6.6
1749	22.35	0	419	1.2			0	4.5	5.0	11.2	275	12.4	0.1	0.4	7.4
2070	22.35	0	422	0.8			0	3.7	4.9	12.6	312	12.7	0.0	0.3	4.4
2120	22.35	0	422	1.7			0	4.6	4.9	15.1	274	12.4	0.0	0.7	5.9

**All trace metal, physical and nutrients concentrations are source from Rolison et al., 2017*

***The Cd-isotopes were measured at University of Otago by Claudine Stirling's lab group*

The bottom of the chemocline marks a dramatic change in the dissolved Cd isotopic composition from $\delta^{114/110}$Cd= 0.43 ‰ at 105 m to $\delta^{114/110}$Cd= 5.5 ‰ at 145 m. This shift to isotopically heavy values of aqueous Cd coincides with a similar peak for dissolved Fe and V concentrations at ~160 m. The dissolved Cd isotopic composition returns to lighter values (~1.5 ‰) by 248 m. This trend continues in the deep-waters with a dissolved Cd isotopes value of $\delta^{114/110}$Cd= -0.04 ‰ at 500 m. These variations lead to an isotopic offset between the deep-water at 500 m and the water above the chemocline (~0.4 ‰). The available data for Cd isotopes is constrained to the first 500 m of the water column at this time; however, the water column displays sulfidic conditions for a majority of the profile. Thus, few major changes are likely to occur in deeper waters below 500 m. In contrast with Cd, dissolved Mo concentrations display minor variations though the chemocline and gradually decrease through the deep-waters, coinciding with increasing concentrations of H_2S.

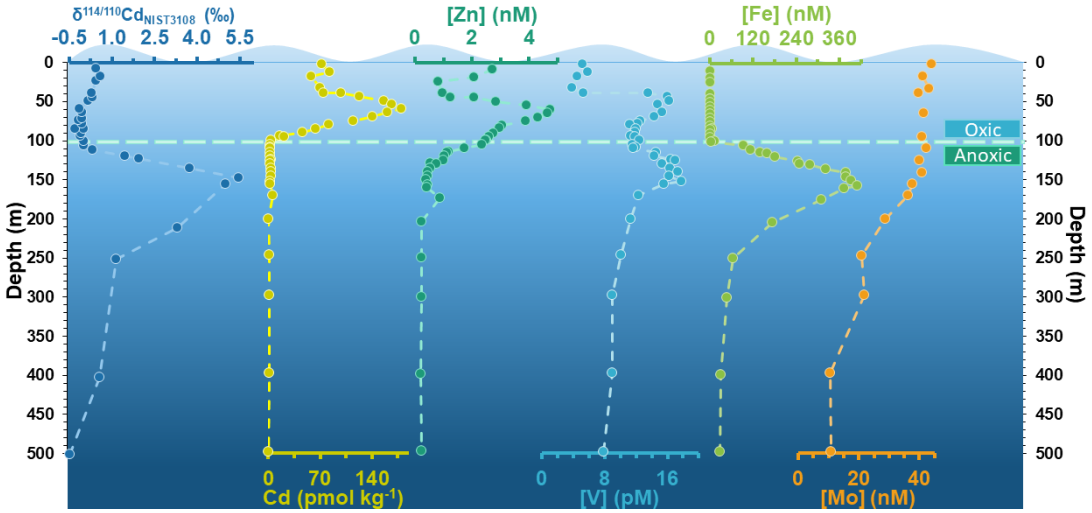


Figure 5.2: Water column profile of the top 500 m water depth for dissolved Cd concentrations (solid, yellow circles) and isotopic compositions (solid, dark blue circles) from deep basin in the Black Sea, along with other trace metal concentrations including Zn, V, Fe, and Mo. Error bars for the Cd isotopes measurements represent the 2 SE on the sample, and is smaller than the data markers.

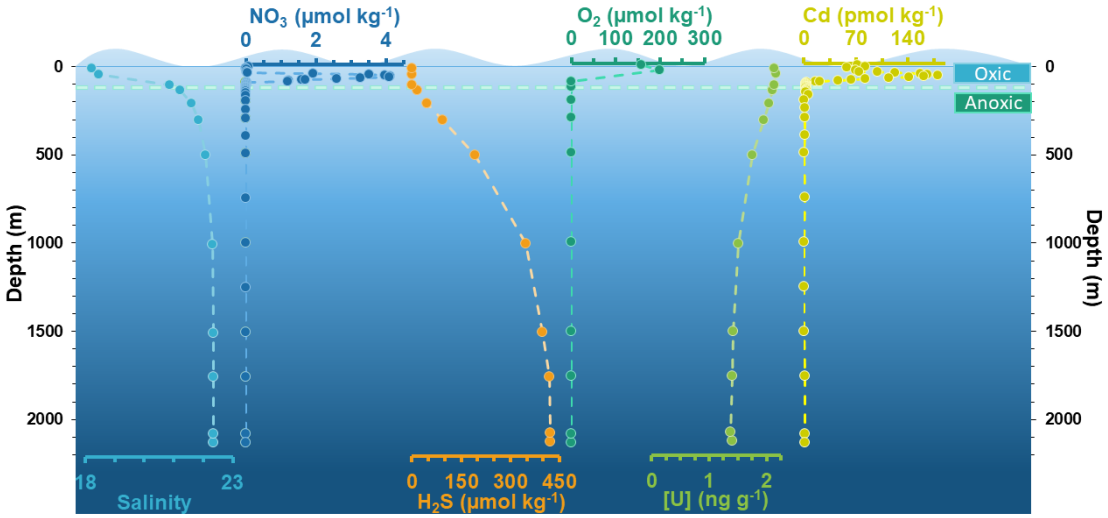


Figure 5.3: Water column profile of Cd concentration, along with physical and nutrients concentrations data from the surface to the bottom of the depth profile at 2120 m in the deep basin in the Black Sea.

5.4.2 Cd concentrations and isotope variations across the sediment-water interface

The transfer of Cd from the benthic-waters into the sediments can be discerned from the Cd concentrations and isotopic compositions of core-top samples, along with corresponding concentrations of dissolved Cd, NO_3^- and H_2S in the sediment pore-waters (see Figure 5.4 and Tables 5.3, 5.4, and 5.5). The variations in Cd concentrations and isotopic compositions for the core-tops relate to differences in the amounts of NO_3^- and/or H_2S concentrations in the overlying water column. The core-tops collected within oxygenated waters on the shelf (stations 7, 8 and 13) are characterised by isotopically lighter values of Cd and lower concentrations of Cd compared to sites with overlying euxinic bottom-waters. The core-top samples collected in oxygenated waters have Cd concentrations between 0.09 $\mu g\ g^{-1}$ and 0.41 $\mu g\ g^{-1}$ and Cd isotopic compositions between $\delta^{114/110}Cd$ = -0.04 $\pm$ 0.06 ‰ and $\delta^{114/110}Cd$ = 0.13 $\pm$ 0.07 ‰. The core-top sample collected from station 14 has a Cd concentration of 0.23 $\mu g\ g^{-1}$ and a Cd isotopic composition of $\delta^{114/110}Cd$= 0.07 $\pm$ 0.08 ‰. This core is located on the shelf-edge (station 14) with significantly lower dissolved oxygen concentrations compared to the other cores in this study, and is characterised as a site with overlying hypoxic bottom-waters.

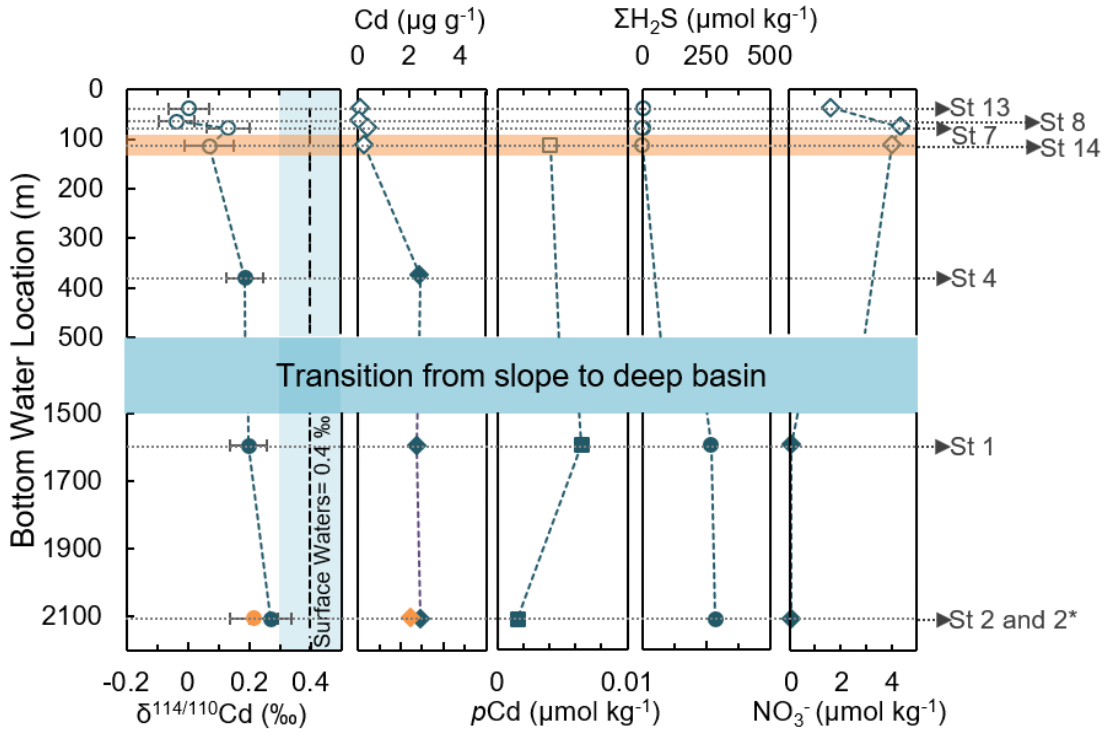


Figure 5.4: Cadmium isotope values and concentrations of core-top sediments (0 to 0.25 cm) collected along a redox transect from the oxic, northwestern shelf of the Black Sea to the adjacent anoxic basin, along with porewater Cd (pCd), H_2S, and NO_3^- concentrations in the pore-waters. The open symbols represent oxic conditions and closed symbols signify anoxic sites. The blue, shaded area represents the range of uncertainty on the Cd isotopes value of the surface water above the chemocline. The orange, shaded area at approximately 105 m represents the transition from oxic to anoxic conditions in the water column. The orange dots represent the data for the cross-over station 2 from the GEOTRACES, MedBlack research cruise.

Table 5.3: Physical and nutrients concentration data in the pore-waters retrieved from a transect of shallow multi-cores obtained from the oxic, coast to the anoxic, deep basin of the Black Sea

Depth interval (cm)	pH	Alkalinity (mM eq)	DIC (μM)	PO_4^{3-} (μM)	Si (μM)	NH_4^+ (μM)	$NO_3^- + NO_2^-$ (μM)	NO_3^- (μM)	NO_2^- (μM)	ΣH_2S (μM)	TOC (%)	CH_4 (μM)
Station 1, 43°21.05'N, 30°22.3'E, 1596 m (water depth)												
0.25		4.6	3946	8.9	434.6	138.4	138.4		1.5	419.6		0.7
0.75		5.0	4243	9.4	448.9	142.9	256.3		1.4	468.8		
1.75		4.8	4320	9.7	462.6	148.9			1.7	457.2		
2.5		4.9	4482	9.9	463.6	153.6			2.9	512.4		2.5
3.5		5.3	4595	10.2	463.0	163.1			1.9	483.2		
5.5		5.2	4682	10.6	462.0	170.8			1.8	559.6		3.9
6.5		5.6	5212	12.4	476.3	168.6			1.9	569.6		
7.5			4634	11.6	464.2	169.8			2.2	445.2		4.6
8.5		5.0	4472	10.7	464.2	168.5			1.5	526.8		
9.5		5.0	4357	10.3	452.3	168.4			1.7	435.6		2.6
11		5.0	4401	10.5	456.2	176.5			1.0	502.4		
13		5.0	4344	10.5	453.7	180.3			0.4	388.4		3.0
15			4582	11.4	459.6	186.4			0.9	507.6		3.0
19		5.4	4501	12.0	461.1	201.0			0.6	550.8		2.4
21			4461	12.0	462.5	194.4			1.3	487.2		2.2
23			4544	12.2	451.5	201.3			1.2	523.2		1.4
27		5.6	4780	13.3	473.5	210.5			1.0	503.2		2.2
32.5		6.1	5029	15.9	476.4	228.2	125.9		0.5	636.0		1.6
35.5			5078	15.4	476.9	235.6	158.3		1.3	635.6		1.6
39.5		6.3	5253	18.3	466.3	236.0			3.5	590.8		2.1
42		6.4	5489	19.6	487.1	256.3			1.6	795.6		1.2
Station 2, 42°53.8'N, 30°40.7'E, 2107 m (water depth)												
0.25	7.95	4.8	3993	8.8	406.2	125.9			0.3	405.2		
1.25	7.99	4.9	4358	8.6	419.4	130.3			0.5	382.4		
1.75	7.97		4480	9.2	426.4	133.3			2.0	402.8		
2.5	7.92	4.9	4583	9.5	436.6	139.2			1.9	423.2		
3.5	8	4.9	4653	9.5	432.0	138.6			1.8	470.8		
5.5	8.01	4.8	4617	8.4	418.0	142.9			2.0	457.2		
6.5	7.95	4.9	4819	8.7	386.4	154.5			2.3	494.4		
7.5	7.93	4.9	4760	9.4	417.0	151.9			1.7	506.4		
9.5	7.91	4.9	4646	9.5	410.9	156.9			1.4	502.8		
13	7.94	4.8	4647	9.1	401.4	158.3			1.4	403.2		

Table 5.3: continued

Depth interval (cm)	pH	Alkalinity (mM eq)	DIC (µM)	PO_4^{3-} (µM)	Si (µM)	NH_4^+ (µM)	$NO_3^- + NO_2^-$ (µM)	NO_3^- (µM)	NO_2^- (µM)	ΣH_2S (µM)	TOC (%)	CH_4 (µM)
Station 7, 42°53.8'N, 29°58.6'E, 78 m (water depth)												
0.25	7.95	3.5	3274	2.1	54.2	29.0	3.9	2.5	1.4	1.2	0.5	
0.75	7.93	3.4	3274	2.1	105.1	24.2	2.5	1.8	0.7	1.2		
1.75	7.95	3.5	3383	2.4	109.3	32.0	1.7	0.8	0.9	1.2		
3.5	8.06	3.3	3291	5.0	104.7	39.2	1.0	0.6	0.4	1.2		
5.5	7.91	3.5	3385			44.5	1.1	0.5	0.6	1.2		
Station 13, 44°36.45'N, 29°27.4'E, 39 m (water depth)												
0.75	7.76	3.9	3328	7.7	290.5	79.2	1.6	1.1	0.6	0.4	2.9	
1.25	7.69	4.4	3741	44.9	380.1	132.1	3.3	2.3	1.1	0.4	1.9	
2.5	7.83	6.4	4983	33.1	423.5	287.0	2.4	0.9	1.5	0.4	2.2	
3.5	7.62	6.7	6397	76.9	504.4	402.1	2.2	0.7	1.5	0.4	1.9	
4.5	7.6	8.5	7964	96.3	573.2	528.5	2.3	1.4	0.9	0.4	2.2	
5.5	7.65	9.7	9738	116.1	602.7	665.1	1.3	0.6	0.7	0.4	2.5	
6.5	7.65	10.9	11251	146.0	669.0	751.2	2.8	1.7	1.2	0.4	2.3	
7.5	7.6	13.0	12324	165.5	685.1	849.1	1.8	0.9	1.0	0.4	2.4	
8.5	7.76	14.5	13341	195.4	736.6	970.6	1.6	0.7	0.9	0.4	2.0	
9.5	7.7	16.0	15228	220.6	740.3	1028.4	1.3	0.6	0.7	0.4	2.1	
11	7.73	18.0	16827	243.5	731.9	1113.6	1.3	0.9	0.4	0.4	2.2	
13	7.7	21.3	19497	291.0	778.4	1314.2	0.9	0.5	0.4	0.4	2.3	
15	7.72	23.6	22110	326.2	806.3	1431.4	0.7	0.4	0.3	0.4	2.4	
17	7.83	25.1		335.7	778.4	1543.8	2.0	1.4	0.6	0.4	2.3	
19	7.83	25.6	24387	329.5	723.6	1618.1	0.7	0.2	0.4	0.4	2.0	
21.5	7.83	26.4	25269	329.6	716.1	1738.1	0.5	0.1	0.4	0.4	2.5	
24.5	7.81	26.9	26076	301.3	675.2	1792.9	1.5	0.5	1.0	0.4	2.1	

**The physical and nutrients concentration data was measured by the participants of the Fe-Vici cruise*

Table 5.4: Trace metal concentrations from pore-waters retrieved from the anoxic, deep basin of the Black Sea (station 1 and 2)

Depth interval (cm)	[Ba] (ng g^{-1})	[U] (ng g^{-1})	[Cr] (ng g^{-1})	[Fe] (ng g^{-1})	[Zn] (ng g^{-1})	[Mo] (ng g^{-1})	[Al] (ng g^{-1})	[Cd] (ng g^{-1})
Station 1, 43°21.05'N, 30°22.3'E, 1596 m (water depth)								
0.25	89.7	2.0	8.1	358.4	183.2	5.8	260.2	0.7
7.5	69.6	5.2	7.0	626.1	69.7	16.7	371.8	0.7
13	59.1	4.2	4.4	83.5	59.5	9.3	61.8	0.4
15								
19	54.7	3.1	3.2	44.7	24.2	6.3	28.3	0.3
21								
23	67.2	4.5	4.4	59.9	64.2	15.0	77.5	0.6
27	35.4	1.0	4.5	54.9	46.3	3.7	33.8	0.2
Station 2, 42°53.8'N, 30°40.7'E, 2107 m (water depth)								
0.25			0.7	178.2	36.5		37.1	
2.5			0.6	86.5	13.9		11.2	
3.5	59.0		0.0	60.8	17.2		12.8	
6.5			1.2	91.7	16.6		13.5	
7.5			1.0	72.3	24.2		22.2	
9.5			1.9	71.9	27.4		43.2	
13	54.6		0.7	142.4	32.7		37.8	

Table 5.5: Cadmium concentrations and isotope compositions from a transect of shallow multi-cores obtained from the oxic, coast to the anoxic, deep basin of the Black Sea, along with major and trace metal concentrations data

Depth interval (cm)	[Cd] (μg g^{-1})	$\delta^{114/110}Cd_{NIST}$ (‰)	2σ	[U] (μg g^{-1})	[Mo] (μg g^{-1})	[V] (μg g^{-1})	[Mn] (mg g^{-1})	[Fe] (mg g^{-1})	[Re] (ng g^{-1})	[Al] (mg g^{-1})	[Ni] (μg g^{-1})	[Cu] (μg g^{-1})
Station 1, 43°21.05'N, 30°22.3'E, 1596 m (water depth)												
0.25	2.07	0.20	0.06	8.28	31.21	91.25	0.36	7.11	9.20	9.53	49.40	73.52
0.75	1.81	0.22	0.08	10.06	37.17	82.25	0.34	10.98		8.73	50.89	72.67
1.75	1.62	0.17	0.08	11.04	52.30	111.27	0.54	16.14		9.09	63.63	76.38
2.5	1.19	0.14	0.07	13.66	46.04	89.93	0.54	15.07	0.44	6.48	55.34	57.43
3.5	1.24	0.04	0.10	15.54	47.99	91.76	0.57	15.38	1.53	7.48	55.75	59.18
5.5	0.80	0.16	0.08	19.27	59.52	118.89	0.64	18.79	4.91	7.78	62.92	71.72
6.5	0.88	0.04	0.07	17.04	22.66	49.18	0.35	13.48	5.61	5.52	40.56	45.27
7.5	0.93	0.11	0.08	19.51	66.41	113.45	0.62	16.99	6.29	5.19	66.90	68.72
8.5	1.02	0.10	0.06	18.49	35.91	73.74	0.43	14.22	8.62	8.66	57.40	63.70
9.5	0.65	0.03	0.06	17.50	36.78	49.81	0.36	8.65	0.73	5.10	39.56	42.86
11	0.54	0.00	0.08	13.98	25.99	37.93	0.35	7.12	0.48	1.33	36.28	40.12
13	0.49	0.01	0.07	12.17	14.73	27.34	0.22	4.54	5.20	4.19	32.61	33.62
15	0.89	0.17	0.07	20.56	69.87	111.24	0.59	16.62	5.20	4.68	69.03	65.72
19	0.76	0.15	0.08	15.80	40.23	63.42	0.39	16.23	7.85	5.91	67.84	49.44
21	0.60	0.11	0.09	16.78	63.37	64.83	0.44	11.19	4.68	4.05	56.14	49.89
23	0.43	-0.01	0.08	12.11	26.24	36.85	0.23	5.93	5.85	5.33	40.99	36.89
27	0.90	0.14	0.06	11.30	54.98	79.30	0.35	22.18	8.48	5.61	83.37	51.52
32.5	1.38	0.26	0.05	13.00	74.23	157.25	0.49	105.07	10.84	52.53	90.98	89.17
35.5	0.85	0.08	0.06	31.74	58.60	105.38	0.27	20.51	13.92	5.98	67.79	65.31
39.5	1.33	0.21	0.06	12.40	78.74	145.74	0.20	38.02	10.99	52.60	83.38	79.92
Station 2, 42°53.8'N, 30°40.7'E, 2107 m (water depth)												
0.25	2.22	0.27	0.07	6.40	51.21	136.38	0.40	16.82		16.78	54.67	78.09
1.25	2.10	0.06	0.08	9.72	30.48	99.97	0.37	7.62	8.99	10.18	53.13	76.26
1.75	2.37	0.12	0.06	11.11	48.88	110.92	0.40	17.97		19.33	54.54	77.23
2.5	1.27	0.13	0.06	5.31	28.84	57.53	0.19	11.95		10.32	34.28	47.22
3.5	2.41	0.22	0.05	9.17	36.87	94.71	0.39	22.25	6.52	15.02	62.73	81.05
5.5	1.36	0.16	0.07	16.68	44.73	81.14	0.54	15.91	1.32	5.47	56.23	59.30
6.5	1.35	0.07	0.05	18.79	30.90	84.23	0.45	19.01	7.73	10.25	56.75	61.95
7.5	1.20	0.11	0.08	23.10	60.46	123.93	0.70	21.53	16.86	6.92	71.86	81.25
9.5	1.10	0.18	0.07	23.71	65.88	120.03	0.65	18.37	14.82	2.80	76.43	78.19
13	0.43	0.29	0.07	11.47	109.40	242.44	0.27	7.29	15.11	5.41	29.94	31.81
Station 4, 43°40.6'N, 30°07.5'E, 380 m (water depth)												
0.25	2.44	0.19	0.06	7.49	111.67	160.16	0.47	16.78		17.24	64.37	91.61
Station 14, 43°45.9'N, 30°04.0'E, 114 m (water depth)												
0.25	0.23	0.07	0.08	0.34	6.59	23.74	13.28	14.05		7.21	106.59	16.64
Station 7, 42°53.8'N, 29°58.6'E, 78 m (water depth)												
0.25	0.41	0.13	0.07	0.38	9.41	19.31	14.68	6.04		2.24	124.57	22.84
0.75	0.30	0.11	0.06	0.72	10.25	35.95	13.84	8.99		2.38	106.84	33.82
1.75	0.23	0.08	0.06	1.31	4.91	40.96	9.99	8.05		1.14	85.96	39.37
3.5	0.23	0.08	0.09	5.79	1.91	63.47	2.41	8.61		1.49	56.39	46.74
5.5	0.11	0.05	0.06	3.85	0.56	49.26	0.83	9.73		1.53	56.04	39.69

Table 5.5: continued

Depth interval (cm)	[Cd] (µg g^{-1})	$\delta^{114/110}Cd_{NIST}$ (‰)	2σ	[U] (µg g^{-1})	[Mo] (µg g^{-1})	[V] (µg g^{-1})	[Mn] (mg g^{-1})	[Fe] (mg g^{-1})	[Re] (ng g^{-1})	[Al] (mg g^{-1})	[Ni] (µg g^{-1})	[Cu] (µg g^{-1})
Station 8, 44°14.7'N, 29°43.4'E, 64 m (water depth)												
0.25	0.09	-0.04	0.06	0.36	0.96	15.08	1.88	6.13		4.59	21.07	12.66
0.75	0.16	-0.01	0.05	1.38	1.00	53.30	2.20	4.12	2.23	1.28	45.38	34.87
1.25	0.13	-0.02	0.07	1.99	0.57	74.22	0.87	5.79	2.21	3.84	51.75	42.00
1.75	0.44	0.16	0.05	3.27	1.31	81.36	0.62	16.12		17.64	54.96	43.48
2.5	0.18	0.01	0.05	4.52	1.01	66.94	0.36	4.49	2.85	2.19	45.79	32.28
3.5	0.15	-0.05	0.09	4.40	1.01	71.29	0.34	11.71		7.41	46.42	31.87
4.5	0.11	-0.07	0.05	3.70	0.40	56.79	0.28	5.96	0.06	3.40	39.43	27.72
6.5	0.10	-0.07	0.06	3.79	0.30	46.96	0.30	5.34	0.06	1.96	40.74	27.79
7.5	0.13	-0.04	0.07	5.96	0.75	60.29	0.40	8.47		6.03	44.87	30.06
8.5	0.14	-0.03	0.06	7.70	0.51	43.67	0.34	6.45	0.08	3.69	42.73	28.06
13	0.11	-0.01	0.09	3.91	3.13	45.90	0.46	10.19		6.67	40.96	19.34
Station 13, 44°36.45'N, 29°27.4'E, 39 m (water depth)												
0.75	0.11	0.00	0.07	2.03	1.08	126.36	0.66	28.44		47.66	65.79	51.42
1.25	0.14	0.04	0.06	1.86	0.99	131.00	0.65	25.73		51.67	69.56	58.17
2.5	0.21	-0.01	0.04	1.96	0.82	106.26	0.62	23.01	2.58	48.94	57.34	50.81
3.5	0.56	-0.13	0.10	2.51	0.40	94.89	0.17	24.56		59.21	14.19	12.07
4.5	0.33	0.05	0.06	1.76	1.12	133.97	0.75	30.52	2.51	81.59	68.19	59.38
5.5	0.11	-0.10	0.06	2.40	0.88	100.47	0.18	23.80		64.10	15.62	13.93
6.5	0.36	0.11	0.05	1.62	1.30	118.90	0.74	0.45	2.44	1.18	60.93	54.67
7.5	0.75	0.19	0.18	1.98	0.66	82.94	0.13	16.23	2.75	49.61	11.85	10.50
8.5	1.22	0.30	0.09	2.68	0.04	103.77	0.18	29.20	2.73	58.73	17.08	15.92
9.5	1.15	0.31	0.09	2.65	0.28	120.85	0.18	30.61	2.67	67.46	17.68	16.79
11	0.93	0.09	0.10	2.59	0.97	124.56	0.17	29.85	2.51	70.29	17.07	15.92
13	0.46	0.17	0.09	2.50	0.49	110.14	0.16	28.73	2.97	66.42	16.37	15.55
15	0.46	0.13	0.10	2.45	0.13	102.05	0.16	27.69	2.63	59.04	15.54	14.57
17	0.35	0.10	0.10	2.48	0.18	108.78	0.16	28.21	2.40	67.52	15.98	14.84
19	0.28	0.01	0.12	2.74	0.97	116.71	0.16	27.86	2.67	64.82	17.03	14.80
21.5	0.50	0.15	0.11	3.29	1.44	117.44	0.15	29.35	2.49	67.54	16.75	16.49
24.5	1.46	0.25	0.10	2.95	1.26	116.72	0.18	26.33		64.44	16.65	18.60

The core-top samples retrieved from sites with overlying euxinic water conditions (stations 1, 2 and 4) have Cd concentrations between 2.07 µg g^{-1} and 2.44 µg g^{-1} and Cd isotopic compositions between $\delta^{114/110}$Cd= 0.19 ± 0.06 ‰ and $\delta^{114/110}$Cd= 0.27 ± 0.07 ‰. The core-tops collected from the deep basin have the highest Cd concentration values and Cd isotopic compositions closest to the surface water above the chemocline (~0.4 ‰). The near-surface sediment core collected in the deep basin from station 2 reported a Cd isotopes value (~0.27 ‰) that is indistinguishable within analytical uncertainty from the surface water above the chemocline (~0.4 ‰).

5.4.3 Trace metal concentrations in sediment pore-waters

The distribution of measured trace metals and nutrient and chemical parameters in the pore-waters from station 1 and 2 in the anoxic, deep basin are reported in Tables 5.4 and 5.3 and Figure 5.5. Cadmium concentrations varied from 0.2 ng g^{-1} to 0.7 ng g^{-1}, with an overall decrease down core, expect for a distinctive peak at 23 cm at station 1. This positive peak in sedimentary Cd concentration at 23 cm is similarly observed

Table 5.6: Cadmium concentrations and isotope compositions from a shallow multi-core obtained from the deep basin of the Black Sea (St 2) during the GEOTRACES MedBlack cruise

Depth interval (cm)	[Cd] ($\mu g\ g^{-1}$)	$\delta^{114/110}Cd_{NIST}$ (‰)	2σ
Station 2, 42°52.2′N, 31°40.2′E, 2120 m (water depth)*			
0.5	1.88	0.22	0.05
1.5	1.99	0.11	0.05
2.5	1.41	0.18	0.05
3.5	1.48	0.22	0.06
4.5	1.31	0.21	0.06
5.5	1.14	0.25	0.05
6.5	0.81	0.18	0.05
7.5	1.01	0.20	0.05
8.5	1.40	0.19	0.06
9.5	0.73	0.23	0.05
11	0.60	0.28	0.05
12	0.46	0.22	0.05
12	0.48	0.28	0.06
13	0.77	0.25	0.04
14	0.84	0.34	0.05
15	0.73	0.33	0.05
16	0.68	0.28	0.05
18	0.85	0.26	0.05
19	0.15	0.02	0.06
20	0.15	0.07	0.05
21	0.27	0.17	0.06
22	0.64	0.26	0.05
22	0.66	0.22	0.05
23	0.41	0.26	0.05
24	0.70	0.27	0.05
25	0.52	0.28	0.05

GEOTRACES, MedBlack Cruise were measured at University of Otago by Claudine Stirling's lab group

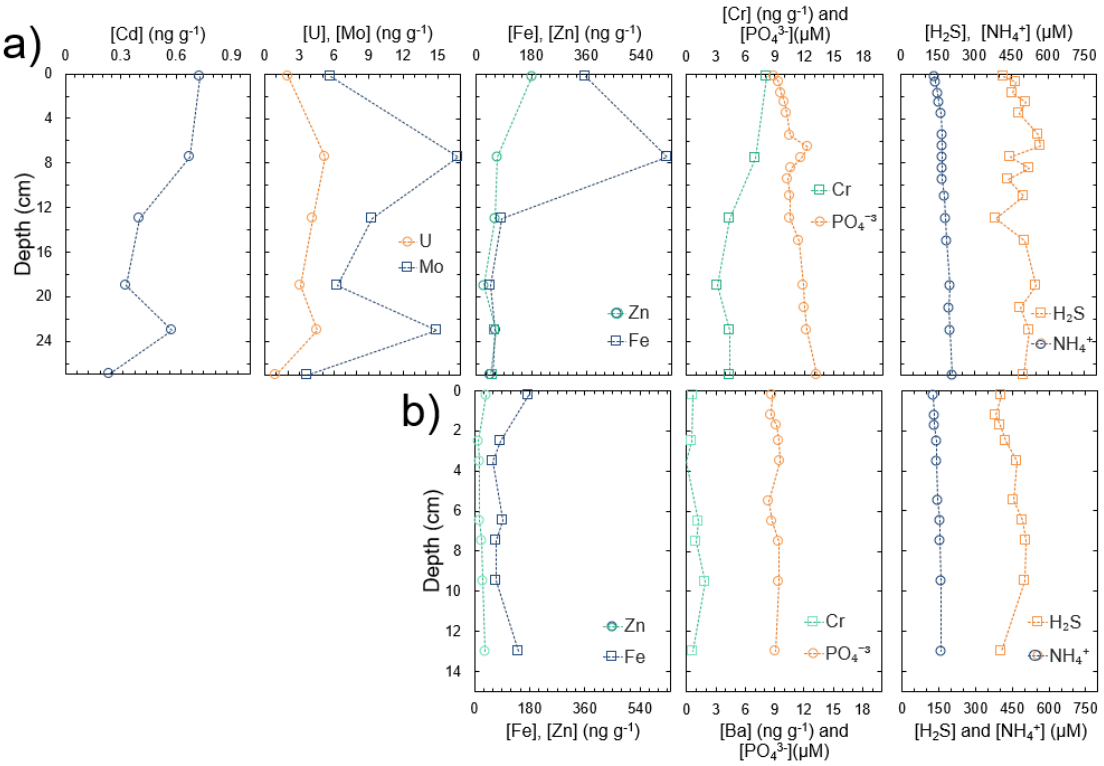


Figure 5.5: Distribution of select trace metals, along with phosphate (PO_4^{3-}), ammonium (NH_4^+), and hydrogen sulphide (H_2S) species in the pore-waters from (a) station 1 and (b) station 2 in the deep basin of the Black Sea.

for Mo and U concentrations. The pore-waters confirm that the conditions are sulfidic with H_2S in the pore-waters remaining high throughout the core, between 382 μmol kg^{-1} and 796 μmol kg^{-1}. Similarly, NH_4^+ concentrations display an incremental increase in both of the deep basin cores from 138 μmol kg^{-1} at 0.25 cm to 256 μmol kg^{-1} in the deepest measured samples.

The concentration trend of selected nutrient and chemical parameters in the pore-waters from oxygenated bottom water conditions is reported in Table 5.3 and Figure 5.6. Cadmium and other trace metals were not measured at these sites; however, the relationship between Cd and NO_3^- concentrations will be explored in later sections. In general, an inverse relationship exists between PO_4^{3-} and NO_3^-, with PO_4^{3-} increasing and NO_3^- decreasing down core. The coastal site (station 13) is the closest to the shore, consequently has a significantly higher input of organic material. It has a high accumulation of DIC and nutrients as well.

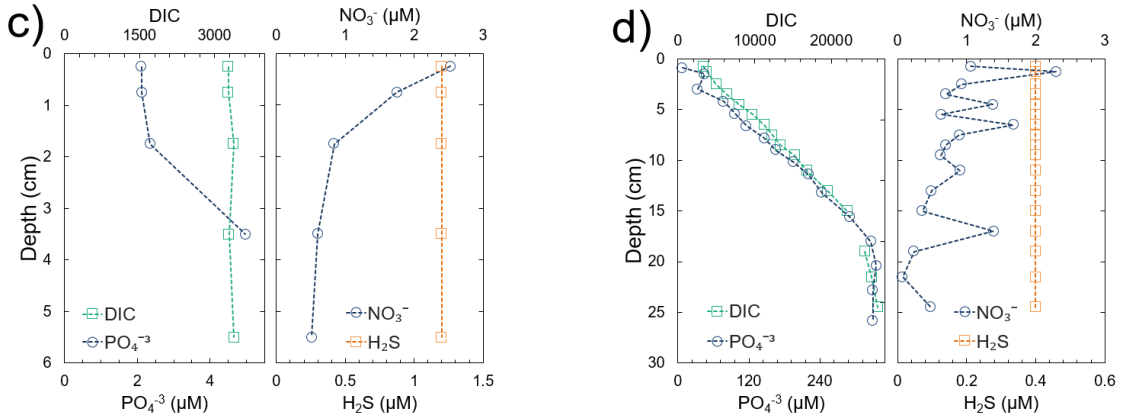


Figure 5.6: Distribution of dissolved inorganic carbon (DIC), phosphate (PO_4^{3-}), nitrate (NO_3^-), and hydrogen sulphide (H_2S) species in the pore-waters from (c) station 7 on the shelf and (d) station 13 on the coast of the Black Sea.

5.4.4 Cd concentrations and isotopic compositions in near-surface sediments

The deep basin cores from stations 1 and 2 represent conditions with overlying euxinic deep-waters (see Table 5.5, Figure 5.7, and Figure 5.8). These sites are characterised by higher Cd concentrations and isotopically heavier compositions of Cd compared to the other cores in this study. Within these two sites, station 2 is in the deepest portion of the basin and is represented by a Cd isotopic composition of $\delta^{114/110}$Cd= 0.27 $\pm$ 0.07 ‰ for the core-top sediment sample, which is heavier than the Cd isotopic composition of station 1 at $\delta^{114/110}$Cd= 0.20 $\pm$ 0.06 ‰. Similarly, station 2 has a slightly higher Cd concentration (2.22 µg g^{-1}) compared to station 1 (2.07 µg g^{-1}) for the core-top sediments. Throughout both sedimentary profiles, the Cd concentrations and isotopic compositions show a similar trend, but have poor correlation. The results are reported in Table 5.5 and shown in Figure 5.7 and 5.8.

The down core variations for Cd concentrations and isotopic compositions from Station 1 ranges from 0.43 µg g^{-1} to 2.07 µg g^{-1} and $\delta^{114/110}$Cd= -0.01 $\pm$ 0.08 ‰ to $\delta^{114/110}$Cd= 0.26 $\pm$ 0.05 ‰, shown graphically in Figure 5.7. Most notable is the distinct increase in Cd isotopes at 32.5 cm to values (0.26 ‰), within error of the waters above the chemocline (~0.4 ‰). The overall down core pattern coincides with shifts in the concentrations of other elements such as Mo, V, Cu, Ni, Re, and U, which are known

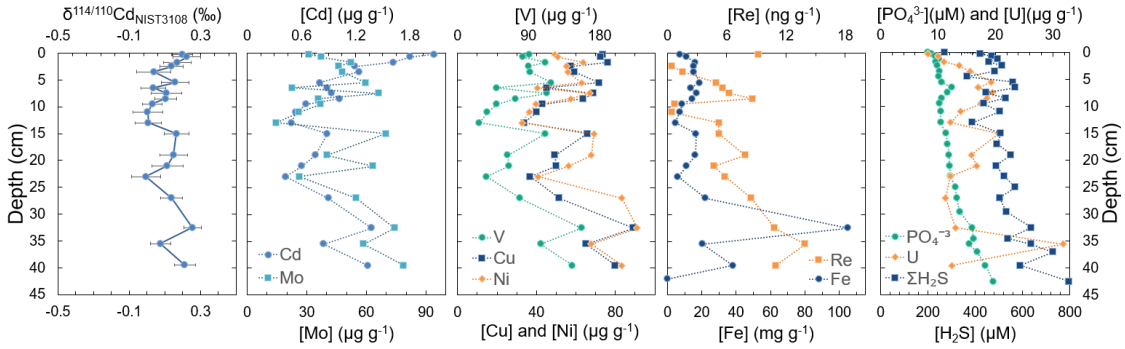


Figure 5.7: Cadmium concentrations and isotopic compositions and selected trace metal concentrations in a sediment depth profile from the deep basin at a water depth of 1596 m at station 1.

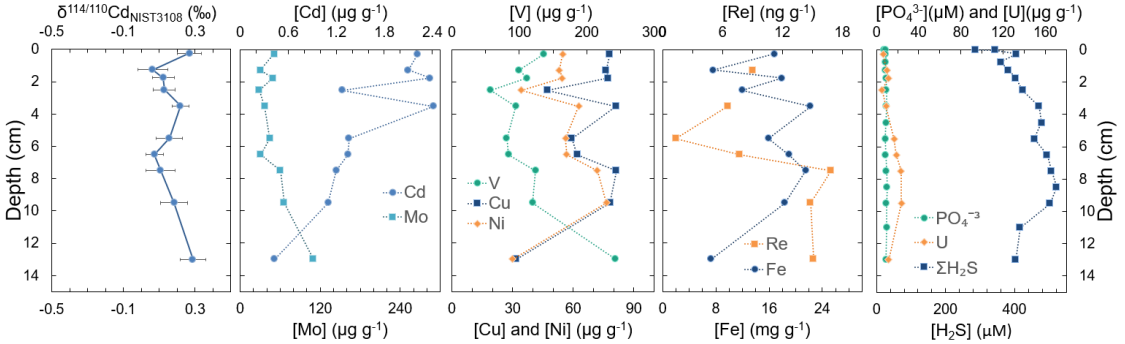


Figure 5.8: Cadmium concentrations and isotopic compositions and selected trace metal concentrations in a sediment depth profile from the deep basin at a water depth of 2107 m at station 2.

to have an affinity for removal from the pore-waters under different redox regimes. The down core variations in Cd compositions and isotopic concentrations might be linked to changes in redox conditions within the sediments, and will be discussed further in the sections below. The concentrations of H_2S, PO_4^{3-}, NH_4^+, and DIC exhibit a steady increase through the measured section, suggesting remineralisation of organic material is likely impacting the distribution of the redox front.

The Cd concentrations and isotopic compositions from Station 2 show a similar trend down core, but poor correlation, with a range from 0.43 μg g^{-1} to 2.41 μg g^{-1} and $\delta^{114/110}$Cd= 0.06 ± 0.08 ‰ to $\delta^{114/110}$Cd= 0.29 ± 0.07 ‰, shown graphically in Figure 5.8. Contrary to station 1, Cd concentration does not exhibit any relationship with other redox-sensitive elements like Mo, V, and U. These elements display a significant enrichment peak at 3.5 cm, co-occuring with a levelling out of the concentrations of

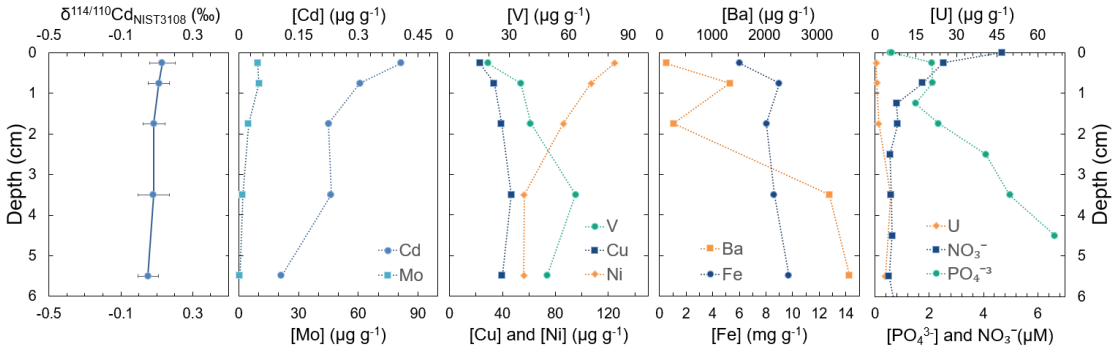


Figure 5.9: Cadmium concentrations and isotopic compositions and selected trace metal concentrations in a sediment depth profile from the shelf at a water depth of 78 m at station 7.

H_2S, DIC, PO_4^{3-}, NH_4^+ levels. Overall, the concentrations of PO_4^{3-} are low in the core, compared to station 1, supporting a low export of organic matter and a system dominated by sulphide formation for sedimentary Cd enrichment. The connection to Cd isotopes and concentration will be further discussed below.

The near-surface core collected on the shelf (station 7) with oxygenated bottom-waters shows a very gradual decrease in sedimentary Cd concentration from 0.41 µg g^{-1} to 0.11 µg g^{-1} and no variation in the Cd isotopic composition outside of analytical uncertainty, with an average $\delta^{114/110}Cd$ of 0.09 $\pm$ 0.09 ‰ (see Figure 5.9 and Table 5.5). The decrease in solid phase Cd concentrations coincides with the decrease in NO_3^- concentrations and an increase in PO_4^{3-} concentrations in the pore-waters. Similarly, other measured elements gradually increase in the solid phase once NO_3^- concentrations decrease, indicating a changing redox state. However, it is important to note that this core is only the first 6 cm of the sediment vertical profile.

The Cd concentrations and isotopic compositions of sediments in the near-surface sediment core from the mid-shelf (station 8) exhibits distinctive variations in Cd concentrations and distinguishable isotope fractionation of Cd in sediments relative to the overlying surface-waters that range from 0.09 µg g^{-1} to 0.44 µg g^{-1} and $\delta^{114/110}Cd$ from -0.07 $\pm$ 0.06 ‰ to $\delta^{114/110}Cd$= 0.16 $\pm$ 0.05 ‰ (see Figure 5.10 and Table 5.5). The down core variations coincide with changes in the concentrations of other trace metals including Mo, V, U, Cu, Ni, and Ba. The Fe concentrations exhibits a more inverse

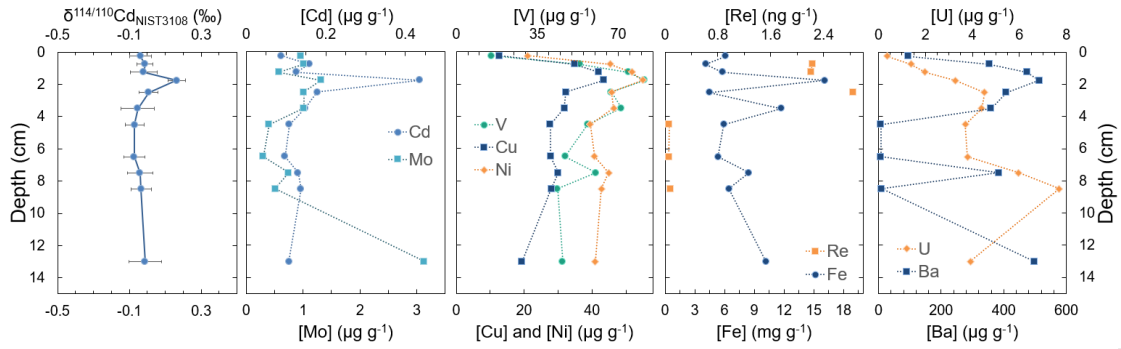


Figure 5.10: Cadmium concentrations and isotopic compositions and selected trace metal concentrations in a sediment depth profile from the mid-shelf at a water depth of 64 m at station 8.

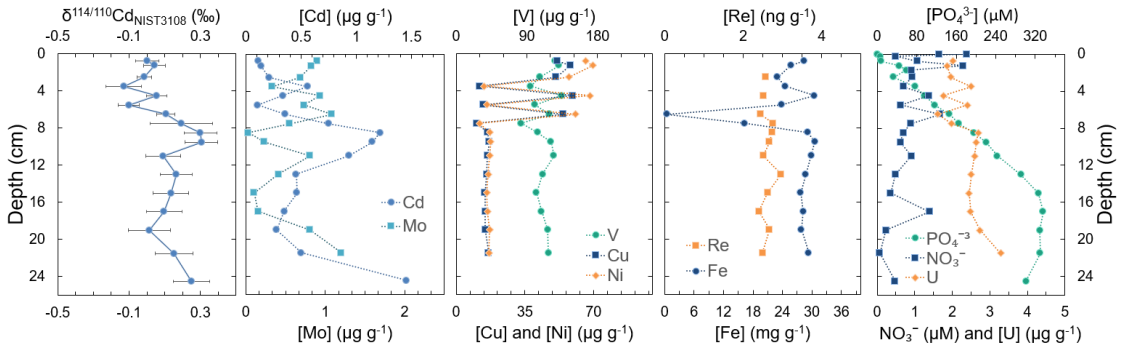


Figure 5.11: Cadmium concentrations and isotopic compositions and selected trace metal concentrations in a sediment depth profile from the coast at a water depth of 39 m at station 13.

pattern compared to Cd and the other metals in the core at the top of the core, possibly relating to the formation and dissolution of Fe-Mn oxyhydroxides.

The near-surface sediment core from station 13 is from a coastal setting with the largest variation in Cd isotopic compositions and the highest Cd concentration in all the cores collected with oxygenated water columns. The down core variations for Cd concentrations and isotopic compositions from Station 13 ranges from 0.11 $\mu g\ g^{-1}$ to 1.46 $\mu g\ g^{-1}$ and $\delta^{114/110}$Cd= -0.13 $\pm$ 0.10 ‰ to $\delta^{114/110}$Cd= 0.31 $\pm$ 0.09 ‰, shown graphically in Figure 5.11 and detailed in Table 5.5. The most significant sedimentary enrichment for Cd occurs at 9.5 cm, corresponding with an excursion to the heaviest Cd isotopes value in the sedimentary profile (0.31 ‰). This increase is quickly followed by a decrease in Cd concentration. These shifts are similarly shown by other elements such as Mo, U, V, Cu, and Ni, with an inverse relationship shown by the pore-waters NO_3^- concentrations. These trends suggest a changing redox front in the sediments.

5.4.5 Interlab Comparison for Station 2

The sediment samples presented in this study from the GEOTRACES MedBlack cruise were measured at the University of Otago and thus an interlaboratory comparison was undertaken on data measured for two sediment cores collected in the deep basin sites, labeled as St 2 (Fe-Vici) and St 2 (GEOTRACES MedBlack) (see Figure 5.1). The Cd concentrations and isotopic compositions of the sediment samples exhibit good agreement between two laboratories with an R-squared value of 0.73. Also, all of the samples through the profile having the same Cd isotopic composition within analytical error (see Figure 5.12 and Table 5.6).

5.5 Discussion

5.5.1 Cause of the observed Cd isotope fractionation effect in the water column

The input of Cd to the Black Sea is predominately from the Mediterranean Sea by way of the Bosporus Straight (~33 m sill depth), as shown by the dramatic increase in Cd concentrations between approximately 45 m and 85 m in the water column (Figure 5.2). This inflow of Mediterranean Sea water increases the oxygen and trace metal concentrations, resulting in the dissolved Cd isotopic composition to be characterized by ~0.4 ‰ above the chemocline. The dominant source of water from the eastern Mediterranean Sea suggests that the Cd isotope composition of the sub-surface Black Sea waters should be similar to those of the open ocean. This contention is supported by the similar near-surface Cd concentrations in the Mediterranean Sea as in the open deep ocean [41].

The near-complete removal of dissolved Cd into the solid phase across the transition from oxygenated to anoxic to euxinic water conditions is probably caused by the thermodynamically driven precipitation of insoluble CdS complexes [91, 165]. Cadmium concentrations experience a 50-fold decrease by the depth of H_2S detection. This observation suggests that Cd is precipitated with H_2S below the levels of detection [91] and is nearly quantitatively removed by the bottom of the chemocline. The continued

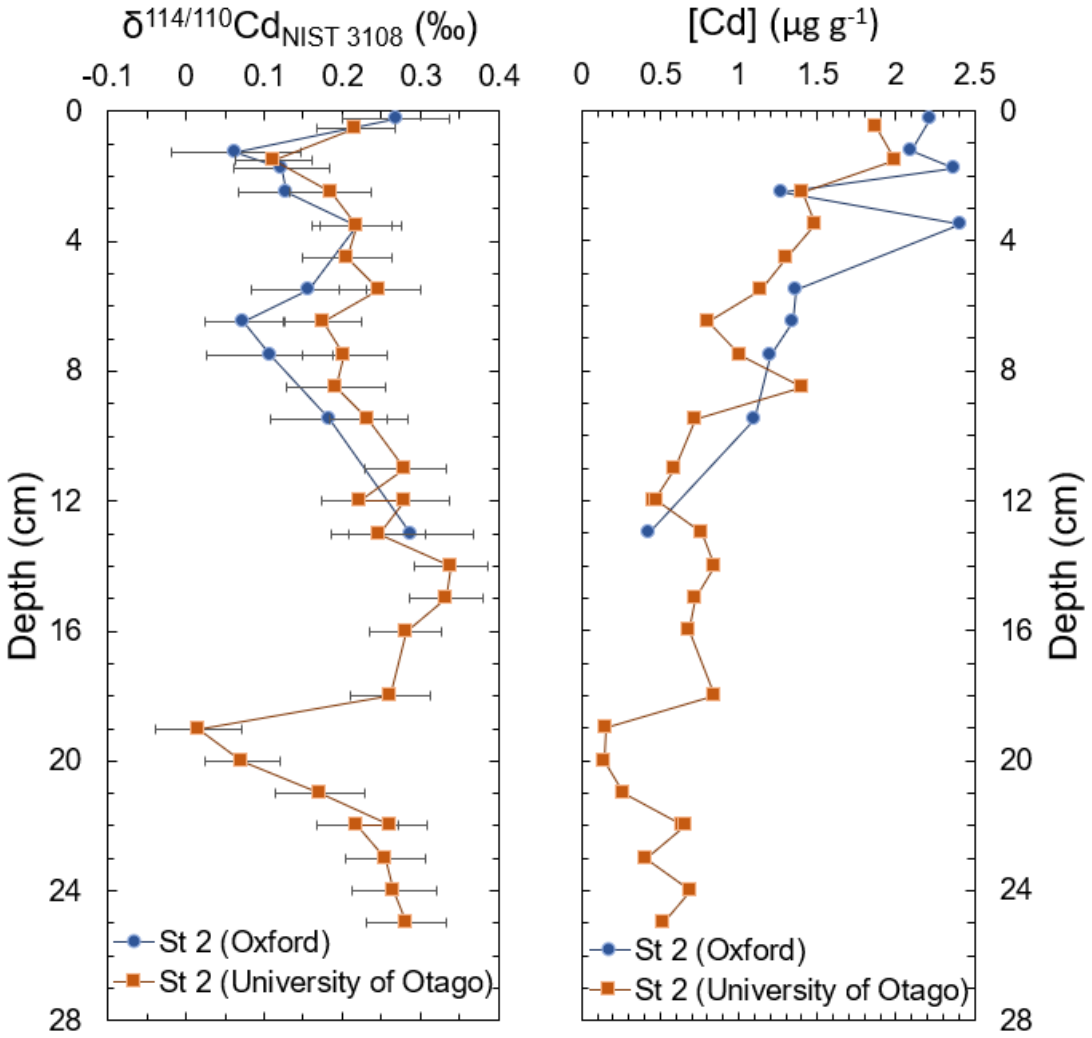


Figure 5.12: Cadmium concentration and isotopic composition of the sediment depth profile from the two sites in the deep basin collected from the Fe-Vici Cruise and the GEOTRACES, MedBlack Cruise.

precipitation of the small percentage of remaining dissolved Cd in the sulfidic deep-waters leads to a large magnitude of fractionation between the solid and aqueous Cd phases. This process peaks at 145 m, where the remaining aqueous pool of Cd is very isotopically heavy (~5.5 ‰).

The observed Cd behaviour across the chemocline from oxygenated to sulfidic water conditions is consistent with Rayleigh trends that indicate an open-system (irreversible) equilibrium isotope effect. The magnitude of fractionation is governed principally by the fraction of Cd precipitated with hydrogen sulphide in the water column, resulting in a fractionation factor of 1.00005 (Figure 5.13). The data from the Black Sea display strong

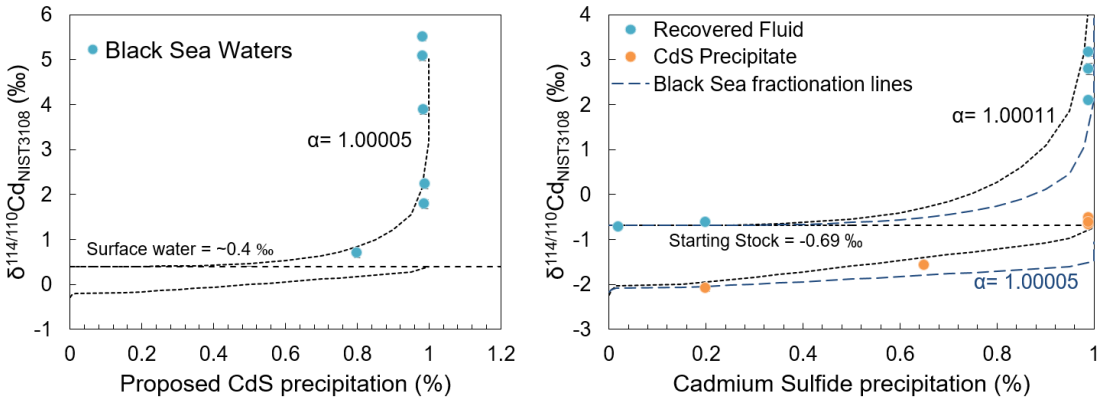


Figure 5.13: Rayleigh isotope fractionation curve using Cd isotopes of the water column from the Black Sea (blue circles) with an alpha value of 1.00005 (Left). The horizontal line at $\delta^{114/110}$Cd= 0.4 ‰ represents the water Cd isotopic composition above the chemocline. Isotopic compositions of dissolved Cd (blue circles) and Cd sulphide precipitate (orange circles) from controlled CdS precipitation experiments completed with synthetic seawater in an oxygen-free atmosphere with an alpha value of 1.00011 (Right). The horizontal line at $\delta^{114/110}$Cd= -0.69 ‰ represents the bulk starting composition. The best-fit Rayleigh fractionation curves for the Black Sea are included (blue, dashed lines). Error bars represent 2 SE of each sample. The errors bars are smaller than the markers.

agreement between the laboratory CdS experiments presented in Chapter 3.

5.5.2 Redox reaction zones defined by other trace metals in the water column

The mechanism for immobilization of the other trace metals from the aqueous pool into solid phases across the chemocline is variable. The depth of trace metal enrichment is different for different metals. It is traditionally defined by a vertical sequence of redox reaction zones in the pore-waters. The order of the zones follow free energy yield: aerobic respiration to NO_3^- reduction, Mn and Fe reduction, and sulfate reduction [181]. This redox depth profile is typically observed within sediments. However, in anoxic, stratified basins, it occurs at the chemocline within the water column. This feature impacts the solubility of redox-sensitive trace metals. At the top of the chemocline and bottom of the oxic zone, Fe and Mn oxides have likely scavenged V and Ni [165]. Similarly, the decrease in dissolved Cd concentrations results from precipitation with trace hydrogen sulphide formed by sulfate-reducing microbes [90] and adsorption onto Fe and Mn oxides. As the Fe and Mn oxides are dissolved through the chemocline, the Cd, V, Ni,

Fe, Mn, and other associated trace metals will be released into aqueous species. At this point, any released Cd will likely be rapidly removed to form CdS species [91]. As H_2S concentrations increase below the chemocline, redox-sensitive trace metals, like Fe and Mo, change oxidation states leading to abotic and biotic driven chemical reactions that remove these metals from the dissolved pool to the solid pool [165, 169]. As observed with Cd, these other metals likely form sulphide complexes as well [182–185].

5.5.3 Explanation for the Cd isotopic compositions in the deep-waters

The sulfidic deep-waters exhibit minimal variations in Cd concentrations. Conversely, the Cd isotopic compositions show a gradual shift to isotopically lighter values with increasing depth. The behaviour of Cd below the chemocline to approximately 200 m is impacted by the breakdown of remaining organic material and formation of insoluble CdS complexes. The explanation for the continued shift towards a lighter isotopic composition of Cd from 200 m till the last measured dissolved Cd sample at 500 m is more of an unknown. The shift could represent the degradation of a small amount of organically-bound Cd with a very light Cd isotope value. Alternatively, it may represent the formation of authigenic carbonates or oxides that preferentially remove the heavy isotopes; however, the fractionation caused by incorporation into carbonates or adsorption to oxides would likely be small as shown from laboratory experiments [85, 86]. Likewise, as mentioned above, Cd remain at very low concentrations below 200 m. It is worth noting that the relationship between Cd isotopes and H_2S concentrations show very good correlation (R-square value = 0.95) from the chemocline to 500 m, suggesting that the rates of Cd and H_2S diffusion are coupled in the deep-waters. More Cd isotope data are required to fully constrain the processes controlling the behaviour of Cd in the deep-waters (below ~200 m).

5.5.4 Authigenic enrichment of Cd in sediments

The elemental enrichment factor (EF) was calculated for the sediments (see Table 5.7). In this equation, as described in Chapter 4, the Cd and other elemental concentrations were normalized to Al in order to determine the detrital contribution to the sediments using the “average shale” value from Wedepohl (1995) [149]. The enrichment factor ranged

from 1.3 to 16.1 in the most oxygenated sites, while the anoxic, deep basin exhibited a significant enrichment ranging from 19.6 to 315.9. This supports the contention that some of the samples may have a detrital influence in the oxygenated sites, particularly near the coast, while the deep-waters are primary derived from the deposition of organic matter or formation of authigenic minerals in the water column.

5.5.5 Source of Cd to the sediment-water interface

The primary sink of solid fraction Cd to the sediments deposited below the chemocline is likely the authigenic enrichment of CdS complexes that primarily formed in the deep-waters. This is evident by the Cd concentration diminishing to ~1.2 % of the initial Cd concentrations above the chemocline. Other minor components include aqueous Cd species and possibly a small component of sinking organic matter. The export of sinking organic matter in the anoxic portion of the basin is supported by a gradual increase in DIC and PO_4^{3-} concentrations in the pore-waters throughout the core at station 1, along with the core-top sediment sample having the highest Cd concentration in the core (2.07 $\mu g\ g^{-1}$). This pattern may reflect an input of organic material near the top of the profile, resulting in the release of Cd from the solid phase into the pore-waters during degradation of remaining organic matter, and subsequent preferential removal of light Cd isotopes with insoluble CdS complexes.

Conversely to station 1, the trend at station 2 depicts a system that is dominated by sulphide formation. This statement is supported by the low and minimal variability of PO_4^{3-} concentrations in the pore-waters through the core, suggesting that remineralization of TOC in the sediments is negligible. Additionally, this implies minimal diffusive flux of PO_4^{3-} into the sediments from the overlying water column, advocating for a low export of organic matter to the sediments. The consequence is the main source of Cd to the sediments is CdS species precipitated in the overlying sulphide-containing waters.

The Cd in near-surface sediments deposited under oxygenated bottom-waters near the basin margins is likely sourced from sinking organic material and dissolved Cd ions associated with chloro complexes. The main support for this claim is the high

Table 5.7: Calculated enrichment factors for select trace metals

Depth interval (cm)	EF [Cd]	EF [U]	EF [Mo]	EF [V]	EF [Mn]	EF [Fe]
Station 1, 43°21.05'N, 30°22.3'E, 1596 m (water depth)						
0.25	168.0	26.9	181.2	14.0	5.6	1.9
0.75	160.4	35.7	235.5	13.8	5.7	3.2
1.75	137.6	37.6	318.2	17.9	8.7	4.5
2.5	142.5	65.3	392.9	20.3	12.3	5.8
3.5	128.3	64.3	354.7	17.9	11.1	5.2
5.5	79.8	76.8	423.4	22.3	12.1	6.1
6.5	124.2	95.7	227.2	13.0	9.3	6.1
7.5	139.1	116.4	707.3	31.9	17.5	8.2
8.5	91.7	66.2	229.5	12.4	7.2	4.1
9.5	98.3	106.2	398.5	14.3	10.5	4.3
11	315.9	326.8	1084.8	41.8	38.5	13.5
13	90.2	90.0	194.3	9.5	7.7	2.7
15	146.6	136.1	825.9	34.7	18.4	8.9
19	99.1	82.9	376.7	15.7	9.8	6.9
21	115.5	128.4	865.8	23.4	16.0	6.9
23	61.9	70.4	272.4	10.1	6.2	2.8
27	124.3	62.4	542.2	20.7	9.1	9.9
32.5	20.3	7.7	78.2	4.4	1.4	5.0
35.5	109.7	164.4	542.1	25.8	6.6	8.6
39.5	19.6	7.3	82.8	4.0	0.6	1.8
Station 2, 42°53.8'N, 30°40.7'E, 2107 m (water depth)						
0.25	102.4	11.8	168.9	11.9	3.5	2.5
1.25	159.7	29.6	165.7	14.4	5.3	1.9
1.75	95.0	17.8	139.9	8.4	3.0	2.3
2.5	95.4	15.9	154.5	8.1	2.7	2.9
3.5	124.4	18.9	135.8	9.2	3.8	3.7
5.5	193.0	94.5	452.5	21.7	14.5	7.3
6.5	101.7	56.8	166.8	12.0	6.4	4.7
7.5	134.6	103.4	483.3	26.2	14.8	7.8
Station 13, 44°36.45'N, 29°27.4'E, 39 m (water depth)						
0.75	1.8	1.3	1.2	3.9	2.0	1.5
1.25	2.1	1.1	1.1	3.7	1.8	1.2
2.5	3.3	1.2	0.9	3.2	1.9	1.2
3.5	7.3	1.3	0.4	2.3	0.4	1.0
4.5	3.2	0.7	0.8	2.4	1.3	0.9
5.5	1.3	1.2	0.8	2.3	0.4	0.9
7.5	11.8	1.2	0.7	2.4	0.4	0.8
8.5	16.1	1.4	0.0	2.6	0.4	1.2
9.5	13.2	1.2	0.2	2.6	0.4	1.1
11	10.3	1.1	0.8	2.6	0.4	1.1
13	5.3	1.2	0.4	2.4	0.4	1.1
15	6.1	1.3	0.1	2.5	0.4	1.2
17	4.0	1.1	0.2	2.4	0.4	1.0
19	3.3	1.3	0.8	2.6	0.4	1.1
21.5	5.8	1.5	1.2	2.5	0.3	1.1

*Reference Al concentration data to calculate enrichment factors is 77440 µg g-1, as detailed in Wedepohl (1995)

TOC amounts (up to 2.9 %) and the significantly higher PO_4^{3-} concentrations compared to the anoxic, deep basin sites.

5.5.6 Quantitative Cd removal from the waters and into the sediments

The dissolved Cd concentrations and isotopic compositions in the core-top samples have a relationship with the redox conditions in the bottom-waters, where shallow, oxygen-rich waters have a light Cd isotope signal relative to the overlying bottom-waters and deep, sulfidic bottom-waters have a Cd isotope signal similar to waters above the chemocline. The behaviour of Cd in the deep basin supports quantitative removal of Cd, as the majority of Cd will be in the solid fraction by the base of the chemocline and remain precipitated through the sediment-water interface. The CdS complexes will likely remain insoluble because of the high stability coefficient of cadmium sulphides [186, 187]. The deep basin site (station 2) recorded an isotopic offset between the core-top sediment sample and the waters above the chemocline (~0.4 ‰) of $\Delta^{114/110}Cd_{\text{core top sediment}-\text{surface waters}} = -0.13 \pm 0.10$ ‰. The analytical error for the measurements on the core-top sample and water sample would overlap, suggesting little to no resolvable fractionation between the seawater and sediments. This means the core-top samples in the deep basin with sulfidic bottom-waters is recording the isotopic composition of the surface-waters. In contrast to the deep basins, the oxygenated bottom-waters on the shelf and coast resulted in a larger isotopic offset, ranging from $\Delta^{114/110}Cd_{\text{core top sediment}-\text{surface waters}} = -0.27 \pm 0.10$ ‰ to $\Delta^{114/110}Cd_{\text{core top sediment}-\text{surface waters}} = -0.44 \pm 0.10$ ‰.

The Cd isotope composition compared to the Cd concentration in the core-top sediment samples from all the stations are primarily impacted by the redox conditions in the pore-waters. The one end-member are stations within oxygenated bottom-waters that are dominated by aerobic bacterial oxidation and record non-quantitative removal, leading to a reported Cd isotopic composition that is lighter than the overlying bottom-waters. The other end-member are the stations with euxinic bottom-waters that are likely exhibiting quantitative removal with H_2S to form CdS species, reporting a Cd isotopic signature that is the same as surface-waters in this study. The mixing between a signal

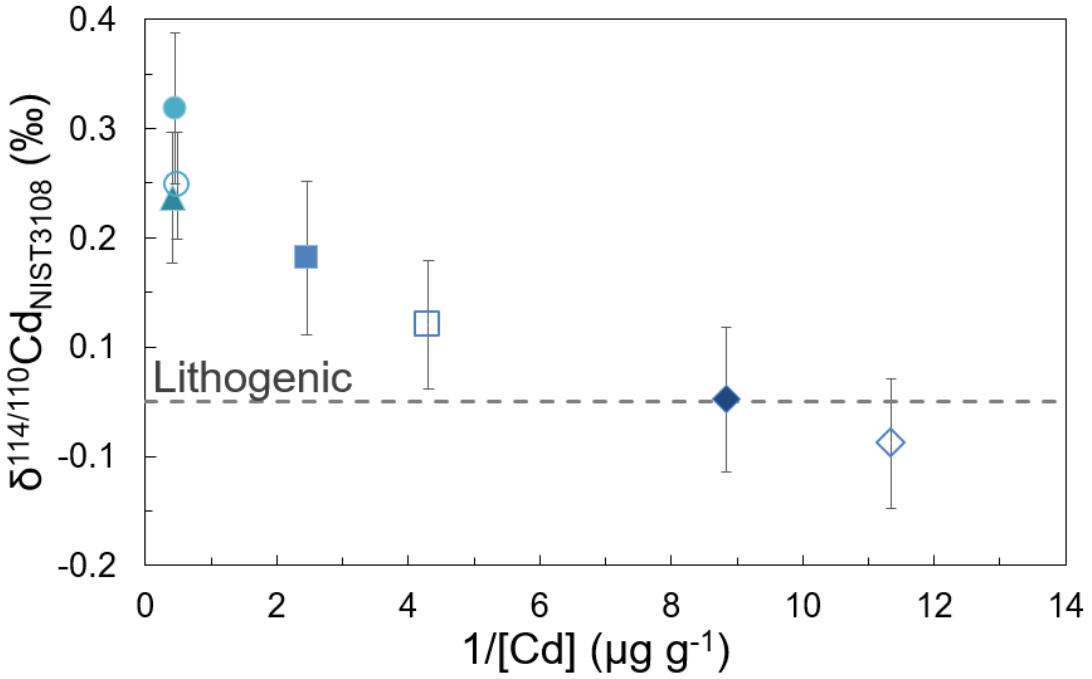


Figure 5.14: Cadmium isotope composition relative to 1/Cd concentration in core-top sediment samples from station 1 (open circle), station, 2 (filled circle), station 4 (filled triangle), station 14 (open square), station 7 (filled square), station 8 (open diamond), and station 13 (filled diamond).

that supports quantitative removal with a Cd isotopic composition similar to the overlying water above the chemocline and non-quantitative removal with a CdS derived signature (~-0.1 ‰) is shown graphically in Figure 5.14.

5.5.7 Cadmium-sulphide interactions in the sedimentary depth profile

The sedimentary depth profiles from the Black Sea show the relationship between variable bottom water redox conditions and the distribution of trace metals and Cd isotopes. In all the sites, the primary mechanism for authigenic Cd enrichment down core is by precipitation of CdS species from the pore-waters or directly sourced from the overlying water column below the chemocline.

The distribution of Cd concentrations and isotopes, along with other redox-sensitive elements in the near-surface sediment core with overlying euxinic bottom-waters indicate a system that has undergone minimal diagenetic alternations, indicating stable, sulfidic deep-water conditions. This scenario implies that Cd and other trace metals are reflecting

minimal post-depositional remobilization in the down-core record. The minor variability in the pore-waters and sediments is likely caused by immobilization of newly released, dissolved Cd from sinking organic matter with H_2S to from CdS species, particularly for station 1 [110]. For example, the similar decrease in sedimentary concentrations of Cd and Fe at St 2 coincide with an excursion to isotopically lighter values (~0.06 ‰) compared to the core-top value (~0.27 ‰). This trend may signify a large input of organic material and subsequent bacterial degradation that release a large quantify of trace metals to the pore-waters, leading to the formation of CdS and FeS species in the solid fraction through the profile. Likewise, iron sulphides, polysulphides, and other sulphide complexes are known to remove metals like Cu, Zn, Co, and Mo from the pore-waters and into the solid fraction [164, 182, 183, 185, 188]. The formation of sulphide complexes may help to explain the similar, but not statistically significant, trends between Cd concentration and concentrations of other redox-sensitive elements such as Mo, V, Cu, U, and Re.

The distribution of trace metals and the behaviour of Cd in the near-surface sediments retrieved from sites with oxygenated water columns differ from those collected in the deep basin. The shelf and margin cores contain a traditional sequence of microbially-mediated redox reactions, along with physical disruption from bioturbation and likely a higher input of organic material and sedimentation rates compared to the deep basin. These chemical reactions cause a redistribution of Cd and other elements. Cadmium concentrations exhibit a strong relationship to peak nitrate reduction, as noted in Chapter 4 for samples from the South Atlantic at 40°S. The near-surface sediments from the coastal site exhibit the most isotopically heavy value of Cd in all the cores at 9.5 cm (~0.31 ‰), right at a decline in NO_3^- concentration. This Cd isotope value coincides with an increase in the concentrations of several redox-sensitive trace metals such as V and Fe, highlighting the likely role of redox transformations in governing the accumulation and speciation of Cd in the sediments. The rapid increase in PO_4^{3-} concentrations in the pore-waters and declining NO_3^- concentrations lead to the use of the oxidant with the next highest free energy yield, in this case specialized sulfate-reducing microbes [90, 119]. While no H_2S was detected in the core, Cd is known to be an indicator of sulphide production for sulfate reduction, even if the concentrations are very low [181]. The peaks

in Cd concentration in these cores may be reflecting microenvironments of trace H_2S, leading to the precipitation of insoluble CdS [90]. The NO_3^- concentrations in the coastal core always remain above the detection limits. This trait is likely caused by the physical mixing from bioturbation, causing a shift of the redox front.

5.6 Conclusions

This study provides constraint on the composition of Cd in near-surface sediments accumulating under varying redox conditions, and compares these compositions with those of the overlying surface-waters. Our results exhibit a strong link between redox state in the bottom-waters and the degree of Cd isotope fractionation of the core-top sediments relative to the overlying surface-waters above the chemocline. Additionally, the most significant variability in Cd concentration and isotope composition in the water column and the near-surface sediments coincides with changes in redox conditions, suggesting the dominating role of the precipitation of dissolved Cd with available hydrogen sulphide to form insoluble cadmium sulphide complexes on the cycling of Cd.

6

Redox cycling control on the cadmium isotope composition of waters, pore-waters, and near-surface sediments in a seasonally anoxic basin (Saanich Inlet, Vancouver)

Contents

6.1 Introduction 135
6.1.1 Study site 135
6.2 Sediment sampling procedures 138
6.3 Methods 140
6.3.1 Measurement of total organic carbon concentrations 140
6.4 Results 140
6.4.1 Cd concentrations and isotope compositions of water depth profiles 140
6.4.2 Cd concentrations and isotope compositions of sediment depth profiles 142
6.4.3 Comparison of Cd concentrations with other trace metals in the near-surface sediment cores 147
6.4.4 Cd concentrations and isotope compositions of pore-water depth profiles 149
6.5 Discussion 151
6.5.1 Origin of Cd isotopic variation in the Saanich Inlet water column 151
6.5.2 Explanation for the Cd isotopic composition of near-surface sediments 153
6.5.3 Evidence for primary depositional signal record by Cd isotopes 155

6.5.4 A mechanism for the authigenic enrichment of Cd in sediments 155
6.5.5 Co-variance between Cd and select trace metals in sediments . 157
6.6 Conclusion 159

Abstract

Cadmium (Cd) isotopes have provided insights into the biogeochemical cycling of Cd in the modern oceans, and may be used to provide information about past ocean chemistry. Cadmium is removed from seawater into marine sediments, but the isotopic composition of this output flux, and the processes that control the isotope composition of the marine sediments, are poorly constrained. The precipitation of cadmium sulphide (CdS) species as a controlling mechanism on the isotopic composition of sediments accumulating in low oxygen settings has been demonstrated by field observations from the South Atlantic Ocean and from the Black Sea. However, the stability of the precipitated CdS species to episodically elevated oxygen levels is not understood. This study investigates the role of redox conditions as a control on the Cd isotope compositions of marine waters, pore-waters, and sediments in an oxygen-depleted setting with seasonal reventilation events (Saanich Inlet, Vancouver Island). Saanich Inlet experiences an annual transition from oxic conditions in early autumn to anoxic conditions in late summer with detectable hydrogen sulphide in the deep-waters. Water column Cd-isotope data depict a near-quantitative removal of dissolved Cd to insoluble cadmium sulphide species across the chemocline, resulting in a short-lived excursion to isotopically heavy isotopes of Cd in the residual dissolved pool. The transition is best fit with a Rayleigh isotope fractionation trend that is similar in magnitude to the Black Sea. Despite this similarity, however, the Cd concentrations and isotope compositions in Saanich Inlet core-top sediments are notably lighter than in the overlying surface-waters, with an average $\Delta^{114/110}\mathrm{Cd}_{\mathrm{core\,top-surface\,waters}}$ of -0.38 $\pm$ 0.07 ‰. This isotopic offset is similar to those found in the oxic South Atlantic Ocean, and to sediments accumulating in oxygenated waters and pore-waters above the Black Sea chemocline. These observations suggest that CdS forming in anoxic marine sediments might not be stable under the

conditions of annual reventilation experienced in Saanich Inlet, with a projected release of isotopically heavy Cd back into pore fluids and seawater. These findings imply that the hydrographic state, as well as the redox state, of ancient marine basins need to be properly evaluated before accurate interpretations of sedimentary Cd isotopes can be made.

6.1 Introduction

The previous chapters have shown that cadmium has a high affinity to form insoluble cadmium sulphides in sulfidic water columns, within short-lived, reducing microenvironments found in ODZs, and with trace hydrogen sulphide (H_2S) during sedimentation and early diagenesis. These findings support the contention that cadmium (Cd), similar to other redox sensitive elements like U, Mo, and Re is a promising tool for deciphering redox conditions in ancient marine environments. However, the stability of CdS formation to annual reoxygenation events is unknown.

This chapter investigates the Cd concentrations and isotopic compositions of waters, near-surface sediments, and sedimentary pore-waters in a setting with seasonal variations in productivity and oxygen. The hypothesis for this study is that the Cd isotopes signature of the near-surface sediments will be impacted by seasonal, water column re-oxygenation events. Saanich inlet provides an ideal setting to study the annual transition from euxinic conditions in the deep-waters in winter through summer to rapid, brief renewals of oxygen-rich waters in early autumn.

6.1.1 Study site

Saanich Inlet is an intermittently anoxic fjord located in southeastern Vancouver Island, British Columbia that was formed by an uplifted convergent margin [169]. It has a maximum length of 26 km and depth of 238 m [189], which is significantly smaller and shallower than the Black Sea. The inlet is bounded by a 70m bedrock sill at the north end of the fjord, limiting deep-water circulation and water exchange between the inlet and the open ocean waters in the Georgia and Haro straits via the Satellite Channel [184, 189–192]. The water from the southern Georgia and Haro straits that manages to infiltrate into the inlet and other nearby basins is a mixture of high salinity seawater from the

Pacific Ocean and freshwater from the Fraser River [193, 194]. The water properties in the straits are highly impacted by processes on the coast, such as El Niño – Southern Oscillation events [193]. Overall, the restricted water exchange between the inlet and Georgia and Haro straits results in anoxic conditions within the inlet below approximately 200m water depth for nearly the entire year.

The surface water pattern within Saanich Inlet is controlled by tidal cycles and wind, along with estuarine circulation from the Satellite Channel in the northern part of the inlet above the sill depth. The estuarine circulation in the surface-waters above the sill inhibits exchange of bottom-waters in the fjord with those of the water from the Haro Strait, leading to decreased deep-water circulation and water column stratification [189, 191]. Additionally, high primary productivity rates lead to increased organic matter fluxes to a stratified deep basin where microbial respiration will rapidly consume oxygen after the autumn oxygenation events, followed by alternative oxidants. Nitrate is depleted by late winter, leading from denitrification by denitrifying microbes to sulfate-reducing microbes respiring detectable (H_2S) in the deep-waters in spring through late summer [191].

At some point in the late summer through autumn, the deep-waters undergo a re-oxygenation event when the water column stratification is destabilized and saline water from Haro strait mixes with the inlet's deep-waters [189, 191, 195]. This event is only able to occur when the surface water salinities in the Haro Strait are greater than those of the deep-waters of the inlet [191, 194, 195]. The salinity in the strait is at its lowest in late spring and early summer, as a result of freshwater from the Fraser River [191]. As the input of freshwater decreases to a minimum in late summer through autumn, then the salinity of the surface-waters in Haro Strait exceeds those salinity values in the deep-waters of the inlet, initiating the renewal event of well-oxygenated waters to deep-waters of the inlet [191, 194, 195].

These renewal events between late summer and autumn are modulated by fortnightly tidal mixing [191, 195], occurring over the course of 8 to 10 days each month to a depth of 100m, however the degree and frequency of this renewal is variable [194]. Renewal events that reach the bottom of the inlet occur less often and are not observed every year [191]. The annual shifts described above have occurred for the past century

in the inlet [194]. The rapid, relatively predictable progression from oxygenated to sulfidic conditions and the easy accessibility of the inlet makes it an ideal setting for a comprehensive redox reaction study.

The anoxic conditions in the deep-water is further evident by a lack of benthic fauna and preservation of seasonal shifts in the sedimentation of fine-grained, organic-rich and terrigenous sediments [194]. The sediments are predominately dark silts and clays that are deposited during the fall and spring with carbonaceous and diatomaceous laminae deposited during spring and summer blooms [184]. Previous studies have reported laminations with systematic annual deposits that are visible in the sediments, termed varves [196, 197]. The signature of anoxia is maintained because the annual re-oxygenation events of the deep-waters are too rapid for benthic fauna to re-inhabit the basin seafloor [184, 189, 190]. The preservation of the varves in the sediments provides an ideal basin to study the influences of the annual re-oxygenation events and tidal cyclicity on the measured Cd concentrations and isotopic compositions of the near-surface sediment cores in this study.

Russell and Morford (2001) observed the varves and noted that the annual laminations are occasionally overprinted by massive layers of clayey silts [192]. The origin of these sedimentary units is likely to be from gravity flows or increased bioturbation, as supported by brackish, shallow-water benthic foraminifers and coarse-grain sediments [197–200].

The drainage basins for Saanich Inlet is small compared to other fjords in British Columbia with no major rivers surrounding the inlet [194]. The inflow of terrigenous sediments that does occur into the inlet is limited to a small contribution from the Goldstream river and a significant input $(9\text{x}10^4 \text{ tons per yr})$ of sediment from the Cowichan River, located 50 km northeast of the inlet [194, 196, 201]. The greater inflow of terrigenous material from the Cowichan River into the inlet is most distinctly shown by the higher sedimentation rates and less organic-rich sediments in the northern portion of the inlet compared to the southern parts [194]. Likewise, the river inputs provide fresh water to sustain lowered salinity conditions (31 PSU) down to approximately 50 m [189, 190, 195, 196]. The terrigenous sediments entering the basin were mainly deposited during the last glaciation and the Holocene [202, 203]. The sediments from the last

glaciation consisted of till, sand and gravel, while those in the Holocene consist of fluvial, marine, lacustrine, and organic-rich material [194]. The reported sedimentation rates are significantly higher than other restricted basins at approximately 2–6mm per yr, with an annual deposition of $0.24 \text{ to } 0.36 \text{ g per cm}^3$ of dry sediment [190, 194, 198]. Budemeier (1969) stated an average accumulation rate based on radiocarbon dating for the past 3860 years to be approximately 4.9mm per yr [198].

6.2 Sediment sampling procedures

Water samples were collected during a time series of cruises over a nine month period from September 2016 to April 2017 with fortnightly cruises to the same location in Saanich Inlet to study the temporal progression of redox reactions. The samples in this study were collected when the water column was stagnant with a distinct chemocline and detectable H_2S concentrations in the deep-waters during the Saanich Inlet Redox Experiments (SaanDox). The sampling site is located at 48° 37.53'N, 123° 29.91'W (see Figure 6.1). Depth at our sampling location was roughly 210 m. Typically, 10 casts were completed at this station with a stainless steel CTD frame fitted with 6, 10 litre bottles with external springs. Each cast was focused on a different part of the water column.

The core data measured either during or after each cruise included trace metal concentrations (Fe, Mn, Cu, Zn, and Cd) and speciation for Fe along with hydrographic, and nutrients concentrations: temperature, salinity, oxygen, H_2S, nitrate-NO_3, nitrite-NO_2, ammonium, and N_2 gas. The samples for Cd concentration and isotopic analyses were collected in acid-cleaned, 10 litre high density polyethylene containers at six depths through the water column: at the surface, immediately above the chemocline, at the middle of the oxic-anoxic interface, at the bottom of the chemocline, in the deep-waters, and at the bottom of the water column. The samples were immediately filtered through an AcroPak (0.45 μm) and acidified with ultra-pure HCl to a pH of 1.7 (0.024 M). Please note that the collection of water samples and measurement of physical and nutrient parameters in the waters presented in this study were not completed by myself, but the participants of the SaanDox cruises.

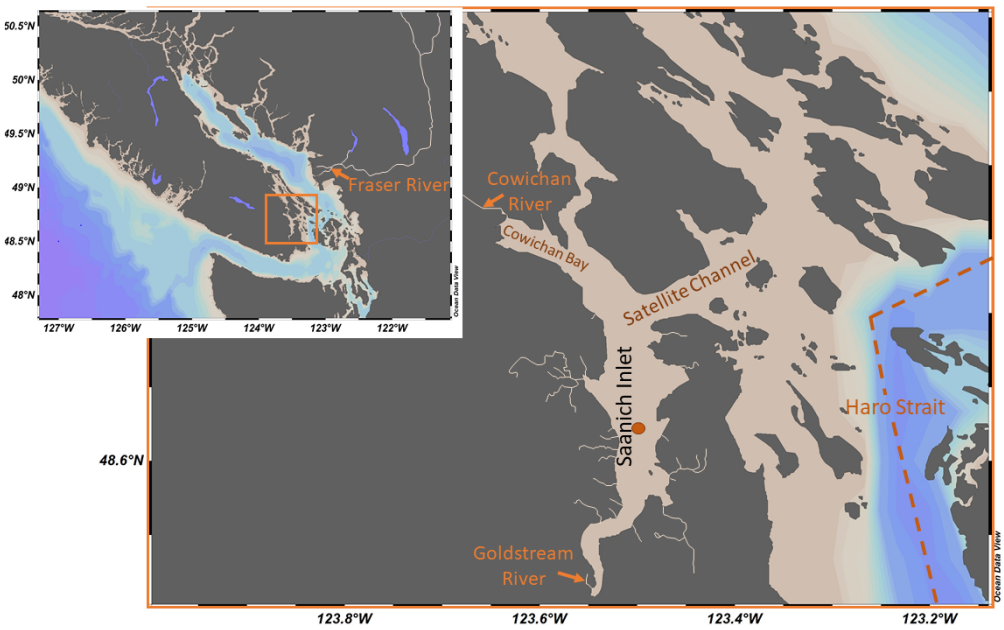


Figure 6.1: Map of Saanich Inlet showing the time-series, water station (orange circle), along with nearby rivers and sites of interest. The smaller overlying insert shows a zoomed-out view of the geographic location of Saanich Inlet.

The sediment samples were collected during a separate cruise to two locations in the inlet that represent hypoxic and euxinic conditions in the deep-waters. The hypoxic station was located at 48°39.131'N, 123°29.212'E and a water depth of 94 m. The euxinic station was located at 48°39.092'N, 123°29.500'E and a water depth of 120 m. The samples were retrieved with the Pedersen gravity corer. Sediment sampling was attempted unsuccessfully at stations with oxygenated bottom-waters.

The cores were transferred to the on-board laboratory and an extruding system was used to extract the sediments from the coring tube. As the sample is extruded above the top of the tube, a thin metal sheet and a spacer ring (1 cm thick) are used to assure 1 cm slices. The samples were placed into acid-cleaned 50 mL polypropylene centrifuge tubes, seal with Parafilm, and placed into a sealed plastic container. Once the ship returned to port, the samples were transferred to a laboratory and immediately centrifuged at 4000 rpm for 20 minutes. The spun sediments were placed inside a Cole Palmer glove bag under an N_2 atmosphere. The pore-water was decanted into an acid-cleaned 15 mL polypropylene centrifuge tube and placed inside a refrigerator. The solid fraction was further subsampled for additional analyses including trace metal concentrations

and measurement of Cd isotopes.

6.3 Methods

Please refer to Chapter 2 for details on the digestion and chemical separation protocols for the natural samples, along with analytical procedures.

6.3.1 Measurement of total organic carbon concentrations

Rock-Eval pyrolysis was used to measure the hydrocarbons in order to calculate the total organic carbon (TOC) in the near-surface sediment cores from Saanich Inlet. The TOC concentration of each near-surface sediment sample was measured at the University of Oxford using a Rock Eval 6 analyser from Vinci Technologies. For each sample, 40 mg of dried and homogenized sediment was weighed into crucibles, placed on a carousel, and loaded into the instrument. An internal standard was measured after every 9 samples. The internal standard was a sample from the Blue Lias formation in St Audries Bay, Somerset labelled as SAB134 [204]. The standard error on SAB134 was 0.2 % (n=6, 2 SE).

6.4 Results

6.4.1 Cd concentrations and isotope compositions of water depth profiles

The relationship between Cd and the properties of anoxic marine environments can be examined by investigating their vertical distribution, along with other chemical species and trace metals. The vertical distribution of dissolved Cd concentration and isotopic composition in a depth profile from a station in the deep basin of Saanich Inlet is reported in Table 6.1 and Figure 6.2, along with oxygen, H_2S, and selected trace metals. The dissolved Cd concentrations slightly decrease from 0.43 nmol kg^{-1} at the surface to 0.42 nmol kg^{-1} at the chemocline, then decrease monotonically through the ~30 m of the chemocline. Hydrogen sulphide is detectable at 115 m, and increases in concentration towards the bottom of the basin. Cadmium isotope values remain constant within propagated error from the surface to the top of the chemocline (~0.4 ‰). The observed

Table 6.1: Cd concentrations and isotope compositions from a water column profile in the deep basin, along with physical and other trace metals concentration data

Location	Water Depth (m)	Temperature (°C)	O_2 (µM)	H_2S (µM)	[Cd] (nmol kg^{-1})	$\delta^{114/110}Cd_{NIST}$ (‰)	2σ	[Ba] (ng g^{-1})	[Cr] (ng g^{-1})	[Mo] (ng g^{-1})	[Pb] (ng g^{-1})	[Al] (ng g^{-1})	[Cr] (ng g^{-1})
Deep basin station, 48° 37.53'N, 123° 29.91'E													
Surface	5	7.86	257.15		0.43	0.42	0.05	8.50	0.23	9.66	0.06	0.73	0.14
75m(2)	75	7.81	224.91		0.42	0.39	0.04	8.36	0.24	9.52	0.06	1.04	0.23
90m(2)	90	8.67	141.44		0.29	0.41	0.03	8.35	0.18	9.50	0.05	0.82	0.15
115m	115	9.62	3.28	2.68	0.03	0.78	0.07	10.16	0.17	8.79	0.06	0.94	0.17
160m	160	9.61	2.86	4.96	0.11	-0.47	0.13	9.23	0.23	8.09	0.06	0.96	0.15
180m	180	9.59	1.55	10.98	0.01	-1.42	0.09	9.21	0.25	7.67	0.06	1.57	0.22

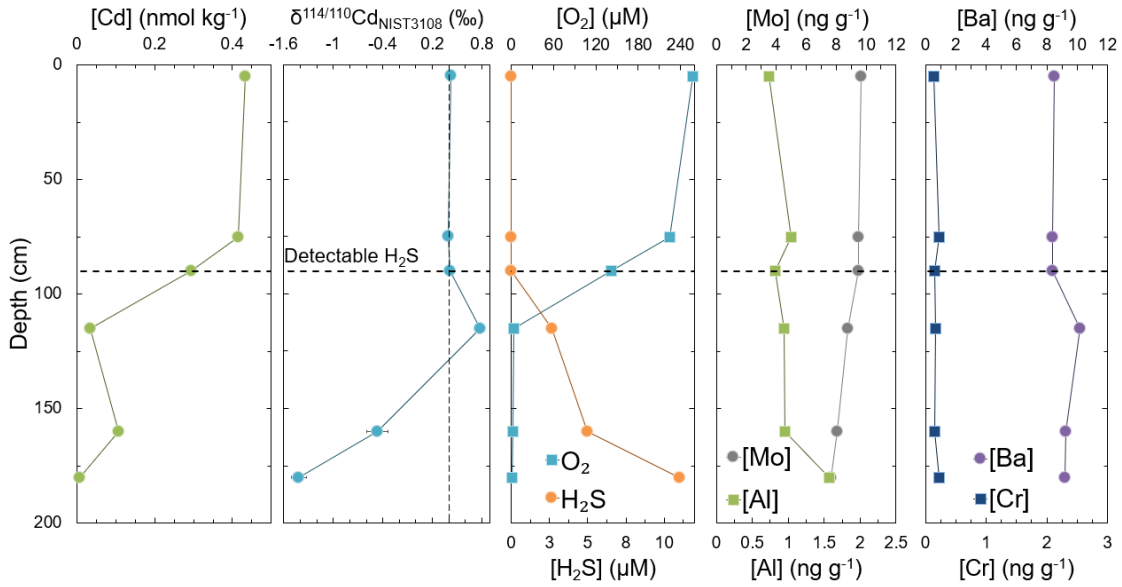


Figure 6.2: Dissolved Cd concentrations and isotopic compositions over the full depth of the water column in Saanich Inlet, shown with dissolved Mo, Al, Ba, Cr, oxygen, and hydrogen sulphide concentrations. The horizontal dashed line represents the transition to water conditions with detectable hydrogen sulphide. The vertical line represents the Cd isotopes value in the surface water (~0.4 ‰). Error bars on $\delta^{114}Cd$ denote the analytical uncertainty (2 SE).

Cd concentration rapidly decrease across the chemocline, while the Cd isotope value of the dissolved pool becomes briefly enriched in the heavy isotopes below the chemocline (up to ~0.8 ‰). In the remainder of the deep-waters of the basin, the Cd concentration continues to decrease from 0.03 nmol kg^{-1} to 0.01 nmol kg^{-1}, while the values of the Cd isotopic signature in the seawater decrease monotonically from $\delta^{114/110}Cd$= 0.78 ± 0.07‰ to $\delta^{114/110}Cd$= -1.42 ± 0.09 ‰ near the sediment-water interface.

The distribution of dissolved concentrations of molybdenum (Mo), aluminium (Al), barium (Ba), and chromium (Cr) are represented in Table 6.1 and shown in Figure 6.2.

The trends for these elements show minor influence by redox reactions. As oxygenated waters transition from anoxic to sulfidic conditions, the solubility of metals will change in the water column. Barium displays a slight decrease with declining oxygen concentrations in the chemocline, followed by a slightly increase below the chemocline at the same depth as the heaviest dissolved Cd isotopes sample ($0.78^{o}/_{oo}$). The [Mo] and [Cr] remain relatively stable through the water column with a gradual decrease in dissolved [Mo] in the deep-waters. A similar [Mo] trend was observed by Algeo and Lyons (2006) in the inlet, with gradual and continuous decrease in [Mo] through the water column [169]. These authors attributed the shallow concentration gradient to scavenging of [Mo] by Fe-Mn oxyhydroxides.

6.4.2 Cd concentrations and isotope compositions of sediment depth profiles

The relationship between near-surface sediments and the overlying hypoxic and euxinic deep-waters was investigated in the seasonally anoxic marine environment, along with sedimentary depth profiles in the Cd concentrations and isotopic compositions. The results are detailed in Table 6.2 and shown graphically in Figure 6.3.

Table 6.2: Cadmium concentrations and isotope compositions from three, near-surface cores obtained fro the deep basin with either hypoxic or anoxic overlying deep-waters, along with major and trace metal concentrations data

Depth interval (cm)	[Cd] µg g^{-1}	$\delta^{114/110}Cd_{NIST}$ (‰)	2σ	TOC (wt%)	[Cr] µg g^{-1}	[Co] µg g^{-1}	[Ni] µg g^{-1}	[Cu] µg g^{-1}	[V] mg g^{-1}	[Mn] mg g^{-1}
Station 1, Core 1, 48°39.131'N, 123°29.212'E, 94 m (water depth)										
0.5				1.08	77.86	14.59	32.38	27.46	0.14	0.55
1.5	0.72	0.03	0.05	0.91	66.83	12.30	27.44	21.42	0.12	0.51
2.5	1.49	-0.12	0.05	0.76	71.34	14.59	31.69	43.95	0.13	0.48
3.5	0.69	-0.07	0.06	0.92	80.47	14.57	33.41	28.12	0.14	0.55
4.5	1.27	0.10	0.07	0.94	80.56	13.49	32.81	27.63	0.13	0.51
5.5	1.18	-0.02	0.05	0.69	83.02	17.73	39.17	38.04	0.16	0.49
6.5	0.62	-0.15	0.07	0.74	73.40	14.09	31.69	30.51	0.13	0.65
7.5	1.00	0.02	0.06	0.77	83.95	16.30	38.40	39.57	0.15	0.48
8.5	0.89	0.05	0.05	0.59	100.86	19.41	47.97	54.80	0.18	0.56
9.5	1.00	0.07	0.06	0.66	91.75	18.02	43.90	49.14	0.16	0.57
10.5	1.09	0.09	0.05	0.94	90.34	15.05	38.54	35.40	0.15	0.44
11.5	1.37	0.09	0.05	0.81	81.75	14.38	36.26	33.58	0.15	0.46
12.5	0.83	-0.04	0.05	0.67	84.71	16.05	38.17	37.32	0.16	0.49
13.5	0.83	-0.07	0.05	0.61	97.84	16.94	41.81	40.78	0.17	0.55
14.5	0.25	0.08	0.04	0.74	79.84	13.86	33.18	32.83	0.14	0.56
15.5	0.82	-0.01	0.06	0.49	95.90	16.92	40.12	38.91	0.18	0.53
16.5	0.55	0.24	0.05	0.40	95.75	19.61	44.54	51.47	0.19	0.66
17.5	0.23	0.16	0.07	0.27	101.54	20.24	46.19	52.80	0.19	0.73
18.5	0.20	0.05	0.08	0.28	104.75	22.33	51.11	62.97	0.20	0.67
19.5					102.49	22.37	51.15	65.07	0.19	0.67
20.5	0.11	0.17	0.11	0.24	98.04	19.59	48.68	61.36	0.19	0.63
Station 3, Core 1, 48°39.092'N, 123°29.500'E, 120 m (water depth)										
0.5	0.69	0.05	0.06	0.28	68.62	11.42	37.03	38.31	0.12	0.40
1.5	1.48	-0.03	0.04	2.52	65.90	12.02	39.28	38.07	0.12	0.31
2.5	1.85	0.06	0.05	2.20	66.96	12.44	38.95	36.29	0.12	0.40
3.5	2.23	0.07	0.05	2.21	67.97	12.40	40.73	35.35	0.13	0.40
4.5	2.17	0.07	0.04	2.18	64.14	11.37	37.96	31.44	0.12	0.33
5.5	2.30	0.15	0.04	2.06	64.52	10.96	38.66	31.76	0.12	0.28
6.5	2.18	0.08	0.06	2.11	67.07	11.65	39.62	33.73	0.12	0.31
Station 3, Core 2, 48°39.092'N, 123°29.500'E, 120 m (water depth)										
0.5	0.87	-0.01	0.07	2.09	67.37	11.05	35.41	34.88	0.12	0.39
1.5	0.76	-0.17	0.08	2.74	67.24	11.43	36.51	35.44	0.12	0.40
2.5	0.71	0.01	0.05	2.63	66.58	11.52	36.33	37.52	0.12	0.41
3.5	1.24	0.01	0.05	2.56	79.53	13.46	43.99	46.90	0.14	0.43
4.5	1.30	0.12	0.05	2.38	50.85	9.51	30.46	29.96	0.10	0.25
5.5	1.12	0.11	0.04	2.20	67.96	12.60	39.54	34.68	0.13	0.45
6.5	1.46	0.06	0.06	2.16	65.17	11.62	38.87	33.52	0.12	0.41
7.5	1.56	-0.20	0.07	2.38	62.85	11.57	37.82	31.22	0.12	0.40
8.5	1.08	-0.04	0.05	2.23	56.11	10.28	34.22	28.13	0.11	0.35
9.5	2.08	0.20	0.04	2.06	63.44	11.95	39.77	32.40	0.12	0.34
10.5	1.22	0.06	0.07	2.06	59.66	11.04	36.50	29.17	0.11	0.37
11.5	1.17	0.06	0.05	2.11	56.08	10.40	34.06	27.85	0.11	0.35

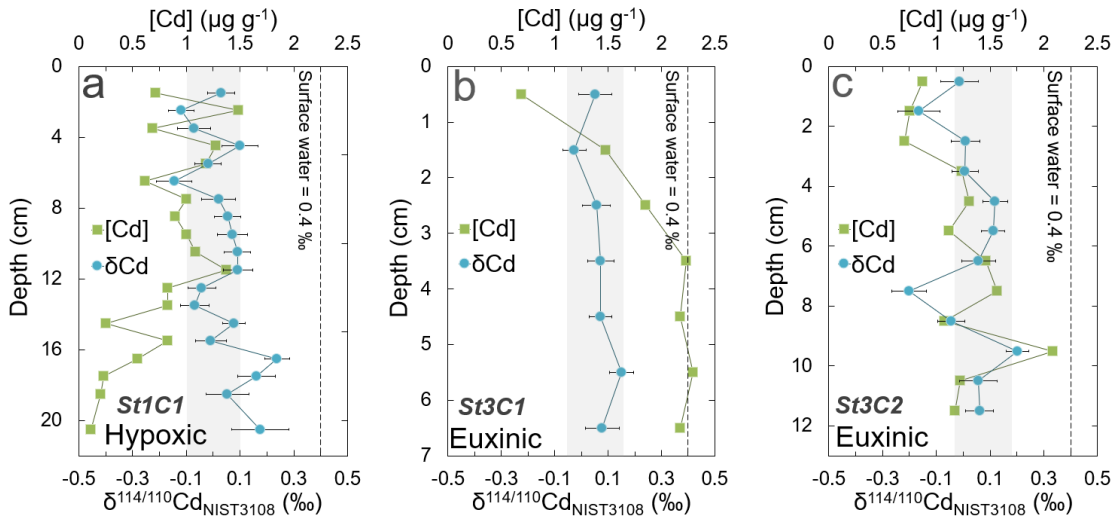


Figure 6.3: Sedimentary depth profile of Cd concentrations (solid, green squares) and isotopic compositions (solid, blue circles) of three cores collected under hypoxic overlying water conditions (a) and euxinic overlying water conditions (b, c). The shaded box represents a 0.2 ‰ range from the core-top value. Error bars on $\delta^{114}\mathrm{Cd}$ denote the analytical uncertainty (2 SE).

Sediments were sampled from the surface to a depth between 7 and 20.5 cm, depending the core. The cores represent a duration of deposition between 23.3 yrs and 68.3 yrs, assuming a sedimentation rate of ~3 mm per yr^{-1} [194]. Generally, the TOC concentration decreases down-core with an average TOC value of 0.68% in the near-surface core with overlying hypoxic water conditions and 2.17% in the near-surface cores with overlying euxinic water conditions.

The sediment budget for Cd is primarily controlled by the enrichment or depletion of authigenic Cd, along with Cd associated with organic material and detrital minerals. The relative enrichment of Cd in the sediments was calculated using the elemental enrichment factor (EF). In this approach, the Cd concentration was normalized to Al in order to determine the detrital contribution to the sediments, then subsequently compared to the average of the upper continental crust in Wedepohl et al. (1995). This provides the following equation:

$$\mathrm{EF_{Cd}} = (\mathrm{Cd/Al})_{\mathrm{sediment\,sample}}/(\mathrm{Cd/Al})_{\mathrm{upper\,continental\,crusts}},$$

where an EF greater than 1 indicates authigenic enrichment of the trace metal and less than 1 implies depletion in the sediments. The EF for Cd varied from 0.5 to 63.7 in

Table 6.2: continued

Depth interval (cm)	[Zn] µg g^{-1}	[Mo] µg g^{-1}	[Re] ng g^{-1}	[Th] µg g^{-1}	[U] µg g^{-1}	[Sr] mg g^{-1}	[Ba] mg g^{-1}	[Al] mg g^{-1}	[Mg] mg g^{-1}	[Fe] mg g^{-1}	[Ca] mg g^{-1}
Station 1, Core 1, 48°39.131'N, 123°29.212'E, 94 m (water depth)											
0.5	75.83	1.59	48.09	4.14	2.18	0.31	0.45	60.64	11.06	40.95	11.67
1.5	64.96	1.26	31.98	2.79	1.84	0.33	0.42	120.50	23.57	71.63	33.16
2.5	66.69	1.49	43.47	0.84	2.40	0.24	0.38	15.22	1.16	41.72	5.94
3.5	67.85	1.71	43.53	2.66	2.81	0.33	0.42	110.90	24.19	73.84	30.65
4.5	71.72	1.79	48.39	3.01	3.09	0.29	0.43	61.34	11.48	38.42	10.61
5.5	75.94	1.64	44.59	0.98	2.39	0.16	0.24	23.22	3.04	45.22	6.97
6.5	66.71	1.69	36.34	2.93	2.67	0.32	0.44	119.26	24.90	71.58	30.92
7.5	78.84	2.10	42.52	0.89	3.06	0.16	0.28	23.84	2.36	43.91	5.70
8.5	93.35	2.59	41.67	1.04	4.18	0.14	0.25	25.25	3.03	50.24	6.03
9.5	86.09	1.97	41.44	1.89	3.98	0.17	0.32	34.07	6.38	45.76	7.05
10.5	79.57	2.09	50.75	1.23	4.24	0.16	0.26	25.83	2.51	43.45	6.95
11.5	78.78	2.66	53.50	1.02	4.68	0.17	0.29	26.23	2.35	41.31	6.08
12.5	79.77	1.84	42.21	1.03	3.95	0.16	0.26	23.52	2.44	43.58	6.42
13.5	84.53	1.51	48.93	1.45	3.83	0.18	0.34	30.39	3.53	44.46	8.22
14.5	68.48	1.57	36.65	3.50	3.68	0.33	0.45	130.99	26.87	77.44	36.95
15.5	78.29	1.27	45.34	1.32	3.89	0.18	0.28	28.33	3.17	47.33	7.95
16.5	86.83	0.92	34.80	1.82	3.19	0.17	0.31	34.52	4.80	55.28	9.44
17.5	84.55	0.54	28.50	1.75	2.52	0.18	0.37	33.44	5.81	50.29	8.45
18.5	96.21	0.64	28.63	1.13	2.18	0.14	0.27	22.57	3.32	52.63	6.17
19.5	93.81	0.58	26.27	0.84	2.00	0.13	0.25	19.00	2.81	53.13	5.20
20.5	82.59	0.56	28.95	3.54	2.12	0.22	0.38	63.87	10.68	51.56	13.12
Station 3, Core 1, 48°39.092'N, 123°29.500'E, 120 m (water depth)											
0.5	102.96	8.17	24.71	4.30	3.00	0.18	0.36	94.93	25.81	60.94	13.19
1.5	97.55	24.33	34.93	2.11	4.36	0.09	0.22	20.50	4.79	34.38	3.33
2.5	89.97	19.67	35.01	3.81	4.32	0.16	0.34	49.31	12.95	39.16	6.10
3.5	90.74	23.31	37.78	4.35	4.75	0.17	0.35	56.24	14.08	38.60	6.95
4.5	83.48	23.75	36.15	2.86	4.28	0.12	0.27	32.16	8.16	33.60	4.37
5.5	81.96	20.95	38.78	1.55	4.38	0.10	0.22	20.26	3.33	33.14	3.67
6.5	86.78	20.25	41.36	1.73	4.03	0.09	0.20	18.70	2.96	32.42	3.54
Station 3, Core 2, 48°39.092'N, 123°29.500'E, 120 m (water depth)											
0.5	97.69	9.15	25.70	4.50	2.84	0.17	0.36	103.22	27.05	65.39	13.87
1.5	96.02	10.75	25.19	4.33	3.01	0.18	0.36	112.24	29.10	72.06	16.50
2.5	98.75	11.59	22.70	4.21	3.18	0.18	0.35	104.75	27.65	67.74	14.85
3.5	133.91	12.96	35.19	3.74	3.97	0.16	0.35	32.87	5.93	44.37	6.71
4.5	73.85	16.53	34.30	1.30	2.54	0.07	0.17	21.14	5.38	28.05	3.61
5.5	83.32	14.99	23.77	4.47	3.94	0.19	0.38	112.20	29.09	71.98	17.97
6.5	81.31	18.10	31.15	4.42	4.49	0.18	0.37	83.50	21.20	51.50	9.46
7.5	79.36	20.50	23.03	4.31	4.70	0.18	0.36	109.94	29.35	71.76	16.73
8.5	71.78	20.33	20.72	3.93	4.23	0.17	0.33	94.32	24.69	60.34	16.00
9.5	80.92	25.44	34.58	2.32	4.67	0.10	0.23	23.62	4.89	34.22	4.00
10.5	75.72	24.35	22.91	4.13	4.65	0.19	0.35	94.01	24.59	59.69	14.34
11.5	71.76	22.21	27.57	3.88	4.15	0.16	0.32	68.69	18.46	44.28	8.14

Table 6.3: Calculated enrichment factors for select trace metals

Depth interval (cm)	EF Cd	EF V	EF Zn	EF Mo	EF U	EF Fe
Station 1, Core 1, 48°39.131'N, 123°29.212'E, 94 m (water depth)						
0.5	11.2	3.3	1.9	1.5	1.1	1.7
1.5	4.7	1.4	0.8	0.6	0.5	1.5
2.5	43.3	12.4	6.5	5.4	4.9	6.9
3.5	5.5	1.8	0.9	0.9	0.8	1.7
4.5	7.4	3.1	1.7	1.6	1.6	1.6
5.5	27.3	9.9	4.9	3.9	3.2	4.9
6.5	4.6	1.6	0.8	0.8	0.7	1.5
7.5	18.7	9.3	4.9	4.9	4.0	4.6
8.5	19.6	10.3	5.5	5.7	5.1	5.0
9.5	15.0	7.0	3.8	3.2	3.6	3.4
10.5	22.9	8.5	4.6	4.5	5.1	4.2
11.5	28.0	8.2	4.5	5.6	5.5	3.9
12.5	16.8	9.9	5.1	4.3	5.2	4.6
13.5	12.3	8.1	4.1	2.8	3.9	3.7
14.5	3.3	1.6	0.8	0.7	0.9	1.5
15.5	16.8	9.4	4.1	2.5	4.3	4.2
16.5	6.4	7.9	3.7	1.5	2.9	4.0
17.5	4.1	8.4	3.8	0.9	2.3	3.8
18.5	3.1	12.8	6.3	1.6	3.0	5.8
19.5	0.5	15.0	7.4	1.7	3.3	7.0
20.5	0.9	4.4	1.9	0.5	1.0	2.0
Station 3, Core 1, 48°39.092'N, 123°29.500'E, 120 m (water depth)						
0.5	7.0	1.8	1.6	4.8	1.0	1.6
1.5	32.0	8.6	7.1	65.6	6.6	4.2
2.5	19.9	3.7	2.7	22.1	2.7	2.0
3.5	20.7	3.2	2.4	22.9	2.6	1.7
4.5	36.9	5.3	3.9	40.8	4.1	2.6
5.5	57.2	8.5	6.0	57.2	6.7	4.1
6.5	63.7	9.4	6.9	59.9	6.7	4.3
Station 3, Core 2, 48°39.092'N, 123°29.500'E, 120 m (water depth)						
0.5	7.4	1.6	1.4	4.9	0.9	1.6
1.5	5.9	1.5	1.3	5.3	0.8	1.6
2.5	7.3	1.6	1.4	6.1	0.9	1.6
3.5	23.2	6.2	6.1	21.8	3.7	3.4
4.5	37.6	6.7	5.2	43.3	3.7	3.3
5.5	9.6	1.7	1.1	7.4	1.1	1.6
6.5	17.5	2.2	1.5	12.0	1.7	1.5
7.5	13.1	1.6	1.1	10.3	1.3	1.6
8.5	10.4	1.6	1.1	11.9	1.4	1.6
9.5	52.0	7.2	5.1	59.6	6.1	3.6
10.5	12.8	1.8	1.2	14.3	1.5	1.6
11.5	15.9	2.2	1.6	17.9	1.9	1.6

*Reference Al concentration data is 77440 µg g^{-1}, as detailed in Wedepohl (1995)

all the sediment samples. These values were either similar or higher than sites in other known restricted basins, such as the Black Sea and Cariaco Basin ([122]). The EF was calculated for the other trace metals presented in this study, detailed in Table 6.3.

The Cd isotopic composition of the core-top sediments was isotopically lighter than

the surface-waters and isotopically heavier than the overlying deep-waters. All the core-top samples in the basin have overlapping error bars and thus no resolvable fractionation was observed despite varying redox conditions of the overlying water column. The isotopic offset between sedimentary Cd in the core-tops and aqueous Cd in the overlying surface-waters ranged from ranged from $\Delta^{114/110}\mathrm{Cd}_{\mathrm{core\,top\,sediment-surface\,waters}} =$ –0.35 ‰ to -0.41 ‰, with an average magnitude of fractionation of -0.38 ± 0.07 ‰. This range is similar to the isotopic offset values from oxygenated sites in the Black Sea and the South Atlantic at 40°S, presented in previous chapters.

The Cd concentrations and isotopic compositions in depth profiles for the three cores have a similar overall pattern. Cadmium concentrations and isotopic compositions are inversely related down-core above approximately 5 cm, and then positively covary through the remainder of the core with an R-square value of 0.72 (Table 6.2 and Figure 6.3 and 6.4). The concentrations of Cd range from 0.69 μg g^{-1} to 2.30 μg g^{-1} in the euxinic cores and 0.11 μg g^{-1} to 1.49 μg g^{-1} in the hypoxic core. The isotopic compositions of Cd range from -0.20 ‰ to 0.20 ‰ in the euxinic cores and -0.15 ‰ to 0.24 ‰ in the hypoxic core for the 37 sediment samples. Results are shown in Figure 6.3, in which the shaded box represents the 0.2 ‰ range of the three measured core-top samples. Almost all core sediment data points have uncertainties that overlap with this range. The Cd isotopic compositions of the samples within the error bars fall within a narrow range of $\delta^{114/110}\mathrm{Cd}$= -0.1 ‰ to 0.1 ‰, with an average value of $\delta^{114/110}\mathrm{Cd}$= 0.03 ‰. The largest Cd isotope variations occur below 16 cm in the hypoxic core and 7 cm in the euxinic cores. The excursion to heavier Cd isotope values near the bottom of the hypoxic (16 cm) and euxinic (9 cm) cores approach the isotope composition of the surface-waters (~0.4 ‰).

6.4.3 Comparison of Cd concentrations with other trace metals in the near-surface sediment cores

A suite of redox-sensitive metals, including U, Mo, Re, and Fe, were studied to identify how different dissolved oxygen concentrations in the overly bottom-waters influenced their speciation and concentration in the sediments (see Table 6.2 and Figure 6.4).

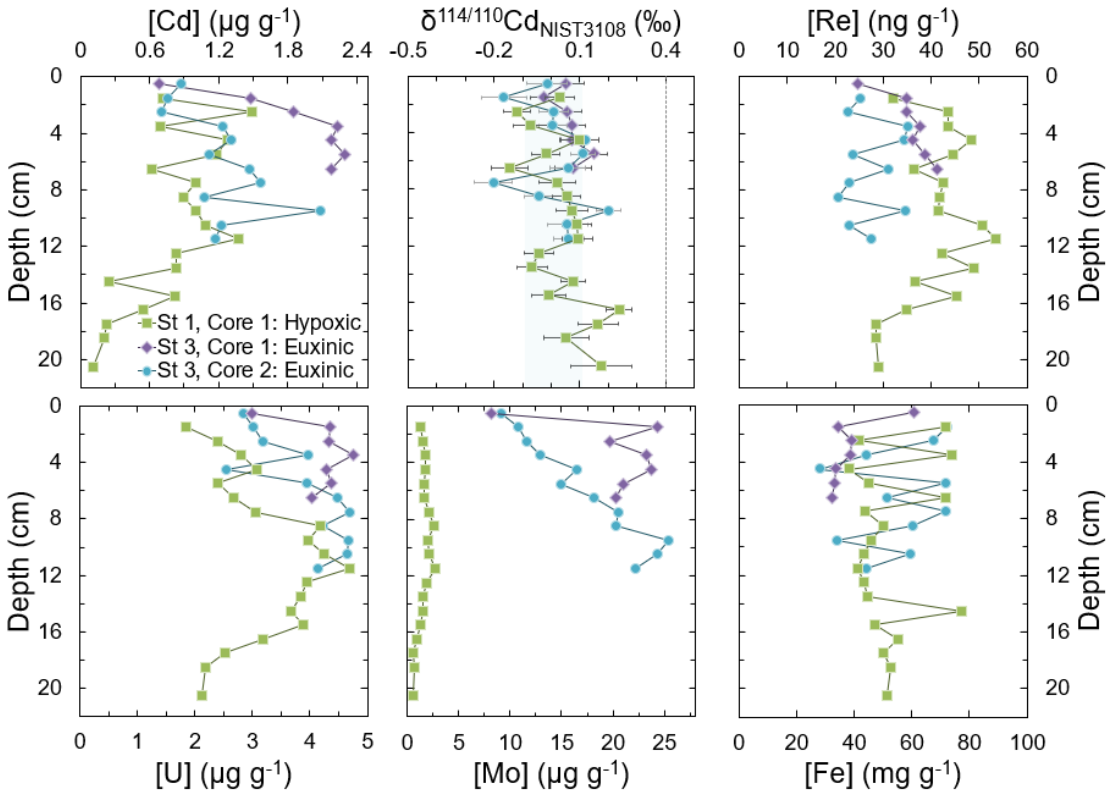


Figure 6.4: Sedimentary depth profile of Cd concentrations and isotopic compositions, along with Re, U, Mo, and Fe for the three cores collected under hypoxic overlying water conditions (green squares) and under euxinic overlying water conditions (blue circles and purple diamonds). The shaded box represents a 0.2 ‰ range and error bars on δ^{114}Cd denote the analytical uncertainty (2 SE).

Uranium appears to have a good correlation with Cd in all the cores, and Mo only for the euxinic cores; however, the statistics indicate a poor R-square value for U:Cd and Mo:Cd ratios. Conversely, Re shows a good correlation with Cd in the euxinic cores, resulting in an R-square value of 0.78.

The sedimentary concentrations of Cd, Mo, Re, U, and other trace metals, including Cr, Cu, V, Ba, and Ni increase in the top 3 to 5 cm for all the cores, and Zn only exhibits a slight increase in the euxinic cores and Fe only in the hypoxic core. The [U] exhibits a pronounced increase in the hypoxic and one of the euxinic cores till ~11 cm, then begin to gradually decrease. The [Mo] show a clear vertical increase for one of the euxinic cores (up to 25.4 µg g^{-1} at 9.5 cm), while the hypoxic core remains at a lower value at 2.6 µg g^{-1}. Conversely, Fe and Al steadily decrease in the top 3 to 5 cm of the euxinic cores. Aluminium, Fe, and Ba concentrations display a decrease in the first 2 to 3 cm of

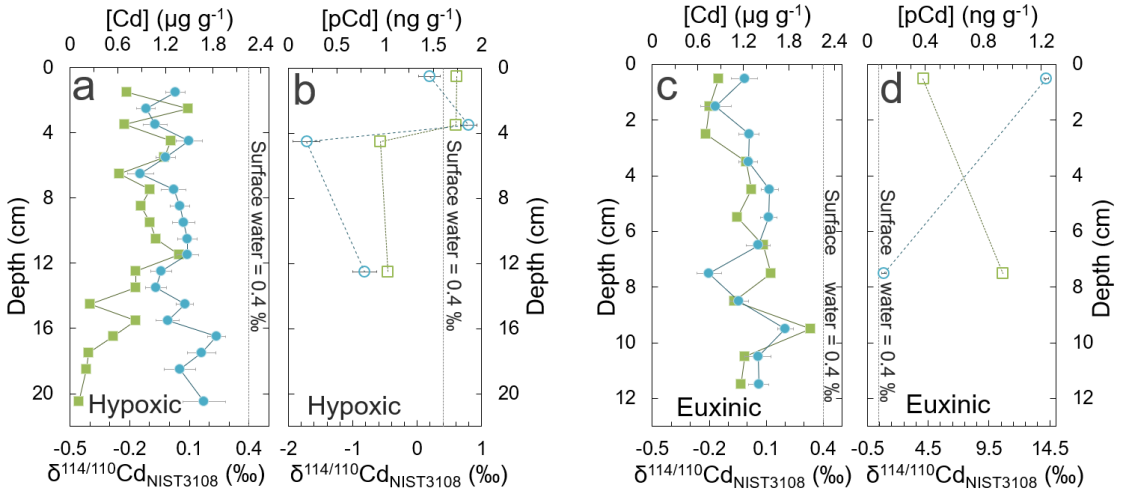


Figure 6.5: Sedimentary depth profile of Cd concentrations (solid and open, green squares) and isotopic compositions (solid and open, blue circles) for sediments (a) and pore-waters (b) collected under hypoxic overlying water conditions and sediments (c) and pore-waters (d) collected under euxinic overlying water conditions. Error bars on $\delta^{114}\mathrm{Cd}$ denote the analytical uncertainty (2SE).

all the cores and exhibit an overall inverse relationship to Cd in the vertical depth profile.

The most noticeable variation in the Cd concentrations and isotopic compositions for the longer euxinic core occurred at 9 cm with a reported $\delta^{114/110}\mathrm{Cd} = 0.20 \pm 0.04$ ‰. This coincided with a sedimentary enrichment in Mo, U, Re, Fe, Ni, Cr, V, Cu, and Zn.

Significant variation of Cd isotopes in the hypoxic core was recorded at 16 cm with $\delta^{114/110}\mathrm{Cd}$ values of 0.24 ± 0.05 ‰. These excursions in the Cd isotopic composition related with increased solid fraction concentrations of Re, U, and Fe just above at 15 cm and Mn, V, Ni, Cr, Cu, and Ba just below at 18 cm.

6.4.4 Cd concentrations and isotope compositions of pore-water depth profiles

The Cd concentrations and isotopic compositions in the sediment core pore-waters were measured in a few samples from the hypoxic and euxinic sites. The Cd in the pore-waters is likely sourced from diffusion of dissolved Cd into the sediments across the sediment-water interface and from dissolution of solid phase or organically-bound Cd into the pore-waters. Results are detailed in Table 6.4 and shown graphically in Figure 6.5.

The Cd concentrations and isotopic compositions of the pore-waters spanned a large range with very isotopically heavy dissolved Cd for the samples above 7 cm in the

Table 6.4: Cadmium concentrations and isotope compositions for pore-waters from three, near-surface cores obtained from the hypoxic and anoxic, deep basin, along with other major and trace metal concentrations data

Depth interval (cm)	[Al] ng g^{-1}	[Cr] ng g^{-1}	[Zn] ng g^{-1}	[Mo] µg g^{-1}	[Ba] µg g^{-1}	[Fe] µg g^{-1}	[U] µg g^{-1}	[Cd] ng g^{-1}	$\delta^{114/110}Cd_{NIST}$ (‰)	2σ
Station 1, Core 1, 48°39.131'N, 123°29.212'E, 94 m (water depth)										
0.5		6.85	24.88	0.72	0.30	0.17	0.06	1.74	0.19	0.17
1.5		5.89	20.01	0.99	0.25	0.64	0.10			
2.5	23.27	7.86	34.02	0.94	0.41	0.57	0.08			
3.5	20.25	3.56	17.90	0.59	0.18	0.12	0.15	1.73	0.80	0.13
4.5	22.83	4.59	20.93	0.64	0.16	0.35	0.19	0.95	-1.72	0.21
5.5		5.82	21.50	0.68	0.16	0.15	0.21			
6.5		5.12	18.52	0.44	0.12	0.14	0.15			
7.5		2.82	9.94	0.71	0.10	0.06	0.12	0.66	0.51	0.31
8.5		2.57	11.13	0.95	0.10	0.08	0.20			
9.5		1.88	10.30	0.81	0.08	0.09	0.14			
10.5	4.40	3.01	8.70	1.68	0.09	0.08	0.33			
11.5	14.27	3.21	14.35	1.19	0.09	0.24	0.18			
12.5		2.52	11.32	1.01	0.12	0.07	0.28	1.03	-0.82	0.18
13.5		2.85	10.54	0.95	0.11	0.07	0.19			
14.5		2.35	10.74	0.82	0.12	0.09	0.20			
Station 3, Core 1, 48°39.092'N, 123°29.500'E, 120 m (water depth)										
0.5	66490.43	78.21	120.73	1.75	0.93	36.52				
1.5	21597.44	38.17	47.65	3.15	1.92	12.69				
2.5	24717.57	63.15	84.78	4.49	1.90	9.88				
3.5	63473.84	73.23	103.97	0.53	0.34	45.55				
4.5	19171.74	74.45	70.57	5.88	2.58	8.91				
5.5	43501.36	95.56	98.72	3.43	2.71	15.64				
6.5	23165.54	94.82	110.76	3.51	2.20	9.71				
Station 3, Core 2, 48°39.092'N, 123°29.500'E, 120 m (water depth)										
0.5		8.08	23.54	3.68	0.41	0.23	0.38	0.38	14.22	0.20
1.5		13.27	35.15	3.90	0.63	0.46	0.73			
2.5		22.96	35.96	1.90	1.13	0.65	0.57			
3.5	42.26	14.86	25.97	0.07	1.04	0.43	0.21			
4.5	37.38	14.00	14.59	0.23	1.44	0.31	0.24			
5.5	17.47	14.06	14.30	1.00	1.45	0.19	0.28			
6.5	20.44	15.14	18.18	0.47	1.68	0.21	0.34	1.17	11.77	0.85
7.5	43.37	16.30	22.03	0.89	1.87	0.34	0.31	0.93	0.85	0.19
8.5	51.83	15.44	15.39	0.12	1.82	0.35	0.28			
9.5	67.70	16.57	18.25	0.74	1.88	0.34	0.27			
10.5	65.38	16.50	15.34	0.75	1.91	0.41	0.28			

euxinic core. Values of $\delta^{114/110}\mathrm{Cd}$ varied from 0.19 ± 0.17 ‰ at ~0.5 cm to -1.72 ± 0.21 ‰ at ~4.5 cm in the hypoxic core. The values of $\delta^{114/110}\mathrm{Cd}$ in the euxinic core ranged from 14.22 ± 0.20 ‰ at ~0.5 cm to 0.85 ± 0.19 ‰ at ~7.5 cm. The isotopic offset between aqueous Cd in the pore-waters from the core-tops and aqueous Cd in the surface-waters (~0.4 ‰) ranged from $\Delta^{114/110}\mathrm{Cd}_{\mathrm{pore-waters-surface\,water}}$ = -0.23 ‰ in the hypoxic core to 13.80 ‰ in the euxinic core.

6.5 Discussion

6.5.1 Origin of Cd isotopic variation in the Saanich Inlet water column

The rapid reoxygenation events in autumn cause high primary productivity and a rapid progression of redox reactions as oxygen becomes quickly depleted in the stratified deep basin, leading to specialized microbes respiring using alternative oxidants (e.g. nitrate and sulfate) [191]. The water samples presented in this study were collected during winter. Consequently, the behaviour of Cd in surface-waters is likely dominated by free, dissolved Cd and chloro complexes of Cd with minimal variations in the surface layer, above the chemocline. Traditionally, Cd displays a nutrient-like behaviour in seawater [205]; however, the surface water conditions in winter are not ideal for significant marine phytoplankton activity, resulting in no isotope fractionation outside of analytical error from the surface to the top of the chemocline at 75 m. At 75 m, a distinct chemocline extended to a depth of ~105 m, with sulfate-reducing microbes respiring detectable $\mathrm{H_2S}$ in the deep-waters. Of particular interest is the behaviour of Cd and other trace metals across the oxic-anoxic-euxinic interfaces.

The primary mechanism that controls the distribution of Cd concentration and isotopic composition across the chemocline and deep-waters is thermodynamically driven fractionation of Cd with preferential removal of light isotopes of dissolved Cd during formation of insoluble cadmium sulphide (CdS) complexes. This relationship between Cd and sulphide explains the decrease in dissolved Cd concentrations from $0.42\,\mathrm{nmol\,kg^{-1}}$ to $0.01\,\mathrm{nmol\,kg^{-1}}$ across the chemocline and subsequent short-lived excursion to isotopically heavy values (~0.78 ‰) below the chemocline. This is a likely scenario as cadmium

has one of the highest stabilities for metal-sulphide complexes based on equilibrium thermodynamics [185], and it is known to form its own sulphide species in sulphidic waters and sediments [164, 182, 183]. Likewise, Cd is a good indicator of trace sulphide production from sulfate reduction, even if it is weak and undetectable, unlike Mo that requires H_2S concentrations to be above a threshold amount [181]. The nonlinear trend between Cd and Mo concentrations in the deep-water indicate different mechanisms for their removal. Cadmium is likely precipitated as insoluble CdS species, while the gradual gradient for Mo concentration depicts an active scavenging on nanoparticulate Fe-Mn oxides [169].

The behaviour of Cd across the chemocline can be described by a Rayleigh isotope fractionation trend (see Figure 6.6). Isotope systematics during precipitation of Cd with H_2S follows a Rayleigh fractionation trend, as continuous addition of surface water through a stratified water column will lead to closed-system behaviour. As Cd diffuses across the chemocline, the precipitated Cd isotope composition should be enriched in the lighter isotopes, and when a large portion of Cd has been removed from the dissolved phase, it will be substantially heavier than the initially formed precipitates. The observed dramatic decrease in Cd concentration supports this idea. This argument is further supported by the cadmium sulphide experiments presented in chapter 3 that shows a Rayleigh isotope fractionation trend with a similar fractionation factor (Figure 6.6).

The dissolved Cd isotopic composition in the water column exhibits a large excursion from $\delta^{114/110}$Cd = 0.78 $\pm$ 0.07 ‰ at 115 m to $\delta^{114/110}$Cd = -1.42 $\pm$ 0.09 ‰ at 180 m. This behaviour may be indicative of a bottom water current delivering organic material and possibly trace metals to the deep basin from the margins. However, the isotopic composition of organic material is unknown a this time. Alternatively, it may represent a reventilation of deeper oxygenated bottom-waters, as the turnover events fully penetrate the surface sediments with oxygen-rich waters. Also, it could suggest remineralization of Cd bound to organic ligands. However, with all of these hypotheses, only a small increase in Cd concentration is observed, but no increase in oxygen concentrations. It is important to note that the dissolved Cd concentrations have decreased to ~1 % from the waters above the chemocline to the benthic-waters. Consequently, large shifts in the

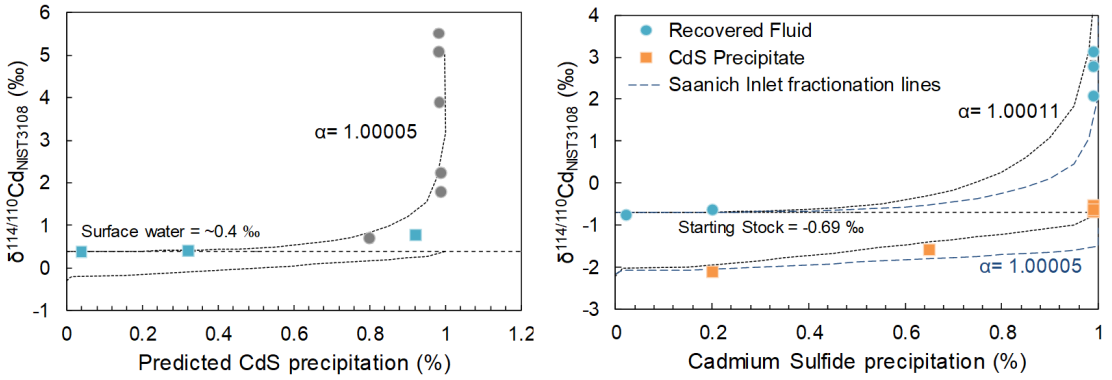


Figure 6.6: Rayleigh isotope fractionation curve using Cd isotopes of the water column from Saanich Inlet (blue squares) and the Black Sea (grey circles) with an alpha value of 1.00005 (Left). The Black Sea is added to show the end member points for CdS precipitation. The horizontal line at $\delta^{114/110}$Cd = 0.4 ‰ represents the water Cd isotope composition above the chemocline. Isotopic compositions of dissolved Cd (blue circles) and Cd sulphide precipitate (orange squares) from controlled CdS precipitation experiments completed with synthetic seawater in an anoxic setting (Right). The horizontal line at $\delta^{114/110}$Cd = -0.69 ‰ represents the bulk starting composition. The dashed lines are Rayleigh fractionation curves with an alpha value of 1.00011. Error bars represent 2 SE of each sample and error bars are smaller than the markers.

dissolved Cd isotopic composition can be caused by very small changes in the mixing of isotopically distinct Cd phases.

6.5.2 Explanation for the Cd isotopic composition of near-surface sediments

The seasonal reventilation event in the marginal marine basin leads to Cd concentrations and isotopic compositions of the near-surface sediments that reflect oxic conditions. The Cd isotope behaviour in the core-top sediments is indicative of a setting with oxygenated overlying bottom-waters that do not support quantitative removal of Cd across the sediment-water interface. Chapter 5 on the permanent anoxic basin, the Black Sea, reported no fractionation of Cd isotopes outside of analytical error between the core-top sediments and overlying surface-waters. Conversely, the hypoxic and euxinic sedimentary core-top samples from Saanich Inlet exhibit a Cd isotopic composition lighter than the overlying surface-waters above the chemocline (by ~0.4 ‰). This observation is similar to Chapter 4 on the South Atlantic with oxygenated deep-waters. The isotopic offset between sedimentary Cd in the core-tops and aqueous Cd in the overlying bottom-waters from the South Atlantic ranged from -0.36 ± 0.08 ‰ to 0.10

$\pm$ 0.07 ‰. Likewise, the average magnitude of fractionation in Saanich Inlet was $\Delta^{114/110}Cd_{\text{core top sediment}-\text{surface waters}}$ = -0.38 $\pm$ 0.07 ‰, within analytical uncertainty of the South Atlantic. The offset was attributed to preferential removal of light Cd isotopes by trace H_2S at the sediment-water interface. This is likely the situation in Saanich Inlet, as supported by an extremely isotopically heavy value of Cd for pore-waters in the core-top sediments within the euxinic basin (~14.2 ‰). It is important to note that the error bars for the euxinic and hypoxic core-top sediment samples overlap, so the magnitude of fractionation cannot be truly distinguished given analytical uncertainties.

The large Cd isotope variation between the core-top sediments and surface-waters is unexpected. In the deep-waters, oxygen diminishes to below 2 μM, H_2S increases to 10.98 μM by the benthic-waters, and Cd concentrations remain at low levels after 84% of Cd was removed into CdS species across the chemocline. These measurements advocate that the highly insoluble CdS complexes will remain stable and reflect a similar Cd isotope composition as the source (~0.4 ‰). Consequently, the Cd speciation at the sediment-water interface is likely to be dominated by particulate CdS phases [187] with additional contribution from aqueous Cd species and remaining organic material [186]. However, the sedimentary core-top samples from Saanich Inlet exhibit a Cd isotopic composition lighter than the overlying surface-waters above the chemocline (by ~0.4 ‰).

The isotopic offset between sedimentary Cd in the core-tops and aqueous Cd in the surface-waters may be described by the rapid bacterial degradation of remaining organic material at the sediment-water interface and in the near-surface sediments. The upward diffusion of H_2S from the sediments and the H_2S in the deep-waters promote a preferential removal of isotopically light Cd to form CdS species from newly released, organically-bound Cd and remaining aqueous Cd species. This process will drive the Cd isotopes in the pore-waters to very heavy values of Cd, as observed (~14.2 ‰). The weakly restricted nature of Saanich Inlet means that the reventilation events cause high primary productivity rates and high amounts of sinking organic material, further supporting this idea. Alternatively, it may represent a delivery of organic material and possibly trace metals to the deep basin from the margins, with a preferential enrichment

of light Cd isotopes to precipitate CdS complexes, as mentioned in the above discussion on the water column.

6.5.3 Evidence for primary depositional signal record by Cd isotopes

The down-core variation of Th normalized redox-sensitive element concentrations, Cd, U, and Mo, and TOC concentrations show evidence of cyclicity in the top 8 cm of the sediment core with hypoxic overlying bottom-waters (see Figure 6.7). While the Th normalized redox-sensitive elements and TOC concentrations are not statistically correlated, an inverse, down-core trend is observed, where a decrease in TOC concentrations corresponds to peaks in Cd/Th, U/Th, and Mo/Th ratios. Conversely, the Cd isotopes in the top 8 cm follow a similar trend as the TOC concentrations. Each cycle spans between approximately 3 and 4 cm. If bulk sedimentation rates is approximately 3 mm per year ([169, 190, 194]), then each cycle corresponds to between 10 and 14 years. The observed trends support the recording of a primary depositional signal in the top of the core that reflects routine fluctuations in depositional conditions, and thus, changes in the composition of biogenic and terrigenous sediments.

The redox shift in the pore-waters during the reventilation events that reach the basin floor with oxygen-rich waters and the rapid return to sulphidic conditions in the pore-waters likely create a complex system where remaining oxygen diffuses upwards as the deep-water returns to anoxic to sulfidic conditions. While a trend is observed between Cd and TOC, it is not possible to decipher the relationship without additional data. However, the primary depositional signal is likely overprinted by further diagenetic alterations on a long-term scale, as observed below 8 cm in the core with hypoxic overlying waters in this study.

6.5.4 A mechanism for the authigenic enrichment of Cd in sediments

The frequency of the reventilation events that extend to the basin floor are enough to cause significant changes in the concentrations of sinking organic material to the sediments and subsequently bacterial degradation. This process will likely alter the

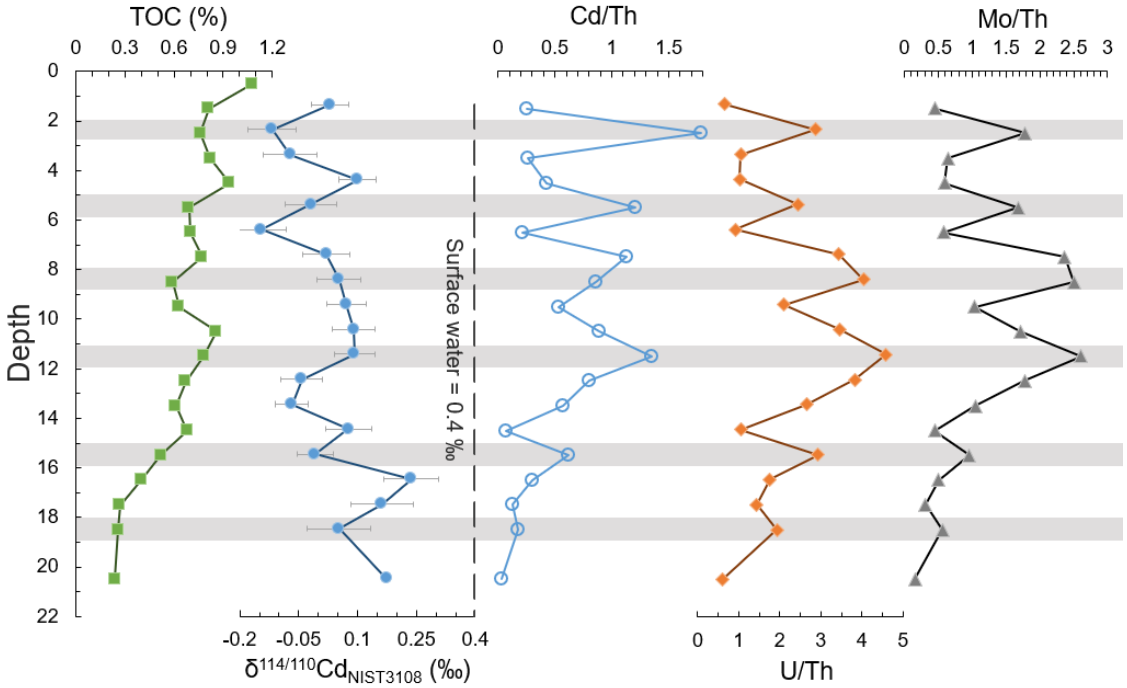


Figure 6.7: Down-core variation of TOC (wt %), Cd isotopes, and Th normalized redox sensitive elements (Cd, Mo, U, V) from the hypoxic, near-surface sediment core. Error bars on $\delta^{114}\mathrm{Cd}$ denote the analytical uncertainty (2 SE). The grey, shaded bars represent each cycle with a minimum peak in Cd/Th, U/Th, and Mo/Th.

redox front, leading to a redistribution of the trace metals during early diagenesis. This statement is further supported by minimal variations in the Cd concentrations and isotopic compositions between the cores collected under different bottom water conditions: hypoxic and euxinic. The majority of the near-surface sediment samples fell within a narrow range and had a mean value of $\delta^{114/110}\mathrm{Cd}$ = 0.03 ‰, considering the analytical uncertainty of 0.10‰. The small excursions in the sedimentary vertical depth profile likely indicate immobilization of Cd from the pore-waters with $\mathrm{H_2S}$ to form insoluble cadmium sulphide phases that do not coprecipitate with iron sulphides (FeS). This contention is support by the lack of a clear relationship between the sedimentary Cd and Fe in the vertical profile, along with poor correlation between Cd and Fe in previous studies on FeS precipitation [192, 206, 207].

Three sediment samples collected from the core with hypoxic overlying water conditions and three samples from the core with euxinic overlying water conditions had Cd isotopic compositions outside of the general range of down-core variation. The excursion

to isotopically heavy isotopes of Cd (~0.20 ‰) and a peak in sedimentary Cd at 9 cm in the euxinic core coincided with solid phase enrichment in Cd, Mo, U, Re, Fe, Ni, Cr, V, Cu, and Zn, supporting either oxygen diffusion into the sediments, causing reoxidation and a movement of the redox boundary during the annual reoxygenation events [124]. The highest magnitude of Cd isotope fractionation in the sediments relative to the overlying surface-waters in the hypoxic core is observed at 16 cm (~0.24 ‰). The shift in Cd isotopes at 16 cm is bound between sedimentary increases in the concentrations of Cd, Re, U, and Fe at 15 cm and Mn, V, Ni, Cr, Cu, and Ba at 18 cm.

It is important to note that the sedimentary Cd concentrations increase before the excursion to isotopically heavier values. The delayed offset in the Cd isotopes compared to Cd concentration is observed in other oxygenated cores presented in previous chapters; however, is not currently understood.

6.5.5 Co-variance between Cd and select trace metals in sediments

The combination of the reoxygenation of the bottom-waters and increased flux of organic material induced by the turnover event in autumn may result in a penetration of oxygen into the sediments and a change of the redox front. This will cause a redistribution of the trace metals in the sediments based on the redox front, as observed in this study and in previous studies for redox-sensitive elements, including Mn, Fe, U, V, Cd, and Re [110, 161, 192, 208–211]. The overall distribution of the sedimentary concentrations of trace metals in the vertical depth profile for all the cores exhibit similar trends, however the relationships are not statistically significant. The majority of trace metals display an increase in solid phase enrichment at the top of the core by adsorption or precipitation, likely with sulphide species. The down-core excursion to a lighter sedimentary Cd isotopic composition at 1 cm and increased Cd and Mo concentrations compared to the core-top in an euxinic core likely represent degradation of remaining organic material with the release of Cd into the pore-waters [186] and rapid precipitation with H_2S to form CdS complexes [110]. Conversely, Fe and Ba decrease at the top of the core, supporting dissolution of oxides and remaining organic material. Continuing down-core, Cd, Mo, U, Re, Cr, Cu, V, Ba, and Ni show a positive peak between 2 to 5 cm. A similar peak

is seen at the same depth for Zn in the euxinic cores and for Fe in the hypoxic core, indicating removal from the pore-waters during precipitation, coprecipitation, and/or scavenging of metals onto newly formed mineral substrate.

The down-core trend for Mo concentrations displays a slight increase in the euxinic cores. However, the sedimentary Mo concentration in the hypoxic core remains at a low value, signifying that conditions remained too oxygenated or concentrations of H_2S are below a threshold amount for Mo precipitation [169]. Unlike Mo, Cd is likely fixed in the sediments with trace H_2S, prior to either sulfate or iron reduction. The sedimentary enrichment peaks for Mo in the euxinic cores, and in all cores for U, likely reflects remobilization and vertical diffusion from previous Mn- and Fe-oxides to reducing conditions and subsequent immobilization [192].

Further down the vertical depth profile, the sedimentary enrichment of Cd and Re shows a similar trend, but poor correlation in all cores, and a lack of association with iron, supporting that they are not incorporated in iron oxides or iron sulphides. Alternatively, Cd and Re are more resistant to oxidation in their authigenic phases during reoxygenation events [188].

Previous studies provide minimal information on the processes that may influence the deposition of Cd. Some factors that may impart a strong control on Cd burial are the grain size of the CdS complexes and the concentration of Cd supply to the sediments. Grain size could play a role in how resistant the CdS are to dissolution, as deposition in deep-waters of the inlet is dominated by fine grained material with a high content of organic material [184, 212]. The other factor is enrichment of Cd in the sediments. The Cd concentrations in the sediments are significantly higher than the studied samples from the South Atlantic and oxygenated portions of the Black Sea in this thesis. This may be due to a combination of factors such as higher input of trace metals from surrounding rivers, anthropogenic influences, and redistribution of sediments from the basin margins to the deep-waters.

6.6 Conclusion

This study investigated the role of redox conditions as a control on the Cd isotope composition of marine waters and sediments in a setting with seasonal variations in oxygen. The Cd biogeochemical cycle in the water column and sediments was similar to other redox sensitive elements. Cadmium concentration and isotopic composition is primarily controlled by redox dynamics across the chemocline. This redox transition leads to a near-quantitative removal of dissolved Cd to insoluble cadmium sulphide species, resulting in a short-lived excursion to isotopically heavy isotopes of Cd in the residual dissolved pool. The transition across the chemocline is best fit with a Rayleigh isotope fractionation trend, similar to the Black Sea.

The isotopic offset between sedimentary Cd in the core-tops and aqueous Cd in the overlying surface-waters advocates for preferential enrichment of light Cd isotopes as remaining organic material undergoes degradation and release heavy isotopes into the pore-waters and to the overlying bottom-waters. The CdS complexes formed across the sediment-water interface likely remain stable, resulting from the prevailing sulfidic conditions. This observation supports the hypothesis that the Cd isotopes signature of the near-surface sediments is impacted by seasonal water-column re-oxygenation events. The post-depositional redistribution of Cd is a process that requires further work.

It is important to further investigate the controlling mechanisms regulating the distribution of Cd and other trace metals in low oxygen settings. The rate and efficiency of redox reactions is what ultimately controls the fate of organic carbon in sediments, the removal of bioavailable nitrogen from the water column, and the speciation of trace elements in the basin. As oxygen deficient zones continue to expand because of warming and increased stratification, redox reactions in low oxygen settings and their impact on trace metals become more globally important. Likewise, it is important to decipher the potential of sedimentary Cd isotopes as a redox proxy for past ocean conditions.

7 Conclusions and Outlook

Contents

7.1 Conclusions 161
- 7.1.1 The precipitation of Cd with H_2S will preferentially remove the light Cd isotopes into the CdS complexes, with an alpha fractionation factor of 1.00005–1.00011 162
- 7.1.2 Redox conditions in benthic-waters controls the degree of Cd isotope offset between the near-surface sediments (core-tops) and overlying benthic-waters 165
- 7.1.3 The majority of the Cd isotopic compositions in the near-surface sediment cores ranged from $\delta^{114/110}Cd$ range of ~-0.4 to 0.4‰ 166
- 7.1.4 CdS complexes may be unstable under frequently changing redox regimes 167

7.2 Outlook 167

7.3 Closing remarks 168

7.1 Conclusions

Our knowledge of Cd in the ocean environment and its variability over time has greatly advanced through the recent acquisition of a great number of Cd concentrations and isotopic compositions of the waters and particulates in the global ocean. However, a mechanistic understanding of what processes control the Cd cycle in the ocean, especially the export and removal of Cd into the sediments, remains poorly constrained. These are

critical gaps in knowledge required to fully decipher the cycling of Cd in the modern oceans and sediments before we can understand the ancient oceans. This thesis undertook the first systematic measurements of the isotopic composition of Cd in marine sediments. The thesis in particular explored the hypothesised relationship between hydrogen sulphide (H_2S) and Cd, and the high affinity for CdS complexes to form within the water column, pore-waters, and near-surface sediments.

This study was completed by measuring the Cd isotopic compositions and concentrations of waters, sinking particles, pore-waters, and surface sediments accumulating under a range of primary productivity and redox conditions in the South Atlantic at 40°S, Saanich Inlet, and the Black Sea, alongside laboratory CdS precipitation experiments. The observations support that the degree of Cd enrichment in marine sediments is largely controlled by the amount of H_2S present in the system, similar to many other redox-sensitive elements (see Figure 7.1).

The key results of each chapter are summarised in the following sections.

7.1.1 The precipitation of Cd with H_2S will preferentially remove the light Cd isotopes into the CdS complexes, with an alpha fractionation factor of 1.00005–1.00011

Chapter 3 quantified the Cd isotope fractionation that accompanied the precipitation of CdS with pure H_2S gas in synthetic seawater under anoxic conditions. The experiments displayed an enrichment of light Cd isotopes during precipitation of insoluble CdS species, reflecting Rayleigh behaviour with a fractionation factor of 1.00011. Similarly, the Cd behaviour across the chemocline of the Black Sea to sulfidic deep-waters is best fit with Rayleigh trend lines and a fractionation factor of 1.00005. The good agreement between experimental and natural samples supports the hypothesis that dissolved Cd behaviour is governed by its interaction with H_2S. These results provide a mechanistic explanation for the lighter Cd-isotopes signature in Cd particulates within prominent ODZs, along with the different Cd:PO_4^{3-} ratios in various OMZs [28, 56, 80, 87]. Likewise, these findings support the hypothesis that CdS precipitation is likely to be the missing 'sink' of isotopically light Cd from the ocean, thus balancing the isotopic offset between the

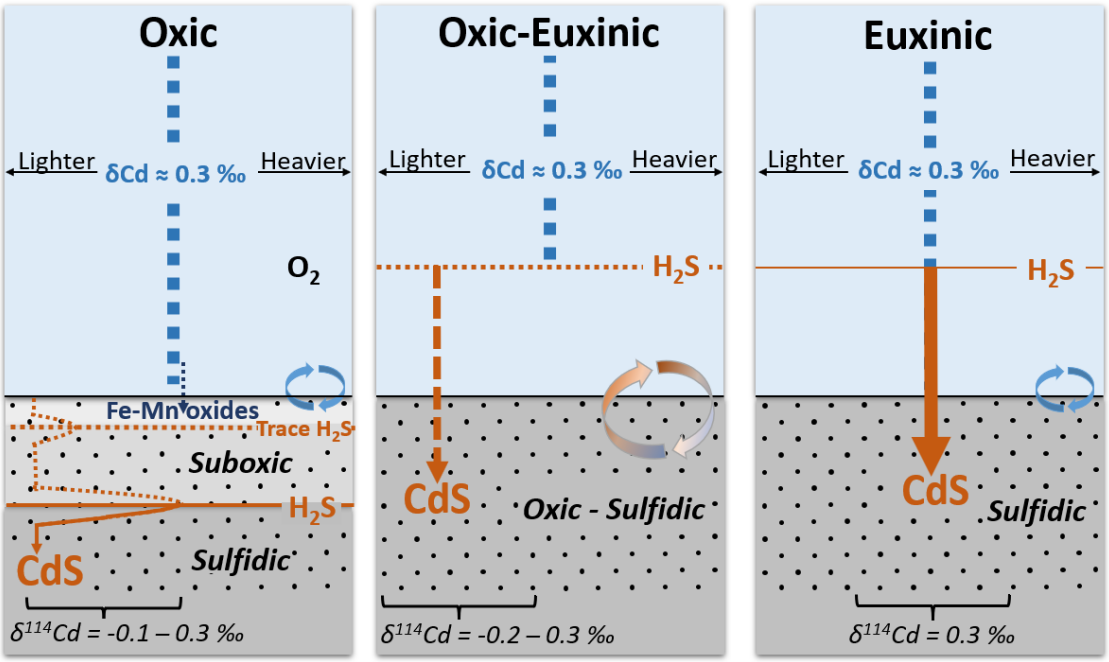


Figure 7.1: Summary schematic of the controls on sedimentary Cd concentration and isotopic composition under deep-water conditions that are oxygenated, seasonally euxinic, and permanently euxinic. The blue shaded area represents the global deep ocean at a Cd isotopic composition of approximately 0.3 ‰. The transition from oxygenated to euxinic conditions in the overlying water-column is indicated by an orange dotted line (seasonally euxinic) or orange straight line (permanently euxinic) to signify production of H_2S. The primary mechanism for removal of dissolved Cd from the water-column and pore-waters is by precipitation of CdS complexes in suboxic to euxinic conditions. An orange straight line represents permanent removal of Cd to form CdS complexes, assuming redox conditions remain stable. Conversely, an orange dotted line represents a system with fluctuating redox conditions in the water column and/or near-surface sediments, where the degree of Cd removal to precipitate CdS species is variable. The stability of CdS species in changing redox conditions is not constrained.
The width of the orange line with an arrow represents the expected degree of Cd removal from the water column and into the sediments relative to the other settings. Likewise, the location of the orange arrow indicates if the core-top sediment sample in each setting has a Cd isotopic composition that is lighter or similar to the global deep ocean (~0.3 ‰). The expected range for $\delta^{114/110}$Cd of the near-surface sediment samples from each setting is shown at the bottom of the box. Additionally, the figure depicts the adsorption and/or incorporation of Cd to the Fe-Mn oxyhydroxides within the oxygenated water-column and near-surface sediments.

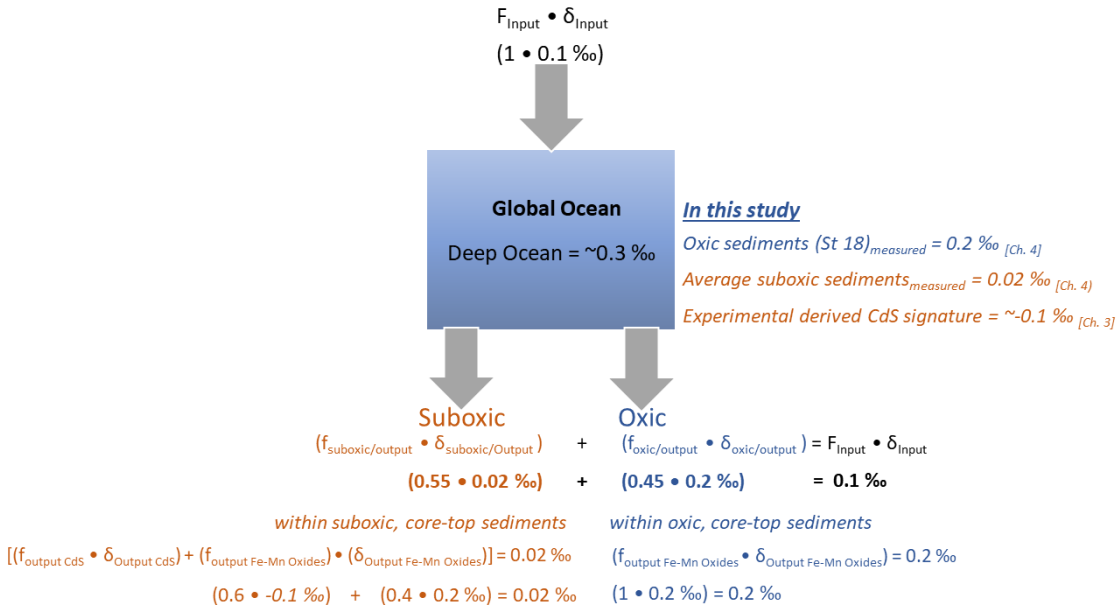


Figure 7.2: Updated Cd mass balance model

deep global oceans (~0.3 ‰) and the lithogenic crust (0.1 ‰, relative to NIST SRM 3108) [28, 54, 57]. This is further discussed in Figure 7.2.

The sedimentary output of Cd in global oceans can be characterized for the first time using the compiled dataset from Chapter 4. The updated mass balance model is presented in 7.2. The model constrains the initial flux between the deep-waters and sediments by only considering the Cd isotopic composition of the core-top sediments. It hypothesizes that the dominate sinks of sedimentary cadmium within the core-top sediments with oxic pore-waters is via pore-water Cd adsorption to and/or incorporation into Fe-Mn oxides. The bulk Cd isotopic composition of core-top sediments with oxic pore-waters has a value of 0.2‰, identical to the average of ferromanganese crusts and nodules in the ocean [93, 104, 114]. Conversely, the bulk Cd isotopic composition of core-top sediments with suboxic pore-waters is lighter than the core-top sediments with oxic pore-waters by nearly 0.2‰. This suggest that we are missing a light sink to the oceans within suboxic sediments [56, 93, 112].

The proposed light Cd sink is precipitation of CdS complexes using trace H_2S, along with pore-water Cd adsorption to and/or incorporation into Fe-Mn oxides. Laboratory experiments in Chapter 3 and by Guinoiseau et al. (2018) reported that precipitation

of dissolved Cd with H_2S gas in synthetic seawater results in preferential association of lighter isotopes with the precipitated CdS phase relative to the bulk solution [80]. These laboratory experiments report an experimentally-derived CdS signature of -0.1‰, and advocate that CdS precipitation may be an important sink in the global ocean to explain the Cd isotopic composition of the sediments with suboxic pore-waters and satisfy the Cd mass balance model. The source of the trace H_2S may either come from the upward diffusion of pore-water from the zone of sulfate reduction or from degrading organic aggregates that form microenvironments with increased respiration and inhibited diffusion that result in precipitation of chalcophile metals at the top of the sediment core [90, 110]. However, it is unknown if an adequate supply of H_2S is available at the sediment-water interface.

The use of CdS complexes as a sink in core-top sediments is potentially the missing sink to balance the global mass balance for Cd in the ocean and explain the bulk, core-top sedimentary Cd isotopic composition with suboxic pore-waters, however the availability of trace H_2S at the sediment-seawater interface remains unknown. Likewise, if trace H_2S is present within suboxic pore-waters, it remains unknown if enough CdS is precipitated to satisfy the Cd mass balance model in 7.2. Further work is required to answer these critical questions. This work should include measurement of the sedimentary and pore-water Cd concentration and isotopic compositions, along with concentrations of pore-water sulphide, nitrate, and dissolved organic carbon and sedimentary total organic carbon.

7.1.2 Redox conditions in benthic-waters controls the degree of Cd isotope offset between the near-surface sediments (core-tops) and overlying benthic-waters

This study is the first constraint on the isotopic composition of Cd in modern, near-surface marine sediments relative to the directly overlying water-column from settings that vary in their level of restriction and redox conditions. The Cd concentrations and isotopic compositions of the core-tops capture a picture of the interactions at the sediment-water interface. The studies in this thesis indicate that the degree of isotopic offset between the core-top sediments and overlying benthic-waters is directly dictated by the amount

of oxygen available and by the sedimentation rates, with removal driven by trace or detectable H_2S to form insoluble CdS complexes within sediments. Oxygenated deep-waters drive the isotopic compositions of the near-surface sediments to lighter values relative to the deep-waters, as seen in the South Atlantic ($\Delta^{114/110}Cd_{\text{core–top sediments – deep waters}}$ ranges from -0.36 ± 0.08 ‰ to 0.10 ± 0.07 ‰); in the seasonally anoxic basin, Saanich Inlet (average $\Delta^{114/110}Cd_{\text{core–top sediments – surface waters}}$ of -0.38 ± 0.07 ‰); and in the oxygenated sites deposited above the chemocline (i.e. shelf and coast) of the Black Sea (average $\Delta^{114/110}Cd_{\text{core–top sediments – surface waters}}$ = -0.30 ± 0.10 ‰).

Conversely, permanently anoxic deep-waters in the Black Sea are minimally offset from the near-surface sediments. The nature of the Black Sea being a permanently anoxic basin supports that the CdS particulates will remain stable in the deep-waters and be exported across the sediment-water interface to the near-surface sediments. This redox condition recorded an isotopic offset between the core-top sediment samples and the waters above the chemocline (~0.4 ‰) of $\Delta^{114/110}Cd_{\text{core–top sediments – surface waters}} = -0.13 \pm 0.10$ ‰. The analytical error for the measurements on the core-top sediment and water samples overlaps, suggesting little to no resolvable fractionation between the surface-waters and sediments. Similarly, suboxic sediments in the South Atlantic exhibited quantitative removal, with the Cd isotopic composition of the suboxic sediments within analytical error of the overlying deep-waters.

7.1.3 The majority of the Cd isotopic compositions in the near-surface sediment cores ranged from $\delta^{114/110}Cd$ range of ~-0.4 to 0.4‰

The South Atlantic Ocean, Black Sea, and Saanich Inlet are three very different locations that vary significantly in their degree of hydrographic restriction, primary productivity, nutrients, trace metal inventories, water depths, basin structure, and sedimentation rates. Despite these differences, the near-surface sediments only spanned a $\Delta^{114/110}Cd$ range of ~-0.4 to 0.4 ‰ for all 164 measurements (excluding outliers) reported in this thesis. This range agrees with the observed range in Late Permian shales and Cenomanian-Turonian (Late Cretaceous) shales (~-0.5 to 0.5 ‰ [121, 162]), indicating that the dominating process governing Cd burial in ancient and modern sediments is the formation of CdS

complexes. More importantly, secular variation of the seawater Cd isotope composition over time may have been very small.

7.1.4 CdS complexes may be unstable under frequently changing redox regimes

The data presented in chapters 5 and 6 support the hypothesis that quantitative removal of Cd to sediments requires stable anoxic conditions in the deep-waters and pore-waters. The key findings from the seasonally-anoxic Saanich Inlet are an isotopic offset between the core-top sediments and the overlying surface-waters above the chemocline of similar magnitude to oxygenated sediments in the South Atlantic at 40°S. This observation may be explained by instability of the CdS particulates formed across the chemocline, at the sediment-water interface or within the near-surface sediments during reventilation events. Conversely, the permanent, anoxic basin, the Black Sea, allows for an export of the CdS particulates formed across the chemocline, and subsequently burial in the sediments to remain immobilised as CdS complexes, as the redox conditions remain stable for ~500 years.

This observation supports the hypothesis that the Cd isotopes signature of the near-surface sediments is impacted by seasonal water column re-oxygenation events. The post-depositional redistribution of Cd under varying redox conditions is a process that requires further work.

7.2 Outlook

The work presented in this thesis tested a range of hypothesis governing Cd cycling in the oceans. Several hypotheses were tested, with a resulting improvement in our knowledge of how Cd and its isotopes behave in marine environments, especially underneath varying redox conditions. However, several clear gaps in knowledge can be clearly identified as targets for future study:

- Constraining the Cd isotope signature of Cd organic complexes in seawater, and the Cd isotopic composition of Cd released during organic matter remineralisation.

This step is required to better constrain the global model of Cd cycling in the oceans.

- Measuring Cd in porewater samples to better constrain its behaviour during the earliest stages of diagenesis in shallow sediments
- Investigating the stability of CdS complexes in the water column and within the sediments to changing redox regimes. Additionally, deciphering the rate of dissolution of the CdS species below the ODZs in the global ocean basins.
- Deciphering whether the different CdS species in nature exhibit different fractionation factors from dissolved Cd, and whether the speciation of dissolved Cd (Cd^{2+}, $CdCl_x$ and others) influences these fractionation factors.
- Completing X-ray adsorption fine structure (XAFS) analyses of sediments and waters to determine Cd speciation in differing environments, and their relationship to isotopes

7.3 Closing remarks

The field of trace metal isotopes offers a range of opportunities to study and better constrain the cycling of trace metals, such as Cd. These metals play an essential role in controlling chemical and biological processes in our oceans, including the carbon cycle and marine life. However, many questions remain left to explore and answer. This makes it an innovative and important area of research to help improve our projections of the ocean's responses to global climate change. It is through the efforts of programmes, such as GEOTRACES that these questions can be answered. I have enjoyed my time at Oxford, and being able to learn and work alongside researchers using a wide range of developmental and challenging techniques to better understand trace metals in our changing oceans.

References

[1] J. J. Wright, K. M. Konwar, and S. J. Hallam. “Microbial ecology of expanding oxygen minimum zones”. In: *Nature Reviews Microbiology* 10.6 (2012), pp. 381–394.

[2] N N Rabalais et al. *Dynamics and distribution of natural and human-caused hypoxia*. Tech. rep. 2010, pp. 585–619.

[3] A. Paulmier and D. Ruiz-Pino. “Oxygen minimum zones (OMZs) in the modern ocean”. In: *Progress in Oceanography* 80.3-4 (2009), pp. 113–128.

[4] K. P. Helm, N. L. Bindoff, and J. A. Church. “Observed decreases in oxygen content of the global ocean”. In: *Geophysical Research Letters* 38.23 (2011), p. L23602.

[5] R. F. Keeling, A. Körtzinger, and N. Gruber. “Ocean Deoxygenation in a Warming World”. In: *Annual Review of Marine Science* 2.1 (2010), pp. 199–229.

[6] S. Kumar. “Fourth assessment report of the Intergovernmental Panel on Climate Change: Important observations and conclusions”. In: *Current Science* 92.8 (2007), p. 1034.

[7] S. Schmidtko, L. Stramma, and M. Visbeck. “Decline in global oceanic oxygen content during the past five decades”. In: *Nature* 542.7641 (2017), pp. 335–339.

[8] A. Oschlies et al. “Drivers and mechanisms of ocean deoxygenation”. In: *Nature Geoscience* 11.7 (2018), pp. 467–473.

[9] R. Anderson et al. “GEOTRACES: Changing the Way We Explore Ocean Chemistry”. In: *Oceanography* 27.1 (2014), pp. 50–61.

[10] H. Elderfield and R. E. M. Rickaby. “Oceanic Cd/P ratio and nutrient utilization in the glacial Southern Ocean”. In: *Nature* 405.6784 (2000), pp. 305–310.

[11] E. A. Boyle and L. D. Keigwin. “Comparison of Atlantic and Pacific paleochemical records for the last 215,000 years: changes in deep ocean circulation and chemical inventories”. In: *Earth and Planetary Science Letters* 76.1-2 (1985), pp. 135–150.

[12] K. W. Bruland. “Oceanographic distributions of cadmium, zinc, nickel, and copper in the North Pacific”. In: *Earth and Planetary Science Letters* 47.2 (1980), pp. 176–198.

[13] W. G. Sunda and S. A. Huntsman. “Iron uptake and growth limitation in oceanic and coastal phytoplankton”. In: *Marine Chemistry* 50.1-4 (1995), pp. 189–206.

[14] F M M Morel and N M Price. “The biogeochemical cycles of trace metals in the oceans.” In: *Science* 300.5621 (2003), pp. 944–7.

[15] J. T. Cullen et al. “Effect of iron limitation on the cadmium to phosphorus ratio of natural phytoplankton assemblages from the Southern Ocean”. In: *Limnology and Oceanography* 48.3 (2003), pp. 1079–1087.

[16] E. S. Lane et al. “Effects of iron limitation on intracellular cadmium of cultured phytoplankton: Implications for surface dissolved cadmium to phosphate ratios”. In: *Marine Chemistry* 115.3-4 (2009), pp. 155–162.

[17] B. S. Twining and S. B. Baines. “The Trace Metal Composition of Marine Phytoplankton”. In: *Annual Review of Marine Science* 5.1 (2013), pp. 191–215.

[18] E. A. Boyle, F. Sclater, and J. M. Edmond. “On the marine geochemistry of cadmium”. In: *Nature* 263.5572 (1976), pp. 42–44.

[19] K. W. Bruland, G. A. Knauer, and J. H. Martin. “Cadmium in northeast Pacific waters”. In: *Limnology and Oceanography* 23.4 (1978), pp. 618–625.

[20] M. J., K.W. Bruland, and W. Broenkow. “Cadmium transport in the California current”. In: *Marine Pollutant Transfer*. Ed. by H.L. Windom and R.A. Duce. Toronto: Lexington Books, 1976, pp. 84–159.

[21] K. W. Bruland. “Complexation of zinc by natural organic ligands in the central North Pacific”. In: *Limnology and Oceanography* 34.2 (1989), pp. 269–285.

[22] K.W. Bruland and M.C. Lohan. “Controls of Trace Metals in Seawater”. In: *Treatise on Geochemistry*. Ed. by H. Elderfield. Vol. 6. Elsevier, 2003, pp. 23–47.

[23] A. Milne et al. “Determination of Mn, Fe, Co, Ni, Cu, Zn, Cd and Pb in seawater using high resolution magnetic sector inductively coupled mass spectrometry (HR-ICP-MS)”. In: *Analytica Chimica Acta* 665.2 (2010), pp. 200–207.

[24] O. Baars and P. L. Croot. “The speciation of dissolved zinc in the Atlantic sector of the Southern Ocean”. In: *Deep-Sea Research Part II: Topical Studies in Oceanography* 58.25-26 (2011), pp. 2720–2732.

[25] W. Abouchami et al. “Modulation of the Southern Ocean cadmium isotope signature by ocean circulation and primary productivity”. In: *Earth and Planetary Science Letters* 305.1-2 (2011), pp. 83–91.

[26] M. Gault-Ringold et al. “Anomalous biogeochemical behavior of cadmium in subantarctic surface waters: Mechanistic constraints from cadmium isotopes”. In: *Earth and Planetary Science Letters* 341-344 (2012), pp. 94–103.

[27] S. C. Yang, D. C. Lee, and T. Y. Ho. “The isotopic composition of Cadmium in the water column of the South China Sea”. In: *Geochimica et Cosmochimica Acta* 98 (2012), pp. 66–77.

[28] T. M. Conway and S. G. John. “Biogeochemical cycling of cadmium isotopes along a high-resolution section through the North Atlantic Ocean”. In: *Geochimica et Cosmochimica Acta* 148 (2015), pp. 269–283.

[29] K. W. Bruland, K. J. Orians, and J. P. Cowen. “Reactive trace metals in the stratified central North Pacific”. In: *Geochimica et Cosmochimica Acta* 58.15 (1994), pp. 3171–3182.

[30] K. Abe. “Cadmium Distribution in the Western Pacific”. In: *Global Environmental Change in the Ocean and on Land* (2004), pp. 189–203.

[31] S. Ripperger et al. “Cadmium isotope fractionation in seawater - A signature of biological activity”. In: *Earth and Planetary Science Letters* 261.3-4 (2007), pp. 670–684.

[32] E. A. Boyle. “Cadmium: Chemical tracer of deepwater paleoceanography”. In: *Paleoceanography* 3.4 (1988), pp. 471–489.

[33] T. M. Marchitto and W. S. Broecker. “Deep water mass geometry in the glacial Atlantic Ocean: A review of constraints from the paleonutrient proxy Cd/Ca”. In: *Geochemistry, Geophysics, Geosystems* 7.12 (2006).

[34] M. C. Makou, D. W. Oppo, and W. B. Curry. "South Atlantic intermediate water mass geometry for the last glacial maximum from foraminiferal Cd/Ca". In: *Paleoceanography* 25.4 (2010).

[35] R. Middag et al. "The relationship between cadmium and phosphate in the Atlantic Ocean unravelled". In: *Earth and Planetary Science Letters* 492 (2018), pp. 79–88.

[36] H. Y. Chen, T. H. Fang, and L. S. Wen. "A preliminary study of the distributions of Cd in the South China Sea". In: *Continental Shelf Research* 25.3 (2005), pp. 297–310.

[37] J. T. Cullen. "On the nonlinear relationship between dissolved cadmium and phosphate in the modern global ocean: Could chronic iron limitation of phytoplankton growth cause the kink?" In: *Limnology and Oceanography* 51.3 (2006), pp. 1369–1380.

[38] H. J.W. de Baar et al. "Cadmium versus phosphate in the world ocean". In: *Marine Chemistry* 46.3 (1994), pp. 261–281.

[39] M. R. Van Der Loeff, E. Helmers, and G. Kattner. "Continuous transects of cadmium, copper, and aluminium in surface waters of the Atlantic Ocean, 50°N to 50°S: correspondence and contrast with nutrient-like behaviour". In: *Geochimica et Cosmochimica Acta* 61.1 (1997), pp. 47–61.

[40] E. Mawji et al. "The GEOTRACES Intermediate Data Product 2014". In: *Marine Chemistry* 177 (2015), pp. 1–8.

[41] R. Schlitzer et al. "The GEOTRACES Intermediate Data Product 2017". In: *Chemical Geology* 493 (2018), pp. 210–223.

[42] B. M. Löscher, J. T.M. De Jong, and H. J.W. De Baar. "The distribution and preferential biological uptake of cadmium at 6°W in the Southern Ocean". In: *Marine Chemistry* 62.3-4 (1998), pp. 259–286.

[43] M. J. Ellwood. "Wintertime trace metal (Zn, Cu, Ni, Cd, Pb and Co) and nutrient distributions in the Subantarctic Zone between 40-52°S; 155-160°E". In: *Marine Chemistry* 112.1-2 (2008), pp. 107–117.

[44] T. Y. Ho et al. "Cadmium and phosphorus cycling in the water column of the South China Sea: The roles of biotic and abiotic particles". In: *Marine Chemistry* 115.1-2 (2009), pp. 125–133.

[45] M. A. Saito et al. "A seasonal study of dissolved cobalt in the Ross Sea, Antarctica: micronutrient behavior, absence of scavenging, and relationships with Zn, Cd, and P". In: *Biogeosciences* 7 (2010), pp. 4059–4082.

[46] E. V. Armbrust et al. "The Genome of the Diatom Thalassiosira Pseudonana: Ecology, Evolution, and Metabolism". In: *Science* 306.5693 (2004), pp. 79–86.

[47] K. R. Hendry et al. "Cadmium and phosphate in coastal Antarctic seawater: Implications for Southern Ocean nutrient cycling". In: *Marine Chemistry* 112.3-4 (2008), pp. 149–157.

[48] J. T. Cullen et al. "Modulation of cadmium uptake in phytoplankton by seawater CO2 concentration". In: *Nature* 402.6758 (1999), pp. 165–167.

[49] R. D. Frew and K. A. Hunter. "Influence of Southern Ocean waters on the cadmium–phosphate properties of the global ocean". In: *Nature* 360.6400 (1992), pp. 144–146.

[50] R. D. Frew. "Antarctic bottom water formation and the global cadmium to phosphorus relationship". In: *Geophysical Research Letters* 22.17 (1995), pp. 2349–2352.

[51] R. C. Xie et al. “The cadmium–phosphate relationship in the western South Atlantic — The importance of mode and intermediate waters on the global systematics”. In: *Marine Chemistry* 177 (2015), pp. 110–123.

[52] R. D. Frew and K. A. Hunter. “Cadmium-phosphorus cycling at the subtropical convergence south of New Zealand”. In: *Marine Chemistry* 51.3 (1995), pp. 223–237.

[53] S. Roshan and J. Wu. “Cadmium regeneration within the North Atlantic”. In: *Global Biogeochemical Cycles* 29.12 (2015), pp. 2082–2094.

[54] W. Abouchami et al. “Biogeochemical cycling of cadmium isotopes in the Southern Ocean along the Zero Meridian”. In: *Geochimica et Cosmochimica Acta* 127 (2014), pp. 348–367.

[55] O. Baars et al. “Dissolved cadmium in the Southern Ocean: Distribution, speciation, and relation to phosphate”. In: *Limnology and Oceanography* 59.2 (2014), pp. 385–399.

[56] D. J. Janssen et al. “Undocumented water column sink for cadmium in open ocean oxygen-deficient zones”. In: *Proceedings of the National Academy of Sciences* 111.19 (2014), pp. 6888–6893.

[57] F. Lacan et al. “Cadmium isotopic composition in the ocean”. In: *Geochimica et Cosmochimica Acta* 70.20 (2006), pp. 5104–5118.

[58] S. Ripperger and M. Rehkämper. “Precise determination of cadmium isotope fractionation in seawater by double spike MC-ICPMS”. In: *Geochimica et Cosmochimica Acta* 71.3 (2007), pp. 631–642.

[59] E. A. Boyle et al. “GEOTRACES IC1 (BATS) contamination-prone trace element isotopes Cd, Fe, Pb, Zn, Cu, and Mo intercalibration”. In: *Limnology and Oceanography: Methods* 10.1 (2012), pp. 653–665.

[60] Z. Xue et al. “A new methodology for precise cadmium isotope analyses of seawater”. In: *Analytical and Bioanalytical Chemistry* 402.2 (2012), pp. 883–893.

[61] Z. Xue et al. “Cadmium isotope variations in the Southern Ocean”. In: *Earth and Planetary Science Letters* 382 (2013), pp. 161–172.

[62] T. M. Conway et al. “A new method for precise determination of iron, zinc and cadmium stable isotope ratios in seawater by double-spike mass spectrometry”. In: *Analytica Chimica Acta* 793 (2013), pp. 44–52.

[63] S. G. John and T. M. Conway. “A role for scavenging in the marine biogeochemical cycling of zinc and zinc isotopes”. In: *Earth and Planetary Science Letters* 394 (2014), pp. 159–167.

[64] T. W. Lane and F. M. M. Morel. “A biological function for cadmium in marine diatoms”. In: *Proceedings of the National Academy of Sciences* 97.9 (2000), pp. 4627–4631.

[65] W. G. Sunda and S. A. Huntsman. “Effect of CO2 supply and demand on zinc uptake and growth limitation in a coastal diatom”. In: *Limnology and Oceanography* 50.4 (2005), pp. 1181–1192.

[66] F. M. M. Morel. “The oceanic cadmium cycle: Biological mistake or utilization?” In: *Proceedings of the National Academy of Sciences* 110.21 (2013), E1877–E1877.

[67] T. J. Horner et al. “Nonspecific uptake and homeostasis drive the oceanic cadmium cycle”. In: *Proceedings of the National Academy of Sciences* 110.7 (2013), pp. 2500–2505.

[68] J. L. Morford and S. Emerson. “The geochemistry of redox sensitive trace metals in sediments”. In: *Geochimica et Cosmochimica Acta* 63.11-12 (1999), pp. 1735–1750.

[69] K. W. Bruland. “Complexation of cadmium by natural organic ligands in the central North Pacific”. In: *Limnology and Oceanography* 37.5 (1992), pp. 1008–1017.

[70] W. G. Sunda. “Trace Metal/Phytoplankton Interactions in the Sea”. In: *Chemistry of Aquatic Systems: Local and Global Perspectives*. Dordrecht: Springer Netherlands, 1994, pp. 213–247.

[71] J.R. Donat and K.W. Bruland. “Trace elements in the oceans”. In: *Trace elements in natural waters*. Ed. by B. Salbu and E. Steinnes. Boca Raton, FL: CRC Press, 1995, pp. 247–280.

[72] W. Stumm and J. J. Morgan. *Aquatic Chemistry: Chemical Equilibria and Rates in Natural Waters; Third Edition*. New York: Wiley, 1995, p. 1022.

[73] L.S. Wen, K.T. Jiann, and P.H. Santschi. “Physicochemical speciation of bioactive trace metals (Cd, Cu, Fe, Ni) in the oligotrophic South China Sea”. In: *Marine Chemistry* 101.1-2 (2006), pp. 104–129.

[74] D. C. Ohnemus and P. J. Lam. “Cycling of Lithogenic Marine Particulates in the US GEOTRACES North Atlantic Zonal Transect”. In: *Deep Sea Research Part II: Topical Studies in Oceanography* 116 (2015), pp. 283–302.

[75] L. Balistrieri, P. G. Brewer, and J. W. Murray. “Scavenging residence times of trace metals and surface chemistry of sinking particles in the deep ocean”. In: *Deep Sea Research Part A, Oceanographic Research Papers* 28.2 (1981), pp. 101–121.

[76] K. A. Hunter. “The adsorptive properties of sinking particles in the deep ocean”. In: *Deep Sea Research Part A, Oceanographic Research Papers* 30.6 (1983), pp. 669–675.

[77] B.A. Ahner and F.M.M. Morel. “Phytochelatin production in marine algae. 2. Induction by various metals”. In: *Limnology and Oceanography* 40.4 (1995), pp. 658–665.

[78] F.L.L. Muller. “Interactions of copper, lead and cadmium with the dissolved, colloidal and particulate components of estuarine and coastal waters”. In: *Marine Chemistry* 52.3-4 (1996), pp. 245–268.

[79] M. J. Ellwood. “Zinc and cadmium speciation in subantarctic waters east of New Zealand”. In: *Marine Chemistry* 87.1-2 (2004), pp. 37–58.

[80] D. Guinoiseau, S. J.G. Galer, and W. Abouchami. “Effect of cadmium sulphide precipitation on the partitioning of Cd isotopes: Implications for the oceanic Cd cycle”. In: *Earth and Planetary Science Letters* 498 (2018), pp. 300–308.

[81] S. E. Calvert and N. B. Price. “Geochemistry of Namibian shelf sediments”. In: *Coastal upwelling: its sediment record. Part A. Responses of the sedimentary regime to present coastal coastal upwelling*. Vol. 10a. Boston, MA: Springer US, 1983, pp. 337–375.

[82] H. J. Brumsack. “Geochemistry of recent TOC-rich sediments from the Gulf of California and the Black Sea”. In: *Geologische Rundschau* 78.3 (1989), pp. 851–882.

[83] T. J Algeo and J. B. Maynard. “Trace-element behavior and redox facies in core shales of Upper Pennsylvanian Kansas-type cyclothems”. In: *Chemical Geology* 206.3-4 (2004), pp. 289–318.

[84] C. H. van der Weijden, G. J. Reichart, and B. J.H. van Os. “Sedimentary trace element records over the last 200 kyr from within and below the northern Arabian Sea oxygen minimum zone”. In: *Marine Geology* 231.1-4 (2006), pp. 69–88.

[85] L. E. Wasylenki, J. W. Swihart, and S. J. Romaniello. “Cadmium isotope fractionation during adsorption to Mn oxyhydroxide at low and high ionic strength”. In: *Geochimica et Cosmochimica Acta* 140 (2014), pp. 212–226.

[86] T. J. Horner, R. E. M. Rickaby, and G. M. Henderson. “Isotopic fractionation of cadmium into calcite”. In: *Earth and Planetary Science Letters* 312.1-2 (2011), pp. 243–253.

[87] D. J. Janssen and J. T. Cullen. “Decoupling of zinc and silicic acid in the subarctic northeast Pacific interior”. In: *Marine Chemistry* 177 (2015), pp. 124–133.

[88] D. E. Canfield et al. “A cryptic sulfur cycle in oxygen-minimum-zone waters off the Chilean coast”. In: *Science* 330.6009 (2010), pp. 1375–1378.

[89] M. T. Carolan, J. M. Smith, and J. M. Beman. “Transcriptomic evidence for microbial sulfur cycling in the eastern tropical North Pacific oxygen minimum zone”. In: *Frontiers in Microbiology* 6 (2015), p. 334.

[90] D. Bianchi et al. “Global niche of marine anaerobic metabolisms expanded by particle microenvironments”. In: *Nature Geoscience* 11 (2018), pp. 1–6.

[91] W.M. Landing and B.L. Lewis. “Thermodynamic Modeling of Trace Metal Speciation in the Black Sea”. In: *Black Sea Oceanography* 351 (1991), pp. 125–160.

[92] J. Yang et al. “Theoretical calculations of Cd isotope fractionation in hydrothermal fluids”. In: *Chemical Geology* 391 (2015), pp. 74–82.

[93] A. D. Schmitt, S. J.G. Galer, and W. Abouchami. “Mass-dependent cadmium isotopic variations in nature with emphasis on the marine environment”. In: *Earth and Planetary Science Letters* 277.1-2 (2009), pp. 262–272.

[94] S. G. John, J. Helgoe, and E. Townsend. “Biogeochemical cycling of Zn and Cd and their stable isotopes in the Eastern Tropical South Pacific”. In: *Marine Chemistry* 201 (2018), pp. 256–262.

[95] S. Yang et al. “The isotopic composition of dissolved cadmium in the water column of the West Philippine Sea”. In: *Frontiers in Marine Science* 1 (2014), p. 61.

[96] T. M. Conway and S. G. John. “The cycling of iron, zinc and cadmium in the North East Pacific Ocean - Insights from stable isotopes”. In: *Geochimica et Cosmochimica Acta* 164 (2015), pp. 262–283.

[97] D.J. Janssen et al. “Fine-scale spatial and interannual cadmium isotope variability in the subarctic northeast Pacific”. In: *Earth and Planetary Science Letters* 472 (2017), pp. 241–252.

[98] J.L. Mero. *The mineral resources of the sea. volumne 1*. Amsterdam, NED: Elsevier, 1965.

[99] E. D. Goldberg and G. O. S. Arrhenius. “Chemistry of Pacific pelagic sediments”. In: *Geochimica et Cosmochimica Acta* 13.2–3 (1958), pp. 153–212.

[100] H. Heinrichs, B. Schulz-Dobrick, and K. H. Wedepohl. “Terrestrial geochemistry of Cd, Bi, Tl, Pb, Zn and Rb”. In: *Geochimica et Cosmochimica Acta* 44.10 (1980), pp. 1519–1533.

[101] B. J. Hay. "Sediment accumulation in the central western Black Sea over the past 5100 years". In: *Paleoceanography* 3.4 (1988), pp. 491–508.

[102] J. R. Hein et al. "Cobalt-Rich Ferromanganese Crusts in the Pacific". In: *Handbook of Marine Mineral Deposits*. Ed. by D.S. Cronan. CRC Press, 2000. Chap. 9, pp. 239–279.

[103] J. R. Hein, A. Koschinsky, and A. N. Halliday. "Global occurrence of tellurium-rich ferromanganese crusts and a model for the enrichment of tellurium". In: *Geochimica et Cosmochimica Acta* 67.6 (2003), pp. 1117–1127.

[104] T. J. Horner et al. "Ferromanganese crusts as archives of deep water Cd isotope compositions". In: *Geochemistry, Geophysics, Geosystems* 11.4 (2010), pp. 1–10.

[105] K.L. Von Damm et al. "Chemistry of submarine hydrothermal solutions at 21 °N, East Pacific Rise". In: *Geochimica et Cosmochimica Acta* 49.11 (1985), pp. 2197–2220.

[106] R. P. Trocine and J. H. Trefry. "Distribution and chemistry of suspended particles from an active hydrothermal vent site on the Mid-Atlantic Ridge at 26°N". In: *Earth and Planetary Science Letters* 88.1-2 (1988), pp. 1–15.

[107] C. R. German, A. C. Campbell, and J. M. Edmond. "Hydrothermal scavenging at the Mid-Atlantic Ridge: Modification of trace element dissolved fluxes". In: *Earth and Planetary Science Letters* 107.1 (1991), pp. 101–114.

[108] T. L. Patterson and R. A. Duce. "The cycle of atmospheric cadmium over the North Pacific Ocean". In: *Tellus B: Chemical and Physical Meteorology* 43.1 (1991), pp. 12–29.

[109] A. M. Shiller and E. A. Boyle. "Trace elements in the Mississippi River Delta outflow region: Behavior at high discharge". In: *Geochimica et Cosmochimica Acta* 55.11 (1991), pp. 3241–3251.

[110] Y. Rosenthal et al. "Authigenic cadmium enrichments in suboxic sediments: Precipitation and postdepositional mobility". In: *Earth and Planetary Science Letters* 132.1-4 (1995), pp. 99–111.

[111] W. Abouchami et al. "A Common Reference Material for Cadmium Isotope Studies - NIST SRM 3108". In: *Geostandards and Geoanalytical Research* 37.1 (2013), pp. 5–17.

[112] M. Lambelet et al. "Isotopic analysis of Cd in the mixing zone of Siberian rivers with the Arctic Ocean-New constraints on marine Cd cycling and the isotope composition of riverine Cd". In: *Earth and Planetary Science Letters* 361 (2013), pp. 64–73.

[113] A. van Geen, D. C. McCorkle, and G. P. Klinkhammer. "Sensitivity of the phosphate-cadmium-carbon isotope relation in the ocean to cadmium removal by suboxic sediments". In: *Paleoceanography* 10.2 (1995), pp. 159–169.

[114] M. Rehkämper et al. "Natural and Anthropogenic Cd Isotope Variations". In: *Handbook of Environmental Isotope Geochemistry*. Ed. by M. Baskaran. Berlin, Heidelberg: Springer, 2012, pp. 125–154.

[115] P. E. Framson and J. O. Leckie. "Limits of Coprecipitation of Cadmium and Ferrous Sulfides". In: *Environmental Science and Technology* 12.4 (1978), pp. 465–469.

[116] T. J. Nameroff, S. E. Calvert, and J. W. Murray. "Glacial-interglacial variability in the eastern tropical North Pacific oxygen minimum zone recorded by redox-sensitive trace metals". In: *Paleoceanography* 19.1 (2004).

[117] H. J. Brumsack. “The trace metal content of recent organic carbon-rich sediments: Implications for Cretaceous black shale formation”. In: *Palaeogeography, Palaeoclimatology, Palaeoecology* 232 (2006), pp. 344–361.

[118] N. Tribovillard et al. “Trace metals as paleoredox and paleoproductivity proxies: An update”. In: *Chemical Geology* 232.1-2 (2006), pp. 12–32.

[119] P.N. Froelich et al. “Early oxidation of organic matter in pelagic sediments of the eastern equatorial Atlantic: suboxic diagenesis”. In: *Geochimica et Cosmochimica Acta* 43.7 (1979), pp. 1075–1090.

[120] D.Z. Piper and S.E. Calvert. “A marine biogeochemical perspective on black shale deposition”. In: *Earth-Science Reviews* 95.1-2 (2009), pp. 63–96.

[121] S. V. Georgiev et al. “Cadmium-isotopic evidence for increasing primary productivity during the Late Permian anoxic event”. In: *Earth and Planetary Science Letters* 410 (2015), pp. 84–96.

[122] S. H. Little et al. “Controls on trace metal authigenic enrichment in reducing sediments: Insights from modern oxygen-deficient settings”. In: *American Journal of Science* 315.2 (2015), pp. 77–119.

[123] H. Elderfield et al. “Chemical diagenesis in Narragansett Bay sediments.” In: *American Journal of Science* 281.8 (1981), pp. 1021–1055.

[124] C. Gobeil, R. W. Macdonald, and Bjørn Sundby. “Diagenetic separation of cadmium and manganese in suboxic continental margin sediments”. In: *Geochimica et Cosmochimica Acta* 61.21 (1997), pp. 4647–4654.

[125] W. B. Homoky et al. “Distinct iron isotopic signatures and supply from marine sediment dissolution”. In: *Nature Communications* 4.1 (2013), p. 2143.

[126] R. F. Anderson et al. “GEOTRACES intercalibration of 230 Th, 232 Th, 231 Pa, and prospects for 10 Be”. In: *Limnology and Oceanography: Methods* 10.4 (2012), pp. 179–213.

[127] C. S. Buck and A. Paytan. “Evaluation of commonly used filter substrates for the measurement of aerosol trace element solubility”. In: *Limnology and Oceanography: Methods* 10.10 (2012), pp. 790–806.

[128] D. C. Ohnemus et al. “Laboratory intercomparison of marine particulate digestions including Piranha: A novel chemical method for dissolution of polyethersulfone filters”. In: *Limnology and Oceanography: Methods* 12 (2014), pp. 530–547.

[129] R. G Behrens and C. F.V Mason. “A mass spectrometric investigation of the vaporization thermodynamics and vapor composition of cadmium oxide”. In: *Journal of the Less Common Metals* 77.2 (1981), pp. 169–184.

[130] P. Holdship et al. “Micro flow injection ICP-MS analysis of high matrix samples: an investigation of its capability to measure trace elements in iron meteorites”. In: *Journal of Analytical Atomic Spectrometry* 33.11 (2018), pp. 1941–1953.

[131] T.J. Horner. “Cadmium Isotope Fractionation in Seawater: Driving Mechanisms and Paleoceanographic Applications”. Doctor of Philosophy in Earth Sciences. University of Oxford, 2012.

[132] J. R. de Laeter et al. “Atomic weights of the elements. Review 2000 (IUPAC Technical Report)”. In: *Pure and Applied Chemistry* 75.6 (2003), pp. 683–800.

[133] C. R. Pearce, A. S. Cohen, and I. J. Parkinson. "Quantitative Separation of Molybdenum and Rhenium from Geological Materials for Isotopic Determination by MC-ICP-MS". In: *Geostandards and Geoanalytical Research* 33.2 (2009), pp. 219–229.

[134] F. Wombacher et al. "Stable isotope compositions of cadmium in geological materials and meteorites determined by multiple-collector ICPMS". In: *Geochimica et Cosmochimica Acta* 67.23 (2003), pp. 4639–4654.

[135] A. J. Dickson et al. "Basin-scale controls on the molybdenum-isotope composition of sea water during Oceanic Anoxic Event 2 (Late Cretaceous)". In: *Geochimica et Cosmochimica Acta* 178 (2016), pp. 291–306.

[136] N.S Belshaw et al. "A new variable dispersion double-focusing plasma mass spectrometer with performance illustrated for Pb isotopes". In: *International Journal of Mass Spectrometry* 181.1-3 (1998), pp. 51–58.

[137] M. Rehkämper and A. N. Halliday. "Accuracy and long-term reproducibility of lead isotopic measurements by multiple-collector inductively coupled plasma mass spectrometry using an external method for correction of mass discrimination". In: *International Journal of Mass Spectrometry* 181.1-3 (1998), pp. 123–133.

[138] X. Zhu et al. "Secular variation of iron isotopes in north atlantic deep water". In: *Science* 287.5460 (2000), pp. 2000–2002.

[139] C. Archer and D. Vance. "Mass discrimination correction in multiple-collector plasma source mass spectrometry: an example using Cu and Zn isotopes". In: *Journal of Analytical Atomic Spectrometry* 19.5 (2004), p. 656.

[140] C. Siebert, T. F. Nägler, and J. D. Kranmers. "Determination of molybdenum isotope fractionation by double-spike multicollector inductively coupled plasma mass spectrometry". In: *Geochemistry, Geophysics, Geosystems* 2.7 (2001).

[141] T. Hirata. "Lead isotopic analyses of NIST standard reference materials using multiple collector inductively coupled plasma mass spectrometry coupled with a modified external correction method for mass discrimination effect". In: *Analyst* 121.10 (1996), pp. 1407–1411.

[142] C. N. Maréchal, P. Télouk, and F. Albarède. "Precise analysis of copper and zinc isotopic compositions by plasma-source mass spectrometry". In: *Chemical Geology* 156.1-4 (1999), pp. 251–273.

[143] W. M. White, F. Albarède, and P. Télouk. "High-precision analysis of Pb isotope ratios by multi-collector ICP-MS". In: *Chemical Geology* 167.3-4 (2000), pp. 257–270.

[144] S. J.G. Galer. "Optimal double and triple spiking for high precision lead isotopic measurement". In: *Chemical Geology* 157.3-4 (1999), pp. 255–274.

[145] M. Waeles et al. "Off Congo waters (Angola Basin, Atlantic Ocean): A hot spot for cadmium-phosphate fractionation". In: *Limnology and Oceanography* 58.4 (2013), pp. 1481–1490.

[146] D. C. Ohnemus et al. "Elevated trace metal content of prokaryotic communities associated with marine oxygen deficient zones". In: *Limnology and Oceanography* 62.1 (2017), pp. 3–25.

[147] R. C. Xie et al. "Non-Rayleigh control of upper-ocean Cd isotope fractionation in the western South Atlantic". In: *Earth and Planetary Science Letters* 471 (2017), pp. 94–103.

[148] L. Xu et al. “Mo isotope and trace element patterns of Lower Cambrian black shales in South China: Multi-proxy constraints on the paleoenvironment”. In: *Chemical Geology* 318-319 (2012), pp. 45–59.

[149] K. H. Wedepohl. “The composition of the continental crust”. In: *Geochimica et Cosmochimica Acta* 59.7 (1995), pp. 1217–1232.

[150] D. C. McCorkle and G. P. Klinkhammer. “Porewater cadmium geochemistry and the porewater cadmium: δ13C relationship”. In: *Geochimica et Cosmochimica Acta* 55.1 (1991), pp. 161–168.

[151] G. W. Luther and D. T. Rickard. “Metal Sulfide Cluster Complexes and their Biogeochemical Importance in the Environment”. In: *Journal of Nanoparticle Research* 4-5 (2005), pp. 389–407.

[152] T. Ho et al. “THE ELEMENTAL COMPOSITION OF SOME MARINE PHYTOPLANKTON 1 Franc”. In: *Journal of Phycology* 39 (2003), pp. 1145–1159.

[153] D. Heggie, D. Kahn, and K. Fischer. “Trace metals in metalliferous sediments, MANOP Site M: interfacial pore water profiles”. In: *Earth and Planetary Science Letters* 80.1-2 (1986), pp. 106–116.

[154] C. Gobeil et al. “Cadmium diagenesis in Laurentian Trough sediments”. In: *Geochimica et Cosmochimica Acta* 51.3 (1987), pp. 589–596.

[155] D. J. Janssen et al. “Particulate cadmium stable isotopes in the subarctic northeast Pacific reveal dynamic Cd cycling and a new isotopically light Cd sink”. In: *Earth and Planetary Science Letters* 515 (June 2019), pp. 67–78.

[156] T. W. Lyons et al. “Tracking Euxinia in the Ancient Ocean: A Multiproxy Perspective and Proterozoic Case Study”. In: *Annual Review of Earth and Planetary Sciences* 37.1 (2009), pp. 507–534.

[157] J. Thomson, N. C. Higgs, and S. Colley. “Diagenetic redistributions of redox-sensitive elements in northeast Atlantic glacial/interglacial transition sediments”. In: *Earth and Planetary Science Letters* 139.3-4 (1996), pp. 365–377.

[158] H. L. Bourne et al. “Global Spatial and Temporal Variation of Cd:P in Euphotic Zone Particulates”. In: *Global Biogeochemical Cycles* 32.7 (2018), pp. 1123–1141.

[159] Y. Rosenthal et al. “Glacial enrichments of authigenic Cd And U in subantarctic sediments: A climatic control on the elements’ oceanic budget?” In: *Paleoceanography* 10.3 (1995), pp. 395–413.

[160] K. R. Chandana, Ravi Bhushan, and A. J. T. Jull. “Evidence of Poor Bottom Water Ventilation during LGM in the Equatorial Indian Ocean”. In: *Frontiers in Earth Science* 5 (Oct. 2017), p. 84.

[161] J. Thomson et al. “Authigenic uranium in Atlantic sediments of the last glacial stage — a diagenetic phenomenon”. In: *Earth and Planetary Science Letters* 98.2 (1990), pp. 222–232.

[162] T. Sweere. “Zn and Cd isotopes as proxies for geochemical change in Mesozoic oceans”. Doctor of Philiosophy in Earth Sciences. University of Oxford, 2018.

[163] T. F. Pedersen, R. D. Waters, and R. W. Macdonald. “On the natural enrichment of cadmium and molybdenum in the sediments of ucluelet inlet, British Columbia”. In: *Science of the Total Environment, The* 79.2 (1989), pp. 125–139.

[164] K. Kremling. “The behavior of Zn, Cd, Cu, Ni, Co, Fe, and Mn in anoxic baltic waters”. In: *Marine Chemistry* 13.2 (1983), pp. 87–108.

[165] J. M. Rolison et al. “Uranium stable isotope fractionation in the Black Sea: Modern calibration of the 238U/235U paleo-redox proxy”. In: *Geochimica et Cosmochimica Acta* 203 (2017), pp. 69–88.

[166] E. Özsoy and Ü. Ünlüata. “Oceanography of the Black Sea: A review of some recent results”. In: *Earth-Science Reviews* 42.4 (1997), pp. 231–272.

[167] C.G. Gunnerson and E. Özturgut. “The Black Sea- Geology, Chemistry and Biology”. In: *American Association of Petrology and Geologists* 20 (1974), pp. 99–114.

[168] J. W. Murray, Z. Top, and E. Özsoy. “Hydrographic properties and ventilation of the Black Sea”. In: *Deep Sea Research Part A. Oceanographic Research Papers* 38 (1991), S663–S689.

[169] T. J. Algeo and T. W. Lyons. “Mo-total organic carbon covariation in modern anoxic marine environments: Implications for analysis of paleoredox and paleohydrographic conditions”. In: *Paleoceanography* 21.1 (2006).

[170] J. S. Turner. “A Physical Interpretation of the Observations of Hot Brine Layers in the Red Sea”. In: *Hot Brines and Recent Heavy Metal Deposits in the Red Sea*. Berlin, Heidelberg: Springer, 1969, pp. 164–173.

[171] H. J. S. Fernando. “Oceanographic implications of laboratory experiments on diffusive interfaces”. In: *Journal of Physical Oceanography* 19.11 (1989), pp. 1707–1715.

[172] E. Özsoy and Ş. Beşiktepe. “Sources of double diffusive convection and impacts on mixing in the black sea”. In: *Geophysical Monograph Series* 94 (1995), pp. 261–274.

[173] J. W. Murray et al. “Unexpected changes in the oxic/anoxic interface in the Black Sea”. In: *Nature* 338.6214 (1989), pp. 411–413.

[174] C. Saydam et al. “Identification of the oxic/anoxic interface by isopycnal surfaces in the black sea”. In: *Deep Sea Research Part I: Oceanographic Research Papers* 40.7 (1993), pp. 1405–1412.

[175] B. B. Jørgensen et al. “Sulfide oxidation in the anoxic Black Sea chemocline”. In: *Deep Sea Research Part A. Oceanographic Research Papers* 38 (1991), S1083–S1103.

[176] T.F. Nägler et al. “Molybdenum isotope fractionation in pelagic euxinia: Evidence from the modern Black and Baltic Seas”. In: *Chemical Geology* 289.1-2 (2011), pp. 1–11.

[177] D. Vance et al. “The oceanic budgets of nickel and zinc isotopes: The importance of sulfdic environments as illustrated by the Black Sea”. In: *Philosophical Transactions of the Royal Society A: Mathematical, Physical and Engineering Sciences* 374.2081 (2016).

[178] T. W. Lyons and R. A. Berner. “Carbon-sulfur-iron systematics of the uppermost deep-water sediments of the Black Sea”. In: *Chemical Geology* 99.1-3 (1992), pp. 1–27.

[179] S. E. Calvert et al. “Low organic carbon accumulation rates in Black Sea sediments”. In: *Nature* 350.6320 (1991), pp. 692–695.

[180] D. M. Karl and G. A. Knauer. “Microbial production and particle flux in the upper 350 m of the Black Sea”. In: *Deep Sea Research Part A. Oceanographic Research Papers* 38 (1991), S921–S942.

[181] G. Chaillou et al. “The distribution of Mo, U, and Cd in relation to major redox species in muddy sediments of the Bay of Biscay”. In: *Marine Chemistry* 80.1 (2002), pp. 41–59.

[182] G.W. Luther III et al. “Metal Sulfides in Estuarine Sediments”. In: *SEPM Journal of Sedimentary Research* 50.4 (1980), pp. 1117–1120.

[183] F. Y. Lee and J. A. Kittrick. “Elements associated with the cadmium phase in a harbor sediment as determined ith the electron beam microprobe”. In: *Journal of Environmental Quality* 13(3).3 (1984), pp. 337–340.

[184] R Francois. “A study on the regulation of the concentrations of some trace metals (Rb, Sr, Zn, Pb, Cu, V, Cr, Ni, Mn and Mo) in Saanich Inlet Sediments, British Columbia, Canada”. In: *Marine Geology* 83.1-4 (1988), pp. 285–308.

[185] R. Al-Farawati and C. M.G. van den Berg. “Metal-sulfide complexation in seawater”. In: *Marine Chemistry* 63.3-4 (1999), pp. 331–352.

[186] T. J. Shaw, E. R. Sholkovitz, and G. Klinkhammer. “Redox dynamics in the Chesapeake Bay: The effect on sediment/water uranium exchange”. In: *Geochimica et Cosmochimica Acta* 58.14 (1994), pp. 2985–2995.

[187] S. L. Borchers et al. “Geochemical signatures of the Namibian diatom belt: Perennial upwelling and intermittent anoxia”. In: *Geochemistry, Geophysics, Geosystems* 6.6 (2005).

[188] L. Olson et al. “Trace metal diagenesis in sulfidic sediments: Insights from Chesapeake Bay”. In: *Chemical Geology* 452 (2017), pp. 47–59.

[189] J. L. Morford, A. D. Russell, and S. Emerson. “Trace metal evidence for changes in the redox environment associated with the transition from terrigenous clay to diatomaceous sediment, Saanich Inlet, BC”. In: *Marine Geology* 174.1-4 (2001), pp. 355–369.

[190] S. M. Gucluer and M. G. Gross. “Recent marine sediments in Saanich Inlet, a stagnant marine basin”. In: *Limnology and Oceanography* 9.3 (1964), pp. 359–376.

[191] J. J. Anderson and A. H. Devol. “Deep water renewal in Saanich Inlet, an intermittently anoxic basin”. In: *Estuarine and Coastal Marine Science* 1.1 (1973), pp. 1–10.

[192] A.D Russell and J.L Morford. “The behavior of redox-sensitive metals across a laminated–massive–laminated transition in Saanich Inlet, British Columbia”. In: *Marine Geology* 174.1-4 (Mar. 2001), pp. 341–354.

[193] R. E. Thomson. “Physical oceanography of the Strait of Georgia-Puget Sound-Juan de Fuca Strait system”. In: *Review of the Marine Environment and Biota of the Strait of Georgia, Puget Sound, Juan de Fuca Strait. Canadian Technical Report of Fisheries and Aquatic Sciences No. 1948*. Ed. by R.C.H. Wilson and J. Beamish, R.J., Aitkens, F., Bell. Ottawa: Department of Fisheries and Oceans, Ottawa, 1994, pp. 36–100.

[194] Shipboard Scientific Party. “Sites 1033 and 1034”. In: *Proceedings of the Ocean Drilling Program, 169S Initial Reports*. College Station, TX: Ocean Drilling Program, 1998, pp. 11–61.

[195] R. H. Herlinveaux. “Oceanography of Saanich Inlet in Vancouver Island, British Columbia”. In: *Journal of the Fisheries Board of Canada* 19.1 (1962), pp. 1–37.

[196] M. G. Gross et al. “Varved marine sediments in a stagnant fjord”. In: *Science* 141.3584 (1963), pp. 918–919.

[197] P.T. Bobrowsky and J.J. Clague. “Holocene sediments from Saanich Inlet, British Columbia, and their neotectonic implications”. In: *Current Research, Part E, Geological Survey of Canada* Paper 90-1E (1990), pp. 251–256.

[198] R.W. Buddemeier. “Radiocarbon study of varved marine sediments of Saanich Inlet, British Columbia”. PhD thesis. University of Washington, Seattle, 1969.

[199] R.I.L. Powys. “The geochemistry and diatom assemblages of varved sediments from Saanich Inlet, B.C. [Ph.D. Dissert.]” PhD thesis. University of British Columbia, 1987.

[200] P. Bobrowsky, J. Clague, and A. Blais. “Late Holocene earthquakes: the geological record from Saanich Inlet, southern Strait of Georgia”. In: *Proceedings, Conference on Large Earthquakes and Active Faults in the Puget Sound Region*. University of Washington, Seattle, Washington, 1993.

[201] R. W. Drinnan. *Saanich Inlet study: water use inventory and water quality assessment*. Tech. rep. B.C.: Ministry of Environment, Lands & Parks, Environmental Protection Department, Water Quality Branch, 1995.

[202] H.E. Blyth and N.W. Rutter. “Quaternary Geology of Southeastern Vancouver Island and Gulf Islands (92B/5, 6, 11, 12, 13 and 14)”. In: *British Columbia Geological Survey Geological Fieldwork* Paper 1993-1 (1993), pp. 407–413.

[203] H.E. Blyth et al. *Surficial geology of the Shawnigan Lake area : NTS 92B/12*. Victoria, British Columbia: Ministry of Energy, Mines and Petroleum Resources, 1993.

[204] S. P. Hesselbo, S. A. Robinson, and F. Surlyk. “Sea-level change and facies development across potential Triassic-Jurassic boundary horizons, SW Britain”. In: *Journal of the Geological Society* 161.3 (2004), pp. 365–379.

[205] K. W. Bruland and R. P. Franks. “Mn, Ni, Cu, Zn and Cd in the Western North Atlantic”. In: *Trace Metals in Sea Water. NATO Conference Series (IV Marine Sciences)*. Ed. by C.S. Wong et al. Boston, MA: Springer, 1983, pp. 395–414.

[206] L. Jacobs and S. Emerson. “Trace metal solubility in an anoxic fjord”. In: *Earth and Planetary Science Letters* 60.2 (1982), pp. 237–252.

[207] J. W. Morse et al. “The Chemistry of the Hydrogen Sulfide and Iron Sulfide Systems in Natural Waters”. In: *Earth-Science Reviews* 24.1 (1987), pp. 1–42.

[208] S. Colley et al. “Post-depositional migration of elements during diagenesis in brown clay and turbidite sequences in the North East Atlantic”. In: *Geochimica et Cosmochimica Acta* 48.6 (1984), pp. 1223–1235.

[209] H.E. Wallace et al. “Active diagenetic formation of metal-rich layers in N. E. Atlantic sediments”. In: *Geochimica et Cosmochimica Acta* 52.6 (1988), pp. 1557–1569.

[210] S. Colley and J. Thomson. “Behaviour and mobility of U series radionuclides in Madeira Abyssal Plain turbidites over the past 750,000 years”. In: *Marine Geology* 109.1-2 (1992), pp. 141–158.

[211] D. C. Colodner et al. “Post-depositional mobility of platinum, iridium and rhenium in marine sediments”. In: *Nature* 358.6385 (1992), pp. 402–404.

[212] T. H. van Andel. “Recent marine sediments of the Gulf of California”. In: *Marine Geology of the Gulf of California: a symposium*. Ed. by T. H. van Andel and G.G.J. Shor. Vol. 3. American Association of Petroleum Geologist, 1964, pp. 216–310.